Synthesis and Evaluation of 2,3-Dihydroquinazolinones as Dual Inhibitors of Angiogenesis and Cancer Cell Proliferation

Gary Michael Chinigo

Monroe, Connecticut

B.S., University of Michigan at Ann Arbor, 2000

A Dissertation Presented to the Graduate Faculty of the University of Virginia in Candidacy for the Degree of Doctor of Philosophy

Department of Chemistry

University of Virginia

January 2007

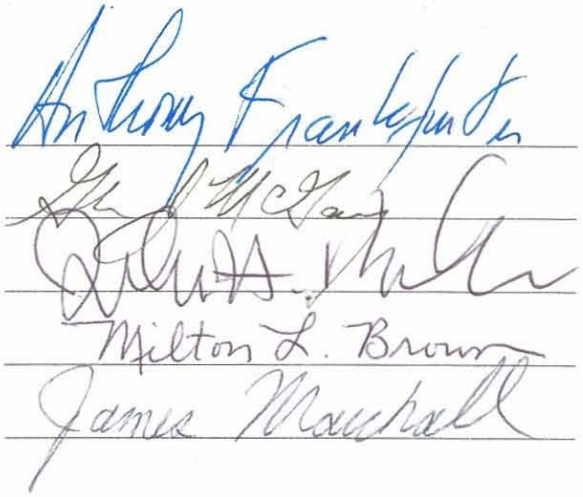

Abstract

Dual inhibitors of cancer cell proliferation and angiogenesis have recently shown remarkable potential for the clinical treatment of several cancers. Inspired by this success, we have employed traditional medicinal chemistry techniques to develop a 2,3-dihydroquinazolin-4-one lead molecule with promising anti-proliferative and anti-angiogenic activity. These molecules, which we originally derived from thalidomide, have evolved into an extremely effective (sub-nanomolar) prospective drug candidate for the treatment of cancer.

Described herein is an account of the many structural modifications made to this lead compound along with the corresponding effects on competitive ^{3}H colchicine displacement from tubulin, microtubule depolymerization, and cytotoxicity toward several human cancer and endothelial cell lines. From these evaluations we were able to design 3rd generation analogs with significantly enhanced potency. Subsequent animal testing suggests these molecules are relatively non-toxic, bio-available, and efficacious at treating tumors *in vivo* – evidence which supports the possibility of our most active analogs being evaluated clinically.

In addition to the SAR studies, we were compelled to develop synthetic methods enabling us to synthesize the enantiomers of these molecules. Exploration of several different approaches eventually led us to a chiral auxiliary based method of synthesis. Preliminary success led to a more thorough exploration of the scope and limitations of this methodology, and ultimately to the synthesis of the R and S enantiomers of both the lead and our most active molecule. Related X-ray crystal structure and biological studies conclusively point to the S isomer as the biologically active enantiomer. Finally, by using molecular modeling in conjunction with all the data gathered thus far, we have developed a hypothesis regarding the likely mode of interaction between tubulin and the molecules in this study.

Table of Contents

List of Figures

List of Tables

List of Schemes

List of Abbreviations

Biological

ADME – adsorption, distribution, metabolism, and elimination

ADMET - adsorption, distribution, metabolism, elimination, and toxicity

CAM – chicken chorioallantoic membrane assay

DNA – deoxyribonucleic acid

EDTA – ethylenediaminetetraacetic acid

ELISA – enzyme-linked immunosorbent assay

FDA – Food and Drug Administration

5FU – 5-fluorouracil

GTP – guanine triphosphate

HMBE – human bone marrow endothelial cells

HMEC – human microvascular endothelial cells

HUVEC – human umbilical vein endothelial cells

IC_{50} / GI_{50} – concentration of drug to inhibit 50% of cell growth

IP or ip – intraperitoneal

LPS – lipopolysaccharide

MTD – maximum tolerated dose

MVD – microvessel density

NCI – National Cancer Institute

PBS – phosphate buffer saline

PDGF – platelet derived growth factor

Pgp – P-glycoprotein

Rr – relative resistance value

SAR – structure-activity relationship

SEM – standard error of the mean

VEGF – vascular endothelial growth factor

WHO – world health organization

Chemical

Å – angstrom

Ac – acetate

Bp – boiling point

Boc – *tert*-butoxy carbonyl

Boc_2O – di-*tert*-butyldicarbonate

Bu – butyl

CAN – ceric ammonium nitrate

DBU – 1,8-diazabicyclo[5.4.0]undec-7-ene

DCM – dichloromethane

DHQZ – 2,3-dihydro-4-quinazolinone

DHPQZ – 2,3-dihydro-2-phenyl-4-quinazolinone

DMAC – dimethylacetamide

4-DMAP – 4-dimethylaminopyridine

DME – 1,2-dimethoxyethane

DMF – dimethylformamide

DMSO – dimethylsulfoxide

EDC – 1-(3-dimethylaminopropyl)-3-ethylcarbodiimide hydrochloride

Et – ethyl

H-Bond – hydrogen bond

HMPA – hexamethylphosphoramide

HOBt – 1-hydroxybenzotriazole

IR – infrared spectroscopy

LAH – lithium aluminum hydride

LDA – lithium diisopropylamide

mCPBA – *meta*-chloroperoxybenzoic acid

Me – methyl

mM – millimolar

MOMCl – chloromethyl methyl ether

Mp – melting point

MS – mass spectroscopy

MT – microtubule

NaH – sodium hydride

NBS – N-bromosuccinimide

nM – nanomolar

NMR – nuclear magnetic resonance spectroscopy

PDC – pyridinium dichromate

Ph – phenyl

TEA – triethylamine

Tf – trifluoromethanesulfonic or triflate

TFA – trifluoroacetic acid

THF – tetrahydrofuran

TLC – thin layer chromatography

TMS – trimethylsilane

p-TsOH – *para*-toluenesulfonic acid

μM – micromolar

Chapter 1: Introduction

Cancer is an extremely serious and often deadly medical condition which has plagued mankind for thousands of years. The earliest written reference to this disease dates back to ca. 1600 B.C. and can be found in an ancient Egyptian scroll known as the Edwin Smith Surgical Papyrus.[1] This document, primarily a surgical treatise, describes a series of ailments and wounds and the treatments that were used. Among these, the papyrus describes 8 cases of tumors of the breast and the methods used to treat them. The author of this document, with obviously limited therapeutic options at his disposal, attempted to cure these breast cancers by cauterization with an enigmatic tool only referred to as "the fire drill." Apparently, after learning that drills of fire are ineffective at treating malignancies, the author concludes with the grim diagnosis "there is no treatment."

Fortunately, significant scientific progress has been made in this field since the days of the Edwin Smith Papyrus. Achievements began to accumulate in the Renaissance era[2] and have now led to a much deeper understanding of this ailment. It is now known, for example, that "cancer" is a term that actually encompasses more than 100 different types of uncontrolled cell growth, each capable of affecting different tissues of the body and possessing its own unique pathology. Because of this, it is unlikely that one single cure for cancer will ever be found – rather, a multitude of different therapies, vaccines, and drugs exist and are continually being developed.

1.1 Cancer

The statistics associated with cancer are staggering (see Fig. 1.1A). According to the American Cancer Society[3], cancer is the second leading cause of death in the United States and is surpassed only by heart disease. Based on historical data, approximately

Figure 1.1A Major Causes of Death in the US in 2002

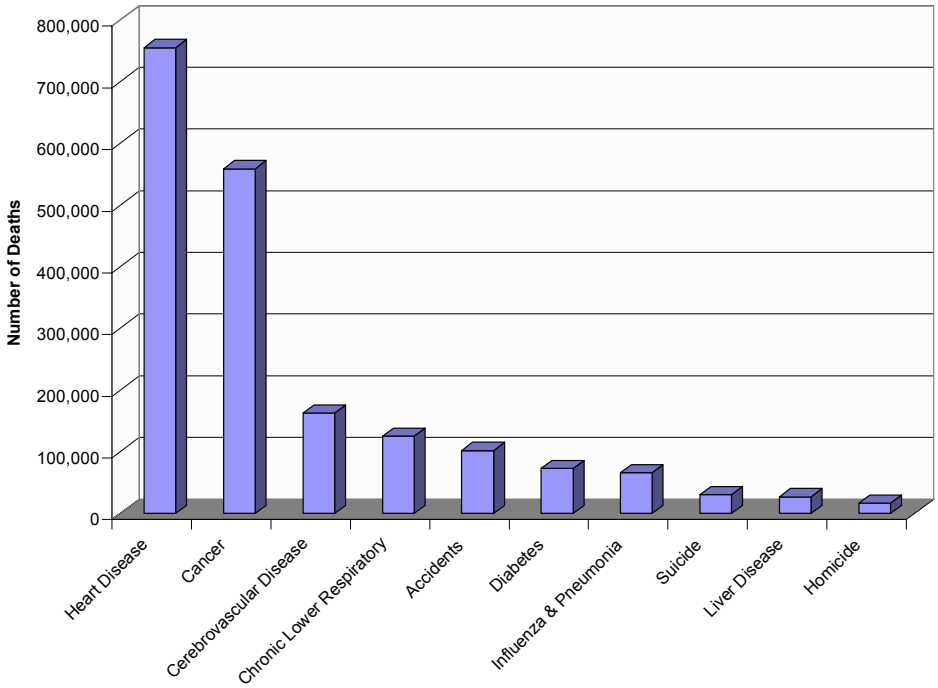

570,280 people are expected to die from cancer related illness this year[3] – that translates to slightly more than 1 person every minute. Although the advancements in oncological therapies have led to an increase in survival over the years, the current 5-year survival rate for cancer patients is only 64 %.[3]

Certain types of cancer tend to be more prevalent based on gender, race, age, and geographic location. As Figure 1.1B indicates, this year an estimated 291,270 males will die from cancer versus 273,560 females.[3] Although the trends in cancer location tend to

be similar between the sexes, there are a significant number of cases of cancer localized to gender specific tissue.

There are currently several options available for those who are diagnosed with cancer. Depending on the stage and nature of the disease, a patient may opt for surgery, radiation therapy, chemotherapy, immunotherapy, or hormonal suppression. The odds that a patient will survive this affliction increase the sooner the cancer is detected and treated. Drug intervention (chemotherapy) is one of the more widely used methods to control cancer and works through any of several different mechanisms of action.

Figure 1.1B 2006 Estimated U.S. Cancer Deaths by Site and Sex

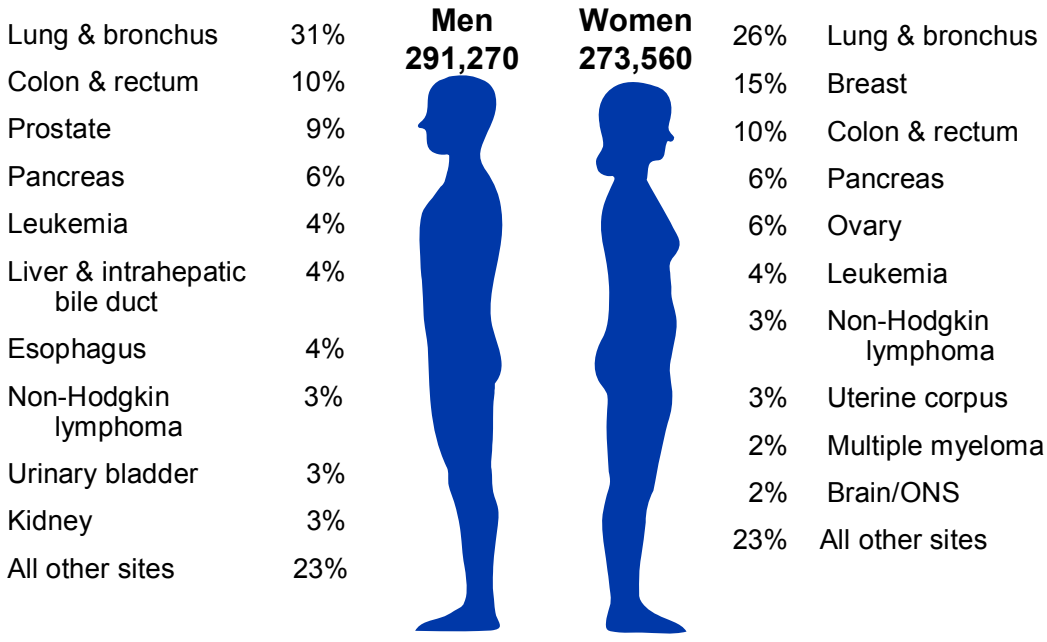

ONS=Other nervous system.
Source: American Cancer Society, 2006.

1.2 Tubulin / Microtubules

Tubulin is a ~50 kDa heterodimeric protein which is composed of an alpha and beta subunit.[4] Both the alpha and beta monomers further exist in at least 13 different isotopic forms which are expressed in a tissue specific manner.[5] The tubulin α/β heterodimer is found in all eukaryotic cells and, when appropriately stimulated, polymerizes to form a critical cellular structure known as the microtubule (see Figure 1.2A).[6]

Figure 1.2A Repeating Alpha and Beta Tubulin Sub-units Form the Microtubule Polymer

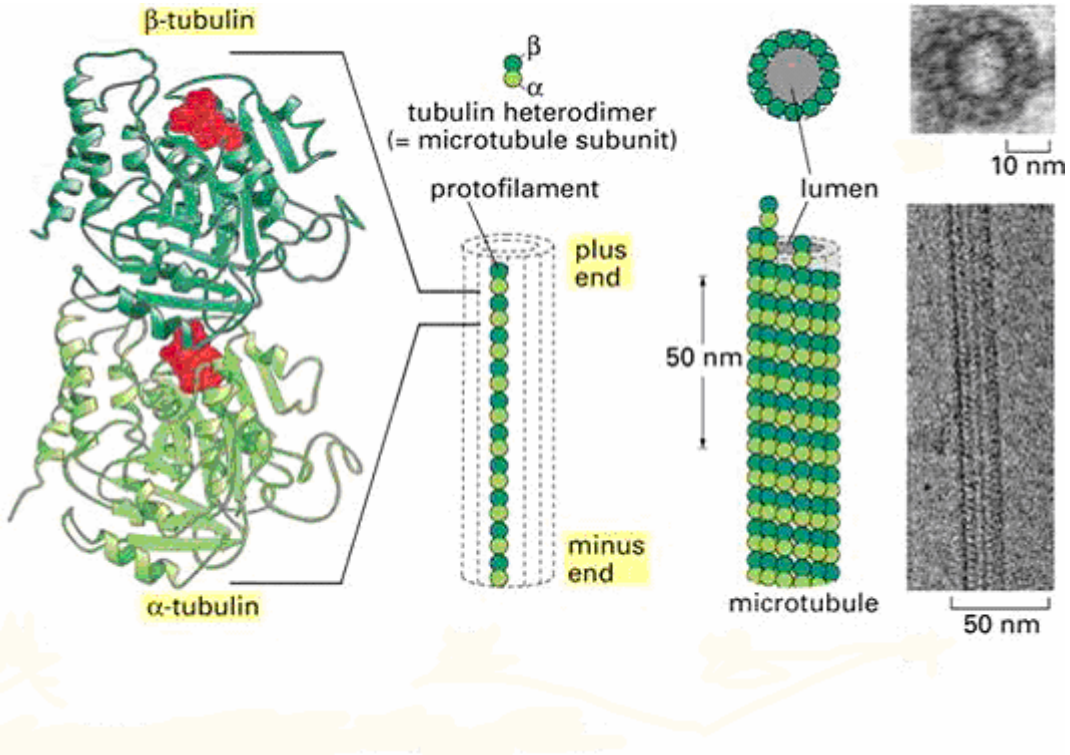

Microtubules are hollow cylindrical structures approximately 25 nm in diameter and are the major constituent of the cellular cytoskeleton. They can be found distributed throughout the cellular cytoplasm and serve a variety of functions essential to the cellular life cycle. They assist in the determination of cell shape,[7] the transportation of cellular

matter throughout the cytoplasm,[8] cellular motility,[9-10] and most importantly, they play a crucial role during mitosis.[11-14]

Microtubules are very dynamic structures – they are continually elongating or shortening according to the needs of the cell.[15] Each microtubule has a "minus" end which is embedded into a structure known as the microtubule organizing center, or centrosome, and a "plus" end which extends away from the centrosome (see Figure 1.2B).[16] When tubulin heterodimers polymerize, they add to the "plus" end and during depolymerization tubulin is removed from the "minus" end.[17-19] The net result is a continually changing cytoskeleton that appears to grow outwards or contract inward, depending on the polymerization event that is occurring.

Figure 1.2B The Organization of Microtubules and Related Structures Within a Cell

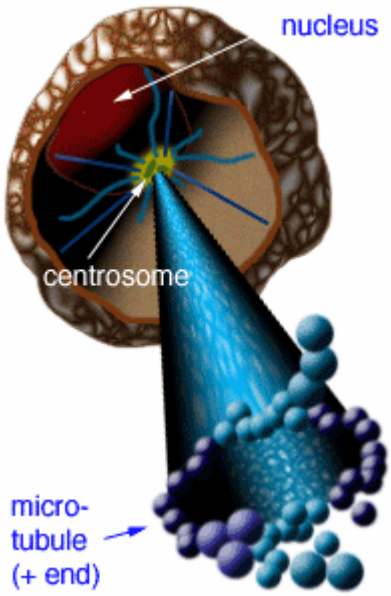

The existence of "plus" and "minus" ends of microtubules provides a sense of polarity to these structures which is exploited during many of a cell's routine functions. Various microtubule-associated motor proteins serve as vehicles carrying cellular freight around the cell by traversing these microtubules to the "plus" or "minus" ends of the tubulin polymer.[20-23] Such is the case during cell division when the newly replicated chromosomes are separated into two different cells (see Figure 1.2C).[24]

Due to the essential function of microtubules during mitosis, antimitotic agents which target them have become an attractive target for medicinal intervention in several cancers.[25-33] These compounds act by interfering with the mitotic spindle, a complex structure (see Figure 1.2C) largely composed of microtubules whose function is primarily chromosome separation and cell division. Tubulin is the known binding partner to several natural and synthetic molecules such as taxol,[29] colchicine,[34] laulimalide,[32,35] podophyllotoxin,[36] epothilone,[37] vinca alkaloids,[38] and combretastatin.[39] There appear to be at least 2 distinct modes of tubulin-drug interaction – spindle poisons that accelerate the depolymerization of the microtubule (e.g. vincas, colchicine, combretastatin)[40-42] and agents that excessively stabilize the polymer (e.g. taxol, laulimalide).[30,43-44] When either of these mechanisms is operative, the microtubule dynamics are affected in such a way which produces cell cycle arrest and ultimately apoptosis.

Figure 1.2C Main Components of the Mitotic Spindle

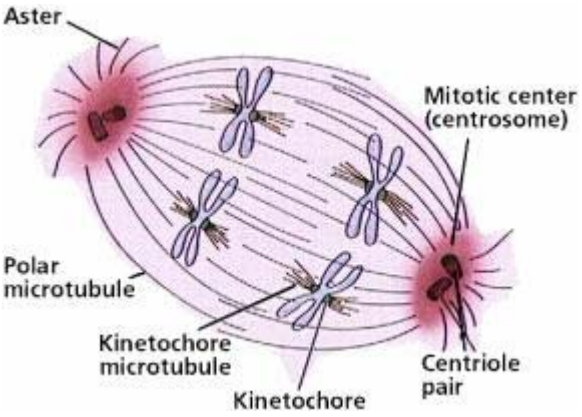

Targeting tubulin and microtubules is a well-established method of combating malignant tumors. One aspect that these tubulin drugs share with most other chemotherapeutics (as well as radiation therapy) is that they directly interact with and destroy the diseased cells. A new approach has emerged in recent years which employs a more indirect mechanism – it derives its therapeutic value from its ability to prevent a tumor from nourishing itself with the body's blood supply.

1.3 Angiogenesis

Angiogenesis is the generation of new blood vessels from a pre-existing vasculature. While it is a normal, healthy phenomenon involved in such processes as wound healing,[45] embryonic development,[46] and the female reproductive cycle,[47-49] it is also a relatively rare event in the adult human body (vascular endothelial cells only divide once every 3 years on average).

Angiogenesis is regulated by a series of chemical signals which act as either activators or inhibitors of new blood vessel growth. Figure 1.3A lists some of these chemical agents. After an angiogenesis activator binds to its receptor on the endothelial cell, a series of events occur which ultimately lead to new blood vessel growth. Initially, there is vascular destabilization of the wall of the blood vessel followed by extracellular matrix degradation by endothelial proteases. This causes the supporting collagen and basement membrane of the parent vessel to break down. Subsequently, the endothelial cells migrate, proliferate, and begin to form a tube-like structure that will become the

Figure 1.3A Various Chemical Activators and Inhibitors of Angiogenesis

Angiogenesis Activators	Angiogenesis Inhibitors
Proteins	**Proteins**
Acidic Fibroblast Growth Factor	Angiostatin
Angiogenin	Endostatin
Basic Fibroblast Growth Factor	Interferons
Hepatocyte Growth Factor	Platelet Factor 4
Interleukin 8	Prolactin 16 Kd fragment
Placental Growth Factor	Thrombospondin
Platelet Derived Endothelial Growth Factor	TIMP-1
Transforming Growth Factor α	TIMP-2
Tumor Necrosis Factor α	TIMP-3
Vascular Endothelial Growth Factor	
Small Molecules	
Adenosine	
1-Butyryl Glycerol	
Nicotinamide	
Prostaglandins E1 and E2	

daughter vessel.[50] Finally the pericytes reattach and the collagen and basement membrane are restored in a process known as vascular stabilization.[51]

Angiogenesis and Disease

As stated previously, angiogenesis is a natural physiological phenomenon that occurs in healthy beings. An excessive or deficient amount of angiogenesis, however, has been linked to some very serious pathologies, as Figure 1.3B indicates.

While extensive work has been done to modulate angiogenesis in order to treat these disorders, by far the most attention has been given to the role of angiogenesis in cancer. One of the earliest references to angiogenesis and cancer was made by Ide and

Figure 1.3B Diseases Resulting from Abnormal Levels of Angiogenesis

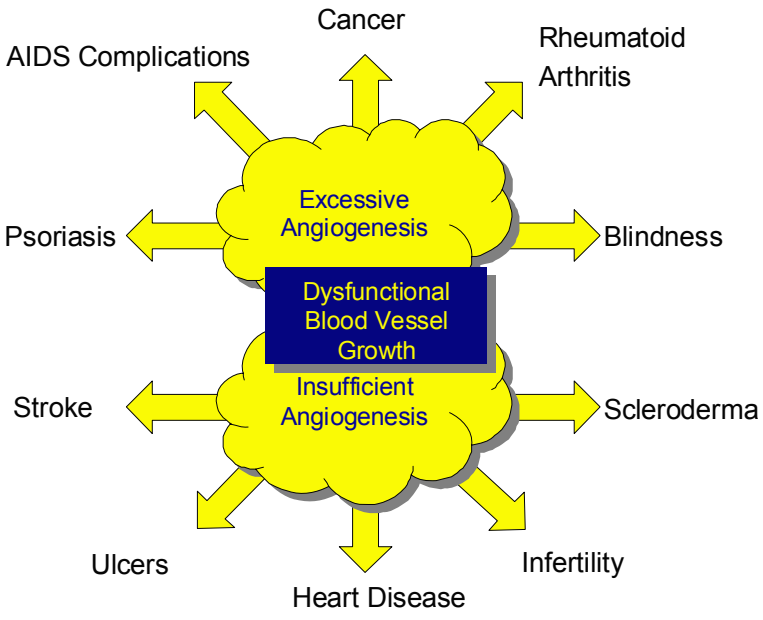

co-workers[52] in 1939 when they observed that tumor growth in a rabbit was accompanied by infiltration of newly formed blood vessels. Then in the mid 1940s when Algire and Chalkeley placed tumors in chambers, then implanted those chambers in mice, they

observed new blood vessels growing toward the encapsulated tumors.[53-54] It was not until 1971, however, when Dr. Judah Folkman published his landmark paper in which he hypothesized that chemical inhibitors of tumor angiogenesis could be used to treat cancer.[55-56] Although his ideas initially met with much resistance, Folkman's ideas have since been proven correct and are now regarded seminal in this field.

Folkman[55] and others have observed that tumors remain dormant until they have established a link with the host's circulation system. It is this connection which supplies a tumor with oxygen and nutrients, as well as a means to remove metabolic waste. Once this stage is reached, no obstacles remain to prevent the tumor from growing indefinitely and spreading to other parts of the body. Indeed, the vascularization of a cancerous mass usually leads to aggressive tumor growth and metastasis. This link between angiogenesis and tumor growth is so strong that the degree of tumor vascularization has been shown to directly correlate with patient survival in all four of the most lethal cancers in the United States: lung, colon, breast, and prostate.[57] The angiogenesis/tumor relationship been studied extensively in the last 30 years and has led to dozens of new therapeutics that are currently in various stages of clinical trials (see Tables 1.3A-C).

The mechanism by which a tumor promotes its vascularization has been exhaustively studied in recent years. Research suggests that angiogenesis is triggered by chemical signals sent from a tumor that is unable to meet its own metabolic needs. Once a dormant early stage non-vascularized tumor reaches a certain critical volume (approximately 1 to 2 cubic millimeters), it is very difficult for oxygen and nutrients to diffuse to the center of the cancerous mass (see Figure 1.3C). This results in a state of

cellular hypoxia which serves as a critical cue for pathological new blood vessel growth.[58]

Table 1.3A Angiogenesis Inhibitors in Current Clinical Trials: Protease Inhibitors

Drug	Mechanism	Sponsor	Trial
Marimastat	Synthetic matrix metalloprotease inhibitor	British Biotech	Phase III for cancer of breast, lung, pancreas, malignant glioma
Bay 12-9566	Synthetic MMPI, inhibitor of tumor growth	Bayer	Phase III for carcinoma of lung, ovary, pancreas
AG3340	Synthetic MMPI	Agouron/Warner-Lambert	Phase III for NSCLC; Phase III for prostate cancer
CGS 27023A	Synthetic MMPI	Novartis	Pase I/II
COL-3	Synthetic MMPI; Tetracycline derivative	Collagenex; NCI	Phase I
BMS-275291	Synthetic MMPI	Bristol-Myers Squibb	Phase I
Penicillamine	Urokinase inhibitor	NCI-NABTT;	Phase II for glioblastoma

Table 1.3B Angiogenesis Inhibitors in Current Clinical Trials: Direct Inhibitors of Endothelial Cell Proliferation/Migration

Drug	Mechanism	Sponsor	Trial
TNP-470	Inhibits endothelial cell growth	TAP Pharmaceuticals	Phase II for advanced adult solid tumors
Squalamine	Inhibits sodium hydrogen exchanger, NIHE3	Magainin	Phase III for NSCLC; Phase III for prostate cancer
Combretastatin	Induction of apoptosis in proliferating Ecs	Oxigene	Phase I/II
Endostatin	Inhibition of Ecs	EntreMed	Phase I
Penicillamine	Blocks EC migration and proliferation	NCI-NABTT	Phase II for glioblastoma
Farnesyl Tranferase Inhibitor	Blocks EC migration and proliferation	NCI-NABTT	Phase I for solid tumors and glioblastoma

Table 1.3C Angiogenesis Inhibitor in Current Clinical Trials: Angiogenesis Antagonist with Distinct Mechanisms

Drug	Mechanism	Sponsor	Trial
CAI	Inhibitor of calcium influx	NCI	Phase II/III for ovarian, NSCL, and renal cancers
ABT-627	Endothelin receptor antagonist	Abbot/NMI	Phase I, prostate and other malignancies; Phase II for glioblastoma
CM101/ZDO101	Group B strep toxin that selectively disrupts proliferating endothelium by interaction with the CM201 receptor	CarboMed/Zeneca	Phase II
Interleukin 12	Induction of interferon gamma	M.D. Anderson Cancer Center/ Temple Univ.	Phase I trials for ovarian, renal cell, melanoma, and GI cancers; phase I/II for Kaposi's sarcoma and solid tumors
IM862	Blocks production of VEGF and bFGF; increases production of the inhibitor IL-12	Cytran	Phase III for AIDS related Kaposi's sarcoma
PNU-145156E	Blocks angiogenesis induced by TAT protein	Pharmacia and Upjohn	Phase I/II for solid tumors

Cells have evolved an extraordinary system for sensing and responding to hypoxia. Hypoxia-inducible factor 1 (HIF-1) is a protein transcription factor which cells continuously synthesize, disseminate, and degrade under normal physiological conditions.[59-61] As the levels of oxygen decline, the cell is unable to degrade HIF-1α, resulting in an exponential increase of this signal.[62] The accumulated HIF-1 transcription factors prompt the biosynthesis of over 40 different pro-angiogenic signaling proteins, most notably vascular endothelial growth factor (VEGF).[63-65] After these proteins are

Figure 1.3C: A non-vascularized tumor lies adjacent to a capillary and requires a blood supply to grow

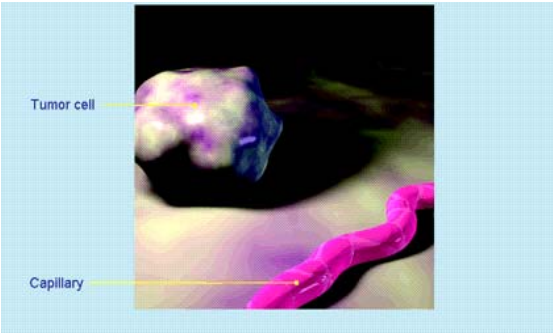

Figure 1.3D: Angiogenic signals from the tumor cause the capillary to vascularize it, enabling metastasis

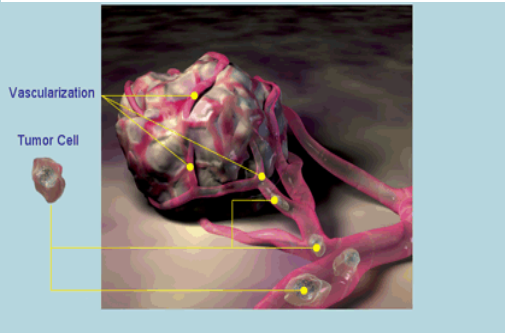

Figure 1.3E Removing the tumor's access to the circulatory system will confine it to 1 area and minimize its size

secreted from the tumor into the surrounding cellular matrix, neighboring blood vessels which possess receptor proteins on their extracellular surface act as binding partners to these angiogenesis signals. Once bound to these receptors, an intracellular chemical cascade stimulates the secretion of matrix metalloproteinases (MMPs) which degrade the collagen of the basement membrane and creates a fissure in the outer wall of the blood vessel.[66] From this deterioration, new blood vessel growth emerges and extends toward the source of the angiogenic stimulus, which in this case is the tumor. This growth continues until the sprouting blood vessels have completely vascularized the cancerous mass, thus eliminating the state of cellular hypoxia and malnourishment. We are now at

a situation where the tumor is not only capable of sustaining indefinite growth via the intake of oxygen and nutrients, but can also excrete small portions of itself into its new blood supply (see Figure 1.3D). It is in this manner in which a cancerous mass can metastasize and spread portions of itself great distances throughout the body. It is thought that by targeting the vascular network which supports the tumor that the size and motility of the cancer can be controlled (see Figure 1.3E).

Unfortunately, compounds which target only angiogenic factors have fallen short of the initially high expectations that were placed upon them. While it appeared that they were not clinically successful in completely controlling cancer when used by themselves, they have shown promise when used in conjunction with other drugs and/or radiation as a chemotherapeutic cocktail.[67-71] Based on these results, we hypothesize that a single drug which demonstrates both anti-angiogenic as well as anti-proliferative activity will provide a unique therapeutic advantage.

1.4 Discovery of Dihydroquinazolinone SC-2-71

For the last several years, the Brown lab has been engaged in the development of dual inhibitors of angiogenesis and cancer cell proliferation. This effort originated with the goal of modifying the structure of the known angiogenesis inhibitor thalidomide into an analogue with less toxicity, teratogenicity, and increased anti-proliferative activity.[72] Figure 1.4A illustrates the chemical evolution of thalidomide into the new lead compound **SC-2-71**, the structure of which serves as the starting point for these studies.

Based on extensive literature precedent which suggests that the glutarimide moiety is not critical to maintaining activity, a series of N-phenylphthalimides were synthesized and evaluated for their anti-proliferative and anti-angiogenic properties.

After some experimentation it became clear that while this class of compound retained much of the activity associated with thalidomide, it was not showing the improvements that we were seeking. Consequently, we designed a new set of compounds based on the ring expansion of the phthalimide heterocycle. The result was a series of isoquinoline analogs that were evaluated in a similar manner as the N-phenylphthalimides.

Figure 1.4A Chemical evolution of Thalidomide into the Lead Compound SC-2-71

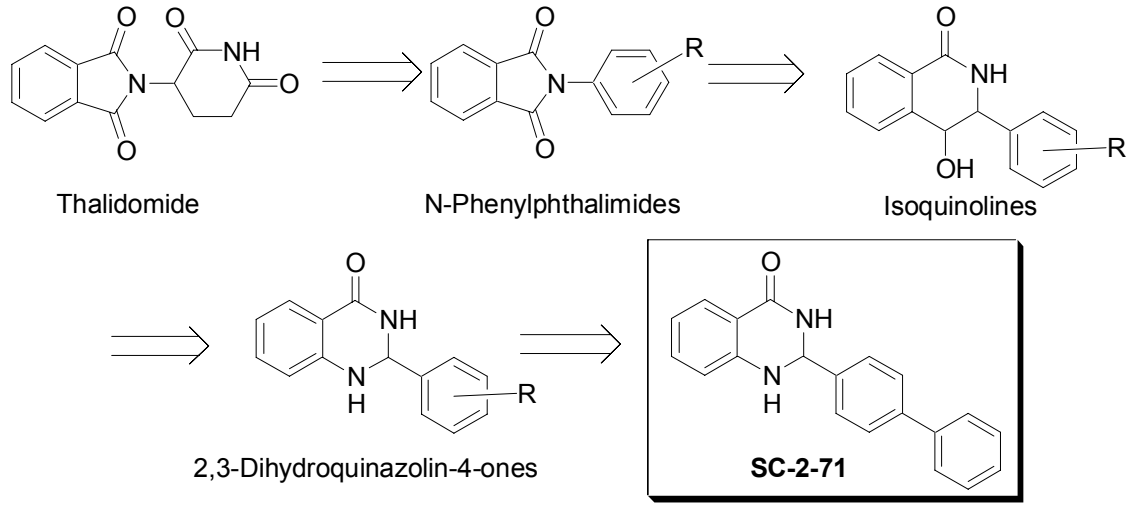

Unfortunately, the biological results for this series of compounds were extremely poor. While similar levels of anti-angiogenic activity were observed, there were no significant anti-proliferative effects associated with these molecules. By using a nitrogen in lieu of the benzylic carbon, the isoquinolines were transformed into a new class of molecule known as 2,3-dihydroquinazolin-4-ones. Again, several analogs were prepared and assayed for their ability to inhibit the proliferation of HMECS and human cancer cells. Most of these analogs had moderate to good activity, but only the quinazolinone **SC-2-71** proved exceptionally potent and appeared to be the lead compound we were

searching for. Figure 1.4B is the result of the National Cancer Institute's 60 cell line screen for **SC-2-71.** These results indicate significant anti-proliferative activity across several different tissue types. It is encouraging to note that there appears to be

Figure 1.4B National Cancer Institute's 60-cell Line Screen for **SC-2-71**

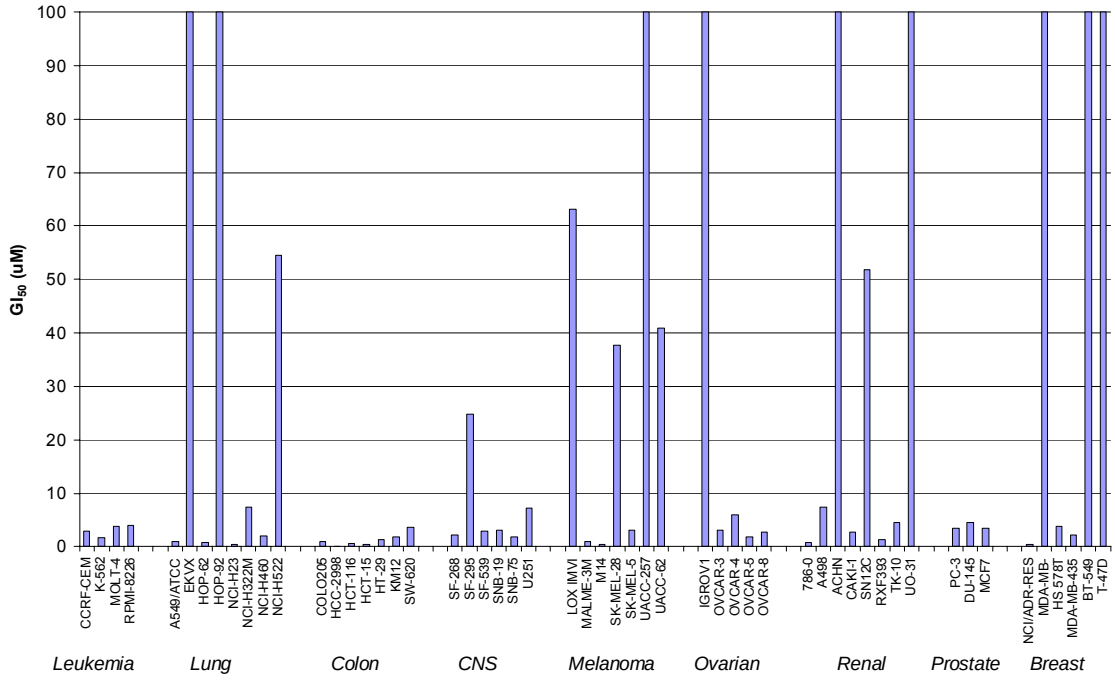

some specificity toward certain cell lines, suggesting there is an underlying biological mechanism guiding the tissue selectivity of this compound and it is not merely toxic to all cells. Particularly striking is the colon cancer data, with GI_{50} values ranging from 3 μM to 500 nM. Due to the large number of deaths and limited treatment options associated with colorectal cancer, we decided to use this type of cancer, specifically the HCC-2998 line (GI_{50} = 500 nM), as the basis of future **SC-2-71** SAR studies.

Because it is our intention to develop a dual inhibitor of cancer cell proliferation as well as angiogenesis, we required information about this compound's ability to inhibit angiogenesis. Table 1.4A conveys the results of an *in vitro* anti-proliferative study of

SC-2-71 and thalidomide on human microvascular endothelial cells (HMVECs). The results show that compared to thalidomide, **SC-2-71** is far superior at inhibiting the growth of blood vessel cells.

Table 1.4A Comparison of Thalidomide versus **SC-2-71** for Angiogenesis Inhibition

	HMEC GI_{50} (μM)		
Thalidomide	> 300		
SC-2-71	10	±	10.1

(All experiments run in triplicate)

To further investigate this angiogenesis-inhibiting behavior, we wanted to see what kind of *in vivo* anti-angiogenic effects this compound had. An *in vivo* experiment would more closely resemble the conditions present in the human body than would an *in vitro* assay, and so a chicken chorioallantoic membrane (CAM) assay was performed. The results of this experiment are shown in Figure 1.4C. At a concentration of 100 μM, **SC-2-71** abolished more than half of the CAM vasculature when compared to the DMSO/ethanol controls.

Figure 1.4C Chorioallantoic Membrane (CAM) Assay for **SC-2-71**

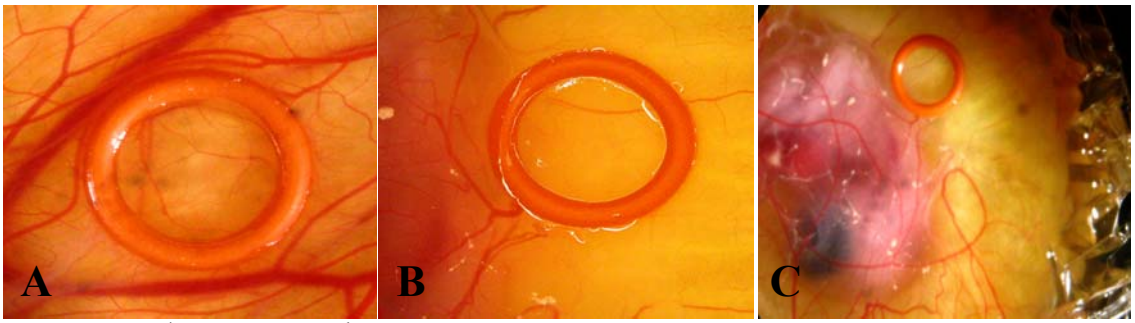

A: DMSO/EtOH Control **B**: SC-2-71 (100 μM) **C**: SC-2-71 (100 μM)

Having already established the anti-proliferative as well as the anti-angiogenic properties of **SC-2-71**, we now wished to put the quantitative results of these experiments into perspective by comparing them with the known values of some other relevant compounds. Table 1.4B shows a comparison between **SC-2-71**, vincristine (a structurally complex tubulin-binding natural product), and 5-fluorouracil (5-FU, currently

Table 1.4B Comparison of Anti-proliferative Activity of **SC-2-71**, Vincristine, and 5-Fluorouracil (5-FU) Across Several Human Cancer Cell Lines

	GI_{50} (μM) Data for Various Human Colon Cancer Cell Lines[a]						
	HT29	*COLO 205*	*HCC-2998*	*HCT-116*	*HCT-15*	*KM12*	*SW-620*
SC-2-71[b]	5	1.02	0.97	0.54	3.03	1.13	3.95
Vincristine	0.11	0.12	0.11	0.12	0.14	0.12	0.11
5-FU	6.7	7.2	1.4	4	5.8	11.1	26.2

[a]Data for vincristine and 5-fluorouracil is from the NCI
[b]SC-2-71 data is the average of 2 separate experiments

the standard FDA-approved clinical treatment for colorectal cancer). While vincristine shows superior activity to both drugs, we were excited to note that **SC-2-71** shows better anti-proliferative activity than 5-FU. Based on this molecule's ability to inhibit angiogenesis and its strong antiproliferative effect, we felt it prudent to investigate this compound further.

1.5 Biological Mechanism of Action

Understanding the biological mechanism of action of a drug is an important aspect of the pharmaceutical development process. In addition to aiding in a researcher's understanding about how the compound functions, this information can be used in conjunction with *in silico* drug design methods to more quickly develop a medicinally efficacious molecule. A survey of related literature reveals that 2,3-dihydroquinazolin-4-

ones are known to interact with tubulin,[73-77] and so a series of experiments was done to gauge how effective **SC-2-71** was at disrupting microtubules.

Figure 1.5A shows qualitatively how **SC-2-71** affects the immortalized HeLa cells during mitosis. Panel A shows the mitotic spindle during as it would normally appear during cell division. The asters and microtubules (green) appear in a symmetrical and highly ordered state, as expected. However, when this same cell line is exposed to **SC-2-71** (panels B – D), we note a visible disruption of the spindle (characterized by multiple asters and a disorganized appearance of the mitotic structures). This experiment seems to support the idea that **SC-2-71** derives its anti-proliferative effects by interacting with microtubules, and so further experiments were carried out to verify this.

Figure 1.5B shows the microtubule depolymerization effects of **SC-2-71** on the microtubules (green). This compound caused a 75% microtubule depolymerization at 33

Figure 1.5A Effects of SC-2-71 on the Cell Division of HeLa Cells

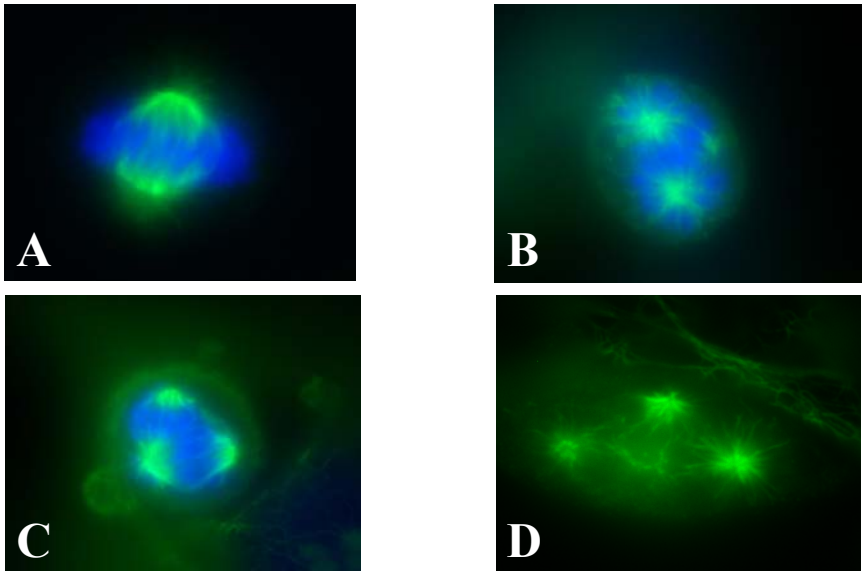

A: Control HeLa Mitosis; B-D: Various Mitotic Stages (17 μM SC-2-71)

μM (panel B) when compared to the control (panel A). While the control system exhibited a normal filamentous microtubule array, **SC-2-71** caused a concentration dependent loss of cellular microtubules – a hallmark response to microtubule disrupting agents.

Figure 1.5B Microtubule Depolymerization in A-10 Cell Caused by **SC-2-71**

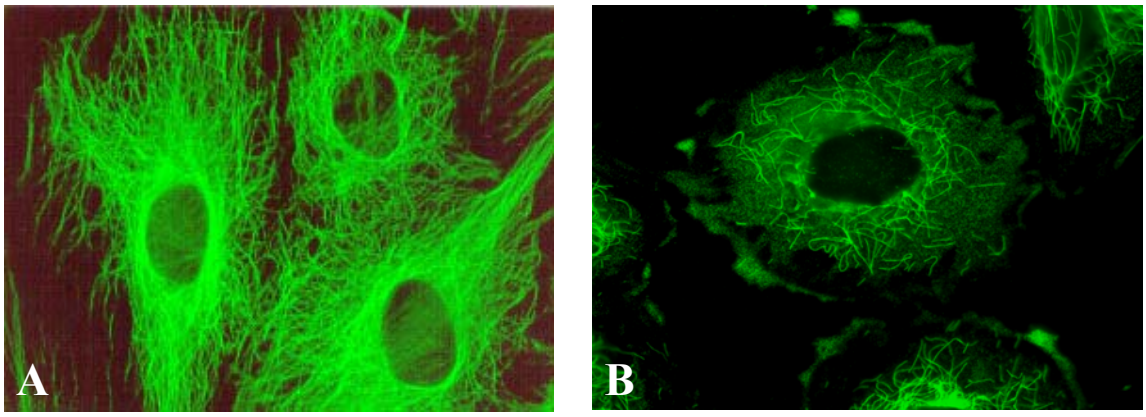

A: Control A-10 Cells B: SC-2-71 (33 μM)

As mentioned previously, tubulin binding agents interact with microtubules in two distinct manners: those that overly stabilize the microtubule, thereby promoting excessive polymerization, and those that destabilize microtubules, thereby causing depolymerization. As we observed in the previous experiment, **SC-2-71** causes pre-existing microtubules to depolymerize, so we may conclude that it is one of the latter tubulin binding agents. This information allows us to categorize **SC-2-71** with other microtubule depolymerizing agents such as colchicine and vinblastine and may further indicate a specific site or area of interaction on the tubulin protein.

Figure 1.5C Structurally Similar Molecules Known to Bind At or Near the Colchicine Site of Tubulin

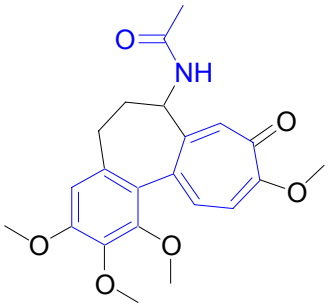

Colchicine

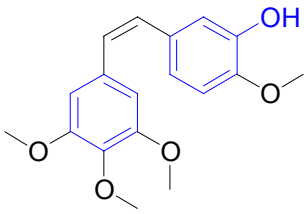

Combretastatin

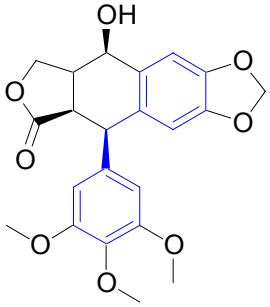

Podophyllotoxin

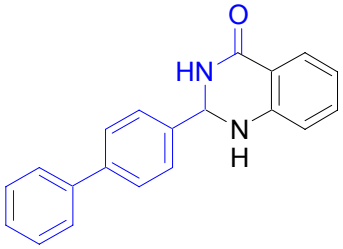

SC-2-71

Colchicine, podophyllotoxin, and combretastatin are 3 structurally comparable molecules that are known to bind to the colchicine site of tubulin. In addition to sharing features with each other, there is enough similarity between these molecules and **SC-2-71** (see Figure 1.5C) to make us suspect that our lead compound may also binds to the colchicine site. To test this hypothesis, a competitive binding assay was done with this quinazolinone and radioactive (tritiated) colchicine. As a result, we learned that a 5 μM concentration of **SC-2-71** was, in fact, able to displace 5.9 % of ^{3}H colchicine from tubulin. This suggests that our lead compound does bind at or near the colchicine site of tubulin.

One final aspect we wanted to investigate is the role the dihydroquinazolinone plays in multi-drug resistance (MDR). MDR, in this context, occurs when a cancer cell develops immunity or resistance toward the chemotherapeutic agent that is supposed to be affecting it. Although there are several mechanisms by which a cell may develop MDR, one of the most common is the expression of an efflux pump.[78] Figure 1.5D illustrates how these transmembrane glycoproteins confer resistance. Normally after a drug enters a cell, it would diffuse throughout the cytoplasm until it reaches the target protein or other site of action which enables it to elicit the desired pharmacological effect. When an efflux pump (such as p-Glycoprotein, for example) is present, the drug enters the cell, binds to the interior domain of the pump, and is immediately expelled back into the extracellular matrix before it is able to influence the cell's physical condition.[79] These proteins have evolved to assist the body in removing harmful substances, but their over-expression can result in making certain drugs less effective. The most abundant of these efflux pumps is known as p-glycoprotein (Pgp) and is the primary cause of multidrug resistant cancer cells.

Figure 1.5D Mechanism by which P-glycoprotein and other Efflux Pumps Remove a Drug from a Cell

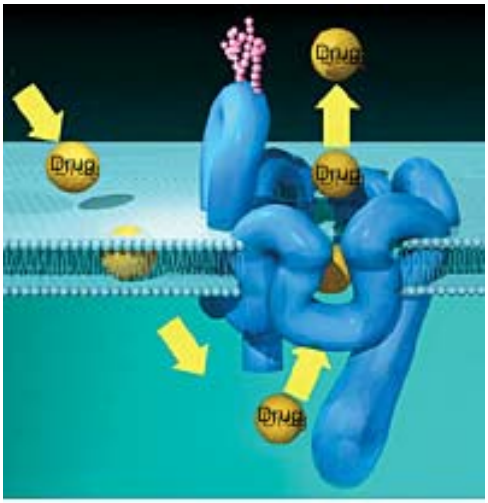

The ability to evade the actions of Pgp would be very valuable in the treatment of tumors which are expressing MDR. **SC-2-71** was therefore examined for its ability to inhibit the proliferation of the Pgp-expressing cell line NCI/ADR. Relative resistance (Rr) is the common method of conveying the ability of a compound to circumvent Pgp and can be calculated by dividing the IC_{50} of the resistant cell line by the IC_{50} of the sensitive cell line. The Rr of taxol in the NCI/ADR and MDA-MB-435 cell lines is 827, suggesting taxol is an excellent substrate for Pgp and therefore not a viable treatment for this type of cancer. **SC-2-71** was measured to have a Rr of 1.5 – 2.9, meaning it is a poor substrate for Pgp and may offer a valuable clinical alternative for people suffering from this form of multi-drug resistant cancer.

1.6 Experimental Design

As a result of the exceptional potential of our biphenyl-substituted dihydroquinazolinone outlined in sections 1.4 and 1.5, it seemed prudent to carry out a

Figure 1.6A Experimental Design for the SAR Study About the **SC-2-71** Scaffold

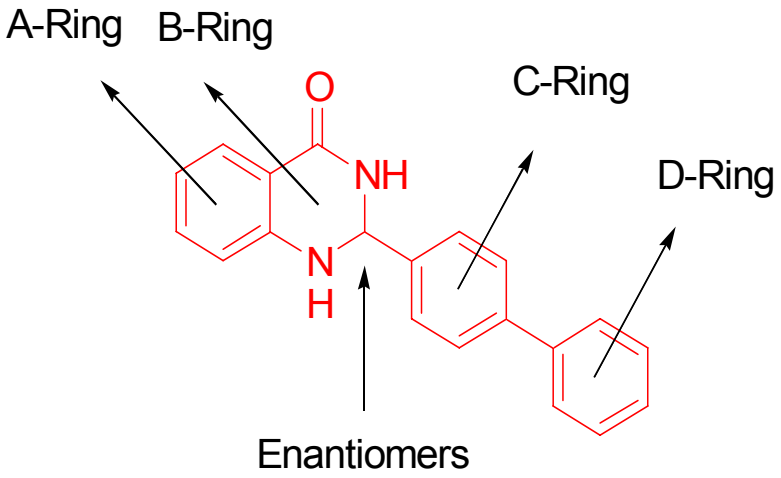

structure-activity relationship (SAR) study on our lead (**SC-2-71**) with the goal of enhancing the anti-proliferative and anti-angiogenic activity as much as possible.

Our experimental plan for this project is to make a series of structural modifications based on the 5 elements present in Figure 1.6A. Traditional medicinal chemistry transformations will be made on all 4 rings present in the lead compound, then evaluated in a series of *in vitro* biological assays that measure 1) the ability of the compounds to displace tritiated colchicine from tubulin, 2) how effective the analogs are at causing the depolymerization of microtubules, 3) the anti-proliferative effects on the cancerous HCC-2998 cell line and 4) the anti-proliferative effects on the human microvascular endothelial cell (HMVEC) line as a measure of the potential to inhibit angiogenesis.

In addition, we would like to determine which enantiomer is responsible for the biological activity that we have observed thus far. Since there is no known preparation or isolation of 2,3-dihydroquinazolin-4-one enantiomers, we anticipate this to be a significant undertaking. Initially, this will entail the development of a general new synthetic methodology that results in pure enantiomers of this class of molecule. Once successful, it will then be advantageous to determine the absolute configuration of the enantiomers in question. Finally, this new methodology will be applied to synthesize enantiomers of any relevant analogs resulting from the SAR study.

Once the work outlined thus far is complete, it will be applied to make a next generation of more active analogs. By incorporating multiple structural changes that increased the biological activity of our lead into one hybrid molecule, we will (hopefully) arrive at a DHQZ that displays enough of an *in vitro* synergistic effect to warrant *in vivo*

studies. Such studies will include determining the maximum tolerated dose (MTD), verification of the bio-availability, as well as pertinent xenograft studies.

1.7 Chapter 1 References

1. The Edwin Smith Surgical Papyrus. http://www.touregypt.net/edwinsmithsurgical.htm (accessed July 2006).
2. MedicineWorld History of Cancer. http://www.medicineworld.org/cancer/history/html (accessed July 2006).
3. Cancer Facts and Figures 2005 - American Cancer Society. http://www.cancer.org/docroot/STT/stt_0.asp (accessed July 2006).
4. Najbauer, J.; Orpiszewski, J.; Aswad, D.W. Molecular Aging of Tubulin: Accumulation of Isoaspartyl Sites in Vitro and in Vivo. *Biochemistry.* **1996**, *35*, 5183 – 5190.
5. Verdier-Pinard, P.; Wang, F.; Martello, L.; Burd, B.; Orr, G.A.; Horwitz, S.B. Analysis of Tubulin Isotypes and Mutations from Taxol-Resistant Cells by Combined Isoelectrofocusing and Mass Spectrometry. *Biochemistry.* **2003**, *42*, 5349 – 5357.
6. Nogales, E.; Wang, H.W.; Structural mechanisms underlying nucleotide-dependent self-assembly of tubulin and its relatives. *Curr. Opin. in Struct. Bio.* **2006**, *16*, 221 – 229.
7. Brown, D.L.; Bouck, G.B. Microtubule Biogenesis and Cell Shape in Ochromonas:II. The Role of Nucleating Sites in Shape Development. *J. Cell. Biol.* **1972**, *56*, 360 – 378.
8. Suh, J.; Wirtz, D.; Hanes, J. Efficient active transport of gene nanocarriers to te cell nucleus. *Proc. Natl. Aca. Sci. U.S.A.* **2003**, *100*, 7, 3878 – 3882.

9. Vasiliev, J.M.; Gelfand, I.M.; Effects of colcemid on morphogenetic processes and locomotion of fibroblasts. *Cell Motility*, **1976**, 279 – 304.

10. Gotlieb, A. I.; May, L. M.; Subrahmanyan, L.; Kalnins, V. I. Distribution of microtubule organizing centers in migrating sheets of endothelial cells. *J. Cell Biol.* **1981**, *91*, 589 – 594.

11. Wilson, L.; Panda, D.; Jordan, M. A. Modulation of microtubule dynamics by drugs: A paradigm for the action of cellular regulators. *Cell Struct. Funct*. **1999**, *24*, 329 – 335.

12. Panda, D.; Miller, H.P.; Islam, L.; Wilson, L. Stabilization of microtubule dynamics by estramustine by binding to a novel site in tubulin: a possible mechanistic basis for its antitumor action. Proc. *Natl. Acad. Sci. U.S.A.*, **1997**, *94*, 10560 – 10564.

13. Hamel, E. Antimitotic natural products and their interaction with tubulin. *Med. Res. Rev.* **1996**, *16*, 207 – 231.

14. Panda, D.; DeLuca, K.; Williams, D.; Jordan, M.A.; Wilson, L. Antiproliferative mechanism of action of cryptophycin-52: Kinetic stabilization of microtubule dynamics by high affinity binding to microtubule ends. *Proc. Natl. Acad. Sci. U.S.A.* **1998**, *95*, 9313 – 9318.

15. Gorbsky, G.J.; Sammak, P.J.; Borisy, G.G. Chromosomes move poleward in anaphase along stationary microtubules that coordinately disassemble from their kinetochore ends. *J. Cell. Biol*. **1987**, *104*, 9 – 18.

16. Desai, A.; Mitchison, T. J.; Microtubule polymerization dynamics. *Annu. Rev. Cell Dev. Biol.* **1997**, *13*, 83 – 117.

17. Kirschner, M.; Mitchison, T.; Beyond Self-Assembly: From Microtubules to Morphogenesis. *Cell*, **1986**, *45*, 329 – 342.

18. Carlier, M. F.; Pantaloni, D. Kinetic analysis of guanosine 5'triposphate hydrolysis associated with tubulin polymerization. *Biochemistry*, **1981**, *20*, 1918 – 1924.

19. Hill, T. L.; Carlier, M.F. Steady-state theory of the interference of GTP hydrolysis in the mechanism of microtubule assembly. *Proc. Natl. Acad. Sci. U.S.A.* **1983**, *80*, 7234 – 7238.

20. Allan, V. Motor proteins: a dynamic duo. *Curr. Biol*.,**1996**, *6*, 630 – 633.

21. Ahmad, F. J.; Echeverri, C. J.; Valee, R. B.; Bass, P. W. Cytoplasmic dynein and dynactin are required for the transport of microtubules into the axon. *J. Cell Biol*., **1998**, *140*, 391 – 401.

22. Echeverri, C. J. Paschal, B. M.; Vaughan, K. T. Vallee, R. B. Molecular characterization of the 50-kDa subunit of dynactin reveals function for the complex in chromosome alignment and spindle organization during mitosis. *J. Cell Biol.,* **1996**, *132*, 617 – 633.

23. Schroer, T. A. New insights into the interaction of cytoplasmic dynein with the actin-related protein, Arpl. *J. Cell Biol.* **1994**, *127*, 1 – 4.

24. Rieder, C. L.; Salmon, E. D. The vertebrate cell kinetochore and its roles during mitosis. *Trends in Cell Biol*. **1998**, *8*, 310 – 318.

25. Jordan, M. A.; Wilson, L. Microtubules and actin filaments: dynamic targets for cancer chemotherapy. *Curr. Opin. Cell Biol.* **1998**, *10,* 123 – 130.

26. Noble, R. L. The discovery of the vinca alkaloids – chemotherapeutic agents against cancer. *Biochem. Cell Biol*. **1990**, *68*, 1344 – 1351.

27. Toso, C.; Lindley, C. Vinorelbine: a novel vinca alkaloid. *Am. J. Health Syst. Pharm*. **1995**, *52*, 1287 – 1304.

28. Owellen, R. J., Root, M. A., Hains, F. O. Pharmacokinetics of vindesine and vincristine in humans, *Cancer Res*. **1977**, *37*, 2603 – 2607.

29. Schiff, P. B.; Fant, J.; Horwitz, S. B. Promotion of microtubule assembly in vitro by Taxol. *Nature* **1979**; *277*, 5698, 665 – 667.

30. Schiff, P. B.; Horwitz, S. B. Taxol stabilizes microtubules in mouse fibroblast cells. *Proc. Natl. Acad. Sci. U.S.A.* **1980**, *77*, 3, 1561 – 1565.

31. Rowinsky, E. K. Taxane analogues: distinguishing royal robes from the "Emperor's New Clothes." *Clin. Cancer Res*. **2002**, *8*, 9, 2759 – 2763.

32. Corley, D. G.; Herb, R.; Moore, R. E.; Scheuer, P. J.; Paul, V. J. Laulimalides: New Potent Cytotoxic Macrolides from a Marine Sponge and a Nudibranch Predator. *J. Org. Chem*. **1988**, *53*, 3644 – 3646.

33. Pettit, G. R.; Cragg, G. M.; Herald, D. L.; Schmidt, J. M.; Lohavanijaya, P. Antineoplastic agents. 84. Isolation and structure of combretastatin. *Can. J. Chem*. **1982**, *60*, 11, 1374 – 1376.

34. Uppuluri, S.; Knipling, L.; Sackett, D. L.; Wolff, J. Localization of the Colchicine-Binding Site of Tubulin. *Proc. Natl. Acad. Sci. U.S.A.* **1993**, *90*, 11598-11602.

35. Quinoa, E.; Kakou, Y.; Crews, P. Fijianolides, polyketide heterocycles from a marine sponge. *J. Org. Chem.* **1988**, *53*, 3642 - 3644.

36. Kelleher, J. K. Tubulin binding affinities of podophyllotoxin and colchicine analogs. *Molecular Pharmacology*, **1977**, *13*, 2, 232 – 241.

37. Bollag, D. M.; McQueney, P.; Zhu, J.; Hensens, O.; Koupal, L.; Liesch, J.; Goetz, M.; Lazarides, E.; Woods, C. M. Epothilones, a new class of microtubule-stabilizing agents with a taxol-like mechanism of action. *Cancer Res.* **1995**, *55*, 2325-2333.

38. The Alkaloids. *Antitumor Bisindole Alkaloids from Catharanthus Roseus (L.)*. Brossi, A., Suffness, M., Eds.; Academic Press: San Diego, 1990; Vol. 37.

39. Pettit, G. R.; Singh, S. B.; Hamel, E.; Lin, C. M.; Alberts, D. S.; Garciakendall, D. Antineoplastic Agents. 145. Isolation and Structure of the Strong Cell-Growth and Tubulin Inhibitor Combretastatin-a-4. *Experientia* **1989**, *45*, 209-211.

40. Uppuluri, S.; Knipling, L.; Sackett, D. L.; Wolff, J. Localization of the Colchicine-Binding Site of Tubulin. *Proc. Natl. Acad. Sci. U.S.A.* **1993**, *90*, 11598-11602.

41. Woods, J. A.; Hadfield, J. A.; Pettit, G. R.; Fox, B. W.; McGown, A. T. The Interaction with Tubulin of a Series of Stilbenes Based on Combretastatin a-4. *Br. J. Cancer* **1995**, *71*, 705-711.

42. Chauvergne, J. Periwinkle alkaloids: vincristine, vinblastine, vindesine. Mechanism of action and antitumor activity. *Bordeaux Medical*, **1980**, *13*, 13, 607 – 614.

43. Thompson, W. C.; Wilsonn, L.; Purich, D. L. Taxol induces microtubule assembly at low temperature. *Cell Motility*, **1981**, *1*, 4, 445 – 454.

44. Mooberry, S. L.; Tien, G.; Hernandez, A. H.; Plubrukarn, A.; Davison, B. S. Laulimalide and isolaulimalide, new paclitaxel-like microtubule-stabilizing agents. *Cancer Res*. **1999**, *59*, 3, 653 – 660.

45. Gospodarowicz, D. Humoral control of cell proliferation: the role of fibroblast growth factor in regeneration, angiogenesis, wound healing, and neoplastic growth. *Prog. in Clin. Biol. Res*. **1976**, *9*, 1 – 19.

46. Werner, R.; Lemmon, V. Changes in the vascular extracellular matrix during embryonic vasculogenesis and angiogenesis. *Develop. Biol*., **1988**, *125*, 2, 441 – 450.

47. Burley, D. M.; Lenz, W. Thalidomide and congenital abnormalities. *Lancet* **1962**, *279*, 271 – 272.

48. Klauber, N.; Rohan, R. M.; Flynn, E.; D'Amato, R. J. Critical components of the female reproductive pathway are suppressed by the angiogenesis inhibitor AGM-1470. *Nat. Med.* **1997**, *3*, 443 – 446.

49. McBride, W. G. Thalidomide and congenital abnormalities. *Lancet* **1961,** *278*, 1358.

50. Ferrara, N. Role of vascular endothelial growth factor inn physiologic and pathologic angiogenesis: therapeutic implications. *Semin. Oncol*. **2002**, *29*, 10 – 14.

51. Folkman, J. D'Amore, P. A. Blood vessel formation: what is its molecular basis? *Cell*, **1996**, *87*, 1153 – 1155.

52. Ide, A. G.; Baker, N. H.; Warren, S. L. Vascularization of the Brown Pearce rabbit epithelioma transplant as seen in the transparent ear chamber. *Am. J. Roentgenol*, **1939**, *42*, 891 – 899.

53. Algire, G. H.; Chalkley, H. W.; Legallais, F. Y.; Park, H. D. Vascular reactions of normal and malignant tumors in vivo. I. Vascular reactions of mice to wounds and to normal and neoplastic transplants. *J. Natl. Cancer Inst*. **1945**, *6*, 73 – 85.

54. Algire, G. H. An adaptation of the transparent-chamber technique to the mouse. *J. Natl. Cancer Inst*. **1943**, *4*, 1 - 11.

55. Folkman, J. Tumor angiogenesis: therapeutic implications. *N. Engl. J. Med.* **1971**, *285*, 1182 – 1186.

56. Folkman, J.; Merler, E.; Abernathy, C. Williams, G. Isolation of a tumor factor responsible for angiogenesis. *J. Exp. Med.* **1971**, *133*, 275 – 288.

57. Borre, M.; Offersen, B. V.; Nwestrom, B.; Overgaard, J. Microvessel density predicts survival in prostate cancer patients subjected to watchful waiting. Br. *J. Cancer* **1998**, *78*, 940 – 944.

58. Hirota, K.; Semena, G. L. Regulation of angiogenesis by hypoxia-inducible factor 1. *Crit. Rev. in Oncol./Hemat.* **2006**, *59*, 15 – 26.

59. Salceda, S.; Caro, J. Hypoxia-inducible factor 1α (HIF-1α) protein is rapidly degraded by the ubiquitin-proteasome system under normoxic conditions. Its staliization by hypoxia depends on redox-induced changes. *J. Biol. Chem*. **1997**, *272*, 22642 – 22647.

60. Maxwell, P. H.; Wiesener, M. S.; Chang, G. W. The tumor suppressor protein VHL targets hypoxia-inducible factors for oxygen-dependent proteolysis. *Nature*, **1999**, *399*, 271 – 275.

61. Huang, L. E.; Gu, J.; Schau, M.; Bunn, H. F. Regulation of hypoxia-inducible factor 1α is mediated by an O_2-dependent degradation domain via the ubiquitin-proteasome pathway. *Proc. Natl. Acad. Sci. U.S.A.* **1998**, *95*, 17987 – 17992.

62. Jiang, B. H.; Semenza, G. L.; Bauer, C.; Marti, H. H. Hypoxia-inducible factor 1 levels vary exponentially over a physiologically relevant range of O_2 tension. *Am. J. Physiol*. **1996**, *271*, 1172 – 1180.

63. Forsythe, J. A.; Jiang, B. H.; Iyer, N.V.; Activation of vascular endothelial growth factor gene transcription by hypoxia-inducible factor 1. *Mol. Cell Biol*. **1996**, *16*, 4606 – 4613.

64. Iyer, N. V.; Kotch, L. E.; Agani, F. Cellular and developmental control of O_2 homeostasis by hypoxia-inducible factor 1α. *Genes Dev.* **1998**, *12*, 149 – 162.

65. Carmeliet, O.; Dor, Y.; Herbert, J. Role of HIF-1α in hypoxia-mediated apoptosis, cell proliferation and tumor angiogenesis. *Nature.* **1998**, *394*, 485 – 490.

66. Moses, M. A. The regulation of newvascularization of matrix metalloproteinases and their inhibitors. *Stem Cells*, **1997**, *15*, 180 -189.

67. Teicher, B. A.; Sotomayor, E. A.; Huang, A. D. Antiangiogenic agents potentiate cytotoxic cancer therapies against primary and metastatic disease. *Cancer Res*. **1992**, *52*, 6702 – 6704.

68. Siemann, D. W.; Warrington, K. H.; Horsman, M. R. Targeting tumor blood vessels: an adjuvant strategy for radiation therapy. *Radiother. Oncol*. **2000**, *57*, 5 – 12.

69. Jain, R. K. Normalization of tumor vasculature: an emerging concept in antiangiogenic therapy. *Science.* **2005**, *307*, 58 – 62.

70. Abdollahi, A.; Lipson, K. E.; Han, X. SU5416 and SU6668 attenuate the angiogenic effects of radiation-induced tumor cell growth factor production and amplify the direct anti-endothelial action of radiation in vitro. *Cancer Res.* **2003**, *63*, 3755 – 3763.

71. Xu, L.; Tong, R.; Cochran, D. M.; Jain, R. K. Blockinng platelet-derived growth factor receptor beta signaling inhibits human renal cell carcinoma progression in an orthotopic mouse model. *Cancer Res*. **2005**, *65*, 5711 – 5719.

72. Capitosti, S. M.; Hansen, T. P.; Brown, M. L. Thalidomide analogues demonstrate dual inhibition of both angiogenesis and prostate cancer. *Bioorg. Med. Chem*. **2004**, *12*, 2, 327 – 336.

73. Lin, C. M.; Kang, G. J.; Roach, M. C.; Jiang, J. B.; Hesson, D. P.; Luduena, R. F.; Hamel, E. Investigation of the mechanism of the interaction of tubulin with derivatives of 2-styrylquinazolin-4(3H)-one. *Mol. Pharmacol.* **1991**, *40*, 827 – 832.

74. Jiang, J. B.; Hesson, D. P.; Dusak, B. A.; Dexter, D. L.; Kang, G. J.; Hamel, E. Synthesis and biological evaluation of 2-styrylquinazolin-4(3H)-ones, a new class of antimitotic anticancer agents which inhibit tubulin polymerization. *J. Med. Chem.* **1990**, *33*, 1721 – 1728.

75. Hamel, E.; Lin, C. M.; Plowman, J.; Wang, H. K.; Lee, K. H.; Paull, K. D. Antitumor 2,3-dihydro-2-(aryl)-4(1H)-quinazolinone derivatives. Interaction with tubulin. *Biochem. Pharmacol*. **1996**, *51*, 53 – 59.

76. Chen, K.; Kuo, S. C.; Hsih, M. C.; Mauger, A.; Linn, C. M.; Hamel, E.; Lee, K. H. Synthesis and biological evaluation of substituted 2-aryl-1,8-naphthyridin-4(1H)-ones as antimitotic agents that inhibit tubulin polymerization. *J. Med. Chem.* **1997**, *40*, 3049 – 3056.

77. Yale, H. J.; Kalkstein, M. Substituted 2,3-dihydro-4(1H)-quinazolinones. A new class of inhibitors of cell manipulation. *J. Med. Chem.* **1967**, *10*, 334 – 336.

78. Choi, C. H. ABC transporters as multidrug resistance mechanisms and the development of chemosensitizers for their reversal. *Cancer Cell Int.* **2005**, *5*, 30.

79. Ozben, T. Mechanisms and strategies to overcome multiple drug resistance in cancer. *FEBS Lett.* **2006**, *580*, 2903 – 2909.

Chapter 2: A-Ring Analogs and B-Ring Analogs

As we saw in Chapter 1, the abundance of data collected regarding the biological properties of **SC-2-71** provides a strong impetus to initiate a SAR study. As this chapter deals with the synthesis and evaluation of A- and B-ring analogs, it is germane to review previous works which have made similar modifications. Such an analysis may provide direction as well as allow us to save time by not reproducing work that has already been done.

The antitumor properties of 2,3-dihydroquinazolin-4-ones (DHQZs) have been known for over 30 years.[1] In 1996, Lee and Hamel published a paper dealing with the biological mechanism of action for these DHQZs as well as a preliminary SAR study.[2] Further work was done by the same authors in 2000 which again included a short SAR study on DHQZ analogs.[3] The results of these works are very straightforward with regards to the A-Ring derivatives: the only analog that has been made and tested has a chlorine atom *para* to the aniline (position R_5) which improved the depolymerization ability when compared to the unsubstituted analog.

The case of the heterocyclic B-ring analogs is a somewhat more complex. Figure 2A illustrates some of the related structures that have been made and tested, but this is by no means an all inclusive list. Several classes of compounds listed do have significant microtubule/anticancer activity, including the 2-phenyl-4-quinolone (**PQ**),[4-7] 2,3-dihydro-2-phenyl-4-quinolones (**DHPQ**),[8] 2-phenyl-1,8-naphthyridin-4-ones (**PN**),[8-10] phenylquinazolinones (**PQZ**),[11] dihydrophenylquinazolinones (**DHPQZ**),[12-13] and 2-styrylquinazolin-4-ones (**SQZ**),[14-15] however none appear to possess the potency that the

DHQZ derivatives do. With that in mind, it was our intention to omit similar structures from the B-ring analogs investigated in our study.

Figure 2A Structures of Quinazolinone Related Analogs

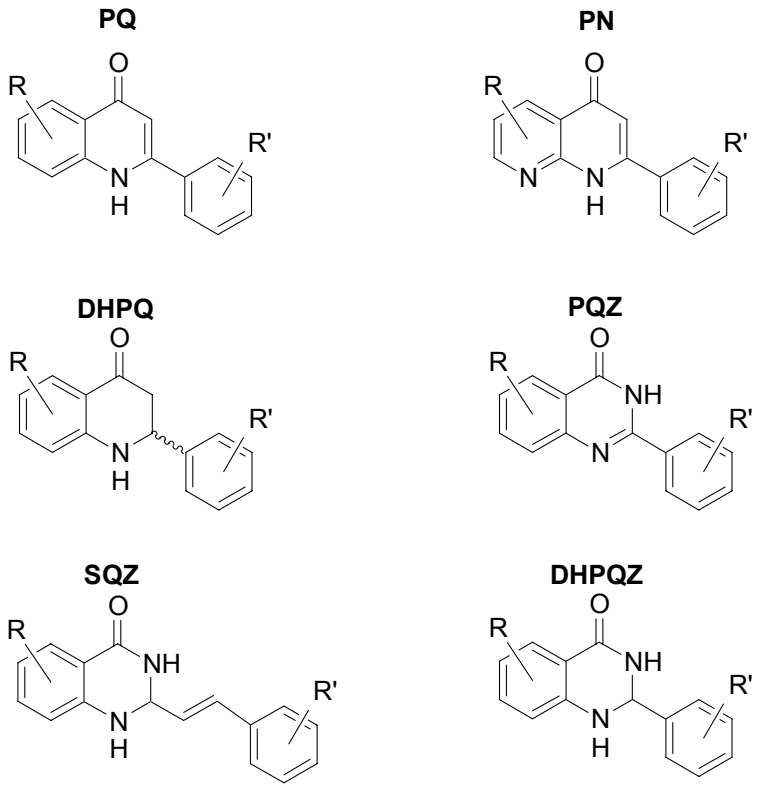

Structurally, the lead **SC-2-71** is a very simple molecule. While we did wish to increase the complexity of subsequent analogs, molecules that could not be realized in less than 5 or 6 steps were deemed to labor intensive for such a preliminary SAR investigation. Figure 2B illustrates the synthetic targets we wished to pursue - the structures outlined herein were chosen on the basis of their structural relevance to the lead compound in addition to their perceived ease of preparation.

Figure 2B Proposed A- and B-Ring Analogs

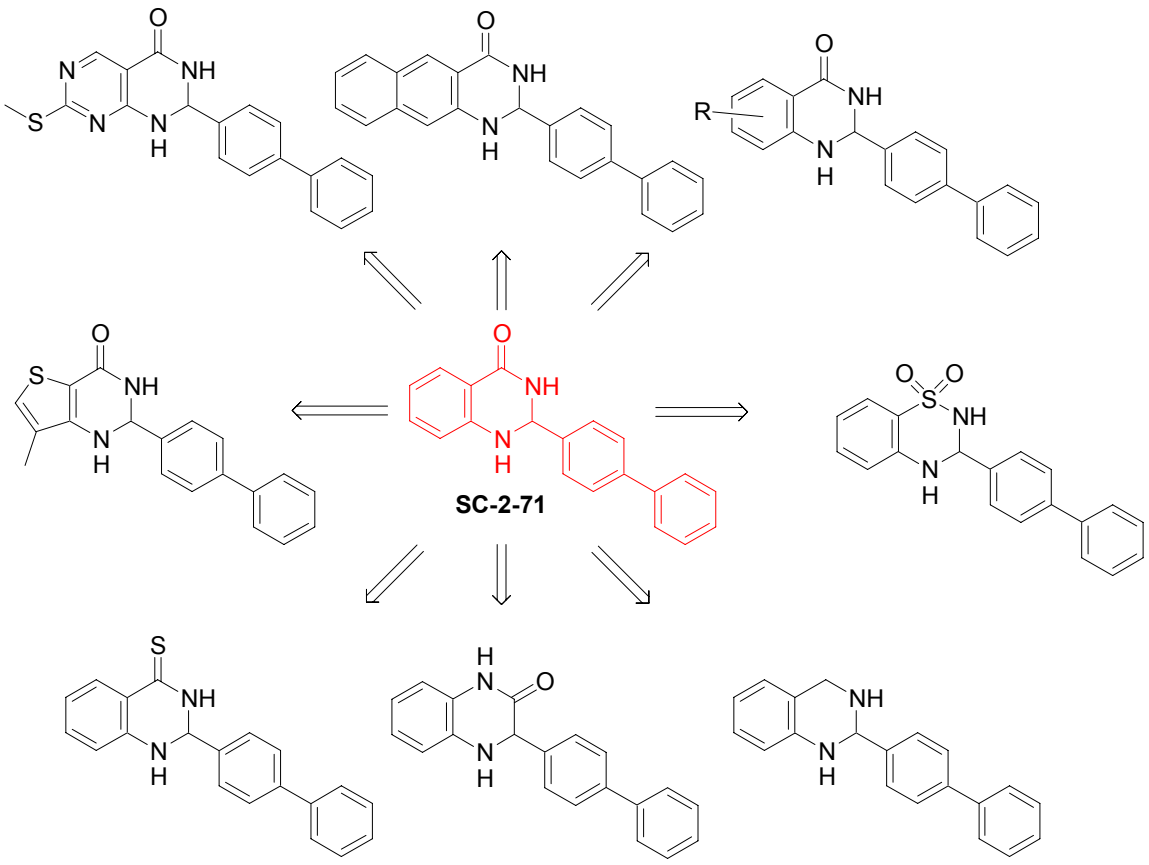

2.1 Synthesis of A-Ring Analogs

In general, the formation of DHQZs is a synthetically simple and convenient reaction to carry out. An anthranilamide analog is reacted with an aldehyde in the presence of a catalytic amount of acid at temperatures ranging from 0°C to 60°C, depending on the nature of the functional groups present. More often than not, the target DHQZ precipitates from solution in a degree of purity high enough to pass elemental

analysis (± 0.4%). When this is not the case, the product is easily purified by recrystallization or column chromatography.

Mechanistically, the aldehyde is initially dehydrated by the aniline to form the imine, which in turn is electrophilic enough to react with the nitrogen of the amide and result in a 6-membered aminal (see Figure 2.1A). The product DHQZs are generally very stable (long shelf-life, high melting point), yet they are sensitive to strong acids and bases.

Figure 2.1A Mechanism of DHQZ formation

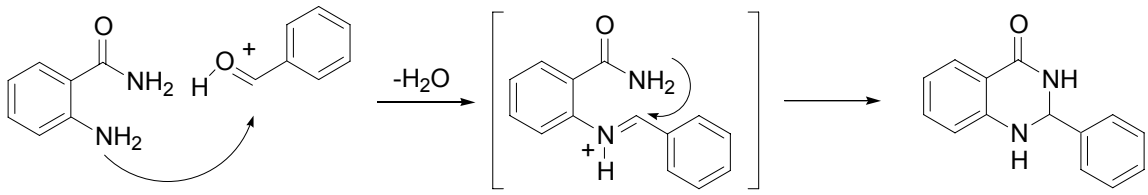

To thoroughly investigate the substitutions necessary for optimal activity, we chose to explore electron withdrawing, electron donating, and neutral substituents on the A-ring. To accomplish this, it seemed the most appropriate route would be to cyclize 4-biphenylcarboxaldehyde with an appropriately substituted anthranilamide. Unfortunately, the majority of anthranilamides were not commercially available, and so had to be synthesized from the corresponding anthranilic acid.[16] In three of these cases, even the acid was not commercially available and so these had to be prepared via the benzylic oxidation of an appropriate aminotoluene derivative.[17] Scheme 2.1A illustrates this approach.

In order to protect the amine from oxidation in the subsequent step, the aminotoluenes **5c**, **8c**, and **10c** were refluxed with acetic anhydride in acetic acid to form

the acetanilides. Upon completion of the reaction, the solvent was removed from the system *in vacuo* and the protected amine was precipitated from solution by addition of saturated aqueous $NaHCO_3$. The precipitate was taken up in water, then $MgSO_4$ and $KMnO_4$ were added and the reaction brought to 100°C. Upon complete oxidation of the benzylic carbon, the crude carboxylic acid was isolated by extraction. Aqueous sodium hydroxide was then added and the solution was refluxed for approximately 5 hours until the acetyl group was fully saponified from the amine. The resulting anthranilic acids were isolated by acid/base extraction and carried on without further purification.

EDC and HOBt were added to DMF solutions of anthranilic acids **1b** – **14b**. After 30 – 40 minutes, ammonium hydroxide was added to form the anthranilamides **1a** – **14a**. The target DHQZs **1** – **14** were finally realized by refluxing the anthranilamides with 4-biphenylcarboxaldehyde and acetic acid in acetonitrile.

Scheme 2.1A Synthesis of A-Ring Analogs **1 - 14**

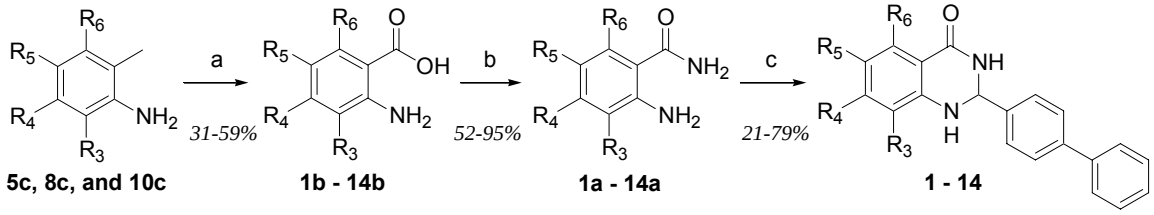

5c, 8c, and 10c **1b - 14b** **1a - 14a** **1 - 14**

	R_3	R_4	R_5	R_6		R_3	R_4	R_5	R_6
1	Cl	H	H	H	**8**	H	H	H	NO_2
2	H	Cl	H	H	**9**	OMe	H	H	H
3	H	H	Cl	H	**10**	H	OMe	H	H
4	H	H	H	Cl	**11**	H	H	OMe	H
5	NO_2	H	H	H	**12**	H	H	H	OMe
6	H	NO_2	H	H	**13**	H	OMe	OMe	H
7	H	H	NO_2	H	**14**	F	F	F	F

a) i. AcOAc, AcOH ii. $KMnO_4$, $MgSO_4$, H_2O iii. NaOH, H_2O b) i. HOBt, EDC, DMF ii. NH_4OH c) 4-biphenylcarboxaldehyde, MeCN, AcOH (cat.)

To further address our questions regarding the A-ring, we proposed the analogs shown in Scheme 2.1B. While these are slightly larger structural changes than we had originally intended to investigate, the anthranilamide starting materials were inexpensive and commercially available. Each was made according to the usual cyclization protocol to afford the indicated dihydroquinazolinones **15 - 17**.

Scheme 2.1B Synthesis of A-ring analogs **15 - 17**

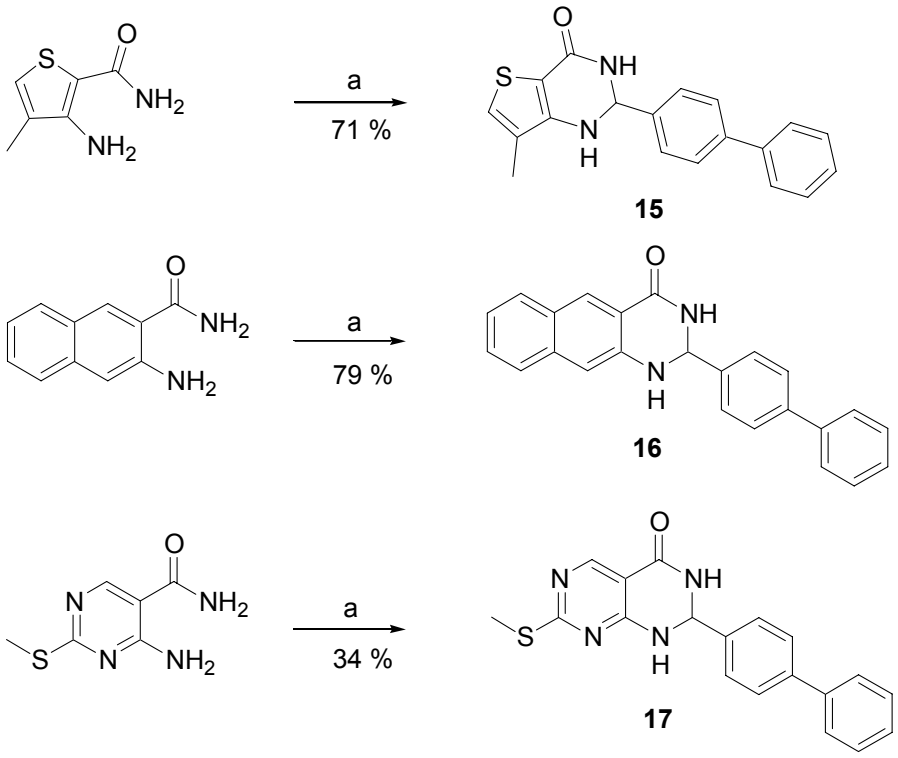

a) 4-biphenylcarboxaldehyde, MeCN, AcOH (cat.)

2.2 Synthesis of B-Ring Analogs

The first alteration made to the heterocycle was the replacement of the oxygen with sulfur. This was accomplished by refluxing **SC-2-71** with Lawesson's reagent[18] in toluene (see Scheme 2.2A). Although the product proved very difficult to isolate cleanly, after much experimentation we found that purification by column chromatography,

followed by trituration and then recrystallization provided **18** in high purity - albeit poor yield.

Scheme 2.2A Synthesis of thioamide **18**

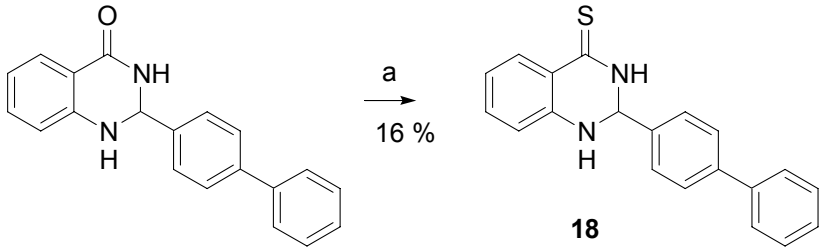

a) Lawesson's reagent, toluene, reflux

Further alterations to the carbonyl were made by the methods indicated in Scheme 2.2B. A net reduction of **SC-2-71** was accomplished by cyclization of 4-biphenylcarboxaldehyde with 2-aminobenzyl amine to form quinazoline **19**. A sulfonamide was analogously installed in the synthesis of compound **20**.

Scheme 2.2B Synthesis of quinazoline **19** and sulfonamide **20**

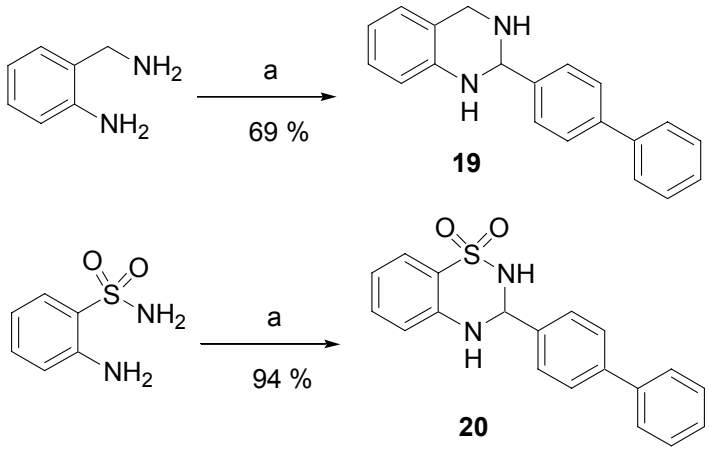

a) 4-biphenylcarboxaldehyde, MeCN, AcOH (cat.)

The last change to the B-ring was an inversion of the amide moiety of the lead compound. A 3-fold excess of biphenyl Grignard reagent was generated, then 1H-quinoxalin-2-one was added to afford compound **21** in modest yield,[19] see Scheme 2.2C.

Scheme 2.2C Synthesis of quinoxaline **21**

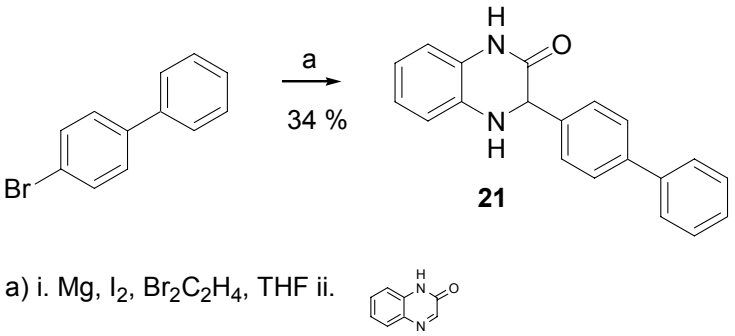

2.3 Biological Evaluation & SAR Conclusions

We initially evaluated the effects dihydroquinazolinones **1 – 21** had upon tubulin and microtubules. Each analog was evaluated in a tubulin polymerization inhibition assay which measured the amount of compound needed to inhibit 50 % of the microtubule formation. IC_{50} curves were determined by first incubating the drug with tubulin at 0 ^{o}C, then polymerization was initiated by warming to 26 ^{o}C and turbidity measurements were taken to determine the degree of polymerization.[7] Analogs that were determined to have an IC_{50} less than 10 μM were then examined for their ability to displace ^{3}[H] colchicine from tubulin in a competitive binding assay.[20]

A summary of these results are shown in **Table 2.3A** and suggest that, like the lead **SC-2-71**, these compounds inhibit tubulin polymerization by binding at or near the colchicines site. Structurally, the presence of a nitro group in the 5-, and to a lesser extent the 4- position, seems to bestow a favorable increase in tubulin depolymerization (see compounds **6**, **7**, **Table 2.3A**). Increased effects on tubulin polymerization were also observed for analogs **14** (with the tetrafluoro motif) and **17** (possessing the methylthiopyrimidine unit *in lieu* of the unsubstituted benzene ring).

One common structural feature among the more potent tubulin depolymerizing analogs in this study thus far is the presence of a strong electron withdrawing effect on

Table 2.3A A-Ring and B-Ring Analogs' Inhibition of Tubulin Polymerization and Displacement of Tritiated Colchicine

Compound	IC_{50} Tubulin Polymerization (μM)	^{3}[H] Colchicine Displacement 5 μM ± SD	50 μM ± SD
1	> 10		
2	> 10		
3	> 10		
4	> 10		
5	> 10		
6	4.9 ± 0.4		19 ± 12
7	4.4 ± 0.5	18 ± 9.5	25 ± 4.9
8	> 10		
9	> 10		
10	> 10		
11	> 10		
12	> 10		
13	> 10		
14	4.3 ± 0.3	7.7 ± 2.9	7.7 ± 1.7
15	> 10		
16	> 10		
17	9.7 ± 0.5	11 ± 8	17 ± 6.2
18	> 10		
19	> 10		
20	> 10		
21	> 10		
SC-2-71	> 10		
Combretastatin	2.0 ± 0.1	99 ± 2	

the aniline nitrogen. Analogs **6**, **7**, and **17** will exert resonance effects, while the tetrafluoro analog **14** will have strong sigma bond induction on the aniline moiety. The net result is the same in each case – a reduction in the availability of the aniline's electron lone pair with a concomitant enhancement in acidity and an increase in NH hydrogen bond donating ability. Whether or not the increased tubulin affinity of these 4 molecules is caused by a more powerful aniline-tubulin hydrogen bond remains speculation at this point.

In addition to the tubulin/microtubule studies, it was necessary to investigate what kind of anti-proliferative effects these compounds have on living cells. As discussed in section 1.4, the human colon cancer cell line HCC-2998 is extremely sensitive to **SC-2-71**, and so this cell line was chosen as a model with which we would guide the anti-proliferative activity of the DHQZs. With this in mind, a growth inhibition assay of all 21 compounds was performed on the HCC-2998 line with Table 2.3B summarizing the results of this screen.

We were pleased to note that the results of the antiproliferation experiment paralleled those of the microtubule assays. With regard to substitutions on the A-ring, the 3-position was, in general, the least-well tolerated of any other position. The addition of functional groups at this position results in a 40 to 100 fold decrease in activity, regardless of the nature of the substitution. It seems that this position is very sensitive to substitution and should be avoided when designing future analogs.

Table 2.3B Anti-proliferative Activities of Analogs **1** – **21** on the Human Colon Cancer Cell Line HCC-2998

Compound	HCC-2998 GI_{50} (μM)	±	SD
1	43.2	±	2.3
2	> 100		
3	1.02	±	0.1
4	8.4	±	0.8
5	16.2	±	0.4
6	1.4	±	0.1
7	0.5	±	0.2
8	> 100		
9	97.8	±	7.5
10	10.7	±	1.2
11	6.4	±	0.4
12	17.3	±	4.3
13	11.2	±	1.6
14	9.2	±	0.6
15	>100		
16	>100		
17	8.4	±	1.5
18	>100		
19	90.4	±	27
20	99.3	±	8.4
21	21.5	±	1.5
SC-2-71	1.2	±	0.1
Combretastatin	< 0.1		

Compound **3**, which has a chlorine atom *para* to the aniline, and compound **7**, with the nitro group at the same position were the only two A-ring analogs to show improved activity over the lead **SC-2-71**. It is interesting that Lee and coworkers also observed a chlorine substitution at this R_5 position of a related DHQZ enhances the biological activity.[2,3] Even a methoxy at the R_5 position (analog **11**), while less active than it's unsubstituted counterpart, still retains significant activity. These results suggest that structural changes at this position are favorable and that future growth on this particular ring should be focused here.

The structural requirements of the B-Ring appear to be more rigid than that of the A-ring. In all cases, synthetic modifications resulted in a partial (analog **21**) or complete loss of activity. The antiproliferative results of compounds **18** – **20** reveal the critical role that the amide oxygen plays in the DHQZ binding affinity.

Table 2.3C Anti-proliferative Activities of Analogs **1** – **21** on the Human Microvascular Endothelial Cell Line (HMVEC) as a Model of Angiogenesis Inhibition

Compound	HMVEC GI_{50} (μM)	±	SD
1	15.1	±	2.8
2	> 100		
3	> 100		
4	10.8	±	0.7
5	8.6	±	0.9
6	9	±	0.6
7	0.7	±	0.04
8	> 100		
9	> 100		
10	10.2	±	0.9
11	0.8	±	0.1
12	10	±	0.9
13	nd		
14	10.9	±	0.9
15	nd		
16	>100		
17	7.1	±	0.6
18	>100		
19	76.2	±	6.2
20	>100		
21	> 100		
SC-2-71	1.2	±	0.02
Combretastatin	< 0.1		

As a model of how these compounds may inhibit the growth of new blood vessels during angiogenesis, we also evaluated the effects of the quinazolinones on the proliferation of blood vessel cells using human microvascular endothelial cells (HMVECs). Table 2.3C summarizes the activities of compounds **1** – **21**. Interestingly,

the results mirror those obtained in the HCC-2998 screen and the microtubule assays. With the exception of compound **3**, all the analogs that were inactive (GI_{50} = 50 μM or more) in one screen, are also inactive in the other. Similarly, the most active analog in all 4 assays was the same (**7**), and had very similar nanomolar level activity in both the anti-proliferation assays. Taken together, these two observations seem to implicate a tubulin-based mechanism of action for the dihydroquinazolinone inhibition of angiogenesis.

Based on the aforementioned SAR data, it seems that electron withdrawing groups (specifically nitro) at position R_5 of the A-ring seem to improve the activity of the lead **SC-2-71** across all the biological measurements that we took. While the correlation between compound **7**'s microtubule depolymerization, tritiated colchicine displacement, HCC-2998 growth inhibition and HMVEC growth inhibition do not align perfectly, there is a strong enough connection between these results to suggest that the nitro group of **7** interacts strongly with some aspect of the tubulin protein.

2.4 Chapter 2 References

1. Yale, H. J.; Kalkstein, M. Substituted 2,3-dihydro-4(1H)-quinazolinones. A new class of inhibitors of cell manipulation. *J. Med. Chem.* **1967**, *10*, 334 – 336.
2. Hamel, E.; Lin, C. M.; Plowman, J.; Wang, K. W.; Lee, K. H.; Paull, K. D. Antitumor 2,3-Dihydro-1-(aryl)-4(1H)-quinazolinone Derivatives. Interaction with Tubulin. *Biochemical Pharmacology*, **1996**, *51*, 53 – 59.
3. Hour, M. J.; Huang, L. J.; Kuo, S. C.; Xia, Y.; Bastow, K.; Nakanishi, Y.; Hamel, E.; Lee, K. H. 6-Alkylamino- and 2,3-Dihydro-3'-methoxy-2-phenyl-4-quinazolinones and Related Compounds: Their Synthesis, Cytotoxicity, and Inhibition of Tubulin Polymerization. *J. Med. Chem.* **2000**, *43*, 4479 – 4487.
4. Brossi, A.; Yeh, H. J.; Chrzanowska, M.; Wolff, J.; Hamel, E.; Lin, C. M.; Quinn, F.; Suffness, M.; Silverton, J. Colchicine and its analogues: recent findings. *Med. Res. Rev.* **1988**, *8*, 77 – 94.
5. Kuo, S. C.; Lee, H. Z.; Juang, J. P.; Lin, Y. T.; We, T. S.; Chang, J. J.; Lednicer, D.; Paull, K. D.; Lin, C. M.; Hamel, E.; Lee, K. H. Synthesis and cytotoxicity of 1,6,7,8- and 4'-substituted 2-phenyl-4-quinolones and related compounds: identification as antimitotic agenst interacting with tubulin. *J. Med. Chem*. **1993**, *36*, 1146 – 1156.
6. Li, L.; Wang, H. K.; Kuo, S. C.; Lednicer, D.; Lin, C. M.; Hamel, E.; Lee, K. H. 2',3',4',5',5,6,7-Substituted 2-phenyl-4-quinolones and related compounds: their synthesis, cytotoxicity, and inhibition of tubulin polymerization. *J. Med. Chem*. **1994**, *37*, 1126 – 1135.

7. Li, L.; Wang, K. H.; Kuo, S. C.; Wu, T. S.; Mauger, A.; Lin, C. M.; Hamel, E.; Lee, K. H. Synthesis and biological evaluation of 3',6',7-substituted 2-phenyl-4-quinolones as antimitotic antitumor agents. *J. Med. Chem*. **1994**, *37*, 3400 – 3407.

8. Xia, Y; Yang, Z. Y.; Xia, P.; Bastow, K. F.; Tachibana, Y.; Kuo, S. C.; Hamel, E.; Hackl, T.; Lee, K. H. Synthesis and biological evaluation of 6,7,2',3',4'-substituted-1,2,3,4-tetrahydro-2-phenyl-4-quinolones as a new class of antimitotic agents. *J. Med. Chem***. 1998***, 41,* 1155 – 1162.

9. Chen, K.; Kuo, S. C.; Hsih, M. C.; Mauer, A.; Linn, C. M.; Hamel, E.; Lee, K. H. 2',3',4',5,6,7-Substituted 2-phenyl-1,8-naphthyridin-4-ones: their synthesis, cytotoxicity, and inhibition of tubulin polymerization. *J. Med. Chem*. **1997**, *40*, 3049 – 3056.

10. Chen, K.; Kuo, S. C.; Hsih, M. C.; Mauger, A.; Lin, C. M.; Hamel, E.; Lee, K. . Synthesis and biological evaluation of substituted 2-aryl-1,8-naphthyridin-4(1H)-ones as antimitotic antitumor agents that inhibit tubulin polymerization*. J. Med. Chem.* **1997**, *40*, 3049 – 3056.

11. Xia, Y.; Yang, Z. Y.; Hour, M. J.; Kuo, S. C.; Xia, P.; Bastow, K. F.; Nakanishi, Y.; Nampoothiri, P.; Hackl, T.; Hamel, E.; Lee, K. H. Antitumor Agents. Part 204:1 Synthesis and biological evaluation of substituted 2-aryl quinazolinones. *Bioorg. Med. Chem. Lett.* **2001**, *11*, 9, 1193 – 1196.

12. Yale, H. J.; Kalkstein, M. Substituted 2,3-Dihydro-4(1H)-quinazolinones. A new class of inhibitors of cell multiplication*. J. Med. Chem.* **1967**, *10*, 334 – 336.

13. Neil, G. L.; Li, L.; Buskirk, H. H.; Moxlcy, T. E. Antitumor effects of the antispermatogenic agent, 2,3-dihydro-2-(1-napthyl)-4(1H)-quinazolinones. *Cancer Chemother.* **1972**, *56*, 163 – 173.

14. Jiang, J. B.; Hesson, D. P.; dusak, B. A.; Dexter, D. L.; Kang, G. J.; Hamel, E. Synthesis and biological evaluation of 2-styryl-quinazolin-4(3H)-ones, a new class of antimitotic anticancer agents which inhibit tubulin polymerization. *J. Med. Chem.* **1990**, *33*, 1721 – 1728.

15. Lin, C. M.; Kang, G. J.; Roach, M. C.; Jiang, J. B.; Hesson, D. P.; Luduena, R. F.; amel, E. Investigation of the mechanism of the interaction of tubulin with derivatives of 2-styrylquinazolin-4(3H)-one. *Mol. Pharmacol*. **1991**, *40*, 827 – 832.

16. Tobe, M.; Isobe, Y.; Tomizawa, H.; Nagasaki, T.; Takahashi, H.; Fukazawa, T.; Hayashi, H. Discovery of Quinazolines as a Novel Structural Class of Potent Inhibitors of NF-kB Activiation. *Bioorg. Med. Chem*. **2003**, *11*, 383 – 391.

17. Rogister, F.; Laeckmann, D.; Plasman, P. O.; Eylen, F.; Ghyoot, M.; Maggetto, C.; Liegeois, J. F.; Geczy, J.; Herchuelz, A.; Delarge, J.; Masereel, B. Novel inhibitors of the sodium-calcium exchanger: benzene ring analogues of N-guanidino substituted amiloride derivatives. Eur. J. Med. Chem. 2001, 36, 597 – 614.

18. Scheibye, S.; Pedersen, B. S.; Lawesson, S. O. Studies on organophosphorous compounds. XXI. The dimer of p-methoxyphenylthionophosphine sulfide as thiation reagent. A new route to thiocarboxamides. *Bull. Soc. Chim. Belg*. **1978**, *87*, 229 - 238.

19. Marxer, A.; Salzmann, U.; Hofer, F. Grignard reactions with haoalkylamines. 6. Aminoalkylation of quinoxalines and quinoxalones. *Helv. Chim. Acta*, **1971**, *54*, 8, 2507 – 2516.

20. Verdier-Pinard, P.; Lai, J. Y.; Yoo, H. D.; Yu, J.; Marquez, B.; Nagle, D. G.; Nambu, M.; White, J. D.; Falck, J. R.; Gerwick, W. H.; Day, B. W.; Hamel, E. Structure-activity analysis of the interaction of curacin A, the potent colchicine site antitmitotic agent, with tubulin and effects of analogues on the growth of MCF-7 breast cancer cells. *Mol. Pharmacol.* **1998**, *53*, 62-76.

Chapter 3 C-Ring and D-Ring Analogs

In chapter 2 we discussed the synthesis and evaluation of A- and B-ring analogs; this chapter will focus on modifications made to the biphenyl moiety. As before, we thought it prudent to survey the literature for related syntheses and SAR studies which may steer our experiments in an effective direction. To our knowledge, there have only been two relevant publications to date describing the antimitotic properties of DHQZ analogs with C-ring substitutions,[1,2] and none at all regarding D-ring analogs. The information therein indicates that C-ring alkoxy groups *ortho* to the D-ring may enhance the desired anti-tumor properties of our lead.[2]

Figure 3A Proposed C- and D-Ring Analogs

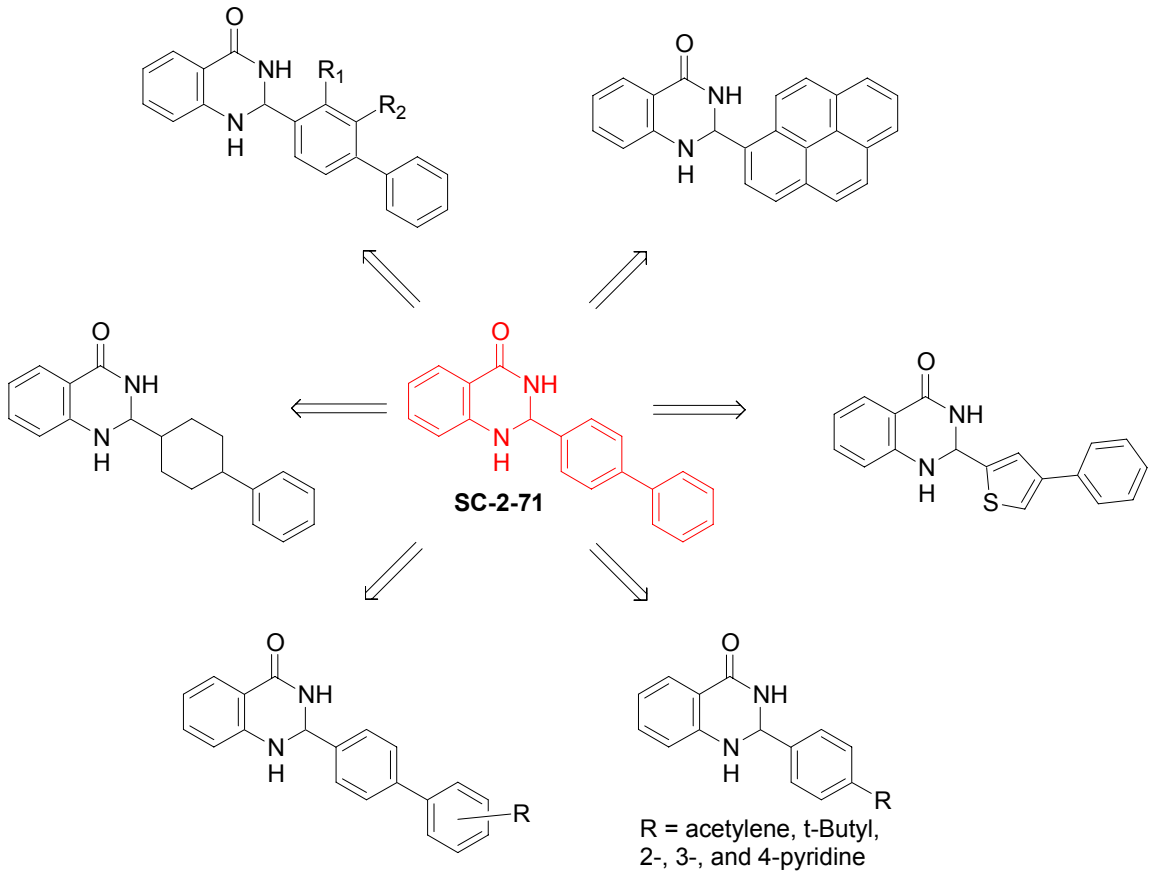

Figure 3A outlines the proposed structural modifications we intended to make to the biphenyl motif. Based on the results of Lee and coworkers[2] we were hopeful that a similar methoxy substitution would result in a favorable change in biological activity, yet we did not want to restrict the range of synthetic targets to that which has already been done. Details regarding the synthesis of the proposed C- and D- ring analogs are in the sections that follow (*vida infra*).

3.1 Synthesis of C-Ring Analogs

Due to a scarcity of appropriate starting materials, the synthesis of the first 8 C-ring analogs required 3 separate approaches to create the necessary aldehyde precursors (see Scheme 3.1A). In the first approach, aldehyde **26a** was made by a Suzuki-Miyaura[3] coupling of 4-formyl-3-fluoro-bromobenzene and phenylboronic acid. In a slightly more circuitous route, triflic anhydride was used in conjunction with various substituted phenols to make the aryl triflates **23b** – **25b**, and **27b – 29b**. The aryl triflates were then reacted with phenylboronic acid under the same Suzuki-Miyaura conditions to form **23a** – **25a** and **27a** – **29a**. In order to make the aldehyde **22a**, we chose to employ the *ortho*-directed lithiation of 4-biphenylcarboxaldehyde.[4] Briefly, this reaction derives its *ortho*-directing ability by initial addition of the N,N,N'-tetramethylethylenediamine anion to the aldehyde to form a hemiaminal. The lone pair of the dimethylamine moiety is believed to coordinate with a lithium cation of another equivalent of butyllithium, thus directing it to deprotonate *ortho* to the aldehyde. The resulting aryl anion was reacted with methyl iodide to form aldehyde **22a**. Each of the aforementioned aldehydes was then cyclized with anthranilamide and a catalytic amount of acid to form DHQZ derivatives **22** – **29**.

Scheme 3.1A Synthesis of C-Ring Analogs **22** – **29**

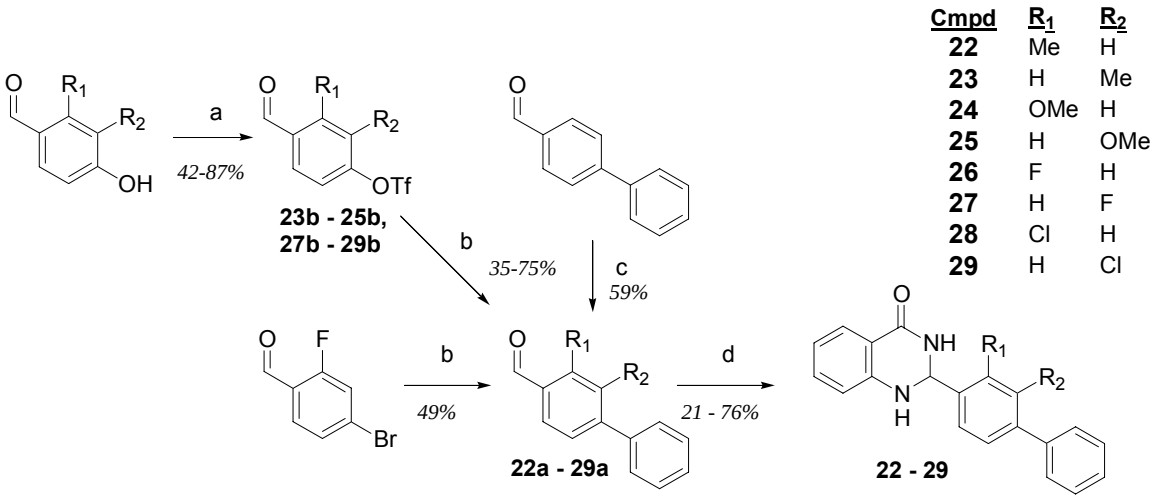

a) Trifluoromethanesulfonic anhydride, pyridine, DCM b) phenylboronic acid, Cs_2CO_3, $Pd(PPh_3)_4$, DME/H_2O
c) *i.* N,N,N'-trimethylethylene diamine, BuLi, benzene *ii.* BuLi *iii.* MeI, -40^oC d) anthranilamide, AcOH, MeCN

The next analog we wished to explore was a cyclohexyl isostere of the C- phenyl ring. Synthesis of the cyclohexane substituted analog **30** was accomplished in 4 steps, beginning with the commercially available 4-phenylcyclohexanone (see Scheme **3.1B**). Wittig olefination[5] provided the expected alkene **30c**, which was then oxidized to the primary alcohol **30b** upon treatment with borane/H_2O_2. As expected, this reaction

Scheme 3.1B Synthesis of C-Ring Analog **30**

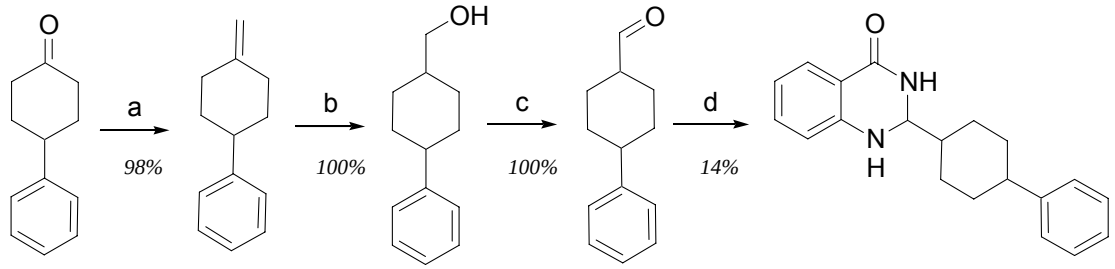

a) Ph_3PMeBr, BuLi, THF b) BH_3, NaOH, H_2O_2, THF c) $(COCl)_2$, DMSO, TEA, DCM, -55 ^oC
d) anthranilamide, MeCN, AcOH (cat.)

proceeded with high regioselectivety in favor of the primary alcohol. Subsequent Swern[6] oxidation provided the aldehyde **30a** which was easily converted by the usual protocol to the target **30**.

The synthesis of analog **31** was done in 2 steps. The bromothiophene derivative shown in Scheme 3.1C was subject to Suzuki-Miyaura[3] conditions and successfully coupled to phenylboronic acid. The resulting aldehyde **31a** was then reacted with anthranilamide to form the DHQZ analog **31**.

Scheme 3.1C Synthesis of C-Ring Analog **31**

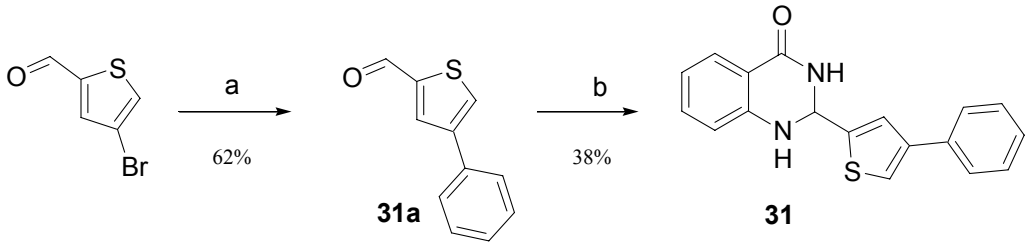

a) $PhB(OH)_2$, Cs_2CO_3, $Pd(PPh_3)_4$, DME/H_2O b) anthranilamide, MeCN, AcOH (cat.).

3.2 Synthesis of D-Ring Analogs

As mentioned earlier, no syntheses or SAR information is available in the literature which deals with the DHQZ D-ring. It was this absence of information, together with the large commercial availability of compatible chemicals, which prompted us to explore the D-ring analogs **32** – **55**. Each compound was made through the same general approach – Suzuki coupling of a substituted aryl bromide with the commercially available 4-formylphenyl boronic acid to form intermediate aldehydes **32a** – **55a** (see Scheme 3.2A), followed by the standard anthranilamide cyclization procedure to form the molecules of interest, **32** – **55**.

Scheme 3.2A Synthesis of D-Ring Analogs **32 - 55**

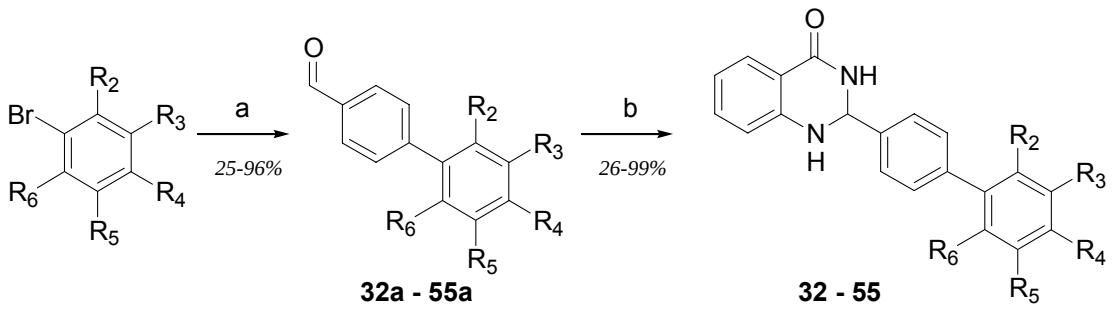

	R2	R3	R4	R5	R6		R2	R3	R4	R5	R6
32	Cl	H	H	H	H	**44**	Me	H	H	H	Me
33	H	Cl	H	H	H	**45**	Ac	H	H	H	H
34	H	H	Cl	H	H	**46**	H	Ac	H	H	H
35	OMe	H	H	H	H	**47**	H	H	Ac	H	H
36	H	OMe	H	H	H	**48**	Ph	H	H	H	H
37	H	H	OMe	H	H	**49**	H	Ph	H	H	H
38	NO_2	H	H	H	H	**50**	H	H	Ph	H	H
39	H	NO_2	H	H	H	**51**	CF_3	H	H	H	H
40	H	H	NO_2	H	H	**52**	H	CF_3	H	H	H
41	Me	H	H	H	H	**53**	H	H	CF_3	H	H
42	H	Me	H	H	H	**54**	F	F	F	F	F
43	H	H	Me	H	H	**55**	CH_2OH	H	H	H	H

a) 4-formylphenylboronic acid, $Pd(PPh_3)_4$, Cs_2CO_3, DME/H_2O b) anthranilamide, MeCN, AcOH (cat.)

In a related procedure, the D-ring analogs **56** – **58** were also realized in two steps each (see Scheme 3.2B). Rather than having a substituent on a phenyl ring, these molecules incorporate a nitrogen at one of three locales in the D-ring, thus forming the 2-, 3-, and 4- pyridine derivatives. Aldehydes **56a** – **58a** were made by Suzuki[3] coupling of 4-formylphenylboronic acid and the corresponding bromopyridine. Each of these aldehydes was then uneventfully cyclized to form DHQZ analogs **56** – **58**.

Scheme 3.2B Synthesis of D-Ring Analogs **56 - 58**

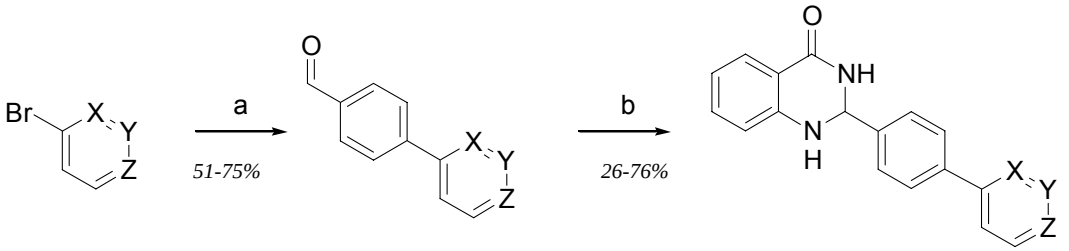

56a - 58a

	X	Y	Z
56	N	CH	CH
57	CH	N	CH
58	CH	CH	N

a) 4-formylphenylboronic acid, $Pd(PPh_3)_4$, Cs_2CO_3, DME/H_2O b) anthranilamide, MeCN, AcOH (cat.)

The last analogs made in this SAR study were the D-ring derivatives **59** and **60**. When **SC-2-71** was first discovered, it was observed that this aromatic D-ring played an important role in the biological activity we observed. It seemed prudent to explore phenyl ring isosteres – in this case, replacement of the outermost ring with an acetylene group and a ^{t}butyl group. Each of these functionalities possesses similar dimensions and electronic properties as a benzene ring, and so the simple, one-step syntheses outlined in Scheme 3.2C were carried out.

Scheme 3.2C Synthesis of D-Ring Analogs **59 - 60**

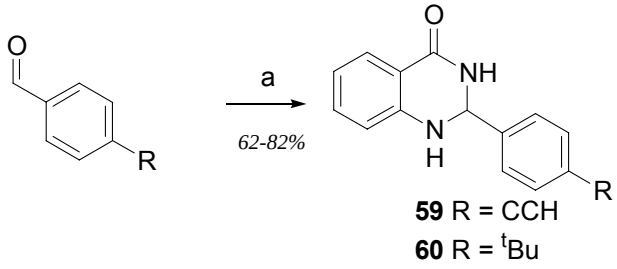

59 R = CCH
60 R = ^{t}Bu

a) anthranilamide, MeCN, AcOH (cat.)

3.3 Biological Evaluation and SAR Conclusions

The ability of these C- and D- ring analogs to trigger the disassembly of the tubulin polymer was measured in two different assays (see Table 3.3A). In the first assay, the percentage of preformed microtubules that were depolymerized in the presence of 15 μM of drug was measured.[7] In a similar assay, the concentration of drug necessary to inhibit the formation of microtubules from a solution of α and β tubulin subunits was measured.[8] If a compound was found to have an IC_{50} less than 10 micromolar in this latter assay, it was further analyzed in a competitive binding experiment with radioactive (tritiated) colchicine.[9]

Compounds **22 – 31** represent the extent of C-ring substitutions that were synthesized for this SAR study. Analysis of this data indicates that position R_2 is a favorable site for substitutions. Analogs **23** and **29** (having a methyl and chloro, respectively) enhance the tubulin binding activity significantly in comparison to **SC-2-71** (see Table 3.3A). As there are not any strong electronic properties associated with these functional groups, this observed increase in activity may be due to the orthogonal torsion angle that is imposed upon the biphenyl system by the presence of these atoms.

With consideration to the D-Ring analogs that were tested, we notice that the changes associated with compounds **32**, **41**, and **51** caused an improvement in the microtubule disrupting abilities. Interestingly, these molecules each have a substituent at the same position on the D-ring (position R_2) which occupies nearly the exact same chemical space as the 2 favorable C-ring analogs (**23** and **29**) that were discussed in the previous paragraph. As for the rest of the D-ring analogs shown, we generally observe a dramatic or complete loss in microtubule activity when there are functional groups

present anywhere else on the D-ring. Since electron withdrawing, donating, and neutral functional groups at positions R_3 and R_4 essentially abolish activity, it appears that the active site in which these drugs are binding may be imposing a steric restriction at these positions.

Table 3.3A C-Ring and D-Ring Analogs' Microtubule Depolymerization, Inhibition of Tubulin Polymerization, and Displacement of Tritiated Colchicine

Compound	Microtubule % Depolymerization (@ 15μM)	IC_{50} Tubulin Polymerization (μM)	^{3}[H] Colchicine Displacement 5 μM ± SD	50 μM ± SD
22	82	>10		
23	100	2.3 ± 0.1	35 ± 2.8	81 ± 0.9
24	0	>10		
25	70	>10		
26	70	>10		
27	55	>10		
28	0	>10		
29	100	3.6 ± 0.2	11 ± 5	49 ± 1.8
30	< 50	>10		
31	< 15	>10		
32	100	0.53 ± 0.02	27 ± 2.9	45 ± 1.7
33	N/D	>10		
34	N/D	>10		
35	25	>10		
36	0	>10		
37	0	>10		
38	< 95	>10		
39	0	>10		
40	0	>10		
41	100	0.76 ± 0.01	33 ± 3.3	60 ± 2.8
42	25	>10		
43	90	>10		
44	< 70	>10		
45	0	>10		
46	0	>10		
47	0	>10		
48	0	>10		
49	0	>10		
50	0	>10		
51	95	9.5 ± 0.5		10 ± 12
52	0	>10		
53	0	>10		
54	< 44	>10		
55	0	>10		
56	N/D	>10		
57	0	>10		
58	0	>10		
59	N/D	>10		
60	0	>10		
SC-2-71	> 50	>10		
Combretastatin	N/D	2.0 ± 0.1	99 ± 2	
Colchicine	100	< 0.1		

In the HCC-2998 anti-proliferation assay shown in Table 3.3B, we see a similar trend as that in the aforementioned microtubule experiments. Three compounds (**23**, **32**, and **41**) demonstrated an increased ability to prevent cell growth when compared to the lead **SC-2-71**. It should be noted that these three analogs also showed improvements in the microtubule assays of Table 3.3A.

In table 3.3C, we see the results of the anti-proliferation experiments of compounds **22** – **60** on the HMVEC cell line. In this assay, we observe an improvement over the lead with analogs **23**, **29**, **32**, and **41**. Again, these "more active" compounds are the same ones highlighted in the microtubule experiments and in the HCC-2998 anti-proliferation assay. Since the HMVECs are not a cancerous cell line, we did not necessarily expect such a strong degree of correlation to exist between this

Table 3.3B Anti-proliferative Activities of Analogs **22** – **60** on the Human Colon Cancer Cell Line HCC-2998

	HCC-2998
Compound	**GI_{50} (μM) ± SD**
22	6.05 ± 0.8
23	<0.1
24	47.4 ± 3.3
25	6.79 ± 0.6
26	7.02 ± 0.6
27	6.67 ± 0.4
28	21.5 ± 1.5
29	2.18 ± 0.5
30	10.24 ± 0.9
31	>100
32	0.67 ± 0.03
33	>100
34	2.8 ± 1.1
35	21.9 ± 8.1
36	>100
37	>100
38	8.16 ± 0.7
39	>100
40	>100
41	0.77 ± 0.1
42	1.76 ± 0.1
43	5.2 ± 0.7
44	43.5 ± 10.4
45	61.7 ± 14.5
46	>100
47	>100
48	23.9 ± 6.1
49	>100
50	>100
51	5.58 ± 0.45
52	>100
53	>100
54	14.3 ± 3.5
55	52.9 ± 5.6
56	88.1 ± 21.6
57	>100
58	>100
59	>100
60	>100
SC-2-71	1.2 ± 0.1
Combretastatin	< 0.1
Colchicine	< 0.1

assay and the HCC-2998 assay. Before considering the significance of this parallel in activity, we wanted to see whether or not there was a statistically strong link. Figure 3.3A graphically plots the GI_{50} values of the HCC-2998 assay versus those of the HMVEC assay for compounds **22** - **60**. As indicated, when a regression line is added to the plot, we observe an R^2 value of 0.902.

As mentioned the Chapter 1, there are many possible mechanisms through which small molecules are known to modulate angiogenesis - for example, by interaction with VEGF, FGF, or other growth factors. To the best of our knowledge, dihydroquinazolinones are a new class of anti-angiogenic compound, and so their mechanism of angiogenesis inhibition is currently unknown. Because the HMVEC results very closely mirror the results obtained in the HCC-2998 assay, we can raise the possibility of a tubulin-based

Table 3.3C Anti-proliferative Activities of Analogs **22** – **60** on the Human Microvascular Endothelial Cell (HMVEC) Line

	HMVEC
Compound	**GI_{50} (μM) ± SD**
22	7.2 ± 0.6
23	0.2 ± 0.3
24	20.4 ± 0.4
25	6.4 ± 0.5
26	7.1 ± 0.5
27	6.3 ± 0.6
28	8.2 ± 0.9
29	1.1 ± 0.1
30	6.54 ± 0.4
31	>100
32	0.77 ± 0.1
33	>100
34	7.77 ± 0.6
35	9.51 ± 0.6
36	>100
37	>100
38	>100
39	>100
40	>100
41	0.73 ± 0.1
42	2.95 ± 0.2
43	8.42 ± 0.4
44	9.26 ± 0.3
45	21 ± 0.8
46	>100
47	>100
48	9.27 ± 0.4
49	>100
50	>100
51	7.6 ± 0.4
52	>100
53	>100
54	3.11 ± 0.1
55	18.7 ± 1.5
56	78 ± 8.2
57	>100
58	>100
59	>100
60	>100
SC-2-71	1.2 ± 0.02
Combretastatin	< 0.1
Colchicine	< 0.1

mechanism for the DHQZ inhibition of angiogenesis. Rather than interfere with one of the proteins or molecules involved in the angiogenesis signaling cascade, it is possible that **SC-2-71** and its analogs may be interacting downstream of these events by interacting with the microtubules of the microvascular endothelial cells and inducing apoptosis in the newly forming blood vessels. Although this is only conjecture at this point, the correlation that exists between the tubulin/microtubule assays and the inhibition of cellular blood vessel growth is very suggestive.

Figure 3.3A Correlation Plot of HMVEC vs. HCC-2998 GI_{50} Values

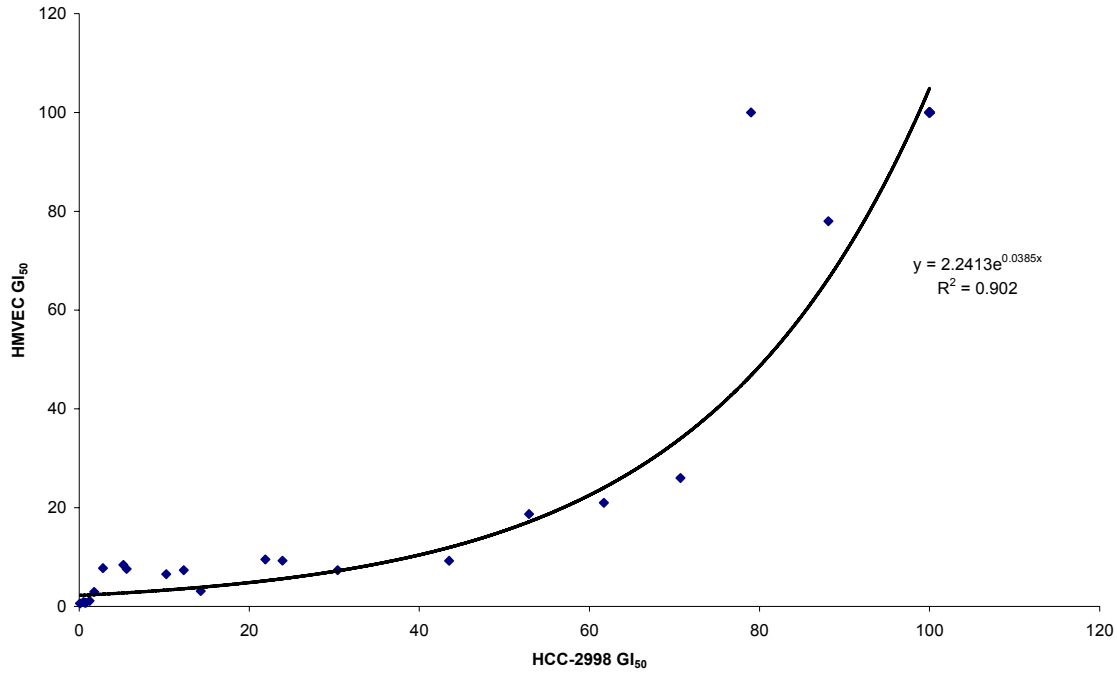

In summary, we have designed and synthesized almost 40 analogs based on the C and D rings of our lead molecule, **SC-2-71**. Biological testing of these compounds confirms that they have a destabilizing effect on microtubules and are able to competitively displace radiolabelled colchicine from β-tubulin. Further, we have demonstrated the potent cytotoxic effect these compounds have on the human colon

cancer cell line HCC-2998 as well as their ability to prevent angiogenesis (they inhibit the growth of HMVEC cells), thus giving them a dual action mechanism of cancer inhibition similar to that of combretastatin. The results of Chapters 2 and 3 have laid the groundwork for the development of a next generation of more active DHQZs.

3.4 Chapter 3 References

1. Hamel, E.; Lin, C. M.; Plowman, J.; Wang, K. W.; Lee, K. H.; Paull, K. D. Antitumor 2,3-Dihydro-1-(aryl)-4(1H)-quinazolinone Derivatives. Interaction with Tubulin. *Biochemical Pharmacology*, **1996**, *51*, 53 – 59.
2. Hour, M. J.; Huang, L. J.; Kuo, S. C.; Xia, Y.; Bastow, K.; Nakanishi, Y.; Hamel, E.; Lee, K. H. 6-Alkylamino- and 2,3-Dihydro-3'-methoxy-2-phenyl-4-quinazolinones and Related Compounds: Their Synthesis, Cytotoxicity, and Inhibition of Tubulin Polymerization. *J. Med. Chem.* **2000**, *43*, 4479 – 4487.
3. Miyaura, N.; Yamada, K.; Suzuki, A. A new stereospecific cross-coupling by the palladium-catalyzed reaction of 1-alkenylboranes with 1-alkenyl or 1-alkynyl halides. *Tet. Lett.* **1979**, *36*, 3437-40.
4. Comins, D. L.; Brown, J. D.; Ortho substitution of m-anisaldehyde via alpha-amino alkoxide directed lithiation. *J. Org. Chem*. **1989**, *54*, 15, 3730 – 3732.
5. Wittig, G.; Geissler, G. *Liebigs Ann. Chem*., **1953**, *580*, 44 – 57.
6. Omura, K.; Swern, D. Oxidation of alcohols by "activated" dimethyl sulfoxide. A preparative, steric and mechanistic study. *Tetrahedron*, **1978**, *34*, 11, 1651 – 1660.
7. Rao, P. N., Cessac, J.W. Tinley, T.L. and Mooberry, S.L**.** Synthesis and antimitotic activity of novel 2-methoxyestradiol analogs. *Steroids.* **2002,** *67*, 1079-1089.
8. Li, L.; Wang, H. K.; Kuo, S. C.; Wu, T. S.; Mauger, A.; Lin, C. M.; Hamel, E.; Lee, K. H. Synthesis and biological evaluation of 3′,6′,7-substituted 2-phenyl-4-quinolones as antimitotic antitumor agents. *J. Med. Chem.* **1994**, *37*, 3400-3407.

9. Verdier-Pinard, P.; Lai, J. Y.; Yoo, H. D.; Yu, J.; Marquez, B.; Nagle, D. G.; Nambu, M.; White, J. D.; Falck, J. R.; Gerwick, W. H.; Day, B. W.; Hamel, E. Structure-activity analysis of the interaction of curacin A, the potent colchicine site antitmitotic agent, with tubulin and effects of analogues on the growth of MCF-7 breast cancer cells. *Mol. Pharmacol.* **1998**, *53*, 62-76.

Chapter 4: Third Generation Hybrid Molecule

Having produced data for sixty 2nd generation analogs of **SC-2-71**, we were now well positioned to use these results to make marked improvements to the potency of these DHQZs. To do so, we planned to incorporate the structural features of two of our more successful analogs from the SAR study into one molecule. Using the HCC-2998 anti-proliferative data generated in Tables 2.3B and 3.3B, we recall that analogs **7** and **41** have GI_{50} values of 770 nM and 530 nM, respectively. These represent significant improvements in activity over the lead, and so it was our intention to create a hybrid molecule with a nitro group *para* to the aniline and a methyl group at R_2 of the D-ring (see Figure 4A). If we were to achieve a synergistic effect by this strategy, it would not be unreasonable to expect a compound exhibiting low to sub-nanomolar growth inhibition.

Figure 4A Design of 3rd Generation Drug

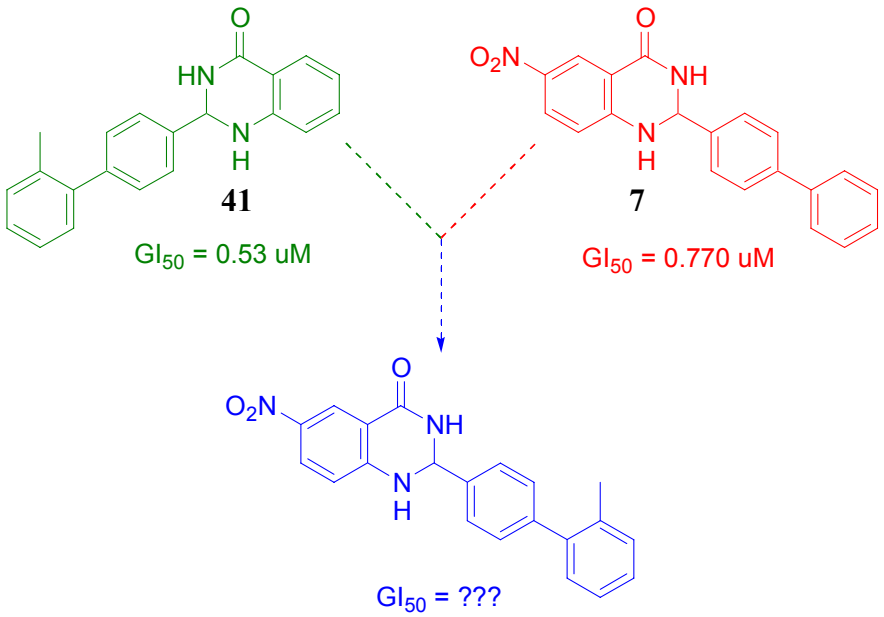

4.1 Synthesis of GMC-5-193

The target dihydroquinazolinone was easily prepared in 3 steps beginning with the Suzuki coupling of 4-formylphenylboronic acid with 2-bromotoluene to form the aldehyde **61a** (see scheme 4.1A). The aldehyde was reacted with 5-nitroanthranilamide (compound **7a**, prepared in Section 2.1) in the standard DHQZ protocol to form 3rd generation analog **61**.

Scheme 4.1A Synthesis of Compound **61**

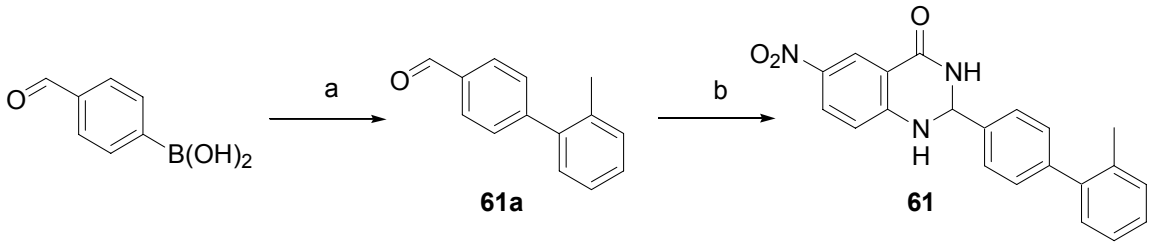

a) 2-bromotoluene, Cs_2CO_3, $Pd(PPh_3)_4$, DME/H_2O, 90 ^oC b) 5-nitroanthranilamide (**7a**), MeCN, AcOH (cat.), reflux

4.2 Biological Testing

Having successfully isolated the desired DHQZ analog, we next needed to evaluate the effectiveness of this compound in biological systems. In order to make an useful comparison to **SC-2-71**, we would need to subject this analog to the same battery of assays as the lead compound.

Figure 4.2A shows the results for **61** in the National Cancer Institute's 60-cell line screen. Particularly striking is the sensitivity of all the leukemia cell lines to this analog. This is an interesting reversal of cancer selectivety considering **SC-2-71** was most effective at inhibiting the growth of colon cancer cells. Analog **61** also appears to be quite successful in preventing the proliferation of cancerous renal cells: we note GI_{50}

values of 1 μM or less in 6 out of 8 renal cell lines. This is a particularly valuable observation when one considers that there are currently no effective chemotherapy options for cancers of the kidney.[1] With regard to the other cell lines in this assay, we are encouraged to note that the GI_{50} values for this compound are in the nanomolar range for a majority of the tested lines.

Figure 4.2A National Cancer Institute's (NCI) 60-Cell Line Screen of **61**

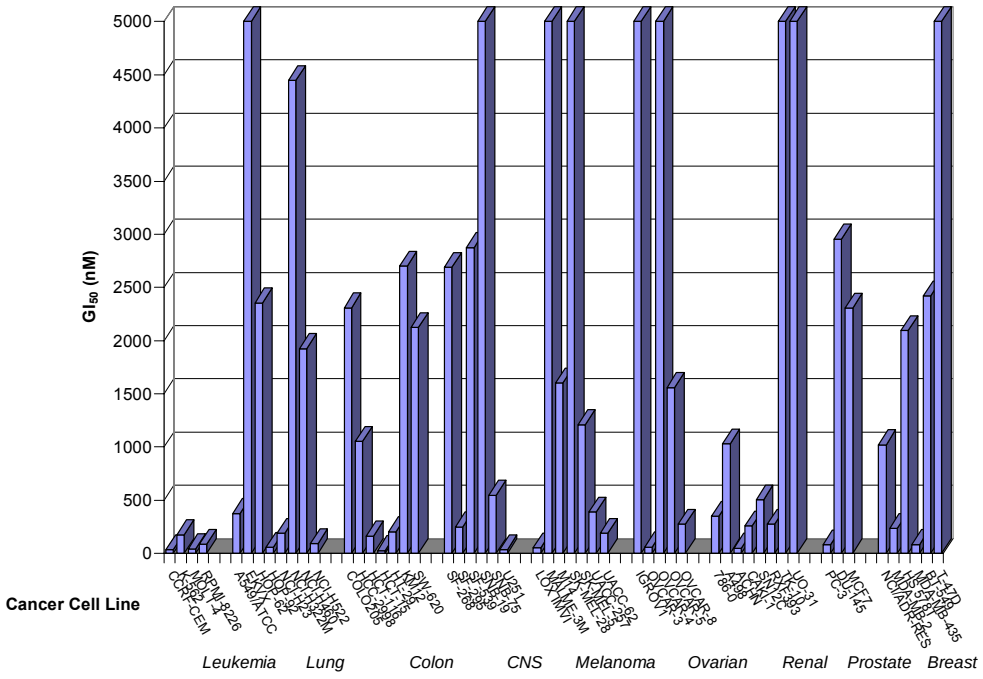

Since one of the goals of this project was to enhance the activity of the lead DHQZ, we were interested in making a head-to-head comparison of the 60 cell line data for **SC-2-71** and **61**, as depicted in Figure 4.2B. As we had anticipated, this 3rd generation analog is significantly more effective at controlling the growth of human cancer cells than its parent compound. It seems that the strategy of incorporating

structural features of successful 2nd generation analogs is a valid approach in this particular system.

Figure 4.2B Comparison of **SC-2-71** and **61** in the NCI 60-Cell Line Screen

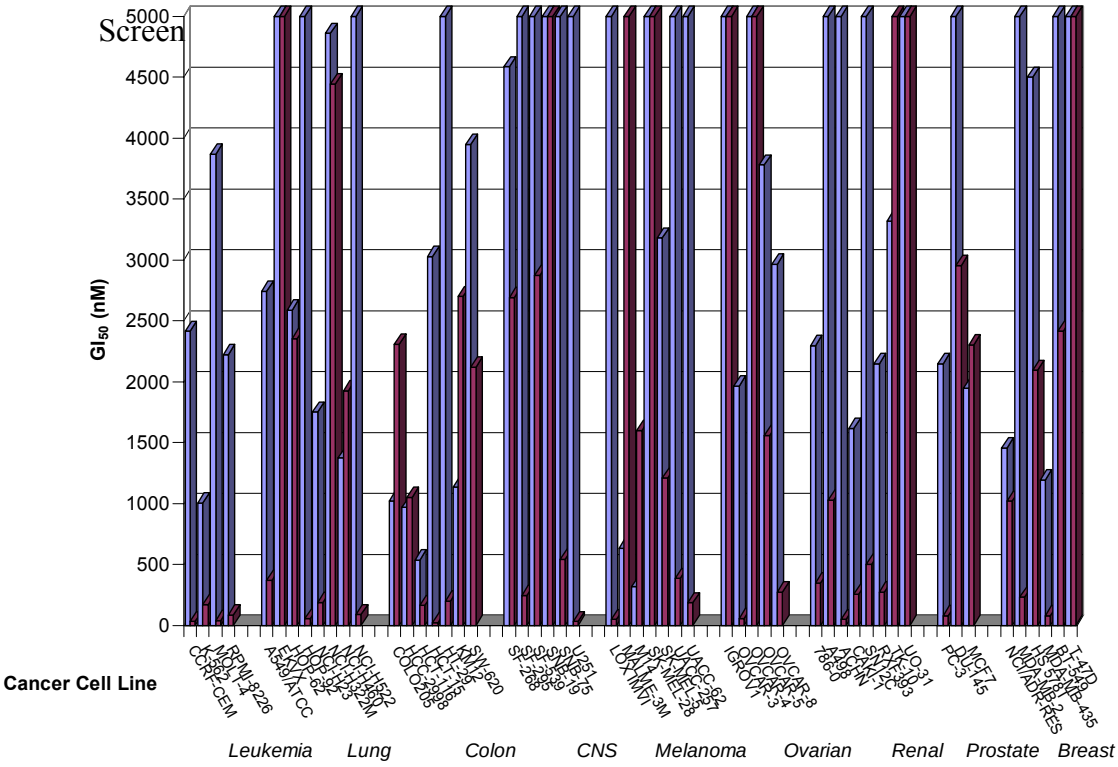

(Blue = Data for **SC-2-71,** Purple = Data for **61)**

We next wanted to measure the inhibitory effects of **61** upon tubulin and microtubules. As Table 4.2A indicates, there is a marked increase in the ability of **61** to depolymerize microtubules and displace tritiated colchicine from tubulin, although these DHQZs are still unable to displace colchicine to the degree that combretastatin can. This apparent lack of affinity for the colchicine site does not necessarily suggest a lack of potency – indeed, as the data presented in Figures 4.2A and 4.2B indicate, this compound is a powerful anti-proliferative agent. These seemingly contradictory results may, in fact,

merely be indicative of a ligand-protein interaction that only sees partial overlap of the DHQZ with the defined "colchicine site".[2] In fact, the DHQZs are also known to displace tritiated vinblastine from the adjacent vinca site of tubulin,[3] an issue we will revisit in chapter 6.

Table 4.2A Tubulin Polymerization Inhibition and Tritiated Colchicine Displacement for **61** and Reference Compounds

Compound	IC_{50} Tubulin Polymerization (μM)	^{3}[H] Colchicine Displacement 5 μM ± SD	50 μM ± SD
61	4.0 ± 0.6	18 ± 9	37 ± 1.4
SC-2-71	>10		
Combretastatin	2.0 ± 0.1	99 ± 2	
Colchicine	< 0.1		

Tables 4.2B and 4.2C show the growth inhibitory effects of **61** on the HCC-2998 and HMVEC cell lines, respectively. With regard to the former, the GI_{50} value was below the limits of detection for this particular experiment. In this case, we know that the true value is less than 100 nM - this represents at least a 10-fold improvement over the lead. The results of the HMVEC assay were more definitive than the previous experiment. As indicated, **61** is a strong inhibitor of human blood vessel proliferation.

Table 4.2B Anti-proliferation Assay of **61** on HCC-2998 Cell Line

Compound	HCC-2998 GI_{50} (μM) ± SD
61	< 0.1
SC-2-71	1.2 ± 0.1
Combretastatin	< 0.1
Colchicine	< 0.1

Table 4.2C Anti-proliferation Assay of **61** on HMVEC Cell Line

Compound	HMVEC GI_{50} (μM) ± SD
61	0.61 ± 0.03
SC-2-71	1.2 ± 0.02
Combretastatin	< 0.1
Colchicine	< 0.1

Having achieved such significant potency and having gathered a relatively large amount of biological data regarding

the mechanism and properties of **61**, we thought it appropriate to begin *in vivo* investigations of this molecule.

4.3 *In Vivo* Testing

An important measurement of a potential new pharmaceutical is its toxicity to living beings. If a drug is able to destroy a virus, bacteria, or tumor while simultaneously causing great harm or death to the patient, it will obviously be of limited to no therapeutic value. The most common method used to estimate the toxicity of a compound is by observing its effects upon an animal while determining the maximum tolerated dose (MTD). The International Union of Pure and Applied Chemistry (IUPAC)[4] defines the maximum tolerated dose as a

"…high dose used in chronic toxicity testing that is expected on the basis of an adequate subchronic study to produce limited toxicity when administered for the duration of the test period. It should not induce (a) overt toxicity, for example appreciable death of cells or organ dysfunction, or (b) toxic manifestations that are predicted materially to reduce the life span of the animals except as the result of neoplastic development or (c) 10 % or greater retardation of body weight gain as compared with control animals. In some studies, toxicity that could interfere with a carcinogenic effect is specifically excluded from consideration."

A group of 5 mice was used in this experiment – two were designated as the control group and received only the drug carrier (peanut oil), while the remaining three received the carrier plus 400 mg/kg of compound **61**. Carrier and/or drug was administered orally (po) once per day (qd) over a 5 day period.

Table 4.3A Daily Mouse Weights in the Maximum Tolerated Dose Study of **61**

Dose	Gross Weight (% loss)				
	Day 1	***Day 2***	***Day 3***	***Day 4***	***Day 5***
Vehicle (N=2)	28 g	27.2 g (-2.9%)	27.4 g (-2.1%)	27 g (-3.6%)	26.3 g (-6.2 %)
400 mg/kg (N=3)	35 g	34.2 g (-2.3%)	34.4 g (-1.8%)	34.5 g (-1.4%)	34.8 g (-0.6%)

%loss calculated as day x weight/day 1 weight X 100.
drug administered po and dosed QD x 5 days

During the course of the experiment, no obvious external signs of toxicity were observed in the mice (eg – erratic behavior, decrease in grooming, hair loss, etc…). As Table 4.3A indicates, by the end of the experiment there was actually an *increase* in the collective weight of the experimental group relative to the control group. From this experiment we may conclude that we have not yet been reached the MTD for **61**, even at the relatively high dose of 400 mg/kg. We must be cautious in interpreting these results, however, due to the relatively short duration of the experiment (the most commonly used MTD studies last 4 weeks). For the sake of comparison, other MTD values of more

Table 4.3B Relative MTD Values of **61** and Some Common Pharmaceuticals

Compound	Animal Model	MTD (mg/kg/day)
Nicotine	Rats	0.8
Sildenafil (Viagra)	Mice	10
Taxol (Paclitaxel)	Mice	20
5-Fluorouracil	Mice	100
Combretastatin-4-phosphate	Mice	800
Ibuprofen	Rats	240
61	*Mice*	*> 400*

familiar compounds are listed in Table 4.3B.[5-7] To provide an even broader perspective of toxicities, Table 4.3C lists some estimated lethal dose levels in humans for some well known substances.[8]

Table 4.3C Estimated Lethal Dose for Some Common Substances

	Probable Oral Lethal Dose for Humans (mg drug/kg of body weight)	Relative Toxicity Range
		practically nontoxic (above 15 g/kg)
Ethyl Alcohol	10,000	slightly toxic (5-15 g/kg)
Sodium Chloride	4,000	moderately toxic (0.5 – 5 g/kg)
Phenobarbitol	150	very toxic (50-500 mg/kg)
Parathion	7	extremely toxic (5-50 mg/kg)
Strychnine	2	super toxic (less than 5 mg/kg)
Nicotine	1	
Tetrodoxin	0.01	
Botulinus Toxin	0.00001	

Armed with the above information regarding the tolerable dosage of **61** in murine models, we were now ready to determine how efficacious this drug is at treating tumors in mice. Accordingly, we performed a mouse tumor xenograft study of **61**. A group of 3 syngeneic nude mice were injected with B-16 melanoma. From that point on, one mouse went untreated while the cancer was allowed to grow and spread unchecked. Two of the mice, however, were intravenously treated with 4.5 mg/kg of **61** (a relatively small dosage in light of our MTD findings) once every other day for 11 days. At the end of the 11^{th} day, all three mice were sacked and their lungs isolated for analysis, as shown in figure 4.3A. In the control mouse with no drug protection (left column), we notice the effects of uncontrolled proliferation of cancer – several tumors are clearly visible on the exterior of the lung while the lung tissue itself has taken on a dark red, diseased hue. In contrast, the 2 mice that were dosed with **61** (middle and right columns) look

comparatively healthy – the lung tissue appears to be a normal color and texture, while the number of visible tumors has dramatically lessened.

Figure 4.3A B-16 Melanoma Metastatic Lung Model with Compound **61**

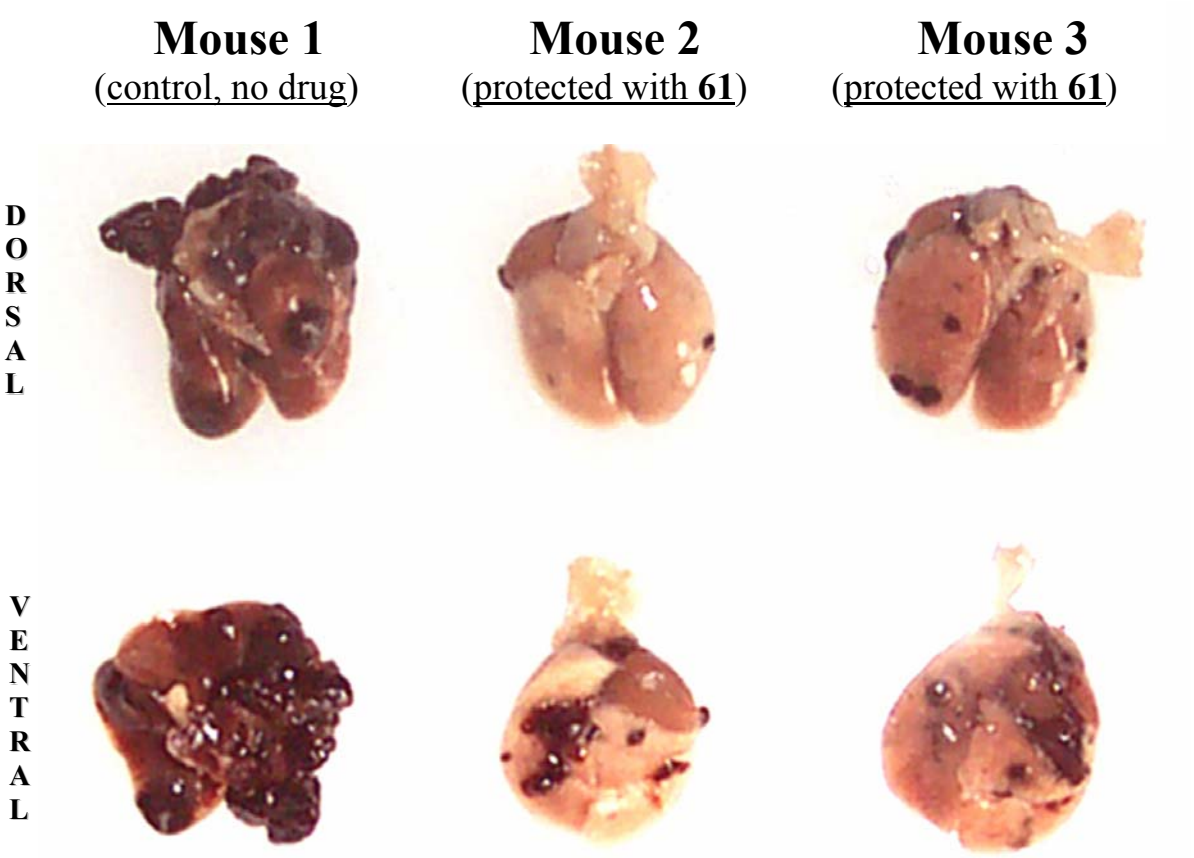

Intravenous dosing of **61** done @ 4.5 mg/kg qd, every other day for 11 days.

In conclusion, we have shown that compound **61** is an extremely potent anti-proliferative agent for a variety of cancerous cell lines. In addition, it retains the angiogenic inhibitory activity that its predecessor DHQZs displayed as is evident from the nanomolar level GI_{50} values measured in the HMVEC cell line. Furthermore, as a

result of our MTD study we have shown compound **61** to be remarkably non-toxic. Finally, our tumor xenograft study clearly demonstrates that **61** is both bio-available and efficacious in treating tumors *in vivo*.

4.4 Chapter 4 References

1. The National Cancer Institute Kidney Cancer Treatment Webpage. http://web.ncifcrf.gov/research/kidney/intro.html (accessed July 2006).
2. Ravelli, R. B., Gigant, B.; Curmi, P. A.; Jourdain, I.; Lachkar, S.; Sobel, A.; Knossow, M. Insight into tubulin regulation from a complex with colchicine and a stathmin-like domain. *Nature*, **2004**, *428*, 198 – 202.
3. Hamel, E.; Lin, C. M.; Plowman, J.; Wang, H. K.; Lee, K. H.; Paull, K. D. Antitumor 2,3-Dihydro-2-(aryl)-4(1H)-quinazolinone Derivatives. Interactions with tubulin. *Biochem. Pharmac.* **1995**, *51*, 53 – 59.
4. International Union of Pure and Applied Chemistry. http://www.iupac.org/dhtml_home.html (accessed July, 2006).
5. Codacci-Pisanelli, G.; Van der Wilt, C. L.; Smid, K. Noordhuis, P.; Voorn, D.; Pinedo, H. M.; Peters, G. J. High-Dose 5-Fluorouracil with Uridine-Diphosphoglucose Rescue Increases Thymidylate Synthase Inhibition but Not 5-fluorouracil Incorporation into RNA in Murine Tumors. *Oncology*, **2002**, *62*, 4.
6. Kim, S. C.; Kim, D. W.; Shim, Y. H.; Bang, J. S.; Oh, H. S.; Kim, S. W.; Seo, M. H. In vivo evaluation of polymeric micellar paclitaxel formulation: toxicity and efficacy. *J. Controlled Rel.* **2001**, 72, 191 – 202.
7. RxList - The internet drug index. http://www.rxlist.com/cgi/generic/viagra_wcp.htm (accessed July 2006).
8. Johns Hopkins Bloomberg School of Public Health. http://ocw.jhsph.edu/courses/EnvironmentalHealth/PDFs/Lecture9.pdf (accessed July 2006).

Chapter 5: Dihydroquinazolinone Enantiomers

From a synthetic perspective, the development of new general methods to create enantiopure aminal stereocenters represents a valuable tool for synthetic chemists. This motif is present abundantly in nature and can be found in such complex products as minfiensine[1], the quadrigemines[2], asperazine[3], and the securamines[4], to name but a few. Current methods for constructing this stereocenter (elegantly exemplified by the syntheses of Overman and coworkers) derive their stereospecificity from the complex chiral scaffolds upon which they are constructed. To the best of our knowledge, the only general method for constructing this aminal motif asymmetrically is via the Curtius rearrangement of a chiral amino acid.[5]

From a medicinal point of view, it is very desirable to isolate or prepare the separate enantiomers of a new pharmaceutical agent. Opposite enantiomers of a single compound can have large differences in biological activity, pharmacokinetics,

Table 5A Effects of Separate Enantiomers of Some Commercially Available Drugs

Racemic Drug	Enantiopure Drug	Treats:	Active Enantiomer	Difference in Activity
Omeprazole *(Prilosec)*	Esomeprazole *(Nexium)*	Acid Reflux Disorder	S-isomer	Clinical trials show Esomeprazole to be somewhat more active than the racemic Omeprazole
Ofloxacin *(Floxin)*	Levofloxacin *(Levaquin)*	Penicillin resistant pneumococci infections	S-isomer	Levofloxacin is twice as active as the racemic mixture; it also has been shown to cause fewer skin, GI, and CNS side effects than the racemic mixture
Albuterol *(Proventil)*	Levalbuterol *(Xopenex)*	Asthma	R-isomer	R-isomer is a strong bronchiodilator, while the S-isomer is actually a weak bronchioconstrictor
Methylphenidate *(Ritalin)*	Dexmethylphenidate *(Focalin)*	ADD/ADHD	d-enantiomer	Dexmethylphenidate is better absorbed and more active than the racemic methylphenidate
Citalopram (Celexa)	Escitalopram (Lexapro)	Depression	S-enantiomer	The S-enantiomer is at least 100 times more active than the R-enantiomer and twice as active as the racemate

pharmacodynamics, and toxicity (see Table 5A).[6,7] In fact, the differing properties are so significant that the FDA now requires that all stereoisomers of a racemic drug be identified and characterized by their respective manufacturer.[8]

It would be difficult to find a more dramatic example of the importance that enantiomers play in medicine than that of the thalidomide tragedy. Thalidomide is a sedative that was first synthesized at Chemie Grünenthal in West Germany in 1953 and was largely prescribed to pregnant women to combat morning sickness.[9] It was not until the early 1960s that thalidomide was discovered to be teratogenic – it caused horrible deformities in an estimated 12,000 children in 46 different countries. Approximately 25 % of pregnant women who took thalidomide during their first trimester gave birth to children with flipper-like appendages in place of arms and/or legs (phocomelia).[10] Although these were the most obvious defects, the effects of thalidomide did not end there. Addition parts of the body that were affected include the eyes, ears, genitals, nervous system and various internal organs. These deformities and teratogenic effects were so severe that only 2/3 of those children survived beyond 1 year of age. It was not until studies investigating the biological roles of thalidomide's enantiomers were done that the details behind this tragedy began to become clear.

Thalidomide is administered as a racemic mixture; however, it is now understood that the glutarimide moiety undergoes spontaneous hydrolysis and fast chiral interconversion when exposed to physiological conditions.[11-14] It was not until non-racemizable thalidomide analogs were prepared that it was proposed the S-enantiomer was solely responsible for the teratogenic effects while the R-enantiomer was responsible for the desired hypnotic and sedative effects (see Figure 5A).[13,15-16]

Figure 5A Biological Roles of the Thalidomide Enantiomers

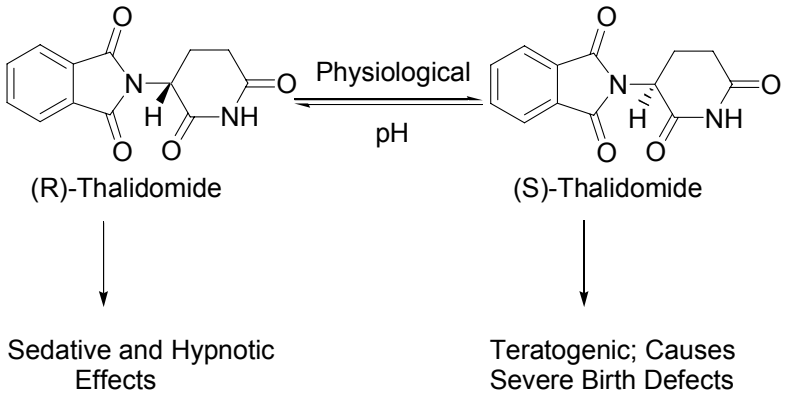

In addition to achieving the general effects of reduced toxicity and enhanced potency, we were further motivated to create the DHQZ enantiomers because of their relationship to thalidomide. Recall from chapter 1 that our investigations into this class of molecule began with making derivatives and analogs of thalidomide. The lead **SC-2-71**, analog **61**, and thalidomide share similar chemical structures as well as similar biological properties (such as inhibition of angiogenesis). Admittedly, this does not definitively indict the DHQZ enantiomers as having serious teratogenic properties, however such similarities to thalidomide underscore the importance of studying the physiological effects of each DHQZ enantiomer.

As we saw in chapters 2 – 4, DHQZs represent a class of compound with significant potential in the field of oncology. In addition to their anti-tumor properties, various DHQZ analogs have also been noted as antibiotics[17], antidefibrillatory agents[18], anti-spermatogenics[19], vasodilators[20], and analgesics[21]. Despite efforts by Lee[22], Priego[23], and possibly others, neither the enantiomeric synthesis nor the separation of these important compounds has yet been reported. It is the potential contribution to the field of organic synthesis as well as medicinal chemistry that has motivated us to explore

various methods of creating or isolating the enantiomers of the DHQZ heterocycle. A synopsis of our efforts will be discussed in the following sections.

5.1 Asymmetric Organolithium Addition

The first approach we chose to pursue was the asymmetric addition of a biphenyl organolithium to the imine moiety of a quinazolin-4-one. It was our hope that previous work in the field of asymmetric nucleophilic additions to imines would be compatible with our system, and so we searched the literature for related reactions.

In the early 1990s, Denmark and co-workers demonstrated that bis-oxazolines and (-)-sparteine are very effective promoters of lithium reagents to a variety of aldimines[24-25] (see Figure 5.1A). There are 2 main differences between the imines in Denmark's studies and the quinazolinone imine to which we must add our organolithium reagent.

On one hand, the imine moiety of the quinazolinone is part of a ring system which firmly locks it into one geometric shape (see Scheme 5.2B). Contrast this with the

Figure 5.1A Denmark's Asymmetric Imine Addition

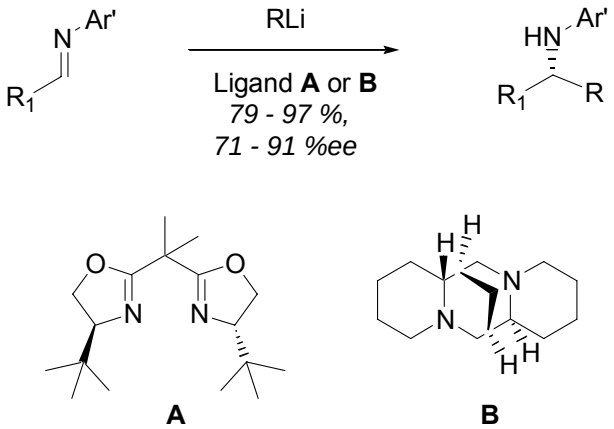

typical imine which is capable of E/Z isomerization about the N=C bond, resulting in a decrease in enantioselectivety over the course of these types of reactions. By virtue of being incorporated into a ring, our quinazolinone could not experience this isomerization event, therefore it would not be unreasonable to expect a higher degree of enantioselectivety.

On the other hand, the aldimine in the quinazolinone substrate has a nitrogen at the alpha position, the effects of which are uncertain with regard to this reaction. We expect that it will make the imine carbon less electrophilic, but hopefully not to an extent that prevents the reaction from occurring. Further, the imines in Denmark's studies are presumed to be in the more stable E configuration, but as noted previously, the quinazolinone is a ring structure which locks its imine into the Z geometry.

With the above considerations in mind, we began to prepare the bis-oxazoline ligand by the methods of Denmark[25] as illustrated in Scheme 5.1A. With compound **63** in hand, we synthesized the quinazolinone substrate in one step. *Para*-methoxybenzylamine was reacted with isatoic anhydride in DMF, then upon completion of the reaction as indicated by TLC the acid catalyzed cyclization with triethylorthoformate provided the PMB-protected quinazolinone **64** (see Scheme 5.1B).

Scheme 5.1A Preparation of Chiral bis-Oxazoline Ligand **63**

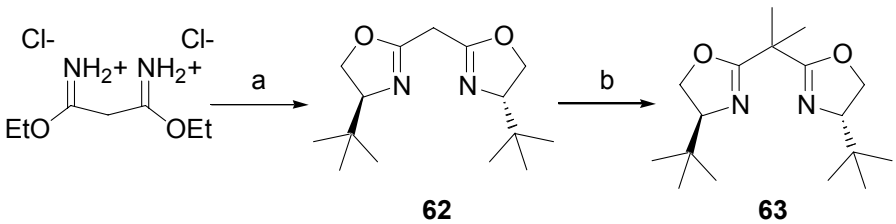

62 **63**

a) L-leucinol, DCM, RT b) *i.* LDA, TMEDA, -78^{o}C, THF *ii.* MeI

Scheme 5.1B Attempted Chiral Formation of **65**

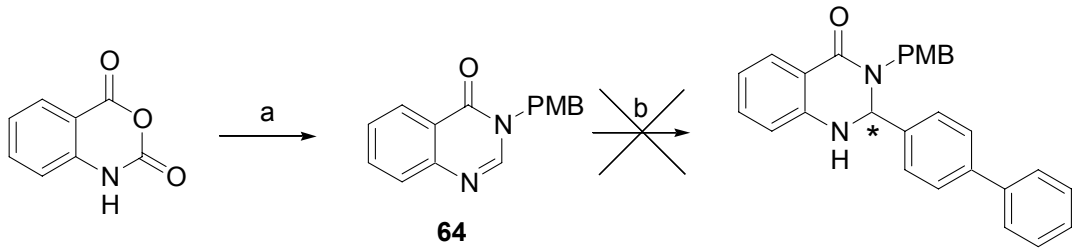

a) *i. para*-methoxybenzylamine, DMF, 80^{o}C *ii.* triethylorthoformate, p-TsOH, MeCN, 60^{o}C b) *i.* biphenyllithium bromide, **63** or (-)sparteine, various solvents *ii.* **64**

Unfortunately, even after screening a variety of solvents and reaction conditions, we were unable to isolate the target by this approach. After extensive investigation, the bis-oxazolines were abandoned and we explored the use of (-)-sparteine as the source of chirality. We were again disappointed to learn that this approach resulted in a range of outcomes, from no reaction to intractable product mixtures.

Before abandoning this approach, we wanted to experiment with a chiral ligand that differs from the previous two in that it does not make use of a diamine motif to chelate the cation of the aryllithium nucleophile. Tomioka and co-workers[26] have enjoyed a great deal of success by using chiral diether ligands in the asymmetric delivery of various organolithium reagents, so we pursued a similar approach illustrated in Scheme 5.1C.

Scheme 5.1C Synthesis of **65** via the Tomioka Method

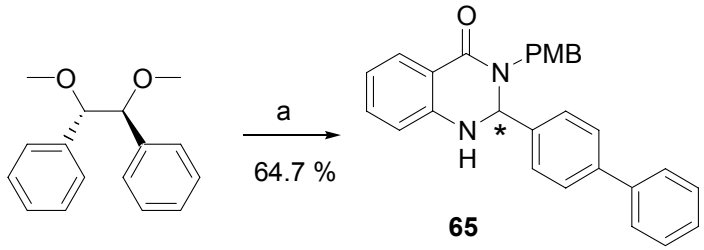

a) *i.* biphenyllithium bromide, **64**, ether/toluene, -45^{o}C

We were please to note that this reaction proceeds with much greater ease than the previous ones. The product was successfully isolated, however the complete lack of optical activity suggests that either the ligand was ineffective at forming **65** stereoselectively, or the product had racemized at some point during the reaction. In either case, this approach was deemed ineffective and was consequently abandoned.

5.2 Asymmetric Hydrogenation

The next approach we pursued was the asymmetric hydrogenation of a 2-biphenyl substituted quinazolinone. Somewhat similar to the approach described in section 5.1, this method attempts to operate on a ketimine rather an aldimine.

One of the more successful examples of asymmetric hydrogenations comes from the lab of Ryoji Noyori. Noyori and coworkers have developed a ruthenium based catalyst which incorporates a chiral diamine to asymmetrically reduce ketones[27-29] and imines[30] to alchohols and amines, respectively. The reported yields and enantiomeric excesses are extremely high, while the reaction conditions are fairly mild. The catalyst preparation is shown in Scheme 5.2A and was operationally simple to carry out.

Scheme 5.2A Preparation of Noyori's Ruthenium Catalyst **67**

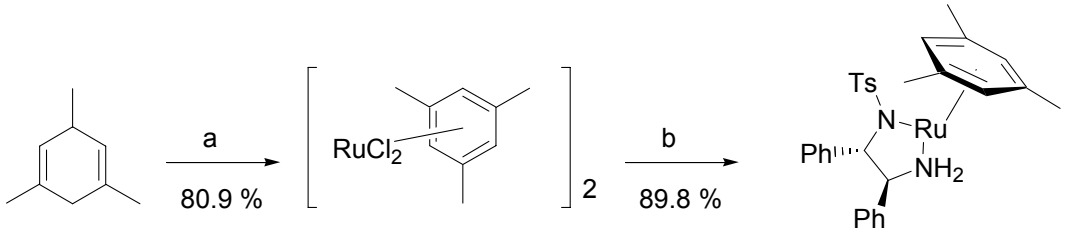

66 **67**

a) $RuCl_3$ monohydrate, EtOH, reflux b) (1S,2S)-N-tosyl-1,2-diphenylethylenediamine, TEA, iPrOH, 80°C

In Scheme 5.2B, we begin with the synthesis of the quinazolinone substrate **68**. Isatoic anhydride was reacted with *para*-methoxybenzyl amine in dimethylacetamide, then 4-biphenylcarboxoyl chloride was added to form the intermediate diamide. Reflux in ethanol caused intramolecular ring closure and concomitant dehydration to form **68**.

When the transfer hydrogenation of **68** was attempted with the ruthenium catalyst, we did not observe any reaction whatsoever. We screened a variety of conditions – alternate solvents, temperatures, catalyst loadings, and pressures – all to no avail. In order to see if this substrate was merely incompatible with the ruthenium, hydrogenation using palladium was explored, but again we did not observe any consumption of starting materials.

Scheme 5.2B Attempted Asymmetric Transfer Hydrogenation of **68** with Noyori's Ruthenium Catalyst

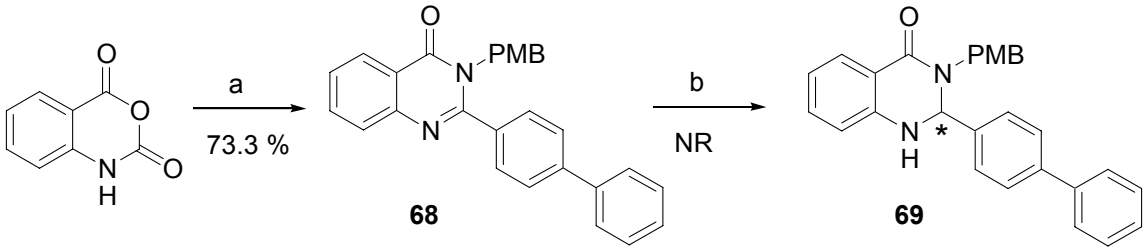

a) *i.* p-methoxybenzylamine, DMAC, 80^{o}C *ii.* 4-biphenylcarboxoyl chloride *iii.* reflux in EtOH b) **67** triethylamine, formic acid, DMF or MeCN or DMSO, RT or Heat

5.3 Curtius Rearrangement

To the best of our knowledge, the only general route which provides access to a chiral aminal is via the Curtius rearrangement of a protected amino acid.[5] This reaction

has been shown to retain the stereochemistry of the starting material, and so we thought this would be a next logical step in our pursuit of the DHQZ enantiomers.

Scheme 5.3A outlines the approach we pursued to arrive at the target. In order to create the enantiomers of **SC-2-71** by this approach, we would need to synthesize an unnatural chiral amino acid with a biphenyl moiety at the alpha position. Although this is a viable undertaking, we did not yet know if the Curtius strategy would be successful, and so we used a simpler amino acid as a test reaction. We chose valine as it is inexpensive, both enantiomers are commercially available, and the isopropyl group should be completely unreactive during the course of these experiments.

We initially coupled 2-iodobenzoyl chloride with L-valine to form the amide **70**. The acyl azide was formed upon reaction of **70** with diphenylphosphoryl azide (DPPA) and the modified Curtius[31] rearrangement occurred upon subsequent heating to provide the intermediate isocyanate. The isocyanate was then trapped as the carbamate **71** after the addition of 2-trimethylsilylethanol.

Buchwald and associates have described several examples of copper and palladium catalyzed coupling between amines,[32-34] amides,[35,36] and carbamates[36] with aryl halides or aryl triflates. Having successfully made our chiral aminal, we now hoped to use this chemistry to do an intramolecular ring closure by fusing the carbamate to the aryl iodide. Although there are currently no published examples of this type of ring closure using an aminal substrate, the similarities between **71** and the molecules that have successfully undergone this type of reaction are close enough to make us believe this would be a viable approach. Unfortunately, we were never able to accomplish this key step. We carried out an extensive screen of reaction conditions, but despite our efforts

we observed the same result for each reaction – the starting material would form trace amounts of product (as judged by TLC) and eventually decompose. We were disappointed to conclude that this type of chemistry would not enable access to our desired DHQZ enantiomers, and so we sought yet another approach.

Scheme 5.3A Approach to Synthesize DHQZ Enantiomers via the Curtius Rearrangement

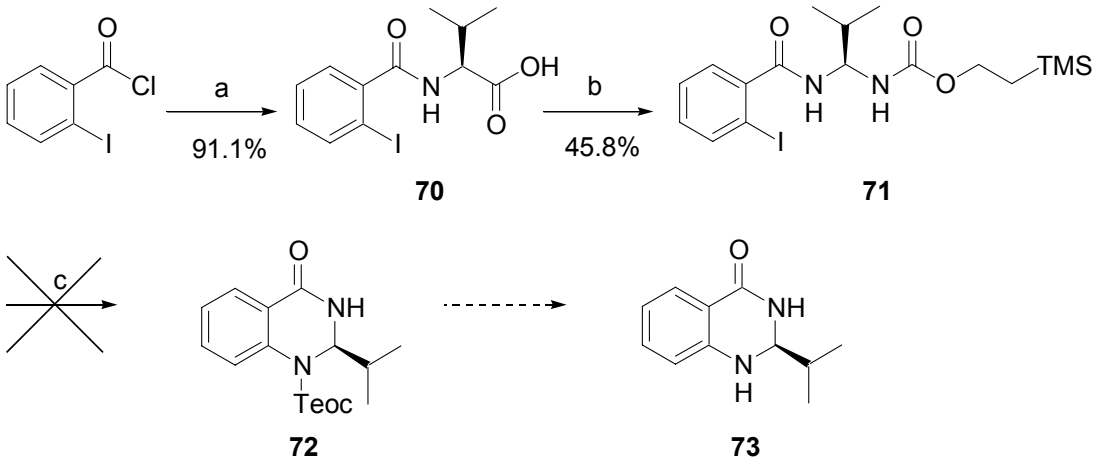

a) L-valine, 1M NaOH, THF b) *i.* TEA, diphenylphosphoryl azide, toluene, sieves, 110^{o}C *ii.* $TMSCH_2CH_2OH$ c) several Pd and Cu based reagents, variety of conditions

5.4 Chiral Auxiliaries

Our next attempts to synthesize the enantiomers were based on the work of Priego and coworkers[23] in which chiral amino acids were used to create dihydroquinazolinone diastereomers that were separable by chromatography. Unfortunately they were unable to remove the chiral auxiliary after separating the diastereomers, thus making this approach of limited utility (see Scheme 5.4A).

Scheme 5.4A Priego *et al* dihydroquinazolinone diastereomer synthesis

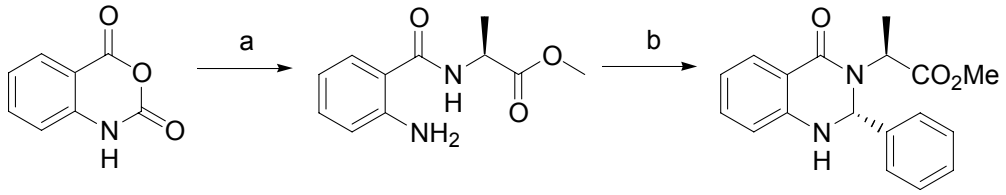

a) L-Alanine methyl ester, TEA/toluene/ethyl acetate 40°C b) Benzaldehyde, DCM, p-TsOH

We began by synthesizing similar amino acid based diastereomers according to the very reproducible methods of Priego with the hope that we would be able to remove the auxiliary from the amide moiety. We envisioned two routes that would be capable of doing this, each of which were met with mixed results. After separating the isomers, hydroxyl-iodine exchange of a serine based auxiliary, followed by reaction with magnesium successfully cleaved the auxiliary from the amide (see Scheme 5.4B, path A). When the enantiomeric purity was assessed by polarimetry and chiral HPLC, however,

Scheme 5.4B Approaches leading to auxiliary cleavage and the inadvertent racemization of the stereocenter

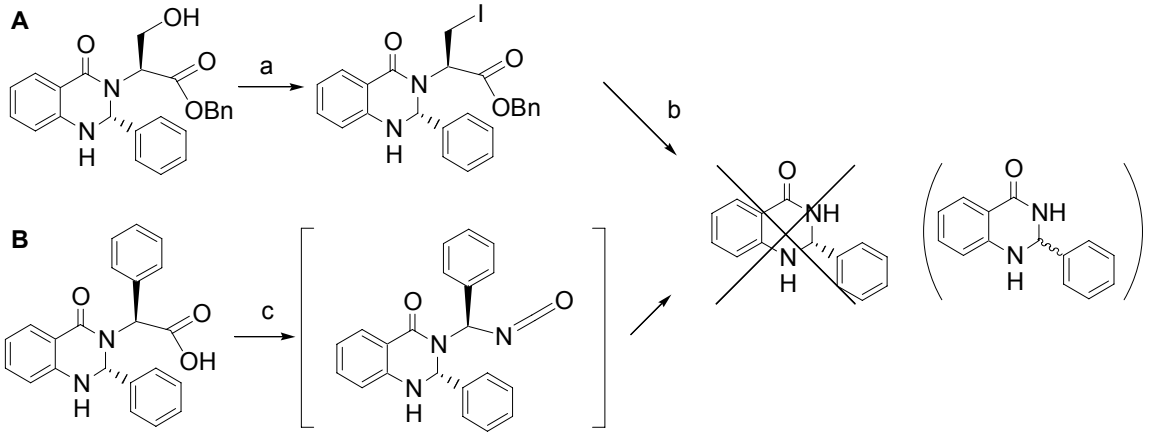

a) I_2, PPh_3, imidazole, DCM b) Mg, THF, 50 - 60°C c) *i.* DPPA, THF, 60°C *ii.* H_2O

complete racemization of the desired chiral center was observed. To overcome this we executed a similar strategy that employed somewhat gentler conditions. The free acid of the chiral auxiliary was reacted with diphenylphoshorylazide (DPPA), then heated to 40 – 60 ^{o}C (Curtius conditions, see Scheme 5.4B, path B). The intermediate isocyanate was hydrated *in situ*, thus causing decarboxylation and collapse of the unstable aminal bond. While the auxiliary was successfully cleaved, to our dismay the desired stereocenter had once again racemized.

It seems that the stereocenter is too fragile to survive when even a transient negative charge is placed on the heterocycle. With this in mind, we hypothesized that the undesired racemization was occurring through a mechanism similar to that illustrated in Figure 5.4A. To circumvent this, we sought a similar approach that met the following criteria: 1) the diastereomers must be separable by solubility differences or chromatographic methods, 2) in order to avoid problems with complete or partial racemization, the chiral auxiliary should not be directly bound to the heterocycle, 3) during auxiliary removal, no strong bases or acids may be used as they would destroy the stereocenter, and 4) the chiral auxiliary should be as inexpensive and effective as possible.

Figure 5.4A Putative Anionic Racemization Mechanism

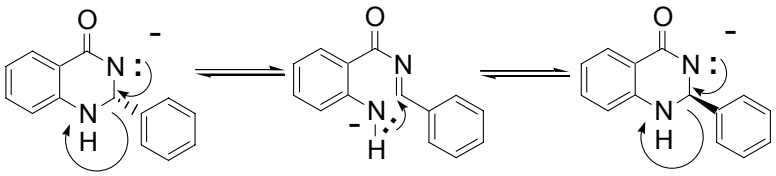

Figure 5.4B illustrates the solution we envision that would satisfy all four of the above criteria. By putting the auxiliary on the aromatic ring, we now have a much more sturdy substrate to manipulate while the source of asymmetric induction retains its

Figure 5.4B Chiral Auxiliary-Based Approach to Synthesize the DHQZ Enantiomers

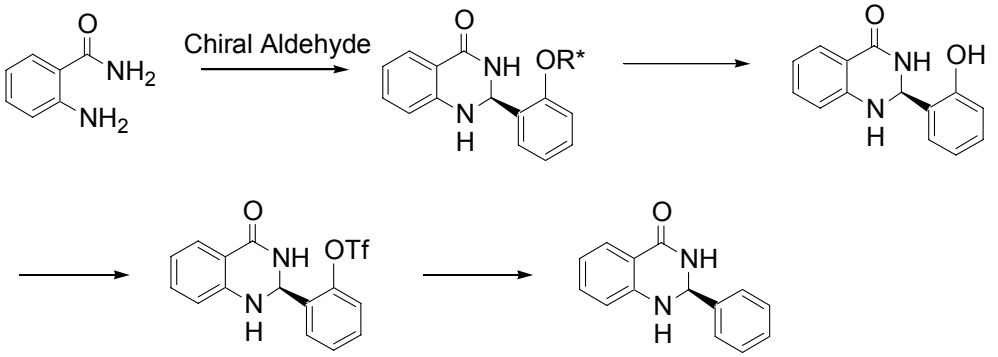

close proximity to the new stereocenter. After finding a suitable auxiliary, we would have to find conditions that would enable us to reduce the aromatic ring without harming the newly formed chiral center.

Towards this end, a series of chiral salicylaldehyde derived esters were prepared, then each subjected to acid-catalyzed cyclization with anthranilamide and screened for their ability to create separable diastereomers. The results of the screen, along with the yields of the major diastereomers formed and the associated diastereomeric ratio are tabulated in Table 5.4A. Regarding the last three entries, we were interested to note that increasing the steric bulk of the auxiliary from methyl to isopropyl to *tert*-butyl significantly enhances the diastereoselectivity (and yield) of the reaction. In addition, we were pleasantly surprised to discover that the diastereomers are not only separable by chromatography, but they are readily separable by solubility differences. During most of these cyclizations, the major diastereomer precipitates from solution as a single pure

isomer. It seems that the minor diastereomers (always the TLC spot with the higher R_f) does not even exist as a crystalline solid; rather, we found it to be an amorphous foam or thick oil. These dramatic solubility differences obviate the need for tedious purifications and/or multiple columns which are often associated with purifying diastereomers of very similar R_f values. These conditions are ideally suited for making preparatively useful quantities of these materials.

To remove the auxiliary and isolate the target DHQZ enantiomers, we sought conditions which would cleave the ester without the strong pH conditions traditionally associated with this type of chemistry. A screen of several hydride reducing agents proved to be incompatible with the DHQZ diastereomers as we observed them deprotonate the amide and racemize the stereocenter. We finally discovered that reaction with hydrazine was able to cleanly and quickly cleave the ester at ambient temperatures to produce the phenol with no detectable racemization.

Reaction of the phenol enantiomer with N-phenyl-bis-triflimide in the presence of Hunig's base proved very effective in selectively forming the aryl triflate over the triflic amide. The triflate enantiomer was then reduced with ammonium formate and $Pd(dppf)Cl_2$ to finally yield the desired enantiomerically pure DHQZ, as indicated by chiral HPLC.

Table 5.4A Screen of Several Chiral Auxiliaries

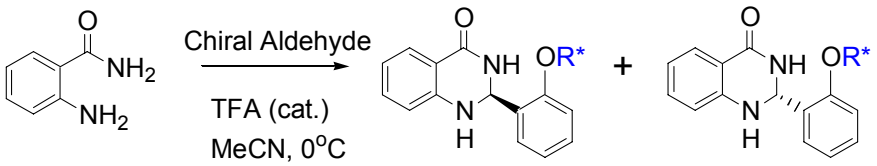

Chiral Aldehyde	Result	
	% Yield[a]	D/R
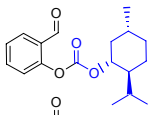	Inseparable Diastereomers	
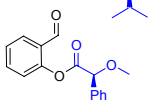	Inseparable Diastereomers	
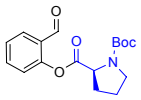	Inseparable Diastereomers	
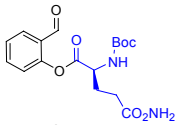	Inseparable Diastereomers	
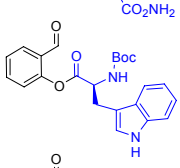	Inseparable Diastereomers	
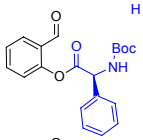	26.4	71:29
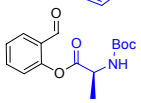	47.1	55:45
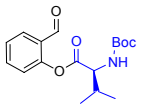	75.4	83:17
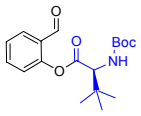	84.6	91:9

[a] *yield refers to the major diastereomer formed*

5.5 New Methodology – Scope and Limitations

In order to probe the scope and limitations of this new methodology, we cyclized the chiral aldehydes in Scheme 5.5A with a variety of anthranilamide analogs. The anthranilamides chosen encompass electron donating, electron withdrawing, and sterically crowded functional groups. The results of this screen are tabulated in Scheme 5B.

Scheme 5.5A Synthesis of the Chiral Aldehydes **74** and **75**

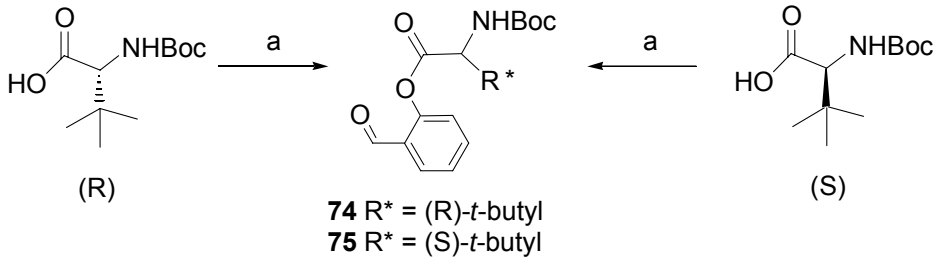

74 R* = (R)-*t*-butyl
75 R* = (S)-*t*-butyl

a) *i.* DCC, HOBt, DMF *ii.*salicylaldehyde

With respect to entries a and b, we were pleased to note that inverting the chirality of the auxiliary inverts the chirality of the new stereocenter, as expected. We also notice that the most deleterious effects on yield and selectivety occur with electron donating substituents (see entries **76d** and **76i**) at R_5, a similar phenomenon was also observed by Lee and coworkers. Examination of the electron withdrawing nitro groups (entries e, f) show similar diastereoselectivety to **77a** and **76b**, but a somewhat reduced yield. These conclusions must be weighed carefully, however, as the nitro containing molecules required reaction conditions 40 – 50 ^{o}C higher that the remaining compounds listed. We also see, with entries **76j** and **76k**, an intolerance toward alteration of the carbonyl of the

Scheme 5.5B Effects of Anthranilamide Substituents on Stereocenter Formation

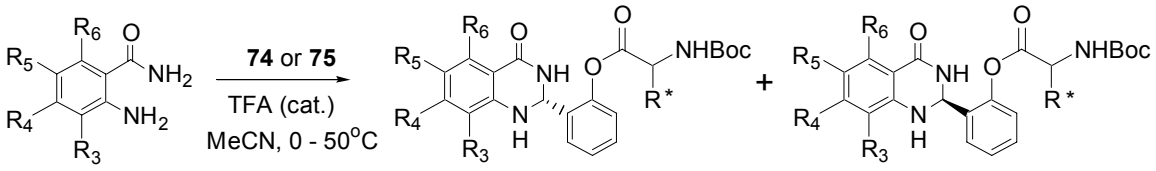

76 **77**

Entry	R_3	R_4	R_5	R_6	Chiral Aldehyde	% Yield[a]	D/R 76 : 77	
a	H	H	H	H	74	71	11	*89*
b	H	H	H	H	75	85	*91*	9
c	H	MeO	H	H	75	78	*85*	15
d	H	H	MeO	H	75	36	*75*	25
e	H	NO_2	H	H	75	66	*85*	15
f	H	H	NO_2	H	75	58	*89*	11
g	Me	H	H	H	75	62	*79*	21
h	H	H	H	Me	75	34	*83*	17
i	H	H	Cl	H	75	59	*83*	17
j	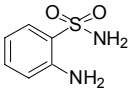				75	*Inseparable Diastereomers*		
k	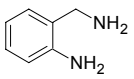				75	*Product not detected*		

[a] *yield refers to the major diastereomer formed*

amide moiety. In both cases we did not observe separable diastereomers upon cyclization.

Having successfully isolated a variety of DHQZ enantiomers, we were now in a convenient position to determine the absolute configuration of the stereocenter. X-ray crystallographic analysis for compound **76b** is show in Figure 5.5A. It seems that using an L-amino acid auxiliary (S-stereochemistry) induces the DHQZ stereocenter to adopt the R-configuration. Further, the crystal structure reveals an interesting intramolecular interaction between the carbamate oxygen and the aniline hydrogen. This structure

appears to form an unusual 11-membered hydrogen bonding ring between these two functionalities.

Figure 5.5A X-Ray Crystal Structure of Diastereomer **76b**

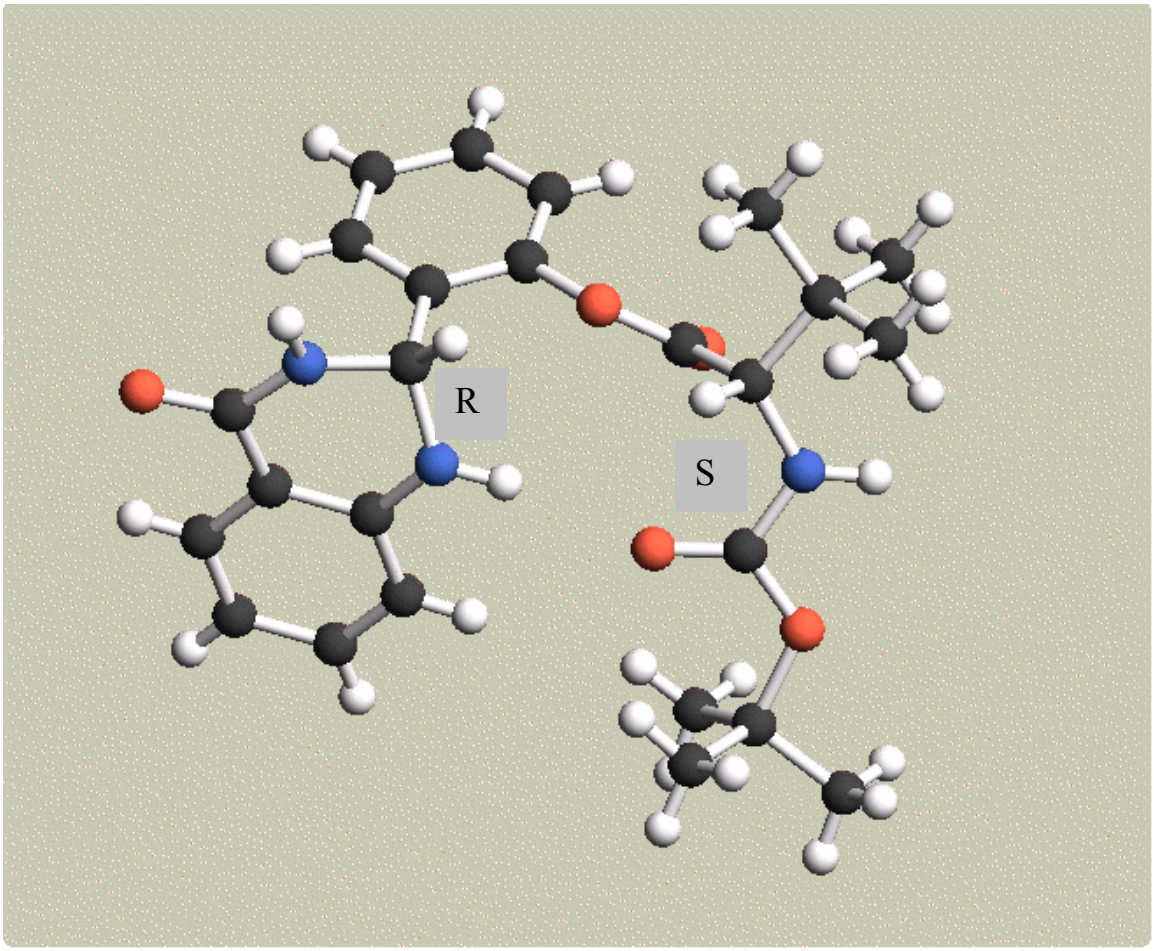

To remove the auxiliary and isolate the target DHQZ enantiomers, we sought conditions which would cleave the ester without the strong pH conditions traditionally associated with this type of chemistry. A screen of several hydride reducing agents proved to be incompatible with the DHQZ diastereomers as we observed them deprotonate of the amide and racemize the stereocenter. We finally discovered that

reaction with hydrazine was able to cleanly and quickly cleave the ester at ambient temperatures to produce the phenol with no detectable racemization.

In order to ensure that the chiral auxiliary cleavage protocol we developed was compatible with the anthranilamide substituents that we examined, we removed the auxiliaries of **76b** – **76i** and **77a** as described previously (*vida supra* or see Scheme 5.5C). Reaction with hydrazine cleaved the chiral esters and left the chiral phenol derivatives. The phenols were crystallized with chloroform and triflated to form **78a** – **78i**. After we isolated the aryl triflates, the C-ring was reduced as shown to provide the enantiomers **79a** – **79i** in enantiomerically pure form (as indicated by chiral HPLC).

Scheme 5.5C Removal of the Chiral Auxiliary for **77a** and **76b** – **76i**

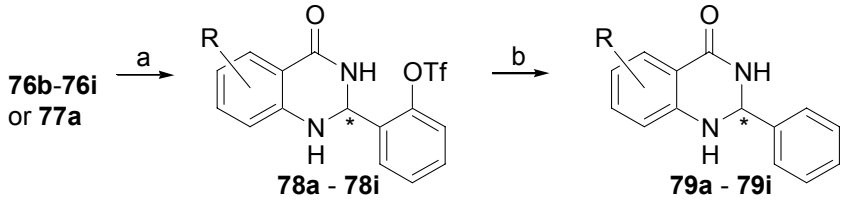

a) *i.* hydrazine, THF, 23°C *ii.* $PhN(Tf)_2$, Hunigs, THF, 23°C b) HCO_2H, TEA, $Pd(dppf)Cl_2$, DMF, 90 - 100°C

5.6 Synthesis of Fourth Generation Hybrid Enantiomers

As mentioned at the beginning of this chapter, the isolation or resolution of dihydroquinazolinone enantiomers is currently unreported in the literature, so accordingly it is also unknown which enantiomer elicits the observed biological responses. To ascertain this information we applied this newly developed synthetic methodology from sections 5.4 and 5.5 to synthesize both isomers of **61** via the approach outlined in Scheme 5.6A.

Suzuki-Miyaura coupling initially provided phenol **80**, which then underwent a regioselective Duff formylation with paraformaldehyde to form aldehyde **81**. Coupling the D- and L- Boc-protected chiral auxiliaries to the phenol created aldehydes **82** and **85**, respectively. Each was cyclized with 5-nitroanthranilamide, then the auxiliary subsequently removed according to the methods disclosed in section 5.4 to form opposite enantiomers **84** and **87**.

Scheme 5.6A Synthetic Preparation of the Enantiomers of Compound **61**

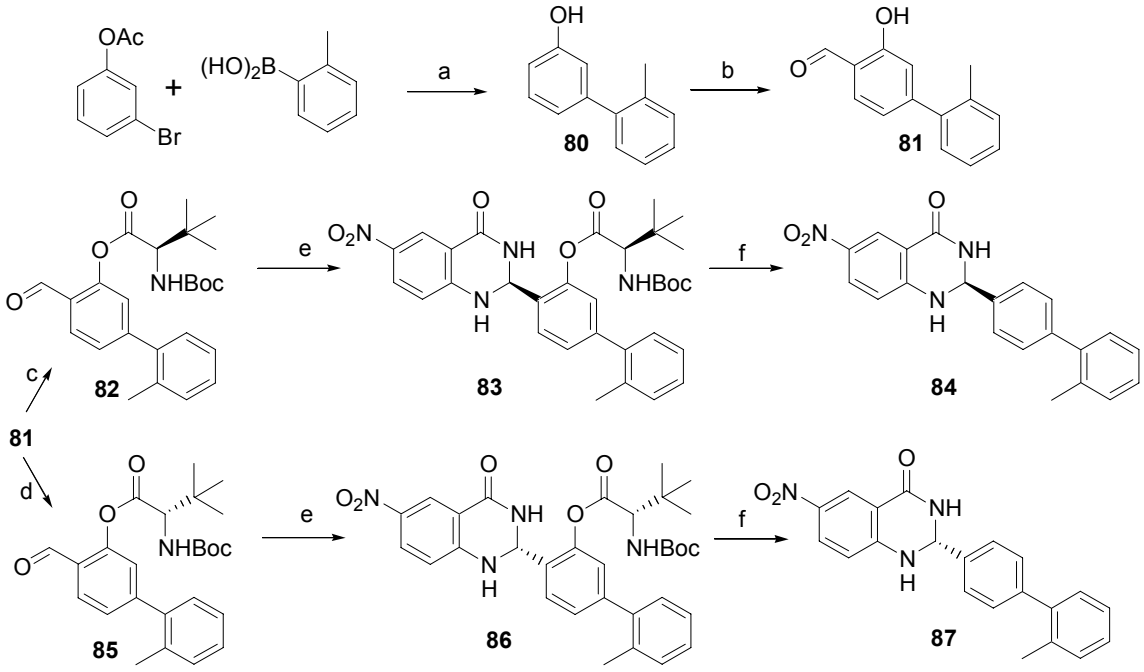

a) *i.* $Pd(PPh_3)_4$, Cs_2CO_3, dioxane, 90°C *ii.* EtOH b) i. MeMgBr, THF, 0°C ii. paraformaldehyde, TEA, benzene, reflux c) D-Boc-*tert*-leucine, DCC, HOBt, DMF d) L-Boc-*tert*-leucine, DCC, HOBt, DMF e) 5-nitroanthranilamide, TFA (cat.), MeCN, 45°C f) *i.* hydrazine, THF *ii.* $PhN(Tf)_2$, diisopropylethyl amine, THF *iii.* HCO_2H, TEA, $Pd(dppf)Cl_2$, DMF, 90°C

5.7 Biological Evaluation

Racemic **61** and each enantiomer (**84** and **87**) were separately assayed against 2 different human cancer cell lines and evaluated for their anti-proliferative effects. As

Table 5.7A shows, both cell lines appear to be significantly more sensitive to compound **84** (S-configuration) when compared to the racemate. Interestingly, the "inactive" enantiomer **87** still retains significant cytotoxicity (ca. 1μM), though significantly less so than either **84** or the racemate. Most noteworthy is the picomolar level inhibition of **84** on the MDA-MB-435 cell line, approximately 10 times more active than taxol – a particularly remarkable feat when one considers the structural complexity of taxol versus that of **84** (see Figure 5.7A) .

Table 5.7A Anti-proliferative Activities of **61**, **84**, and **87**

	MDA-MB-435 *(breast)*	**HCT-116** *(colon)*
61 (racemic)	100 nM	300 nM
87 (R)	1100 nM	930 nM
84 (S)	0.1 nM	100 nM
Taxol	1.15 nM	2.3 nM

Figure 5.7A Structure of Taxol vs. **84**

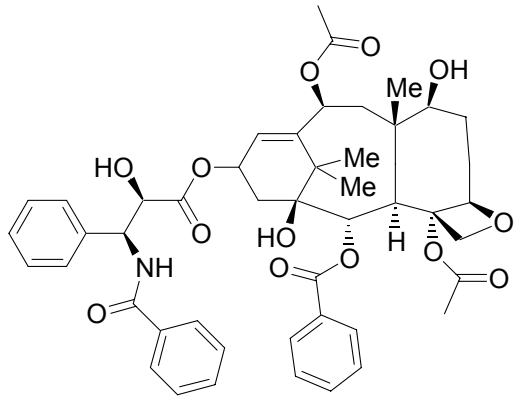

Taxol

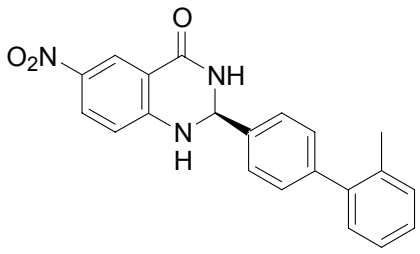

84

5.8 Chapter 5 References

1. Dounay, A. B.; Overman, L. E.; Wrobleski, A. D. Sequential Catalytic Asymmetric Heck-Iminium Ion Cyclization: Enantioselective Total Synthesis of The Strychnos Alkaloid Minfiensine. *J. Am. Chem. Soc.* **2005**, *127*, 29, 10186-10187.
2. Lebsack, A. D.; Link, J. T.; Overman, L. E.; Steams, B. A.; Enantioselective Total Synthesis of Quadrigemine C and Psycholeine. *J. Am. Chem. Soc.* **2002**, *124*, 31, 9008 – 9009.
3. Govek, S. P.; Overman, L. E. Total Synthesis of Asperazine. *J. Am. Chem. Soc.* **2001**, *123*, 38, 9468 – 9469.
4. Rahbæk, L.; Christophersen, C. Marine Alkaloids. 19. Three New Alkaloids, Securamine E – G, from the Marine Bryozoan *Securiflustra securifrons*. *J. Nat. Prod.* **1997**, *60*, 175 – 177.
5. Panagiota, M. M.; Iphigenia, P. Some applications of the Curtius rearrangement. *J. of the Chem. Soc. Perkins Trans. 1*. **1985**, *11*, 2277 – 2281.
6. Crom, W. R. Effect of chirality on pharmacokinetics and pharmacodynamics. A.. *J. Hosp. Pharm*. **1992**, *49*, S9 – S14.
7. Ariens, E. J. Stereochemistry: a source of problems in medicinal chemistry. *Med. Res. Rev.* **1986**, *6*, 451 – 466.
8. United States Food and Drug Administration. http://www.fda.gov/cder/guidance/stereo.htm (accessed July 2006).
9. Wikipedia. http://en.wikipedia.org/wiki/Thalidomide (accessed July 2006).

10. Mellin, G. W.; Katzenstein, M. The saga of thalidomide. Neuropathy to embryopathy, with case reports of congenital abnormalities. *N. Engl. J. Med*. **1962**, *267*, 1184 – 1193.

11. Wnendt, S.; Finkham, M.; Winter, W.; Ossing, J.; Rabbe, G.; Zwingenberger, K. Enantioselective inhibition of TNF-α release by thalidomide and thalidomide analogs. *Chirality*. **1996**, *8*, 5, 390 – 396.

12. Knoche, B.; Blaschke, G. J. Investigations on the in vitro racemization of thalidomide by high-performance liquid chromatography. *J. of Chromatogr.* **1994**, *666*, 235 – 240.

13. Winter, W.; Frankus, E. Thalidomide enantiomers. *Lancet*, **1992**, *339*, 365.

14. Nishimura, K.; Hahimoto, Y.; Iwasaki, S. Enhancement of phorbol ester-induced production of tumor necrosis factor α by thalidomide. *Biochem. Biophys. Res. Commun*. **1994**, *199*, 2, 455 – 460.

15. Eriksson, T.; Bjorkman, S.; Roth, B.; Fyge, A.; Hoglund, P. *Chirality*, **1996**, *7*, 44.

16. Shealy, Y. E.; Opliger, C. E.; Montgomery, J. A. D- and L- Thalidomide. *Chem. Ind*. **1965**, 1030 – 1031.

17. Russel, H. E.; Alaimo, R. J.; Antibacterial 2,3-dihydro-2-(5-nitro-2-thienyl)-quinazolin-4(1H)-ones. *J. Med. Chem*. **1972**, *15*, 3, 335 – 336.

18. Bonola, G.; Da Re, P.; Magistretti, M. J.; Massarani, E.; Setnikar, I. 1-Aminoacyl-2,3-dihydro-4(1H)-quinazolinone derivatives with choleretic and antifibrillatory activity. *J. Med. Chem.* **1968**, *11*, 1136 – 1139.

19. Neil, G. L.; Li, L. H.; Buskirk, H. H.; Moxlcy, T. E. Antitumor effects of the antispermatogenic agent, 2,3-dihydro-2-(1-napthyl)-4(1H)-quinazolinones. *Cancer Chemother.* **1972**, *56*, 163 – 173.

20. Levin, J. I.; Chan, P. S.; Bailey, T.; Katocs, A. S.; Venkatesan, A. M. The Synthesis of 2,3-Dihydro-4(1H)-quinazolinone Angiotensin II Receptor Antagonists. *Bioorg. Med. Chem. Lett.* **1994**, *4*, 9, 1141 – 1146.

21. Okumura, K.; Oine, T.; Yamada, Y.; Hayashi, G.; Nakama, M. 4-Oxo-1,2,3,4-tetrahydroquinazolines. I. Syntheses and pharmacological properties of 2-methyl-3-aryl-4-oxo-1,2,3,4-tetrahydroquinazolines and their 1-acyl derivatives. *J. Med. Chem.* **1968,** *11*, 348 – 352.

22. Hour, M. J.; Huang, L. J.; Kuo, S. C.; Xia, Y.; Bastow, K.; Nakanishi, Y.; Hamel, E.; Lee, K. H. 6-Alkylamino- and 2,3-Dihydro-3'-methoxy-2-phenyl-4-quinazolinones and Related Compounds: Their Synthesis, Cytotoxicity, and Inhibition of Tubulin Polymerization. *J. Med. Chem.* **2000**, *43*, 4479 – 4487.

23. Escalante, J.; Flores, P.; Priego, J. M. Synthesis of 2,3-dihydro-4(1H)-quinazolinones. *Heterocycles*. **2004**, *63*, 9, 2019 – 2032.

24. Denmark, S. E.; Nakajima, N.; Nicaise, O. J. Asymmetric Addition of Organolithium Reagents to Imines. *J. Am. Chem. Soc.* **1994**, *116*, 8797 – 8798.

25. Denmark, S. E.; Stiff, C. M. Effect of Ligand Structure in the Bisoxazoline Mediated Asymmetric Addition of Methyllithium to Imines. *J. Org. Chem.* **2000**, *65*, 5875 – 5878.

26. Inoue, I.; Shindo, M.; Koga, K.; Kania, M.; Tomioka, K. Enantioselective Reaction of An Iminne with Methllithium Catalyzed by A Chiral Ligand. *Tet. Asymm.* **1995**, *6*, 10, 2527 – 2533.

27. Hashiguchi, S.; Fujii, A.; Takehara, J.; Ikariya, T.; Noyori, R. Asymmetric Transfer Hydrogenation of Aromatic Ketones Catalyzed by Chiral Ruthenium(II) Complexes. *J. Am. Chem. Soc*. **1995**, *117*, 7562 – 7563.

28. Takehara, J.; Hashiguchi, S.; Fujii, A.; Inoue, S.; Ikariya, T.; Noyori, R. Amino alcohol effets on the ruthenium(II)-catalyzed asymmetric transfer hydrogenation of ketones inn propan-2-ol. *J. Chem. Soc., Chem. Commun*. **1996**, 233 – 234.

29. Fujii, A.; Hashiguchi, S.; Uematsu, N.; Ikariya, T.; Noyori, R. Ruthenium(II)-Catalyzed Asymmetric Transfer Hydrogenation of Ketones Using a Formic Acid-Triethylamine Mixture. *J. Am. Chem. Soc*. **1996**, *118*, 2521 – 2522.

30. Uematsu, N.; Fujii, A. Hashiguchi, S.; Ikariya, T.; Noyori, R. Asymmetric Transfer Hydrogenation of Imines. *J. Am. Chem. Soc.* **1996**, *118*, 4916 – 4917.

31. Shioiri, T.; Ninomiya, K.; Yamada, S. Diphenylphosphoryl Azide. A New Convenient Reagent for a Modified Curtius Reaction and for the Peptide Synthesis. *J. Am. Chem. Soc*. **1972**, *94*, 6203 – 6205.

32. Kwong, R. Y.; Buchwald, S. L. Mild and Efficient Copper-Catalyzed Amination of Aryl Bromides with Primary Alkylamines. *Org. Lett*. **2003**, *5*, 793 – 796.

33. Ma, D. W.; Cai, Q.; Zhang, H. Mild Method for Ullman Coupling Reaction of Amines and Aryl Halides. *Org. Lett*. **2003**, *5*, 2453 – 2455.

34. Lu, Z.; Twieg, R. J. A mild and practical copper catalyzed amination of halothiophenes. *Tetrahedron*, **2005**, *61*, 903 – 918.

35. Yin, J.; Buchwald, S. L. Palladium-Catalyzed Intermolecular Coupling of Aryl Halides and Amides. *Org. Lett*. **2003**, *5*, 20, 3667 – 3669.

36. Jiang, L.; Job, G. E.; Klapars, A.; Buchwald, S. L. Copper-Catalyzed Coupling of Amides and Carbamates with Vinyl Halides. *Org. Lett*. **2000**, *2*, 8, 1101 – 1104.

Chapter 6: Molecular Modeling of β-Tubulin

Molecular modeling is an emerging subject which interfaces the disciplines of computer technology, mathematics, chemistry, physics, and often structural biology. The computational chemist can use molecular modeling to study a range of phenomenon, including (but not limited to) thermodynamics, quantum mechanics, and chemical reactions. With respect to the latter, molecular models have been used to predict such diverse phenomenon as transition states of asymmetric reactions,[1] the relative energies of reaction participants,[2] and the results of protein folding.[3] In the field of medicinal chemistry, this technology is most often used to examine and predict how a small drug-like molecule interacts with a protein.[4-6] Details of these *in silico* studies can then be used to make structural changes to a pharmaceutical agent to enhance or modify the protein-drug interaction. If used properly, molecular modeling can greatly accelerate the pace at which a lead molecule is transformed into an analog with significantly enhanced biological properties.

In recent years, many robust computational methods have been developed to design, optimize, or screen databases for new lead molecules.[7-10] Within this "optimize" category, several pieces of software have been developed which attempt to predict how the three dimensional structure of a molecule interacts with the X-ray crystal structure of a protein. This computational method is commonly referred to as "docking". Since molecules are not a static collection of atoms – rather, various moieties within a molecule are able to rotate, vibrate, or exist in many possible conformations – "flexible docking" software has been developed which attempts to take into account several of the low energy conformations of these molecules and docking them into a static X-ray crystal

structure. The wide availability of X-ray, NMR, and model-built structures of medicinally important receptors and proteins have made flexible docking programs prevalent throughout the pharmaceutical industry.

Docking software essentially performs 2 main functions during its course of operation. First, the program must accurately predict the proper position and orientation of the ligand within the protein. The methods that the programs use to do so vary from incremental construction approaches (ie- FlexX),[11-12] to genetic algorithms (ie- GOLD),[13] to shape-based algorithms (DOCK),[14] and also Monte Carlo simulations (LigandFit).[15,16] Second, the programs score these docking results with a series of numbers which attempt to estimate the Gibbs free energy of binding, thus providing an estimate of the ligand's affinity for the protein. Several equations have been developed for this, including G-Score,[17] Chem-Score,[18] D-Score,[19] PMF-Score,[20] and F-Score.[21] Although none of these yet operates with 100% accuracy, they are often used in conjunction to improve the accuracy of their measurements.

6.1 Potential Binding Site

As mentioned in section 1.4, the DHQZs are known to interact at the colchicine site of tubulin and to a lesser extent, the adjacent vinca site as well. Both of these receptor areas are located on the β-subunit of the tubulin heterodimer, and so our initial docking studies were focused on this area of β-tubulin.

6.2 FlexX Docking of Quinazolinones

In order to further our understanding of how these molecules are physically situated within the tubulin protein, the FlexX module of Sybyl 7.0 was used to flexibly dock both enantiomers of analogs **1 - 61** at the colchicine site of tubulin. Although we

were unable to obtain good results by docking our compounds to the tubulin-colchicine complex[22] (PDB entry **1SA0**), excellent results were obtained by docking to the podophylotoxin-tubulin complex[23] (PDB entry **1SA1**). Podophylotoxin also binds to the colchicine site, and in fact, shares a high degree of structural homology with colchicine (see Figure 6.1A).

Figure 6.1A Structural Homology Between Colchicine and Podophyllotoxin

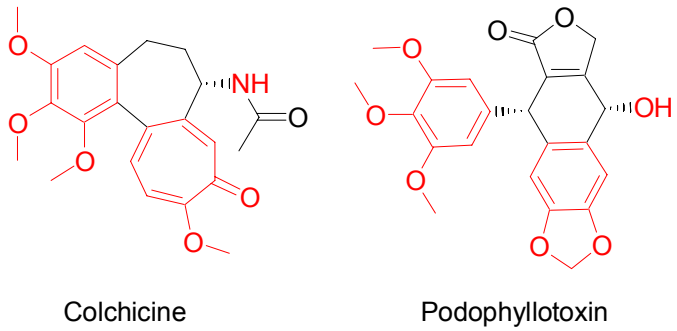

Colchicine Podophyllotoxin

As mentioned above, when we docked the DHQZs into the tubulin-colchicine crystal structure **1SA0**, the FlexX results were visibly flawed. This raises one of the more challenging questions in docking – how does one evaluate the accuracy of a model when the actual protein-ligand crystal structure is unknown? To guide ourselves, we developed the following heuristic criteria for assessing the accuracy of the suggested FlexX solutions.

1) Because the S- enantiomer is most likely solely responsible for the anti-microtubule activity, we expect to find that particular enantiomer to have much better docking results than the R- enantiomer.

2) Most likely there is only one DHQZ binding site on tubulin, therefore the model should place most (if not all) of the analogs in the same position and orientation within the tubulin protein.

3) We should expect that basic chemical principles will be obeyed in any putative binding models (ie – the lipophilic moieties of the ligand will bind in lipophilic sections of tubulin and vice-versa for polar functionalities)

4) The docking results should agree with experimental SAR data that has been accumulated thus far.

With regard to criteria 1 and 2, we were pleased to see that FlexX returned results that suggest the S-enantiomer binds in a consistent, logical fashion while the results for the R-enantiomer were specious at best. In addition, the results of this docking study did not show any obvious violations of steric or electronic considerations outlined in criteria 3. The precise binding mode and its agreement with the structure-activity studies will be described in the following section.

6.3 Correlation with Experimental Data

Analysis of the docking results suggests that poor steric interactions would result from substitutions other than position 5 of the A-ring (Figures 6.3A – 6.3B). This is consistent with the results which show a significantly active 5-chloro, 5-methoxy, and a very active 5-nitro, while substitutions at other positions of the A-ring appear to abolish activity. It also appears that a 5-nitro group is not only within hydrogen bonding distance to the amide of Gln 247, but the close proximity and perpendicular orientation of this electron deficient aromatic ring to the electron rich phenol of Tyr 224 raises the interesting possibility of π-π stacking interactions.

Figure 6.3A Compound **84** Docked with Tubulin

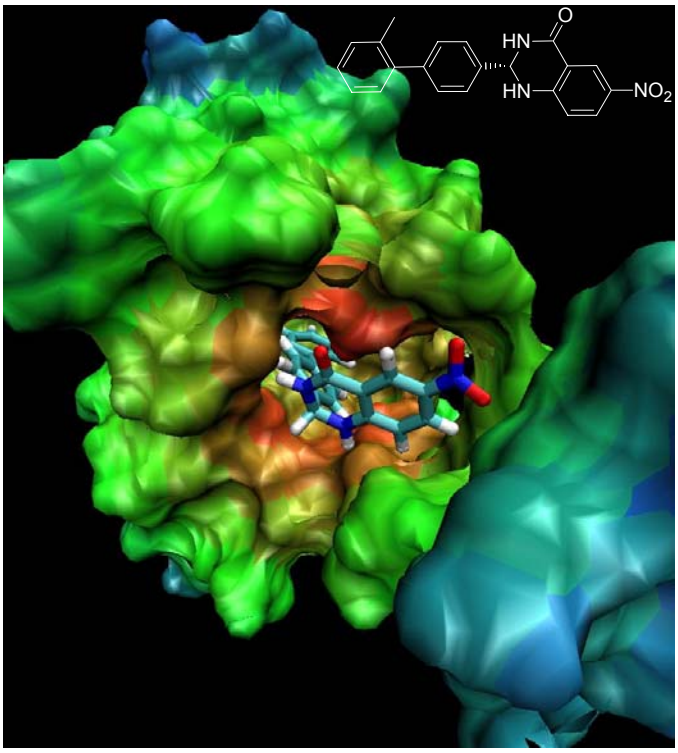

Inspection of the B-ring docking results suggest an intricate network of hydrogen bonding between the heterocycle and various tubulin residues around the cavity leading to the colchicine site (Figure 6.3B). Indeed, this is consistent with the biological results obtained which show a high degree of sensitivity to all changes made to the heterocycle.

Figure 6.3B Proposed Interactions Between Compound **84** and Various Tubulin Residues

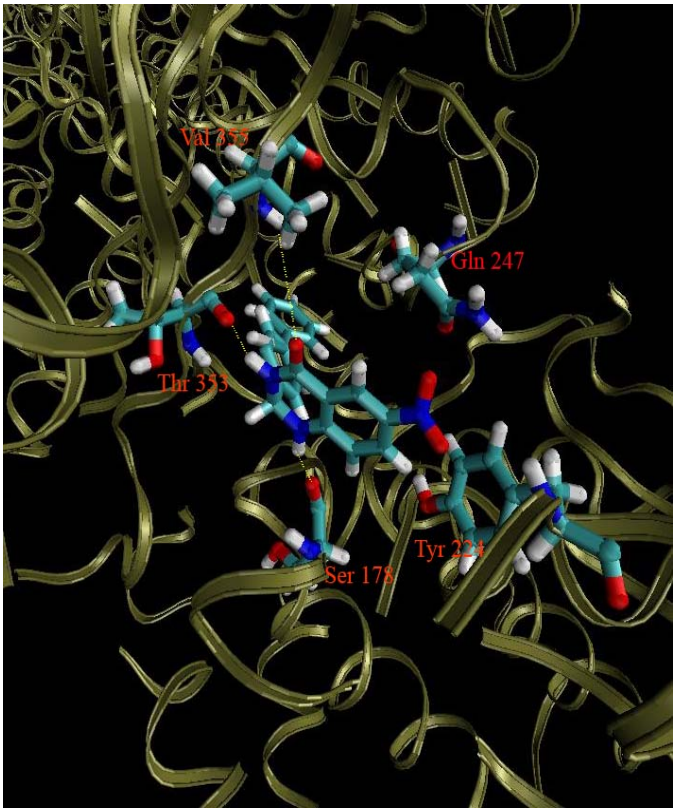

We also notice the C-ring of the biphenyl moiety lying within the lipophilic channel formed by the Leu 248 isopropyl group and the non-polar alkyl side chain of Lys 352. This channel leads to the significantly larger colchicine site cavity which appears to be occupied by the D-phenyl ring (Figures 6.3C – 6.3D). This D-ring lies entirely within the non-polar colchicine site and occupies the same points in space as podophyllotoxin and colchicine (Figures 6.3E). The tight confines of this channel suggest little room for substitutions of any kind at R_2. This is consistent with the biological results obtained showing a loss in activity for all analogs with structural modifications at this position. Biological assays also indicate that R_3 is a favorable site for lipophilic substitutions, again

consistent with the docking model showing a nonpolar portion of the active site capable of interacting with methyl-sized (or larger) lipophilic functional groups (Figure 6.3C).

Figure 6.3C Cutaway of **23** Docked with Tubulin from Perspective of Biphenyl Axis

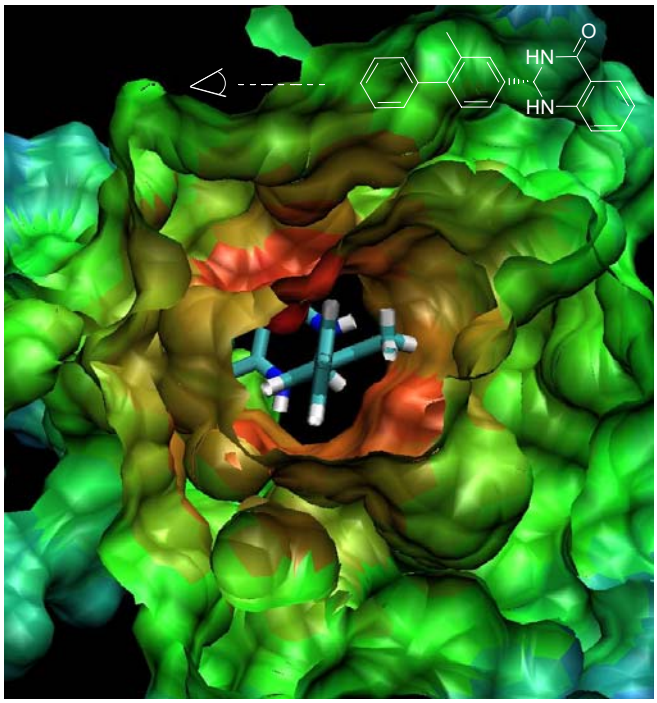

From this docking model, the D-ring appears to sit completely within the colchicine site, and (in the case of the biphenyl analogs) has approximately 1 Å between the *meta* and *para* positions and the active site wall. From this, we would predict that substitutions at these positions would encounter steric resistance within the protein and harm or even abolish activity. This loss in activity was, in fact, what was observed during the biological assays of these particular analogs.

Finally, Figure 6.3E shows the common space occupied by the docked compound **SC-2-71** and the co-crystallized podophyllotoxin found within the X-ray structure. The

structural overlap between the ligand's D-ring and trimethoxybenzene ring of podophyllotoxin may help prioritize future modifications of this ring as well and also raises the possibility of investigating structural hybrids of other colchicine site drugs and dihydroquinazolinones.

Figure 6.3D Analog **23** Docked with Tubulin (Outer Portion of Tubulin Cut Away Over the D-Ring)

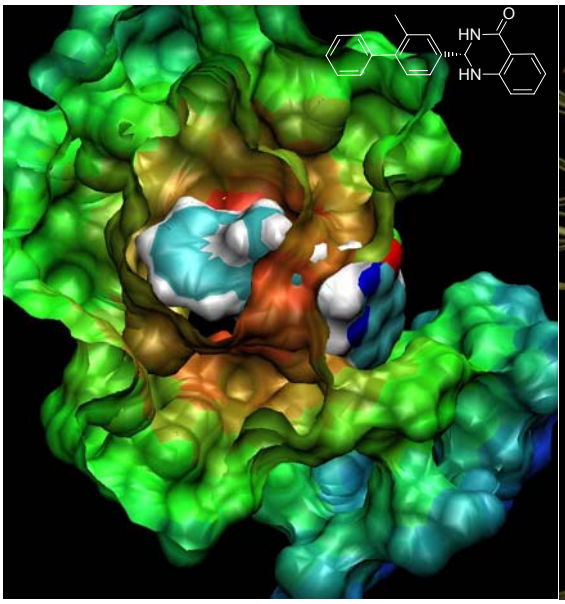

Figure 6.3E SC-2-71 Docked to Tubulin. Shown is the D-Ring Overlap with Podophyllotoxin

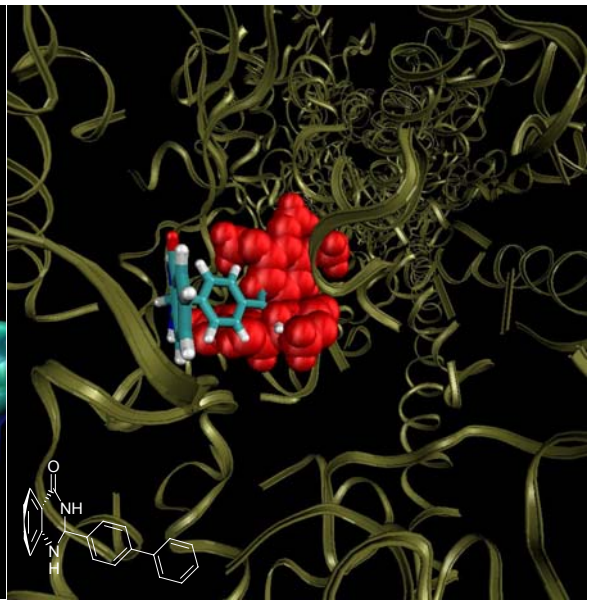

6.4 Preliminary Modeling Conclusions

While the docking model of DHQZ-Tubulin binding presented in the previous section has not been conclusively proven, it does nicely rationalize much of the biological data generated from the SAR study. In addition to correctly predicting the biologically active enantiomer, the model also correlates substitutions across all 4 rings with their relative increases or decreases in activity. Unfortunately, we were unable to find an association between the numerical scoring results of our docking studies and any of the

quantitative *in vitro* results. While it would have been nice to establish a method to link the *in silico* scores with biological activity, the model at least seems to have enough potential to be useful in designing and prioritizing the synthesis of future analogs. Further studies addressing the issue of the DHQZ-tubulin binding will focus on the synthesis of photoaffinity analogs or possibly solving the DHQZ-tubulin X-ray crystal structure.

6.5 Chapter 6 References

7 Norrby, P. O.; Kolb, H. C.; Sharpless, K. B. Toward an Understanding of the High Enantioselectivity in the Osmium-Catalyzed Asymmetric Dihydroxylation. 2. A Qualitative Molecular Mechanics Approach. *J. Am. Chem. Soc*. **1994**, *116*, 8470 – 8478.

8 Zhu, Z. H.; Lu, G. Q. New Insights into NO-Carbon and N2O-Carbon Reactions from Quantum Mechanical Calculations. *Energy and Fuels*, **2003**, *17,* 1057 – 1061.

9 Hao, M. H.; Scheraga, H. A. Optimizing Potential Functions for Protein Folding. *J. Phys. Chem*. **1996**, *100*, 14540 – 14548.

10 He, W.; Li, Y.; Si, H.; Dong, Y.; Sheng, F.; Yao, X.; Hu, Z. Molecular modeling and spectroscopic studies on the binding of guaiacol to human serum albumin. *J. of Photoch. And Photobiol. A: Chem.* **2006**, *182*, 2, 159 – 167.

11 Bikadi, Z.; Hazai, E.; Zsila, F.; Lockwood, S. F.; Molecular modeling of non-covalent binding of homochiral (3S,3'S)-astaxanthin to matrix metalloproteinase-13 (MMP-13). *Bioorg. Med. Chem*. **2006**, *319*, 1-2, 44 – 54.

12 Tramontano, A. The role of molecular modeling in biomedical research. *FEBS Letters*, **2006**, *580*, 12, 2928 – 2934.

13 Gillet, V. J.; De novo molecular design. *Methods Principles Med. Chem*. **2000**, *8*, 46 – 49.

14 Waszkowycz, B. New methods for structure-based de novo drug design. *Adv. Drug Discovery Techniques*. **1998**, 143 – 164.

15 Clark, D. E.; Murray, C. W.; Li, J. Current issues in de novo molecular design. *Reviews in Computational Chemistry*; Lipkowitz, K. B., Boyd, D. B. Eds.; VCH: New York, 1997; 67 – 125.

16 Schneider, G.; Bohm, H. J.; Virtual Screening for Bioactive Molecules. In methods and Principles in Medicinal Chemistry; Mannhold, R., Kubinyi, H., Timmerman, H. Eds.; Wiley-VCH: Weinheim, 2000.

17 Rarey, M.; Kramer, B.; Lengauer, T.; Klebe, G. A. A fast flexible docking method using an incremental construction algorithm. *J. Mol. Biol*. **1996**, *261*, 470 – 489.

18 FlexX was developed at the German National Research Center for Information Technology (GMD) and is distributed by Tripos, Inc., St. Louis MO; www.tripos.com/software/flexx.html.

19 Jones, G.; Willett, P.; Glen, R. C.; Leach, A. R.; Taylor, R. Development and validation of a genetic algorithm to flexible docking. *J. Mol. Biol.* **1997***, 267*, 727 – 748.

20 Kuntz, I. D.; Blaney, J. M.; Oatley, S. J.; Langidge, R.; Ferrin, T. E. A geometric approach to macromolecule-ligand interactions. *J. Mol. Biol.* **1982**, *161*, 269 – 288.

21 Venkatachalam, C. M.; Jiang, X.; Oldfield, T.; Waldan, M. LigandFit: a novel method for the shape-directed rapid docking of ligands to protein active sites. *J. Mol. Graphics Modell.* **2003**, *21*, 289 – 307.

22 Kontoyianni, M.; McClellan, L. M.; Sokol, G. S. Evaluation of docking performance: comparative data on docking algorithms. *J. Med. Chem.* **2004**, *47*, 558 – 565.

23 Jones, G.; Willett, P.; Glen, R. C.; Leach, A. R.; Taylor, R. Development and validation of a genetic algorithm for flexible docking. *J. Mol. Biol.* **1997**, *267*, 727 – 748.

24 Eldridge, M. D.; Murray, C. W.; Auton, T. R.; Paolini, G. V.; Mee, R. P. Empirical scoring functions: I. The development of a fast empirical scoring function to estimate the binding affinity of ligands in receptor complexes. *J. Comp. Aided Mol. Des*. **1997**, *11*, 425 – 445.

25 Kuntz, I. D.; Blaney, J. M.; Oatley, S. J.; Langridge, R.; Ferrin, T. E. A geometric approach to macromolecule-ligand interactions. *J. Mol. Biol.* **1982**, *161*, 269 – 288.

26 Muegge, I.; Martin, Y. C. A general and fast scoring function for protein-ligand interactions: a simplified approach. *J. Med. Chem*. **1999**, *42*, 791 – 804.

27 Rarey, M.; Kramer, B.; Lengauer, T.; Klebe, G. A fast flexible docking method using an incremental construction algorithm. *J. Mol. Biol*. **1996**, *261*, 470 – 489.

28 Ravelli, R. B.; Gigant, B.; Curmi, P. A.; Jourdain, I.; Lachkar, S.; Sobel, A.; Knssow, M. Insight into tubulin regulation from a complex with colchicine and a stathmin-like domain. *Nature*, **2004**, *428*, 198 – 202.

29 Ravelli, R. B.; Gigant, B.; Curmi, P. A.; Jourdain, I.; Lachkar, S.; Sobel, A.; Knssow, M. Insight into tubulin regulation from a complex with colchicine and a stathmin-like domain. *Nature*, **2004**, *428*, 198 – 202.

Chapter 7: Concluding Remarks

The primary goal of this project was to optimize a promising lead compound, **SC-2-71**, into a structurally distinct analog that showed enhanced therapeutic properties towards cancer. The idea which serves as the foundation for this work - that drugs which can target a tumor by both starving it and poisoning it – is rooted in decades of continually evolving scientific work. Through the use of traditional medicinal chemistry techniques in conjunction with a blend of established and new synthetic procedures, we were able to make significant strides in enhancing the potency and therapeutic promise of this class of molecule.

After a methodical approach of functional group substitutions, additions, deletions, and other transformations across all 4 ring systems, the potential of each analog was studied through extensive biochemical and biological evaluation. While most of these modifications were detrimental to the activity of the DHQZ, the SAR study did show us several specific (as well as general) substitutions that enable us to increase the potency of our drug. When we incorporate several of these constructive changes into one hybrid structure, we observed a powerful synergistic effect in the 3rd generation of drug. Upon preliminary examination of this molecule's effects on mice, we were excited to learn that it is both biologically available and has extremely low toxicity.

In addition to the SAR study, we also went to great lengths to develop the first synthetic method to form each of the DHQZ enantiomers. After several failed approaches, we finally arrived at a chiral auxiliary based method which was amenable to these racemization-prone molecules. After exploring the scope and limitations of this approach by pursuing the asymmetric synthesis of several simple analogs, X-ray

crystallography was used in conjunction with polarimetry to determine the absolute configurations of each enantiomer. We then applied this new technique to construct each enantiomer of our most active analog **61**. Related anti-proliferation assays indicate that the R-enantiomer is the one responsible for the biological activity and was measured to have a GI_{50} value of ~100 picomolar in the MDA-MB-435 human breast cancer cell line.

While we remain enthusiastic about the potential of these drugs, future work and significant obstacles still remain. Although the A-ring nitro group was shown to increase activity significantly, this functional group is notorious for creating solubility problems and other complications down the road. Replacing this group with a similar electron withdrawing group such as an acid, ester, or ketone may limit these potential problems as well as provide an additional synthetic handle which we may exploit to add further complexity to our DHQZ. In addition, we have only created one hybrid compound thus far, yet there are other promising 2nd generation analogs with which we may apply this "structural hybrid" concept. Perhaps the most significant obstacle that remains is the relevant ADME studies on these compounds.

Through the use of synthetic and medicinal chemistry we have seen the structure of thalidomide evolve into a significantly different molecule. We have seen how it is possible to tune the properties of a notorious drug with a tragic past into a powerful cancer fighting agent. It is our hope that this work will form the cornerstone of a future cancer medicine and help ease the distress of people suffering from this affliction.

Chapter 8: Experimental Section

8.1 Materials. All reagents were purchased from Aldrich, Lancaster, Fisher, Acros or Strem and were used as received. Unless otherwise indicated, all reactions were run under an inert atmosphere of argon or nitrogen.

8.2 Analytical Procedures. Melting points were determined in open capillary tubes on an Electrothermal melting point apparatus and are uncorrected. ^{1}H and ^{13}C NMR spectra were measured at 25 ^{o}C on compounds solvated in $CDCl_3$ or DMSO-d_6 on a GE 300 MHz or Varian 300 MHz or 500 MHz spectrometer. APCI and ESI mass spectra were obtained on a Finnigan LcQ Classsic. Elemental analyses were performed by Atlantic Microlab, and microanalytical data were within ± 0.4 % of the calculated figures unless otherwise indicated. Thin-layer chromatography (TLC) was performed on precoated aluminum silica gel plates (silica gel 60 F_{254}).

8.3 Synthetic Procedures.

General Procedure A for Preparation of Anthranilic Acids 5b, 8b, and 10b.

Acetic anhydride (1.05 equiv.) was added to a solution of the substituted 2-methylaniline (1 equiv.) in 15 mL acetic acid, then brought to reflux for 2 hours (or until starting material disappears by TLC). The solvent was removed under reduced pressure and a saturated $NaHCO_3$ solution was added to the resulting residue. The precipitated acetanilide was collected by filtration and added to a round bottom flask containing

$MgSO_4$ (1 equiv.) and 150 mL H_2O. $KMnO_4$ (3 equiv.) was added and the purple mixture refluxed for 2 hours before being filtered hot. The brown precipitate was collected, heated in 100 mL H_2O, then filtered again. The volume of the combined aqueous filtrates was reduced to ca. 100 mL, then sodium bisulfite was added until the purple solution turned clear. The aqueous was acidified to a pH of 2 – 3, then extracted three times with ethyl acetate (25 mL). The combined organic layers were evaporated to yield a colorless solid which was taken up in 50 mL H_2O. Sodium hydroxide (3 equiv.) was added and the reaction was refluxed for 5 hours. After cooling to room temperature, the aqueous was acidified to pH of 2 – 3, then extracted three times with ethyl acetate (25 mL). The combined organics were dried with $MgSO_4$ and concentrated to yield the target anthranilic acid derivatives with no further purification.

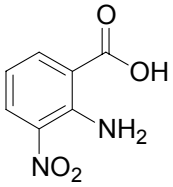

2-Amino-3-nitro-benzoic acid (5b). Compound **5b** was prepared from 2-methyl-6-nitro-phenylamine (2.00 g, 13.14 mmol) according to general procedure A to produce a bright yellow solid (59 %); carried on without further purification/characterization.

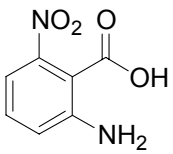

2-Amino-6-nitro-benzoic acid (8c). Compound **8c** was prepared from 2-methyl-3-nitro-phenylamine (2.00 g, 13.14 mmol) according to general procedure A to produce a yellow solid (39 %); carried on without further purification/characterization.

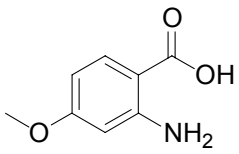

2-Amino-4-methoxy-benzoic acid (10c). Compound **10c** was prepared from 2-methyl-3-nitro-phenylamine (2.00 g, 13.14 mmol) according to general procedure A to produce a colorless solid (31 %): carried on without further purification/characterization.

General Procedure B for the Preparation of Anthranilamide Derivatives (1a-14a). EDC (1.05 equiv.) and HOBt (1.05 equiv.) were added to a solution of the substituted anthranilic acid (1 equiv.) in 25 mL DMF at 0 ^{o}C. After 30 minutes, 3 mL 28% of NH_4OH were added and the cooling bath was removed. After warming to room temperature over 1 hour, the solvent was removed *in vacuo* and the resulting residue was partitioned between ethyl acetate and water. The aqueous layer was extracted twice more, then the combined organics were dried with $MgSO_4$ and filtered. Concentration of the filtrate produced a residue that was purified by flash chromatography (hexane/ethyl acetate 1:1).

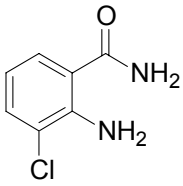

2-Amino-3-chloro-benzamide (1a). Compound **1a** was prepared from 2-amino-3-chloro-benzoic acid (1.00 g, 5.83 mmol) according to general procedure B to yield a colorless solid (84 %); mp: 161 – 162 ^{o}C; NMR (300 MHz, DMSO-d_6): δ 7.93 (s, 1H), 7.52 – 7.57 (d, *J*= 15 Hz, 1H), 7.36 – 7.38 (d, *J*= 12Hz, 1H), 7.34 (s, 1H), 6.71 (s, 2H), 6.53 – 6.56 (t, *J*= 4.5 Hz, 1H); ^{13}C NMR (75 MHz, DMSO-d_6): δ 171.01, 146.16, 132.36, 128.24, 119.50, 116.20, 115.36.

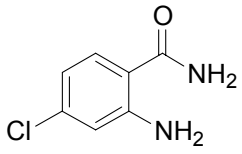

2-Amino-4-chloro-benzamide (2a). Compound **2a** was prepared from 2-amino-4-chloro-benzoic acid (1.00 g, 5.83 mmol) according to general procedure B to yield a colorless solid (81 %); mp: 180 – 182 ^{o}C; ^{1}H NMR (300 MHz, DMSO-d_6): δ 7.79, (s, 1H), 7.52 – 7.57 (d, J= 12 Hz, 1H), 7.17 (s, 1H), 6.83 – 6.86 (s, 2H), 6.73 – 6.77 (d, J= 12 Hz, 1H), 6.49 (s, 1H); ^{13}C NMR (75 MHz, DMSO-d_6): δ 170.90, 151.97, 136.79, 131.05, 115.54, 114.43, 112.79.

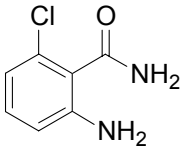

2-Amino-6-chloro-benzamide (4a). Compound **4a** was prepared from 2-amino-6-chloro-benzoic acid (1.00 g, 5.83 mmol) according to general procedure B to yield a colorless solid (82 %); mp: 130 – 132 ^{o}C; ^{1}H NMR (300 MHz, DMSO-d_6): δ 8.06 – 8.10 (t, J= 6 Hz, 1H), 7.11 – 7.16 (d, J= 15 Hz, 1H), 6.96 – 6.97 (d, J= 3 Hz, 1H), 6.63 (s, 2H); ^{13}C NMR (75 MHz, DMSO-d_6): δ 161.31, 150.25, 134.22, 133.41, 120.12, 114.30, 111.13.

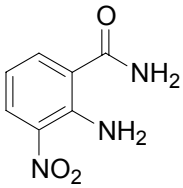

2-Amino-3-nitro-benzamide (5a). Compound **5a** was prepared from 2-amino-3-nitro-benzoic acid (0.74 g, 4.08 mmol) according to general procedure B to yield an orange solid (95 %); mp: 130 – 132 ^{o}C; ^{1}H NMR (300 MHz, DMSO-d_6); δ 8.48 (s, 2H), 8.17 – 8.19 (d, J= 6 Hz, 1H), 8.15 (s, 1H), 7.94 – 7.96 (d, J= 6 Hz, 1H), 7.62 (s, 1H), 6.66 – 6.69 (t, J= 4.5 Hz, 1H); ^{13}C NMR (75 MHz, DMSO-d_6): δ 170.43, 146.53, 136.91, 129.92, 119.28, 114.15, 100.89.

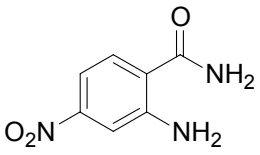

2-Amino-4-nitro-benzamide (6a). Compound **6a** was prepared from 2-amino-4-nitro-benzoic acid (1.00 g, 5.55 mmol) according to general procedure B to yield an orange solid (73 %); mp: 221 – 222 ^{o}C.

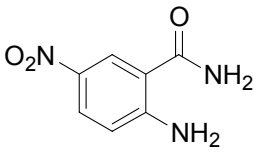

2-Amino-5-nitro-benzamide (7a). Compound **7a** was prepared from 2-amino-5-nitro-benzoic acid (0.75 g, 4.13 mmol) according to general procedure B to yield an orange solid (52 %); mp: 237 – 239 ^{o}C; ^{1}H NMR (300 MHz, DMSO-d_6): δ 8.55 (s, 1H), 8.20 (s, 1H), 7.98 - 8.03 (d, J= 15 Hz, 1H), 7.89 (s, 2H), 7.40 (s, 1H), 6.75 – 6.80 (d, J= 15 Hz, 1H); ^{13}C NMR (75 MHz, DMSO-d_6): δ 170.15, 156.18, 135.28, 127.99, 126.90, 116.44, 112.47.

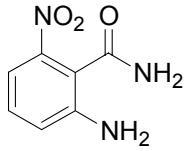

2-Amino-6-nitro-benzamide (8a). Compound **8a** was prepared from 2-amino-6-nitro-benzoic acid (0.74 g, 4.06 mmol) according to general procedure B to yield an orange solid (52 % yield); mp: 237 – 239 ^{o}C.

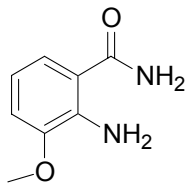

2-Amino-3-methoxy-benzamide (9a). Compound **9a** was prepared from 2-amino-3-methoxy-benzoic acid (1.00 g, 5.98 mmol) according to general procedure B to yield a colorless solid (61 %); mp: 140 – 142 ^{o}C; ^{1}H NMR (300 MHz, DMSO-d_6): δ 7.72 (s, 1H), 7.18 – 7.20 (d, J= 6 Hz, 1H), 7.10 (s, 1H), 6.87 – 6.88 (d, J= 3 Hz, 1H), 6.46 – 6.49 (t, J= 4.5 Hz, 1H), 6.28 (s, 2H), 3.78 (s, 3H); ^{13}C NMR (75 MHz, DMSO-d_6): δ 171.69, 147.35, 140.69, 120.89, 114.11, 113.80, 112.42, 56.00.

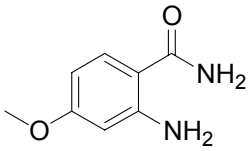

2-Amino-4-methoxy-benzamide (10a). Compound **10a** was prepared from 2-amino-4-methoxy-benzoic acid (0.70 g, 4.19 mmol) according to general procedure B to yield a colorless solid (71 %); mp: 154 – 156 ^{o}C; ^{1}H NMR (300 MHz, DMSO-d_6): δ 7.56 (s, 1H), 7.48 – 7.52 (d, J= 12 Hz, 1H), 6.85 (s, 1H), 6.77 (s, 2H), 6.19 – 6.22 (d, J= 9 Hz, 1H), 6.05 – 6.09 (s, 1H), 3.69 (s, 3H); ^{13}C NMR (75 MHz, DMSO-d_6): δ 171.49, 162.64, 152.88, 130.94, 107.28, 102.61, 99.72, 55.23.

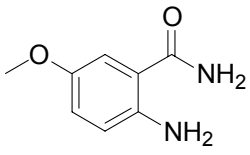

2-Amino-5-methoxy-benzamide (11a). Compound **11a** was prepared from 2-amino-5-methoxy-benzoic acid (1.00 g, 5.98 mmol) according to general procedure B to yield a colorless solid (64 %); mp: 111 – 114 ^{o}C.

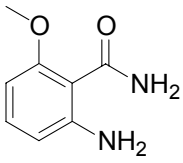

2-Amino-6-methoxy-benzamide (12a). Compound **12a** was prepared from 2-amino-6-methoxy-benzoic acid (1.00 g, 5.98 mmol) according to general procedure B to yield a colorless solid (65 %); mp: 151 – 152 ^{o}C; ^{1}H NMR (300 MHz, DMSO-d_6): δ 7.57 (s, 1H), 7.28 (s, 1H), 7.00 – 7.03 (t, *J*= 4.5 Hz, 1H), 6.37 (s, 2H), 6.31 – 6.32 (d, *J*= 3 Hz, 1H), 6.17 – 6.18 (d, *J*= 3 Hz, 1H), 3.76 (s, 3H); ^{13}C NMR (75 MHz, DMSO-d_6): δ 169.86, 158.99, 151.53, 131.60, 109.92, 105.56, 98.45, 56.02.

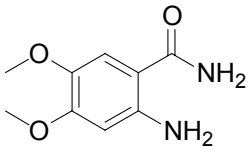

2-Amino-4,5-dimethoxy-benzamide (13a). Compound **13a** was prepared from 2-amino-4,5-dimethoxy-benzoic acid (1.50 g, 7.65 mmol) according to general procedure B to yield a colorless solid (8 %); mp: 141 – 143 ^{o}C; ^{1}H NMR (300 MHz, DMSO-d_6): δ 7.54 (s, 1H), 7.11 (s, 1H), 6.84 (s, 1H), 6.44 (s, 2H), 6.28 (s, 1H), 3.70 (s, 3H), 3.66 (s, 3H); ^{13}C NMR (75 MHz, DMSO-d_6): δ 170.93, 152.95, 146.82, 138.88, 112.98, 104.24, 99.71, 56.59, 55.08..

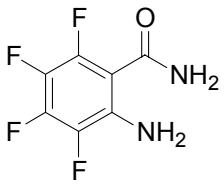

2-Amino-3,4,5,6-tetrafluoro-benzamide (14a). Compound **14a** was prepared from 2-amino-3,4,5,6-tetrafluoro-benzoic acid (0.20 g, 0.96 mmol) according to general procedure B to yield a colorless solid (59 %); mp: 141 – 143 ^{o}C; ^{1}H NMR (300 MHz, DMSO-d$_6$) δ7.85 (bs, 2H), 6.02 (bs, 2H).

General Procedure C for Preparation of Quinazolinone Derivatives (1 – 61). A solution of the aldehyde (1 equiv.) and anthranilamide (1 equiv.) in acetonitrile (25 mL), containing a catalytic amount of glacial acetic acid, was refluxed with stirring for 5-12 hours. If a solid precipitated out of solution after cooling to room temperature, it was collected by suction filtration and recrystallized from ethanol to give the pure quinazolinone analog. If it stayed in solution after cooling, all solvent was removed and the resulting residue was purified by flash chromatography (hexane/ethyl acetate 1:1).

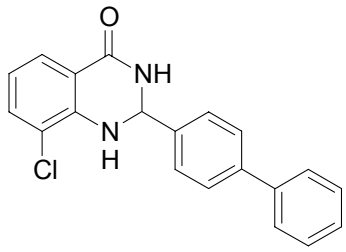

2-Biphenyl-4-yl-8-chloro-2,3-dihydro-1H-quinazolin-4-one (1). Compound **1** was prepared from 4-biphenylcarboxaldehyde (0.32 g, 1.76 mmol) and 2-amino-3-chloro-benzamide **1a** (0.30 g, 1.76 mmol) according to general procedure C to yield a colorless solid (36 %); mp: 183 – 185 ^{o} C; ^{1}H NMR (300 MHz, DMSO-d_6): δ 8.78 (s, 1H), 7.61 – 7.66 (t, *J*= 7.5 Hz, 5H), 7.51 – 7.54 (d, *J*= 9 Hz, 2H), 7.40 – 7.45 (t, *J*= 7.5 Hz, 3H), 7.33 – 7.35 (t, *J*= 3 Hz, 1H), 7.19 (s, 1H), 6.70 – 6.72 (t, *J*= 3 Hz, 1H), 5.86 (s, 1H); ^{13}C NMR (75 MHz, DMSO-d_6): δ 163.08, 143.79, 142.28, 140.71, 140.32, 133.88, 129.60, 128.23, 128.23, 127.39, 127.21, 118.47, 118.17, 117.52, 65.50; APCI *m/z* (rel intensity) 334.9 (M^+, 100); Anal. ($C_{20}H_{15}ClN_2O$) C, H, N; C: calcd, 71.75; found, 71.60; H: calcd, 4.52; found, 4.60; N: calcd, 8.37; found, 8.39.

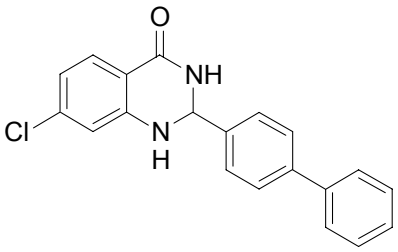

2-Biphenyl-4-yl-7-chloro-2,3-dihydro-1H-quinazolin-4-one (2). Compound **2** was prepared from 4-biphenylcarboxaldehyde (0.32 g, 1.76 mmol) and 2-amino-4-chloro-benzamide **2a** (0.30 g, 1.76 mmol) according to general procedure C to yield a colorless solid (56 %); mp: 271 – 273 ^{o}C; ^{1}H NMR (500 MHz, DMSO-d_6): δ 8.47 (s, 1H), 7.68 – 7.69 (d, *J*= 3 Hz, 2H), 7.64 – 7.65 (d, *J*= 3 Hz, 2H), 7.59 – 7.61 (d, *J*= 6 Hz, 1H), 7.54 – 7.55 (d, *J*= 3 Hz, 2H), 7.44 – 7.47 (m, 3H), 7.34 – 7.37 (t, *J*= 4.5 Hz, 1H), 6.78 – 6.79 (d, *J*= 3 Hz, 1H), 6.67 – 6.89 (m, 1H), 5.85 (s, 1H); ^{13}C NMR (75 MHz, DMSO-d_6): δ 163.38, 149.39, 141.15, 140.31, 138.52, 130.05, 129.63, 129.22, 128.28, 128.01, 127.40, 114.32, 114.11, 66.74; APCI *m/z* (rel

intensity) 335.4 (M^+, 100); Anal. ($C_{20}H_{15}ClN_2O$) C, H, N; C: calcd, 71.75; found, 72.01; H: calcd, 4.52; found, 4.59; N: calcd, 8.37; found, 8.43.

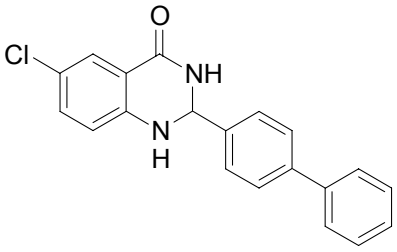

2-Biphenyl-4-yl-6-chloro-2,3-dihydro-1H-quinazolin-4-one (3). Compound **3** was prepared from 4-biphenylcarboxaldehyde (0.80 g, 4.40 mmol) and 2-amino-5-chloro-benzamide (0.75 g, 4.40 mmol) **3a** according to general procedure C to yield a colorless solid (48 %): mp: 247 – 249 ^oC; ^1H NMR (300 MHz, DMSO-d_6): δ 8.56 (s, 1H), 7.57 – 7.70 (m, 4H), 7.48 – 7.56 (m, 3H), 7.36 – 7.57 (m, 4H), 7.27 – 7.31 (m, 1H), 6.78 – 6.82 (d, *J*= 12 Hz, 1H), 5.84 (s, 1H); ^{13}C NMR (75 MHz, DMSO-d_6): δ 162.45, 146.57, 140.46, 139.67, 133.14, 128.97, 127.61, 127.42, 126.73, 126.45, 120.77, 116.46, 116.07, 66.07; APCI *m/z* (rel intensity) 334.9 (M^+, 100). Anal. ($C_{16}H_{12}N_2O$) C, H, N; C: calcd, 71.75; found, 71.41; H: calcd, 4.52; found, 4.35; N: calcd, 8.37; found, 8.27.

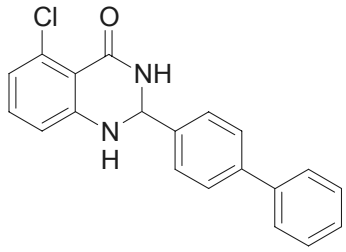

2-Biphenyl-4-yl-5-chloro-2,3-dihydro-1H-quinazolin-4-one (4). Compound **4** was prepared from 4-biphenylcarboxaldehyde (0.32 g, 1.76 mmol) and 2-amino-6-chloro-benzamide **4a** (0.30 g, 1.76 mmol) according to general procedure C to yield a colorless solid (22 %); mp: 225 – 227 ^oC; ^1H NMR (300 MHz, DMSO-d_6): δ 8.51 (s, 1H), 7.64 – 7.70 (t, *J*= 9 Hz, 4H), 7.55 – 7.58 (d, *J*= 9 Hz, 2H), 7.51 (s, 1H), 7.43 – 7.48 (t, *J*= 7.5 Hz, 2H), 7.33 – 7.38 (t, *J*= 7.5 Hz, 1H), 7.14 – 7.20 (t, *J*= 9 Hz, 1H), 6.77 – 6.80 (d, *J*= 9 Hz, 1H), 6.68 – 6.70 (d, *J*= 6 Hz, 1H), 5.72 (s,

1H); ^{13}C NMR (75 MHz, DMSO-d_6): δ 166.74, 156.06, 145.87, 145.35, 145.09, 139.31, 138.53, 134.41, 133.01, 132.44, 132.15, 125.74, 119.47, 117.55, 70.68; APCI *m/z* (rel intensity) 334.9 (MH^+, 100); Anal. ($C_{20}H_{15}ClN_2O$) C, H, N; C: calcd, 71.75; found, 71.80; H: calcd, 4.52; found, 4.63; N: calcd, 8.37; found, 8.39.

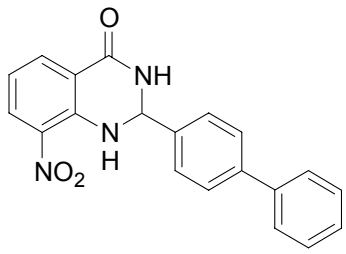

2-Biphenyl-4-yl-8-nitro-2,3-dihydro-1H-quinazolin-4-one (5). Compound **5** was prepared from 4-biphenylcarboxaldehyde (0.20 g, 1.10 mmol) and 2-amino-3-nitro-benzamide **5a** (0.20 g, 1.10 mmol) according to general procedure C to yield an orange-yellow solid (71 %); mp: 171 – 173 ^{o}C; ^{1}H NMR (300 MHz, DMSO-d_6): δ 9.04 – 9.06 (d, *J*= 6 Hz, 1H), 9.01 – 9.03 (d, *J*= 6 Hz, 1H), 8.22 – 8.25 (d, *J*= 9 Hz, 1H), 8.07 – 8.10 (d, *J*= 9 Hz, 1H), 7.60 – 7.66 (m, 3H), 7.40 – 7.49 (m, 3H), 7.33 – 7.36 (t, *J*= 4.5 Hz, 1H), 6.80 – 6.85 (t, *J*= 7.5 Hz, 1H), 6.02 – 6.04 (t, *J*= 3 Hz, 1H); ^{13}C NMR (75 MHz, DMSO-d_6): δ 161.76, 142.91, 141.91, 140.98, 140.24, 136.22, 132.85, 131.28, 129.66, 128.35, 127.69, 127.44, 127.13, 119.37, 116.76, 64.95; APCI *m/z* (rel intensity) 345.3 (M^+, 100); Anal. ($C_{20}H_{15}N_3O_3 \cdot 0.9H_2O$) C, H, N; C: calcd, 66.44; found, 66.14; H: calcd, 4.68; found, 4.37; N: calcd, 11.62; found, 11.39.

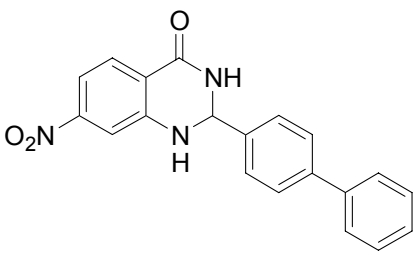

2-Biphenyl-4-yl-7-nitro-2,3-dihydro-1H-quinazolin-4-one (6). Compound **6** was prepared from 4-biphenylcarboxaldehyde (0.40 g, 2.20 mmol) and 2-amino-4-nitro-benzamide **6a** (0.40 g, 2.20 mmol) according to general procedure C to yield an orange-yellow solid (21 %); mp: 233 – 235

^{o}C; ^{1}H NMR (300 MHz, DMSO-d_6): δ 8.78 (s, 1H), 7.81 – 7.85 (m, 2H), 7.63 – 7.71 (m, 4H), 7.54 – 7.58 (m, 3H), 7.41 – 7.48 (m, 3H), 7.33 – 7.38 (t, *J*= 7.5 Hz, 1H), 5.95 (s, 1H); ^{13}C NMR (75 MHz, DMSO-d_6): δ 162.55, 151.47, 148.82, 141.29, 140.91, 140.26, 129.85, 129.66, 128.34, 127.99, 127.54, 127.41,11.73, 109.55, 109.36, 66.66; APCI *m/z* (rel intensity) 345.3, (M^+, 100); Anal. ($C_{20}H_{15}N_3O_3$) C, H, N; C: calcd, 69.56; found, 69.32; H: calcd, 4.38; found, 4.42; N: calcd, 12.17; found, 12.15.

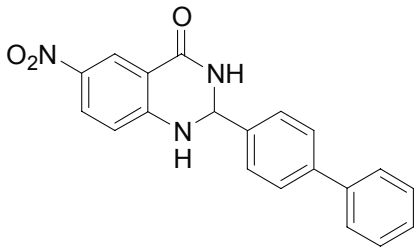

2-Biphenyl-4-yl-6-nitro-2,3-dihydro-1H-quinazolin-4-one (7). Compound **7** was prepared from 4-biphenylcarboxaldehyde (0.15 g, 0.83 mmol) and 2-amino-5-nitro-benzamide **7a** (0.15 g, 0.83 mmol) according to general procedure C to yield an yellow solid (66 %); mp: 263 – 265 ^{o}C; ^{1}H NMR (300 MHz, DMSO-d_6): δ 8.82 (s, 1H), 8.64 (s, 1H), 8.44 – 8.45 (d, *J*= 3 Hz, 1H), 8.10 – 8.14 (dd, *J*= 4 Hz, 1H), 7.71 – 7.74 (d, *J*= 9 Hz, 2H), 7.65 – 7.68 (d, *J*= 9 Hz, 2H), 7.56 – 7.54 (d, *J*= 6 Hz, 2H), 7.54 – 7.56 (d, *J*= 6 Hz, 2H), 7.45 – 7.50 (t, *J*= 7.5 Hz, 2H), 7.38 – 7.40 (t, *J*= 3 Hz, 1H), 6.83 – 6.86 (d, *J*= 9 Hz, 1H), 6.07 (s, 1H); ^{13}C NMR (75 MHz, DMSO-d_6): δ 161.38, 152.16, 140.80, 140.27, 139.57, 137.17, 129.02, 127.73, 127.18, 127.02, 126.76, 124.40, 122.10, 114.35, 112,72, 65.96; APCI *m/z* (rel intensity) 345.7, (M^+, 85); Anal. ($C_{20}H_{15}N_3O_3 \cdot 0.6H_2O$) C, H, N; C: calcd, 67.45; found, 67.41; H: calcd, 4.58; found, 4.50; N: calcd, 11.80; found, 11.70.

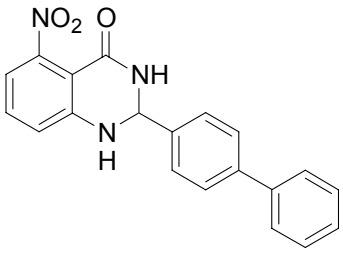

2-Biphenyl-4-yl-5-nitro-2,3-dihydro-1H-quinazolin-4-one (8). Compound **8** was prepared from 4-biphenylcarboxaldehyde (0.40 g, 2.21 mmol) and 2-amino-6-nitro-benzamide **8a** (0.40 g, 2.21 mmol) according to general procedure C to yield an orange solid (79 %); mp: 243 – 245 ^{o} C; ^{1}H NMR (300 MHz, DMSO-d_6): δ 8.79 (s, 1H), 7.95 (s, 1H), 7.65 – 7.73 (m, 4H), 7.58 – 7.61 (d, 2H), 7.43 – 7.48 (t, *J*= 7.5 Hz, 2H), 7.34 – 7.41 (m, 2H), 6.99 – 7.02 (d, *J*= 9 Hz, 1H), 6.88 – 6.91 (d, *J*= 9 Hz, 1H), 5.87 (s, 1H); ^{13}C NMR (75 MHz, DMSO-d_6): δ 160.53, 151.49, 149.74, 141.34, 140.27, 140.02, 134.20, 129.67, 128.35, 128.25, 127.47, 127.43, 118.35, 112.33, 106.84, 65.97; APCI *m/z* (rel intensity) 345.3 (M^+, 100); Anal. ($C_{20}H_{15}N_3O_3$) C, H, N; C: calcd, 69.56; found, 69.46; H: calcd, 4.38; found, 4.47; N: calcd, 12.17; found, 12.23.

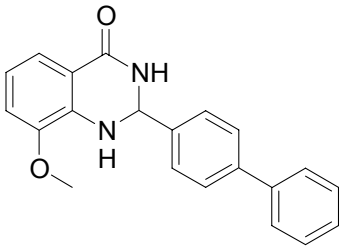

2-Biphenyl-4-yl-8-methoxy-2,3-dihydro-1H-quinazolin-4-one (9). Compound **9** was prepared from 4-biphenylcarboxaldehyde (0.33 g, 1.79 mmol) and 2-amino-3-methoxy-benzamide **9a** (0.30 g, 1.79 mmol) according to general procedure C to yield a colorless solid (79 %); mp: 271 – 273 ^{o} C; ^{1}H NMR (300 MHz, DMSO-d_6): δ 8.42 – 8.43 (d, J= 3 Hz, 1H), 7.61 – 7.63 (d, J= 6 Hz, 4H), 7.43 – 7.50 (m, 4H), 7.33 – 7.35 (d, J= 6 Hz, 1H), 7.21 – 7.24 (d, J= 9 Hz, 1H), 6.93 – 6.96 (d, J= 9 Hz, 1H), 6.59 – 6.62 (t, J= 9 Hz, 2H), 5.74 (s, 1H), 3.78 (s, 3H); ^{13}C NMR (75 MHz, DMSO-d_6): δ 164.01, 146.79, 142.49, 140.60, 140.41, 137.80, 129.60, 128.19, 127.54, 127.36, 127.25, 119.57, 117.04, 115.71, 114.25, 65.96, 56.37; APCI *m/z* (rel intensity)

330.8 (M^+, 100); Anal. ($C_{21}H_{18}N_2O_2 \cdot 0.3H_2O$) C, H, N; C: calcd, 75.13; found, 75.06; H: calcd, 5.58; found, 5.42; N: calcd, 8.34; found, 8.48.

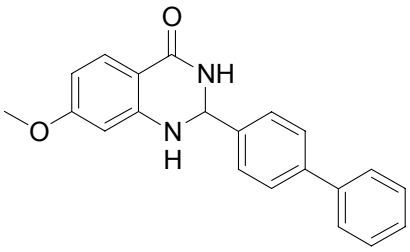

2-Biphenyl-4-yl-7-methoxy-2,3-dihydro-1H-quinazolin-4-one (10). Compound **10** was prepared from 4-biphenylcarboxaldehyde (0.19 g, 1.02 mmol) and 2-amino-4-methoxy-benzamide **10a** (0.17 g, 1.02 mmol) according to general procedure C to yield a colorless solid (53 %); mp: 231 – 233 ^oC; ^1H NMR (300 MHz, DMSO-d_6): δ 8.14 (s, 1H), 7.63 – 7.68 (t, *J*= 7.5 Hz, 3H), 7.53 – 7.55 (m, *J*= 6 Hz, 2H), 7.42 – 7.47 (t, *J*= 7.5 Hz, 2H), 7.35 – 7.37 (t, *J*= 3 Hz, 1H), 7.16 (s, 1H), 6.24 – 6.26 (m, 2H), 5.75 (s, 1H), 3.70 (s, 3H); ^{13}C NMR (75 MHz, DMSO-d_6): δ 164.19, 150.07, 141.77, 140.92, 140.41, 129.94, 129.64, 128.25, 128.00, 127.54, 127.38, 128.37, 109.12, 105.46, 98.44, 66.89, 55.71; Anal. ($C_{21}H_{18}N_2O_2$) C, H, N; C: calcd, 76.34; found, 76.56; H: calcd, 5.49; found, 5.62; N: calcd, 8.48; found, 8.59.

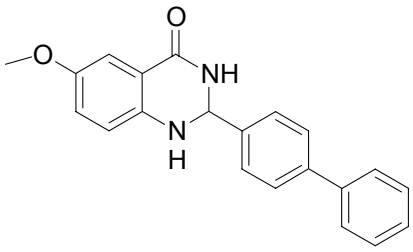

2-Biphenyl-4-yl-6-methoxy-2,3-dihydro-1H-quinazolin-4-one (11). Compound **11** was prepared from 4-biphenylcarboxaldehyde (0.22 g, 1.20 mmol) and 2-amino-5-methoxy-benzamide **11a** (0.20 g, 1.20 mmol) according to general procedure C to yield a colorless solid (26 %); mp: 283 – 285 ^oC; ^1H NMR (300 MHz, DMSO-d_6): δ 8.38 (s, 1H), 7.62 – 7.67 (t, *J*= 7.5 Hz, 4H), 7.54 – 7.57 (d, *J*= 9 Hz, 2H), 7.41 – 7.46 (t, *J*= 7.5 Hz, 2H), 7.34 – 7.36 (t, *J*= 3 Hz, 1H), 7.14 – 7.15 (d, *J*= 3 Hz, 1H), 6.89 – 6.93 (dd, *J*= 4 Hz, 1H), 6.72 – 6.75 (d, *J*= 9 Hz, 1H), 5.72

(s, 1H), 3.66 (s, 3H); ^{13}C NMR (75 MHz, DMSO-d_6): δ 164.32, 152.12, 142.89, 141.35, 140.95, 140.40, 129.64, 128.25, 127.37, 127.26, 122.19, 116.88, 116.40, 110.51, 67.18, 55.95; APCI *m/z* (rel intensity) 330.8 (M^+, 100); Anal. ($C_{21}H_{18}N_2O$) C, H, N; C: calcd, 76.34; found, 76.24; H: calcd, 5.49; found, 5.52; N: calcd, 8.48; found, 8.53.

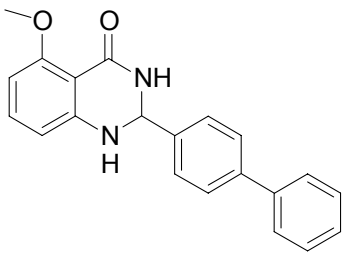

2-Biphenyl-4-yl-5-methoxy-2,3-dihydro-1H-quinazolin-4-one (12). Compound **12** was prepared from 4-biphenylcarboxaldehyde (0.22 g, 1.20 mmol) and 2-amino-6-methoxy-benzamide **12a** (0.20 g, 1.20 mmol) according to general procedure C to yield a colorless solid (55 %); mp: 302 – 304 ^{o}C; ^{1}H NMR (300 MHz, DMSO-d_6): δ 8.07 (s, 1H), 7.63 – 7.68 (m, 4H), 7.52 – 7.55 (d, *J*= 9 Hz, 2H), 7.42 – 7.47 (t, *J*= 7.5 Hz, 2H), 7.32 – 7.37 (t, *J*= 7.5 Hz, 1H), 7.19 (s, 1H), 7.10 – 7.15 (t, *J*= 7.5 Hz, 1H), 6.36 – 6.39 (d, *J*= 9 Hz, 1H), 6.24 – 6.27 (d, *J*= 9 Hz, 1H), 5.71 (s, 1H); ^{13}C NMR (75 MHz, DMSO-d_6): δ 162.71, 161.30, 150.91, 141.32, 140.82, 140.43, 134.17, 129.64, 128.17, 127.38, 127.24, 108.05, 105.23, 101.74, 65.94, 56.02; ESI *m/z* (rel intensity) 330.9 (M^+, 100); Anal. ($C_{21}H_{18}N_2O$) C, H, N; C: calcd, 76.34; found, 75.95; H: calcd, 5.49; found, 5.79; N: calcd, 8.48; found, 8.29.

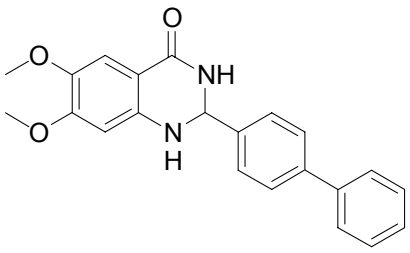

2-Biphenyl-4-yl-6,7-dimethoxy-2,3-dihydro-1H-quinazolin-4-one (13). Compound **13** was prepared from 4-biphenylcarboxaldehyde (0.14 g, 0.76 mmol) and 2-amino-4,5-dimethoxy-benzamide **13a** (0.15 g, 0.76 mmol) according to general procedure C to yield a colorless solid (25 %); mp: 209 –

210 °C; ^{1}H NMR (300 MHz, DMSO-d_6): δ 8.12 (s, 1H), 7.65 – 7.68 (t, *J*= 9 Hz, 4H), 7.56 – 7.57 (d, *J*= 3 Hz, 2H), 7.44 – 7.47 (t, *J*= 9 Hz, 2H), 7.35 – 7.38 (t, *J*= 9 Hz, 1H), 7.11 (s, 1H), 6.85 (s, 1H), 6.37 (s, 1H), 5.73 (s, 1H), 3.72 (s, 3H), 3.67 (s, 3H); ^{13}C NMR (75 MHz, DMSO-d_6): δ 163.78, 153.89, 143.55, 141.49, 141.04, 140.04, 140.23, 139.78, 128.99, 127.58, 127.45, 126.72, 126.60, 109.79, 106.69, 97.97, 66.55, 55.80, 55.40; APCI *m/z* (rel intensity) 360.8 (M^+, 25) 343.8 (100); Anal. ($C_{22}H_{20}N_2O_3 \cdot 0.2H_2O$) C, H, N; C: calcd, 72.59; found, 72.42; H: calcd, 5.65; found, 5.30; N: calcd, 7.70; found, 7.69.

2-Biphenyl-4-yl-5,6,7,8-tetrafluoro-2,3-dihydro-1H-quinazolin-4-one (14).

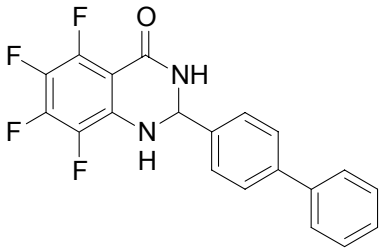

Compound **14** was prepared from 4-biphenylcarboxaldehyde (0.08 g, 0.43 mmol) and 2-amino-3,4,5,6-tetrafluoro-benzamide **14a** (0.14 g, 0.43mmol) according to general procedure C to yield a yellow solid (54.0 %); mp: 209 – 211 °C: ^{1}H NMR (300 MHz, DMSO-d_6): δ ^{1}H NMR (300 MHz, DMSO-d_6) δ 8.84 (s, 1H), 7.92 (s, 1H), 7.31-7.74 (m, 9H), 5.80 (s, 1H); ^{13}C NMR (75 MHz, DMSO-d_6) δ 158.8, 140.5, 139.8, 139.7, 133.6, 129.2, 129.0, 127.6, 127.2, 126.8, 65.3; ESI *m/z* (rel intensity) 371.1 (M-1, 100); Anal. ($C_{20}H_{12}F_4N_2O$) C, H, N; calcd, 64.52; found, 64.59; H: calcd, 3.25; found, 3.29; N: calcd, 7.52; found, 7.53.

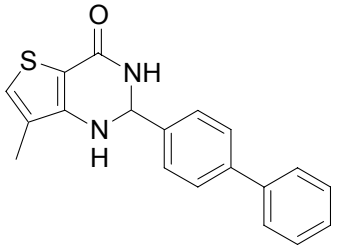

2-Biphenyl-4-yl-7-methyl-2,3-dihydro-1H-thieno[3,2-d]pyrimidin-4-one (15). Compound **15** was prepared from 4-biphenylcarboxaldehyde (0.23 g, 1.28 mmol) and 3-amino-4-methyl-thiophene-2-carboxylic acid amide (0.20 g, 1.28 mmol) according to general procedure C to yield a colorless solid (71 %); mp: 185 – 186 ^{o}C; ^{1}H NMR (300 MHz, DMSO-d_6): δ 8.67 (s, 1H), 8.00 – 8.04 (m, 3H), 7.83 – 7.88 (m, 2H), 7.74 – 7.78 (m, 2H), 7.49 – 7.53 (m, 3H), 7.40 – 7.44 (m, 1H), 7.01 (s, 1H), 2.30 (s, 3H); ^{13}C NMR (75 MHz, DMSO-d_6): δ 165.26, 157.93, 153.32, 143.46, 139.03, 138.10, 134.20, 130.66, 129.62, 129.10, 128.27, 127.20, 126.88, 117.10, 16.82; APCI *m/z* (rel intensity) 320.4 (M^+, 100); Anal. ($C_{19}H_{16}N_2OS$) C, H, N; C: calcd, 71.22; found, 71.53; H: calcd, 5.03; found, 4.63; N: calcd, 8.74; found, 8.37.

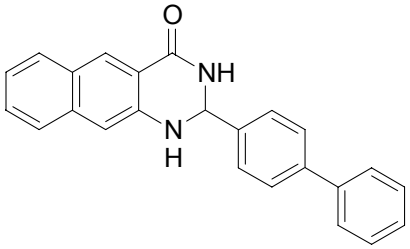

2-Biphenyl-4-yl-2,3-dihydro-1H-benzo[g]quinazolin-4-one (16). Compound **16** was prepared from 4-biphenylcarboxaldehyde (0.32 g, 1.77 mmol) and 3-aminonaphthalene-2-carboxylic acid amide **16a** (0.33 g, 1.77 mmol); mp: 284 - 285 °C (dec); ^{1}H NMR (300 MHz, DMSO-d_6) δ 8.78 (s, 1H); 8.34 (s, 1H), 7.14-7.87 (m, 14H), 7.01 (s, 1H), 5.81 (s, 1H); ^{13}C NMR (75 MHz, DMSO-d_6) δ 163.0, 144.4, 141.2, 140.3, 139.7, 136.7, 129.3, 129.0, 128.7, 128.2, 127.6, 127.4, 126.8, 125.4, 122.6, 118.2, 107.7, 66.1; ESI *m/z* (rel intensity) 190.7 (M-60.1, 100), 350.8 (M^+, 20); Anal. ($C_{24}H_{18}N_2O$) C, H, N; calcd, 80.23; found, 80.02; H: calcd, 5.77; found, 5.54; N: calcd, 8.91; found, 9.09.

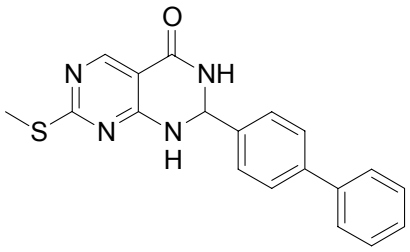

2-Biphenyl-4-yl-7-methylsulfanyl-2,3-dihydro-1H-pyrimido[4,5-d]pyrimidin-4-one (17). Compound **17** was prepared from 4-biphenylcarboxaldehyde (0.20 g, 1.09 mmol) and 4-amino-2-methylsulfanyl-pyrimidine-5-carboxylic acid amide (0.20 g, 1.09 mmol) according to general procedure C to yield a colorless solid (34 %); mp: 267 – 268 ^{o}C; ^{1}H NMR (300 MHz, DMSO-d_6): δ 9.03 (s, 1H), 8.66 (s, 1H), 8.41 (s, 1H), 7.65 – 7.72 (m, 4H), 7.45 – 7.49 (m, 2H), 7.36 – 7.40 (d, *J*= 12 Hz, 1H), 5.96 (s, 1H), 2.45 (s, 3H); ^{13}C NMR (75 MHz, DMSO-d_6): δ 174.93, 161.24, 159.76, 154.35, 140.88, 140.56, 139.57, 128.99, 127.69, 127.02, 126.75, 103.05, 64.95, 13.50; APCI *m/z* (rel intensity) 348.6 (M^+, 100); Anal. ($C_{17}H_{16}N_4OS \cdot 0.4H_2O$) C, H, N; C: calcd, 64.17; found, 64.46; H: calcd, 4.76; found, 4.73; N: calcd, 15.76; found, 15.71.

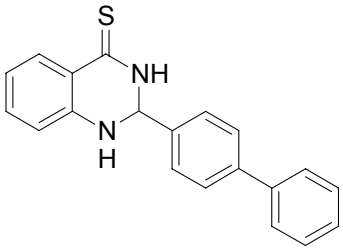

2-Biphenyl-4-yl-2,3-dihydro-1H-quinazoline-4-thione (18). 2-Biphenyl-4-yl-2,3-dihydro-1H-quinazolin-4-one (0.25 g, 0.83 mmol) was refluxed with Lawesson's reagent (0.17 g, 0.42 mmol) in toluene for 3 hours. After cooling to room temperature, the reaction was filtered through celite (which was then washed thoroughly with 3 20 mL portions of acetone). The filtrate was concentrated and purified by flash chromatography (hexane/ethyl acetate 1:1) to yield a yellow solid that still contained significant impurity. The solid was triturated with ethanol, filtered, and the filtrate concentrated. The resulting solid was recrystallized from ethanol to yield yellow crystals (16 %); mp: 210 – 212 ^{o} C; ^{1}H NMR (300 MHz, DMSO-d_6): δ 10.62 (s, 1H), 8.04 – 8.06 (d, *J*= 6 Hz, 1H), 7.63 – 7.68 (m, 5H), 7.42 – 7.52 (m, 4H), 7.35 – 7.38 (d, *J*=

9 Hz, 1H), 7.24 – 7.30 (t, *J*= 12 Hz, 1H), 6.75 – 6.78 (d, *J*= 9 Hz, 1H), 6.64 – 6.69 (t, *J*= 7.5 Hz, 1H), 5.82 (s, 1H); ^{13}C NMR (75 MHz, DMSO-d_6): δ 189.19, 143.37, 140.34, 140.20, 139.63, 134.22, 131.54, 128.99, 128.98, 127.63, 127.11, 126.74, 119.53, 117.42, 114.88, 65.23; APCI *m/z* (rel intensity) 314.6 (M-1.6, 100), 316.2 (M^+, 75); Anal. ($C_{20}H_{16}N_2S$) C, H, N; C: calcd, 75.92; found, 75.75; H: calcd, 5.10; found, 5.05; N: calcd, 8.85; found, 8.85.

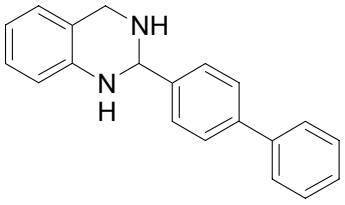

2-Biphenyl-4-yl-1,2,3,4-tetrahydro-quinazoline (19). Compound **19** was prepared from 4-biphenylcarboxaldehyde (0.75 g, 4.12 mmol) and 2-aminomethyl-phenylamine (0.50 g, 4.12 mmol) according to general procedure C to yield a colorless solid (69 %); mp: 129 – 130 ^{o}C: ^{1}H NMR (300 MHz, DMSO-d_6): δ 7.65 – 7.68 (d, *J*= 9 Hz, 4H), 7.57 – 7.60 (d, *J*= 9 Hz, 2H), 7.44 – 7.49 (t, *J*= 7.5 Hz, 2H), 7.33 – 7.38 (s, 1H), 6.90 – 6.95 (t, *J*= 7.5 Hz, 1H), 6.81 – 6.84 (d, *J*= 9 Hz, 1H), 6.60 – 6.63 (d, *J*= 9 Hz, 1H), 6.48 – 6.53 (t, *J*= 7.5 Hz, 1H), 6.19 (s, 1H), 5.16 (s, 1H), 3.96 – 4.00 (d, *J*= 12 Hz, 1H), 3.70 – 3.75 (d, *J*= 15 Hz, 1H), 2.81 (s, 1H); ^{13}C NMR (75 MHz, DMSO-d_6): δ 144.53, 142.07, 140.04, 139.48, 128.95, 127.69, 127.39, 126.66, 126.59, 126.43, 125.71, 120.73, 115.90, 114.21, 67.79, 44.92; APCI *m/z* (rel intensity) 286.9 (M^+, 100); Anal. ($C_{20}H_{18}N_2$) C, H, N; C: calcd, 83.88; found, 83.65; H: calcd, 6.34; found, 6.26; N: calcd, 9.78; found, 9.67.

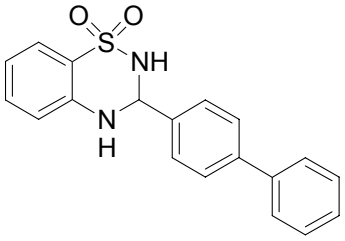

3-Biphenyl-4-yl-3,4-dihydro-2H-benzo[1,2,4]thiadiazine 1,1-dioxide (20). Compound **20** was prepared from 4-biphenylcarboxaldehyde (1.10 g, 5.81 mmol) and 2-amino-benzenesulfonamide (1.00 g, 5.81 mmol) according to general procedure C to yield a colorless solid (94 %); mp: 201 – 203 ^{o}C; ^{1}H NMR (500 MHz, DMSO-d_6): δ 7.94 – 7.96 (d, *J*= 10 Hz, 1H), 7.76 (s, 4H), 7.71 – 7.72 (d, *J*= 5 Hz, 2H), 7.54 – 7.55 (d, *J*= 5 Hz, 1H), 7.48 – 7.51 (t, *J*= 7.5 Hz, 2H), 7.44 (s, 1H), 7.39 – 7.41 (t, *J*= 5 Hz, 1H), 7.31 – 7.34 (t, *J*= 7.5 Hz, 1H), 6.92 – 6.93 (d, *J*= 5 Hz, 1H), 6.76 – 6.79 (t, *J*= 7.5 Hz, 1H), 5.83 – 5.85 (d, *J*= 5 Hz, 1H); ^{13}C NMR (125 MHz, DMSO-d_6): δ 143.95, 141.03, 139.63, 136.44, 132.88, 129.05, 128.23, 127.76, 126.81, 123.81, 121.68, 116.79, 116.44, 68.16; APCI *m/z* (rel intensity) 336.9 (M^+, 35); Anal. ($C_{19}H_{16}N_2O_2S$) C, H, N; C: calcd, 67.84; found, 67.35; H: calcd, 4.79; found, 4.89; N: calcd, 8.33; found, 8.27.

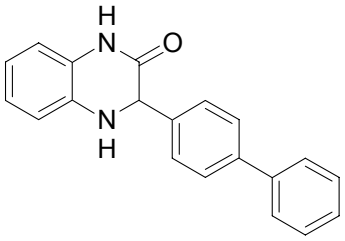

3-Biphenyl-4-yl-3,4-dihydro-1H-quinoxalin-2-one (21). 4-Bromobiphenyl (3.50 g, 15.01 mmol) was added to a mixture of Mg (0.36 g, 15.01 mmol) in ether with a catalytic amount (2-3 crystals) of iodine. After 30 minutes, 1H-quinoxalin-2-one (0.73 g, 5 mmol) was added in one portion. After stirring overnight at room temperature, the reaction was quenched with 50 mL of 10% NH_4Cl and extracted with ethyl acetate (3 x 25 mL). The combined organic extracts were dried with $MgSO_4$, concentrated, and purified by flash chromatography (hexane/ethyl acetate 1:1) to yield a colorless solid (34 %); mp: 190 – 192 ^{o}C; ^{1}H NMR (300 MHz, DMSO-d_6): δ 10.44 (s,

1H), 7.58 – 7.61 (m, 4H), 7.38 – 7.44 (m, 4H), 7.31 – 7.34 (m, 1H), 6.76 – 6.77 (m, 2H), 6.71 – 6.74 (t, *J*= 4.5 Hz, 1H), 6.69 – 6.70 (d, *J*= 3 Hz, 1H), 6.56 – 6.60 (m, 1H), 4.95 (s, 1H); ^{13}C NMR (75 MHz, DMSO-d_6): δ 166.54, 140.46, 140.24, 140.10, 134.49, 130.55, 129.72, 129.60, 128.17, 127.33, 126.05, 123.76, 118.40, 115.54, 114.05, 59.74; APCI *m/z* (rel intensity) 301.1 (M^+, 100); Anal. ($C_{21}H_{18}N_2O$) C, H, N; C: calcd, 79.98; found, 80.16; H: calcd, 5.37; found, 5.43; N: calcd, 9.33; found, 9.39.

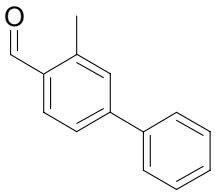

3-Methyl-biphenyl-4-carbaldehyde (22a). To a 0^{o}C solution of N,N,N'-trimethylethylenediamine (7.82 mL, 60.4 mmol) in 50 mL benzene was added BuLi (24.2 mL of a 2.5 M solution in hexanes, 60.4 mmol) over 5 minutes. After 15 minutes, a solution of 4-biphenyl carboxaldehyde (10 g, 54.9 mmol) in 50 mL benzene was added. Fifteen minutes later, BuLi (82.3 mmol) was added and the reaction stirred at 0 – 5 ^{o}C for 2.5 hours before MeI (10.27 mL, 164.7 mmol) was added in 1 portion. After 20 minutes of stirring, the cooling bath was removed and the reaction warmed to room temperature. Saturated ammonium chloride was added and the aqueous was extracted 3 times with ether. The combined organics were dried with $MgSO_4$, concentrated *in vacuo*, and purified by flash chromatography (hexane/ethyl acetate 5:1) to yield a colorless solid (6.4 g, 59.4% yield); ^{1}H NMR (300 MHz, CDCl3): δ 10.30 (s, 1H), 7.86 – 7.89 (d, *J*= 4.7 Hz, 1H), 7.62 – 7.64 (m, 3H), 7.42 – 7.48 (m, 4H), 2.74 (s, 3H); ^{13}C NMR (75 MHz, $CDCl_3$): δ 192.29, 146.14, 141.02, 139.64, 132.88, 132.61, 130.40, 128.89, 128.31, 127.25, 124.92, 19.77.

General Procedure D for the Preparation of Trifluoromethanesulfonic Ester Derivatives (23b - 25b, and 27b – 29b). Trifluoromethanesulfonic anhydride (1.5 equiv.) was added over 5 minutes to a 0 ^{o}C solution of the phenol (1 equiv.) and pyridine (2 equiv.) in 25 mL dichloromethane. The cooling bath was removed and the reaction was allowed to warm to room temperature. After the reaction was complete by TLC (ca. 4 – 12 hours), $NaHCO_3$ (saturated) was added and the organic layer was separated. Two more extractions of the aqueous layer were done with DCM, and the combined organics were washed with a saturated solution of $CuSO_4$. The organics were dried with $MgSO_4$, concentrated *in vacuo*, and purified by flash chromatography (Hexane/Ethyl Acetate 5:1).

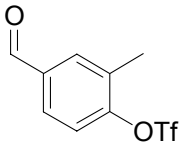

Trifluoro-methanesulfonic acid 4-formyl-2-methyl-phenyl ester (23b). Triflate **23b** was prepared according to General Procedure D from 4-hydroxy-3-methyl-benzaldehyde (0.50 g, 3.67 mmol) to yield a colorless oil (48.1 %); ^{1}H NMR (300 MHz, $CDCl_3$) δ 9.97 (s, 1H), 7.82 (s, 1H), 7.78 (d, *J*= 8.4 Hz, 1H), 7.40 (d, *J*= 8.4 Hz, 1H), 2.43 (s, 3H); ^{13}C NMR (75 MHz, $CDCl_3$) δ 190.5, 152.0, 135.6, 133.2, 132.1, 129.1, 122.1, 118.5 (q, *J* = 319 Hz), 16.2.

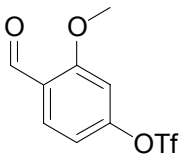

Trifluoro-methanesulfonic acid 4-formyl-3-methoxy-phenyl ester (24b). Triflate **24b** was prepared according to General Procedure D from 4-hydroxy-2-methoxy-benzaldehyde (1.00 g, 6.57 mmol) to yield a colorless oil (42.0 %); ^{1}H NMR (300 MHz, $CDCl_3$) δ 10.28 (s, 1H), 7.76 (d, *J*= 8.4 Hz, 1H), 6.85 (s, 1H), 6.83 (d, *J*= 8.4 Hz, 1H); ^{13}C NMR (75 MHz, $CDCl_3$) δ 187.6, 162.6, 154.0, 130.0, 124.3, 118.5 (q, *J*= 319 Hz), 113.1, 105.5, 55.9.

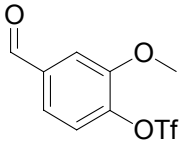

Trifluoro-methanesulfonic acid 4-formyl-2-methoxy-phenyl ester (25b). Triflate **25b** was prepared according to General Procedure D from 4-hydroxy-3-methoxy-benzaldehyde (1.00 g, 6.57 mmol) to yield a colorless oil (87.3 %); ^{1}H NMR (300 MHz, $CDCl_3$) δ 9.95 (S, 1H), 7.54 (d, *J*= 1.8 Hz, 1H), 7.49 (dd, *J*= 8.1, 1.8 Hz, 1H), 7.38 (d, *J*= 8.1 Hz, 1H), 3.96 (s, 3H); ^{13}C NMR (75 MHz, $CDCl_3$) δ 190.4, 152.1, 142.6, 136.7, 123.9, 123.1, 118.6 (q, *J*= 319 Hz), 111.7, 56.4.

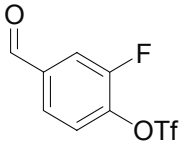

Trifluoro-methanesulfonic acid 2-fluoro-4-formyl-phenyl ester (27b). Triflate **27b** was prepared according to General Procedure D from 4-hydroxy-3-fluoro-benzaldehyde (0.50 g, 3.63 mmol) to yield a colorless oil (72.2 %); ^{1}H NMR (300 MHz, $CDCl_3$) δ 9.96 (d, *J*= 2.1 Hz, 1H), 7.69 (bs, 1H), 7.74 (d, *J*= 1.8 Hz, 1H), 7.53 (dd, *J*= 8.1, 7.4 Hz, 1H); ^{13}C NMR (75 MHz, $CDCl_3$) δ 189.2, 155.8, 152.4, 140.7 (d, *J*= 13.8 Hz), 137.2 (d, *J*= 19.8 Hz), 126.7 (d, *J*= 13.8 Hz), 124.4, 118.5 (q, *J*= 319 Hz), 117.4 (d, *J*= 18.8 Hz).

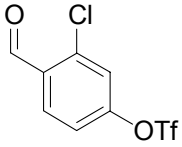

Trifluoro-methanesulfonic acid 3-chloro-4-formyl-phenyl ester (28b). Triflate **28b** was prepared according to General Procedure D from 4-hydroxy-2-chloro-benzaldehyde (1.09 g, 6.96 mmol) to yield a colorless oil (51.0 %); ^{1}H NMR (300 MHz, $CDCl_3$) δ 10.40 (s, 1H), 8.00 (d, *J*= 8.7 Hz, 1H), 7.41 (d, *J*= 2.4 Hz, 1H), 7.32 (dd, *J*= 8.7, 2.4 Hz, 1H) ; ^{13}C NMR (75 MHz, $CDCl_3$) δ 187.7, 152.6, 139.0, 132.1, 131.2, 123.6, 120.6.

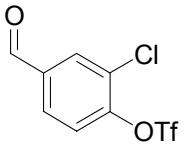

Trifluoro-methanesulfonic acid 2-chloro-4-formyl-phenyl ester (29b). Triflate **29b** was prepared according to General Procedure D from 4-hydroxy-3-chloro-benzaldehyde (1.09 g, 6.96 mmol) to yield a colorless oil (84.8 %); ^{1}H NMR (300 MHz, $CDCl_3$) δ 9.95 (d, *J*= 2.4 Hz, 1H), 8.01-7.99 (m, 1H), 7.85 (d, *J*= 8.4 Hz, 1H), 7.52 (d, *J*= 8.4 Hz, 1H); ^{13}C NMR (75 MHz, $CDCl_3$) δ 189.0, 149.1, 136.5, 131.8, 129.4, 128.5, 123.7, 118.4 (q, *J*= 319 Hz).

General Procedure E for the Suzuki-Miyaura Coupling of Aryl Halides / Triflates with Boronic Acids. A solution of aryl halide / triflate (1 equiv.), aryl boronic acid (1 equiv), Cs_2CO_3 (1.5 equiv), and $Pd(PPh_3)_4$ (.03 equiv.) in dimethoxyethane/water (3:1, 24 mLs) was stirred at 80^{o}C until the disappearance of starting material was observed by TLC (ca. 4 – 12 hours). Upon completion, 50 mL water was added to the reaction and the contents of the flask extracted three times with ether. The combined organics were dried with $MgSO_4$, concentrated *in vacuo*, and purified by flash chromatography (hexanes/EtOAc 5:1).

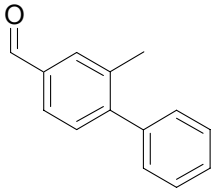

2-Methyl-biphenyl-4-carbaldehyde (23a). Compound **23a** was prepared according to General Procedure E from trifluoro-methanesulfonic acid 4-formyl-2-methyl-phenyl ester **23b** (0.37 g, 1.38 mmol) and phenylboronic acid (0.17 g, 1.38 mmol) to afford a colorless solid (38 %); ^{1}H NMR (300 MHz, $CDCl_3$) δ 10.00 (s, 1), 7.78 (s, 1H), 7.76 (d, *J*= 7.8 Hz, 1H), 7.48-7.30 (m, 6H), 2.33 (s, 3H); ^{13}C NMR (75 MHz, $CDCl_3$) δ 191.8, 147.8, 140.3, 136.1, 135.0, 131.3, 130.2, 128.5, 128.0, 127.3, 127.0, 20.1.

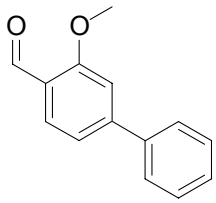

3-Methoxy-biphenyl-4-carbaldehyde (24a). Compound **24a** was prepared according to General Procedure E from trifluoro-methanesulfonic acid 4-formyl-3-methoxy-phenyl ester **24b** (0.78 g, 2.74 mmol) and phenylboronic acid (0.33 g, 2.74 mmol) to afford a colorless solid (49 %); ^{1}H NMR (300 MHz, $CDCl_3$) δ 10.48 (s, 1H), 7.87 (d, *J*= 8.1 Hz, 1H), 7.60 (d, *J*= 8,1 Hz, 2H), 7.49-7.40 (m, 3H), 7.21 (d, *J*= 8.1 Hz, 1H), 7.15 (s, 1H), 3.95 (s, 3H); ^{13}C NMR (75 MHz, $CDCl_3$) δ 189.2, 161.8, 148.7, 139.7, 128.7, 128.4, 127.0, 123.3, 119.4, 110.0, 55.4.

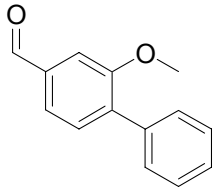

2-Methoxy-biphenyl-4-carbaldehyde (25a). Compound **25a** was prepared according to General Procedure E from trifluoro-methanesulfonic acid 4-formyl-2-methoxy-phenyl ester **25b** (1.60 g, 5.60 mmol) and phenylboronic acid (0.68 g, 5.60 mmol) to afford a colorless solid (74 %); ^{1}H NMR (300 MHz, $CDCl_3$) δ 10.01 (s, 1H), 7.60 (d, *J*= 6.9 Hz, 2H), 7.52-7.38 (m, 6H), 3.85 (s, 3H); ^{13}C NMR (75 MHz, $CDCl_3$) δ 191.4, 156.7, 136.9, 136.6, 136.4, 130.9, 129.1, 127.8, 127.5, 124.0, 109.3, 55.3.

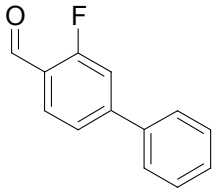

3-Fluoro-biphenyl-4-carbaldehyde (26a). Compound **26a** was prepared according to General Procedure E from 4-formyl-3-fluorophenyl bromide (1.00 g, 4.95 mmol) and phenylboronic acid

(0.60 g, 4.95 mmol) to afford a colorless solid (75 %); ^{1}H NMR (300 MHz, $CDCl_3$) δ 10.38 (s, 1H), 7.93 (t, *J*= 8.1 Hz, 1H), 7.61 (d, *J*= 7.8 Hz, 2H), 7.50- 7.36 (m, 5H).

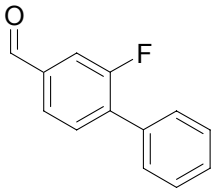

2-Fluoro-biphenyl-4-carbaldehyde (27a). Compound **27a** was prepared according to General Procedure E from trifluoro-methanesulfonic acid 4-formyl-2-fluoro-phenyl ester **27b** (1.00 g, 3.70 mmol) and phenylboronic acid (0.45 g, 3.70 mmol) to afford a colorless solid (49 %); ^{1}H NMR (300 MHz, $CDCl_3$) δ 9.70 (s, 1H), 7.71-7.56 (m, 5H), 7.48-7.41 (m, 3H); ^{13}C NMR (75 MHz, $CDCl_3$) δ 190.3, 161.4, 158.0, 136.8 (d, *J*= 6.3 Hz), 134.9 (d, *J*= 13.8 Hz), 134.2, 131.2, 128.8 (d, *J*= 2.6 Hz), 128.5, (d, *J*= 4.0 Hz), 125.8, 116.0 (d, *J*= 23.6 Hz).

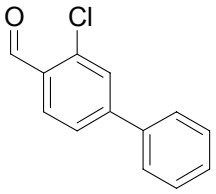

3-Chloro-biphenyl-4-carbaldehyde (28a). Compound **28a** was prepared according to General Procedure E from trifluoro-methanesulfonic acid 4-formyl-3-chloro-phenyl ester **28b** (1.05 g, 6.71 mmol) and phenylboronic acid (0.82 g, 6.71 mmol) to afford a colorless solid (35 %); ^{1}H NMR (300 MHz, $CDCl_3$) δ 10.48 (s, 1H), 7.97 (d, *J*= 8.1 Hz, 1H), 7.64 (d, *J*= 1.5 Hz, 1H), 7.59-7.56 (m, 3H), 7.48-7.44 (m, 3H); ^{13}C NMR (75 MHz, $CDCl_3$) δ 189.2, 147.9, 133.2, 133.1, 130.8, 129.6, 129.0, 128.9, 128.7, 127.1, 125.7.

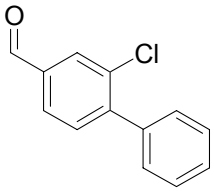

2-Chloro-biphenyl-4-carbaldehyde (29a). Compound **29a** was prepared according to General Procedure E from trifluoro-methanesulfonic acid 4-formyl-2-chloro-phenyl ester **29b** (1.70 g, 5.90 mmol) and phenylboronic acid (0.72 g, 5.90 mmol) to afford a colorless solid (63 %); ^{1}H NMR (300 MHz, $CDCl_3$) δ 9.97 (s, 1H), 7.96 (d, *J*= 1.5 Hz, 1H), 7.79 (dd, *J*= 8.1, 1.5 Hz, 1H), 7.50-7.40 (m, 6H); ^{13}C NMR (75 MHz, $CDCl_3$) δ 190.2, 145.9, 137.8, 136.1, 133.2, 131.8, 130.7, 128.9, 128.2, 128.0, 127.6.

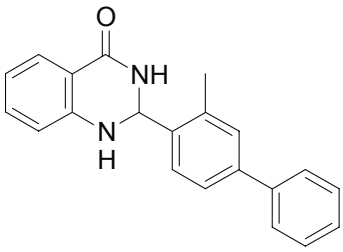

2-(3-Methyl-biphenyl-4-yl)-2,3-dihydro-1H-quinazolin-4-one (22).

Compound **22** was prepared from anthranilamide (0.13 g, 0.97 mmol) and 3-methyl-biphenyl-4-carbaldehyde **22a** (0.19 g, 0.97 mmol) according to General Procedure C to produce a colorless solid (62.9 % yield); mp: 165 – 167 ^{o}C; ^{1}H NMR (300 MHz, DMSO): δ 7.93 – 7.95 (d, J= 7.8 Hz, 1H), 7.75 – 7.77 (d, J= 7.8 Hz, 1H), 7.57 – 7.60 (d, J= 9 Hz, 2H), 7.43 – 7.50 (m, 4H), 7.26 – 7.37 (m, 2H), 6.88 – 6.93 (t, J= 7.5 Hz, 1H), 6.69 – 6.72 (d, J= 9 Hz, 1H), 6.18 (s, 1H), 6.14 (s, 1H), 2.51 (s, 3H); ^{13}C NMR (75 MHz, DMSO): δ 165.62, 147.92, 142.71, 140.44, 136.97, 134.98, 134.29, 130.22, 129.09, 128.99, 128.43, 127.97, 127.35, 125.66, 119.86, 115.00, 65.92, 19.45; ESI *m/z* (rel intensity) 312.8 (M^+, 100); Anal. ($C_{21}H_{18}N_2O \cdot 0.7H_2O$) C, H, N; C: calcd, 77.11; found, 77.06; H: calcd, 5.98; found, 5.88; N: calcd, 8.56; found, 8.27.

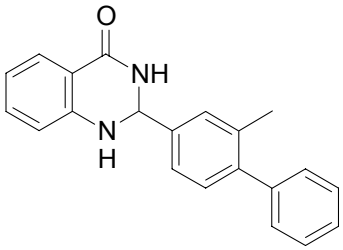

2-(2-Methyl-biphenyl-4-yl)-2,3-dihydro-1H-quinazolin-4-one (23). Compound **23** was prepared from anthranilamide (0.07 g, 0.51 mmol) and 2-methyl-biphenyl-4-carbaldehyde **23a** (0.10 g, 0.51 mmol) according to General Procedure C to produce a colorless solid (30 %); mp: 177-179 °C; ^{1}H NMR (500 MHz, DMSO-d_6) δ 8.33 (s, 1H), 7.65 (d, *J*= 6.5 Hz, 1H), 7.45-7.43 (m, 3H), 7.40-7.35 (m, 2H), 7.32 (d, *J*= 8.0 Hz, 2H), 7.27-7.22 (m, 2H), 7.16 (s, 1H), 6.78 (d, *J*= 7.5 Hz, 1H), 6.69 (t, *J*= 7.5 Hz, 1H), 5.78 (s, 1H), 2.24 (s, 3H); ^{13}C NMR (125 MHz, DMSO-d_6) δ 163.7, 147.9, 141.5, 140.9, 140.6, 134.7, 133.3, 129.6, 129.0, 128.9, 128.3, 127.4, 127.1, 124.6, 117.1, 115.0, 114.4, 66.4, 20.3; ESI *m/z* (rel intensity) 312.7 (M^+, 100); Anal. ($C_{21}H_{18}N_2O$) C, H, N; C: calcd, 80.23; found, 79.84; H: calcd, 5.77; found, 5.97; N: calcd, 8.91; found, 8.93.

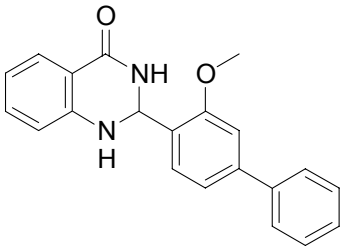

2-(3-Methoxy-biphenyl-4-yl)-2,3-dihydro-1H-quinazolin-4-one (24).

Compound **24** was prepared from anthranilamide (0.18 g, 1.32 mmol) and 3-methoxy-biphenyl-4-carbaldehyde **24a** (0.28 g, 1.32 mmol) according to General Procedure C to produce a colorless solid (21 %); mp: 165 – 168 ^{o}C; ^{1}H NMR (500 MHz, DMSO-d_6) δ 8.10 (s, 1H), 7.69 (d, *J*= 7.5 Hz, 2H), 7.65 (d, *J*= 8.0 Hz, 1H), 7.47 (t, *J*= 7.0 Hz, 3H), 7.38 (dd, *J*= 7.5, 7.0 Hz, 1H), 7.28 (s, 1H), 7.25-7.22 (m, 2H), 6.86 (s, 1H), 6.79 (d, *J*= 7.5 Hz, 1H), 6.80 (dd, *J*= 8.0, 7.0 Hz, 1H), 6.06 (s, 1H), 3.94 (s, 3H); ^{13}C NMR (125 MHz, DMSO-d_6) δ 163.9, 156.8, 148.0, 141.9, 140.0, 133.3, 128.9, 128.2, 127.7, 127.44, 127.39, 127.1, 126.9, 118.6,

117.1, 114.6, 109.6, 61.0, 55.8; ESI *m/z* (rel intensity) 329.8 (M^+, 100); Anal. ($C_{21}H_{18}N_2O_2$) C, H, N; C: calcd, 76.34; found, 75.77; H: calcd, 5.49; found, 5.62; N: calcd, 8.48; found, 8.47.

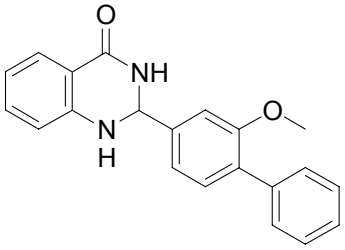

2-(2-Methoxy-biphenyl-4-yl)-2,3-dihydro-1H-quinazolin-4-one (25).

Compound **25** was prepared from anthranilamide (0.09 g, 0.66 mmol) and 2-methoxy-biphenyl-4-carbaldehyde **25a** (0.14 g, 0.66 mmol) according to General Procedure C to produce a colorless solid (64 %); mp: 174-175 °C; ^{1}H NMR (500 MHz, DMSO-d_6) δ 8.37 (s, 1H), 7.66-7.64 (m, 1H), 7.46 (d, *J*= 7.5 Hz, 2H), 7.40 (dd, *J*= 7.5, 7.0 Hz, 2H), 7.33-7.25 (m, 4H), 7.19-7.15 (m, 2H), 6.80 (dd, *J*= 8.0, 3.0 Hz, 1H), 6.70 (dd, *J*= 7.5, 7.0 Hz, 1H), 5.81 (s, 1H), 3.77 (s, 3H); ^{13}C NMR (75 MHz, $CDCl_3$) δ 163.7, 156.0, 148.0, 142.4, 137.8, 133.4, 130.3, 130.0, 129.2, 128.1, 127.4, 127.0, 119.2, 117.2, 115.1, 114.5, 110.4, 66.5, 55.6; ESI *m/z* (rel intensity) 330.0 (M^+, 100); Anal. ($C_{21}H_{18}N_2O_2 \cdot 0.1H_2O$) C, H, N; C: calcd, 75.93; found, 75.78; H: calcd, 5.52; found, 5.64; N: calcd, 8.43; found, 8.47.

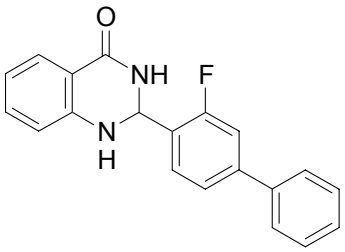

2-(3-Fluoro-biphenyl-4-yl)-2,3-dihydro-1H-quinazolin-4-one (26).

Compound **26** was prepared from anthranilamide (0.34 g, 2.5 mmol) and 3-fluoro-biphenyl-4-carbaldehyde **26a** (0.50 g, 2.5 mmol) according to General Procedure C to produce a colorless solid (72.4 %); mp: 171-173 °C; ^{1}H NMR (500 MHz, DMSO-d_6) δ 8.32 (s, 1H), 7.71 (d, *J*= 7.5 Hz, 2H),

7.68 (d, *J*= 7.5 Hz, 1H), 7.63-7.55 (m, 3H), 7.48 (t, *J*= 7.0 Hz, 2H), 7.42-7.39 (m, 1H), 7.27 (t, *J*= 8.0 Hz, 1H), 7.12 (s, 1H), 6.78 (d, *J*= 8.0 Hz, 1H), 6.72 (t, *J*= 7.5 Hz, 1H), 6.10 (s, 1H); ^{13}C NMR (125 MHz, DMSO-d_6) δ 163.6, 161.1, 159.2, 147.7, 142.6, 138.3, 133.5, 129.1, 129.0, 128.2, 127.4, 127.2 (d, *J* = 13.4 Hz), 126.8, 122.6, 117.4, 114.6 (d, *J* = 28.0 Hz), 113.7 (d, *J* = 21.9 Hz), 60.8; ESI *m/z* (rel intensity) 318.1 (M^+, 100); Anal. ($C_{20}H_{15}N_2OF$) C, H, N; C: calcd, 75.46; found, 75.39; H: calcd, 4.75; found, 4.71; N: calcd, 8.80; found, 8.91.

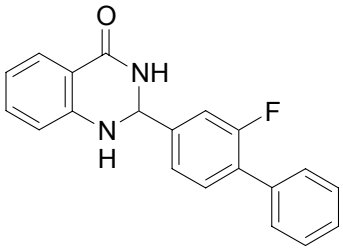

2-(2-Fluoro-biphenyl-4-yl)-2,3-dihydro-1H-quinazolin-4-one (27).

Compound **27** was prepared from anthranilamide (0.36 g, 2.65 mmol) and 2-fluoro-biphenyl-4-carbaldehyde **27a** (0.53 g, 2.65 mmol) according to General Procedure C to produce a colorless solid (54 %); mp: 191-192 °C; ^{1}H NMR (500 MHz, DMSO-d_6) δ 8.49 (s, 1H), 7.64 (d, *J*= 6.5 Hz, 1H), 7.54-7.41 (m, 7H), 7.29-7.27 (m, 2H), 6.80 (d, *J*= 7.5 Hz, 1H), 6.70 (d, *J*= 6.5 Hz, 1H), 5.84 (s, 1H); ^{13}C NMR (75 MHz, $CDCl_3$) δ 163.5, 159.8, 157.8, 147.5, 144.0 (d, *J*= 6.0 Hz), 134.7, 133.5, 130.8, 128.7 (d, *J*= 13.0 Hz), 128.16, 128.0, 127.4, 123.1, 117.4, 115.0, 114.5, 114.3, 65.3; ESI *m/z* (rel intensity) 318.1 (M^+, 100); Anal. ($C_{20}H_{15}N_2OF$) C, H, N; C: calcd, 75.76; found, 75.40; H: calcd, 4.75; found, 4.97; N: calcd, 8.80; found, 8.82.

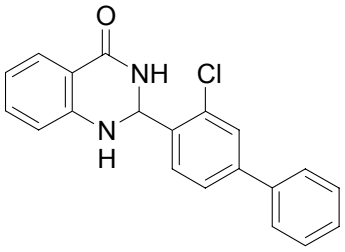

2-(3-Chloro-biphenyl-4-yl)-2,3-dihydro-1H-quinazolin-4-one (28). Compound **28** was prepared from anthranilamide (0.18 g, 1.34 mmol) and 3-chloro-biphenyl-4-carbaldehyde **28a** (0.27 g, 1.34 mmol) according to General Procedure C to produce a colorless solid (52 %); mp: 153-157 °C; ^{1}H NMR (500 MHz, DMSO-d_6) δ 8.31 (s, 1 H), 7.79 (s, 1H), 7.75 (d, *J*= 8.5 Hz, 1H), 7.70-7.69 (m, 5H), 7.48 (t, *J*= 7.5 Hz, 2H), 7.41 (dd, *J*= 7.5, 7.0 Hz, 1H), 7.28 (dd, *J*= 8.0, 7.0 Hz, 1H), 6.82 (d, *J*= 8.0 Hz, 2H), 6.74 (t, *J*= 7.5 Hz, 2H), 6.20 (s, 1H); ^{13}C NMR (125 MHz, DMSO-d_6) δ 163.8, 147.7, 142.2, 138.1, 136.9, 133.6, 132.5, 129.3, 129.2, 128.3, 127.5, 127.4, 126.9, 125.7, 117.6, 114.8, 114.7, 63.6; ESI *m/z* (rel intensity) 334.1 (M^+, 100); Anal. ($C_{20}H_{15}N_2OCl·0.4H_2O$) C, H, N; C: calcd, 70.24; found, 70.09; H: calcd, 4.66; found, 4.55; N: calcd, 8.19; found, 8.14.

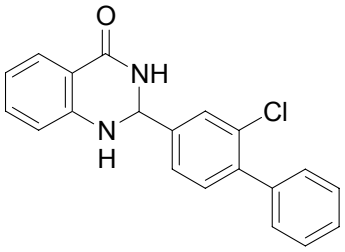

2-(2-Chloro-biphenyl-4-yl)-2,3-dihydro-1H-quinazolin-4-one (29).

Compound **29** was prepared from anthranilamide (0.36 g, 2.68 mmol) and 2-chloro-biphenyl-4-carbaldehyde **29a** (0.54 g, 2.68 mmol) according to General Procedure C to produce a colorless solid (76 %); mp: 207-210 °C; ^{1}H NMR (500 MHz, DMSO-d_6) δ 8.48 (s, 1H), 7.67 (s, 1H), 7.63 (d, *J*= 8.0 Hz, 1H), 7.53 (d, *J*= 8.0 Hz, 2H), 7.48-7.40 (m, 5H), 7.30-7.26 (m, 2H), 6.79 (d, *J*= 8.5 Hz, 1H), 6.70 (dd, *J*= 7.5, 7.0 Hz, 1H), 5.84 (s, 1H); ^{13}C NMR (125 MHz, DMSO-d_6) δ 163.5, 147.5, 143.3, 139.7, 138.3, 133.5, 131.5, 131.2, 129.2, 128.3, 128.2, 127.9, 127.4, 125.8, 117.4, 114.9, 114.5, 65.3; ESI *m/z* (rel intensity) 334.2 (M^+, 100);

Anal. ($C_{20}H_{15}N_2OCl \cdot 0.7H_2O$) C, H, N; C: calcd, 69.15; found, 69.20; H: calcd, 4.76; found, 4.51; N: calcd, 8.06; found, 8.06.

(4-Methylene-cyclohexyl)-benzene (30c).

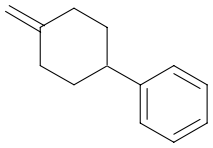

n-BuLi (7.46 mL of a 2.5 M solution in hexanes, 18.65 mmol) was slowly added to a room temperature solution of methyltriphenylphosphonium bromide (6.66 g, 18.65 mmol) in 100 mL THF. After 20 minutes, 4-phenylcyclohexanone (2.50 g, 14.35 mmol) was added to the orange solution and the reaction was allowed to stir overnight. After quenching with saturated NH_4Cl (75 mL), the aqueous was extracted with EtOAc (100 mL x 3), dried with $MgSO_4$, and concentrated *in vacuo*. The resulting residue was purified by distillation (110^oC @ 2 mm Hg) to yield a clear oil (97.5 %); ^1H NMR (300 MHz, $CDCl_3$): δ 7.35 – 7.38 (m, 2H), 7.28 – 7.31 (m, 3H), 4.78 (s, 2H), 2.72 – 2.80 (t, *J*= 12 Hz, 1H), 2.49 – 2.54 (d, *J*= 15 Hz, 2H), 2.23 – 2.51 (m, 2H), 2.06 – 2.10 (d, *J*= 12 Hz, 2H), 1.58 – 1.72 (m, 2H). ^{13}C NMR (75 MHz, $CDCl_3$): δ 149.09, 147.17, 128.69, 127.17, 126.33, 107.75, 44.48, 35.85, 35.49.

(4-Phenyl-cyclohexyl)-methanol (30b).

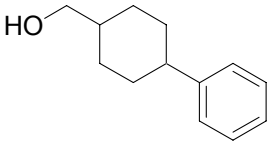

Borane was added to a 0 ^oC solution of 4-methylene-cyclohexyl-benzene **30c** in THF. After warming to room temperature and stirring overnight, NaOH (3.48 g, 87 mmol) in 15 mL water and 30% H_2O_2 (9.86 mL, 87 mmol) were added and stirring continued for and additional hour. Reaction quenched with 100 mL saturated NH_4Cl, extracted with ether (50 mL x 3), dried with $MgSO_4$, concentrated *in vacuo* and purified by flash chromatography (hexane/EtOAc 6:1) to yield

a colorless oil (99.7 %); ^{1}H NMR (300 MHz, $CDCl_3$): δ 7.21 – 7.35 (m, 5H), 3.70 – 3.72 (d, *J*= 6 Hz, 1H), 3.63 – 3.67 (t, *J*= 12 Hz, 1H), 3.50 – 3.52 (d, *J*= 6 Hz, 1H), 1.94 – 1.98 (m, 2H), 1.65 – 1.82 (m, 4H), 1.48 – 1.60 (m, 3H), .95 – 1.00 (t, *J*= 7.5 Hz, 1H).

4-Phenyl-cyclohexanecarbaldehyde (30a).

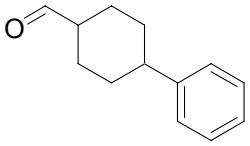

A solution of oxalyl chloride (0.25 mL, 2.89 mmol) in 10 mL of dry CH_2Cl_2 was treated at -78 °C with a solution of DMSO (0.44 mL, 6.31 mmol) in 4 mL of CH_2Cl_2, followed by a solution of (4-phenyl-cyclohexyl)-methanol **30b** (0.50 g, 2.63 mmol) in 4 mL of CH_2Cl_2. After 15 minutes at -78 °C, triethylamine (1.83 mL, 13.15 mmol) was added, and the reaction mixture warmed to room temperature and stirred for an additional 15 minutes. Aqueous HCl (10 mL of a 1 N solution) was added and the layers were separated. The aqueous layer was washed with CH_2Cl_2 (2 x 10 mL), and the combined organic layers were dried ($MgSO_4$) and evaporated *in vacuo* to afford a pale yellow oil (100 %) with no further purification necessary.

2-(4-Phenyl-cyclohexyl)-2,3-dihydro-1H-quinazolin-4-one (30).

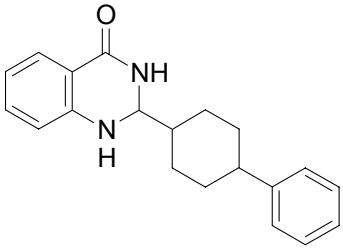

Compound **30** was prepared according to General Procedure C from 4-phenyl-cyclohexanecarbaldehyde **30a** (0.50 g, 2.66 mmol) and anthranilamide (0.37 g, 2.66 mmol) to yield a colorless solid (14.3 %); mp: 198 – 200^{o}C; ^{1}H NMR (300 MHz, $CDCl_3$): δ 7.88 – 7.91 (d, *J*= 7.5 Hz, 1H), 7.26 – 7.35 (m, 4H), 7.18 – 7.21 (t, *J*= 4.5 Hz, 3H), 6.83 – 6.88 (t, *J*= 7.5 Hz, 1H), 6.62 – 6.69

(d, *J*= 10.5 Hz, 1H), 6.16 (s, 1H), 4.72 – 4.74 (d, *J*= 6 Hz, 1H), 2.46 – 2.57 (m, 1H), 2.01 – 2.05 (m, 4H), 1.72 – 1.77 (m, 1H), 1.43 – 1.57 (m, 2H), 1.31 – 1.40 (m, 2H); ^{13}C NMR (75 MHz, $CDCl_3$): δ 165.26, 147.28, 146.61, 133.87, 128.47, 128.39, 126.98, 126.71, 126.12, 119.04, 114.50, 69.44, 44.04, 42.29, 33.31, 27.57; ESI *m/z* (rel intensity) 306.7 (100); Anal. ($C_{20}H_{22}N_2O \cdot 0.5H_2O$) C, H, N; C: calcd, 76.16; found, 76.35; H: calcd, 7.35; found, 7.28; N: calcd, 8.88; found, 8.78.

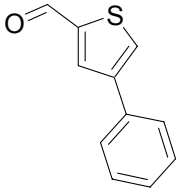

4-Phenyl-thiophene-2-carbaldehyde (31a).

Compound **31a** was synthesized according to General Procedure D from 4-bromothiophene-2-carbaldehyde (1.00 g, 5.23 mmol), and phenylboronic acid (0.63 g, 5.23 mmol) to yield a colorless solid (62.0 %); mp: 53 – 55^{o}C; ^{1}H NMR (300 MHz, $CDCl_3$): δ 9.97 (s, 1H), 8.04 (s, 1H), 7.85 (s, 1H), 7.58 – 7.61 (d, *J*= 9 Hz, 2H), 7.41 – 7.48 (t, *J*= 10.5 Hz, 2H), 7.36 – 7.39 (d, *J*= 9 Hz, 1H); ^{13}C NMR (75 MHz, $CDCl_3$): δ 182.96, 144.33, 143.57, 134.70, 134.28, 129.57, 129.03, 127.99, 126.25.

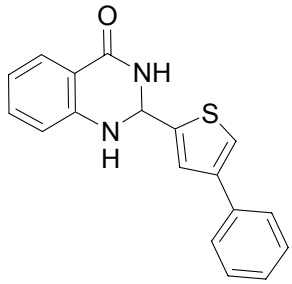

2-(4-Phenyl-thiophen-2-yl)-2,3-dihydro-1H-quinazolin-4-one (31).

Compound **31** was synthesized according to General Procedure C from 4-phenyl-thiophene-2-carbaldehyde **17a** (0.10 g, 0.53 mmol) and anthranilamide (0.07 g, 0.53 mmol) to yield a colorless solid (37.7 %); mp: 228 – 230^{o}C; ^{1}H NMR (300 MHz, DMSO): δ 8.48 (s, 1H), 7.77 (s, 1H), 7.61 – 7.63 (d, *J*= 6 Hz, 3H), 7.56 (s, 1H), 7.37 – 7.42 (t, *J*= 7.5 Hz, 2H),

7.26 – 7.29 (m, 3H), 6.75 – 6.78 (d, *J*= 9 Hz, 1H), 6.67 – 6.73 (t, *J*= 9 Hz, 1H), 6.04 (s, 1H); ^{13}C NMR (75 MHz, DMSO): δ 163.17, 147.30, 140.40, 135.01, 133.47, 129.01, 127.37, 127.25, 125.79, 124.68, 120.90, 117.69, 115.15, 114.78, 62.76; ESI *m/z* (rel intensity) 306.7 (M^+, 100); Anal. ($C_{18}H_{14}N_2OS \cdot 1H_2O$) C, H, N; C: calcd, 70.15; found, 70.03; H: calcd, 4.65; found, 4.35; N: calcd, 9.08; found, 9.02.

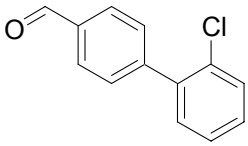

4-(2-chlorophenyl)benzaldehyde (32a). Compound **32a** was prepared according to General Procedure E from 4-formylphenylboronic acid (0.50 g, 3.33 mmol) and 1-chloro-2-iodobenzene (0.79 g, 3.33 mmol) afforded a pale yellow solid (73 %); mp: 71-73 °C; ^{1}H NMR (300 MHz, $CDCl_3$) δ 10.0 (s, 1H), 7.91 – 7.96 (d, *J*= 8.2 Hz, 2H), 7.41-7.53 (m, 4H), 7.60-7.65 (d, *J*= 8.2 Hz, 2H).

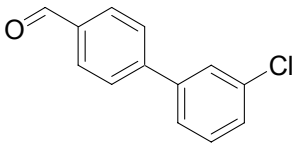

4-(3-chlorophenyl)benzaldehyde (33a). Compound **33a** was prepared according to General Procedure E from 4-formylphenylboronic acid (0.50 g, 3.33 mmol) and 1-chloro-3-iodobenzene (0.79 g, 3.33 mmol) to afford a yellow solid (66 %): mp 44-46 °C; ^{1}H NMR (300 MHz, $CDCl_3$) δ 10.14 (s, 1H), 8.02-8.07 (d, *J*= 8.3 Hz, 2H), 7.70-7.75 (d, *J*= 8.3 Hz, 2H), 7.41-7.62 (m, 4H).

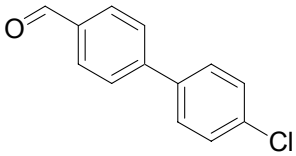

4-(4-Chlorophenyl)benzaldehyde (34a). Compound **34a** was prepared according to General Procedure E from a mixture of 4-formylphenylboronic acid (0.50 g, 3.33 mmol) and 1-chloro-4-iodobenzene (0.79 g, 3.33 mmol) to afford a pale yellow solid (46 %); mp: 113-115 °C; ^{1}H NMR (300 MHz, $CDCl_3$) δ 10.1 (s, 1H), 7.9 (d, *J*= 8.3 Hz, 2H), 7.7 (d, *J*= 8.1 Hz, 2H), 7.6 (d, *J*= 8.5 Hz, 2H), 7.4 (d, *J*= 8.6 Hz, 2H).

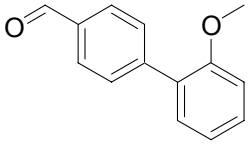

2'-Methoxy-biphenyl-4-carbaldehyde (35a).

Compound **35a** was prepared according to General Procedure E from a mixture of 4-formylphenylboronic acid (0.50 g, 3.33 mmol) and 1-bromo-2-methoxy-benzene (0.62 g, 3.33 mmol) to afford a clear oil (80.2 %); ^{1}H NMR (300 MHz, $CDCl_3$): δ 10.04 (s, 1H), 7.90 – 7.93 (d, *J*= 9 Hz, 2H), 7.70 – 7.90 (m, 2H), 7.33 – 7.41 (m, 2H), 7.00 – 7.09 (m, 2H), 3.82 (s, 3H); ^{13}C NMR (75 MHz, $CDCl_3$): δ 191.86, 156.27, 144.85, 134.65, 130.55, 129.99, 129.56, 129.23, 129.00, 120.81, 111.19, 55.31.

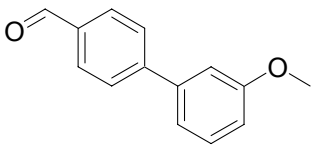

3'-Methoxy-biphenyl-4-carbaldehyde (36a).

Compound **36a** was prepared according to General Procedure E from a mixture of 4-formylphenylboronic acid (0.50 g, 3.33 mmol) and 1-bromo-3-methoxy-benzene (0.62 g, 3.33 mmol) to afford a clear oil (66.4 %); ^{1}H NMR (300 MHz, $CDCl_3$): δ 10.04 (s, 1H), 7.92 – 7.95 (d, *J*= 9 Hz, 2H), 7.72 – 7.75 (d, *J*= 9 Hz, 2H), 7.36 – 7.42 (t, *J*= 9 Hz, 1H), 7.16 – 7.20 (d, *J*= 11.5 Hz, 1H), 7.15 (s, 1H), 6.94 – 6.98 (d, *J*= 11.5 Hz, 1H), 3.87 (s, 3H); ^{13}C NMR (75 MHz, $CDCl_3$): δ

191.79, 159.96, 146.90, 141.03, 135.17, 130.11, 129.95, 127.61, 119.69, 113.66, 113.03, 55.23.

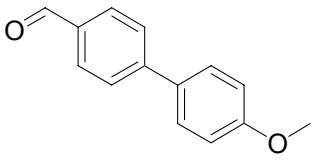

4'-Methoxy-biphenyl-4-carbaldehyde (37a).

Compound **37a** was prepared according to General Procedure E from a mixture of 4-formylphenylboronic acid (0.50 g, 3.33 mmol) and 1-bromo-4-methoxy-benzene (0.62 g, 3.33 mmol) to afford a colorless solid (24.5 %); mp: 101 – 102 ^{o}C; ^{1}H NMR (300 MHz, $CDCl_3$): δ 10.08 (s, 1H), 7.92 – 8.22 (m, 2H), 7.71 – 7.72 (d, *J*= 3 Hz, 2H), 7.59 – 7.62 (d, *J*= 9Hz, 2H), 7.00 – 7.03 (d, *J*= 9 Hz, 2H), 3.88 (s, 3H); ^{13}C NMR (75 MHz, $CDCl_3$): δ 191.88, 160.08, 146.75, 134.62, 132.02, 130.30, 128.47, 127.02, 114.45, 55.37.

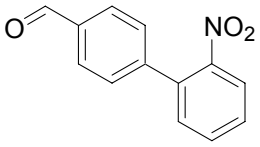

2'-Nitro-biphenyl-4-carbaldehyde (38a).

Compound **38a** was prepared according to General Procedure E from a mixture of 4-formylphenylboronic acid (0.50 g, 3.33 mmol) and 1-bromo-2-nitro-benzene (0.67 g, 3.33 mmol) to afford a colorless solid (93.7 %); mp: 99 – 101 ^{o}C; ^{1}H NMR (300 MHz, $CDCl_3$): δ 10.04 (s, 1H), 7.90 – 7.95 (m, 3H), 7.63 – 7.70 (t, *J*= 10.5 Hz, 1H), 7.52 – 7.58 (m, 1H), 7.41 – 7.48 (m, 3H); ^{13}C NMR (75 MHz, $CDCl_3$): δ 192.01, 144.07, 136.10, 134.75, 133.10, 132.03, 130.23, 129.44, 129.44, 128.97, 128.30, 124.77.

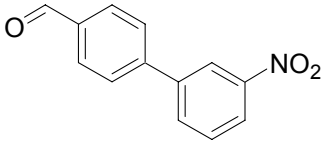

3'-Nitro-biphenyl-4-carbaldehyde (39a).

Compound **39a** was prepared according to General Procedure E from a mixture of 4-formylphenylboronic acid (0.50 g, 3.33 mmol) and 1-bromo-3-nitro-benzene (0.67 g, 3.33 mmol) to afford a colorless solid (68.8 %); mp: 117 – 118 ^{o}C; ^{1}H NMR (300 MHz, $CDCl_3$): δ 10.08 (s, 1H), 8.47 – 8.49 (m, 1H), 8.25 – 8.28 (d, J= 9 Hz, 1H), 8.00 – 8.02 (d, J= 6 Hz, 2H), 7.98 – 7.99 (d, J= 3 Hz, 1H), 7.78 – 7.81 (d, J= 9 Hz, 2H), 7.64 – 7.69 (t, J= 7.5 Hz, 1H); ^{13}C NMR (75 MHz, $CDCl_3$): δ 191.88, 149.00, 144.58, 141.60, 136.29, 133.47, 130.73, 130.32, 128.08, 123.35, 122.44.

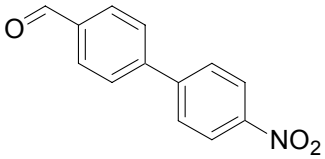

4'-Nitro-biphenyl-4-carbaldehyde (40a).

Compound **40a** was prepared according to General Procedure E from a mixture of 4-formylphenylboronic acid (1.00 g, 6.67 mmol) and 1-bromo-4-nitro-benzene (1.34 g, 6.67 mmol) to afford a colorless solid (59.8 %); mp: 128 – 129 ^{o}C; ^{1}H NMR (300 MHz, $CDCl_3$): δ 10.14 (s, 1H), 8.36 – 8.41 (d, J= 13.5 Hz, 2H), 8.04 – 8.09 (d, J= 13.5 Hz, 2H), 7.82 – 7.87 (m, 4H); ^{13}C NMR (75 MHz, $CDCl_3$): δ 191.91, 146.33, 144.76, 136.56, 130.72, 128.52, 128.38, 127.99, 124.56.

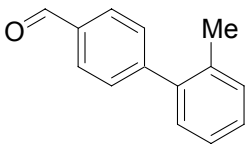

2'-Methyl-biphenyl-4-carbaldehyde (41a). Compound **41a** was prepared according to General Procedure E from 4-formylphenylboronic acid (0.50 g, 3.33 mmol) and 2-iodotoluene

(0.73 g, 3.33 mmol) to afford a colorless solid (74 %); mp: 54-56 °C; ^{1}H NMR (300 MHz, $CDCl_3$) δ 10.11 (s, 1H), 7.93-7.98 (d, *J*= 7.8 Hz, 2H), 7.51-7.54 (d, *J*= 7.8 Hz, 2H), 7.21-7.36 (m, 4H), 2.34 (s, 3H).

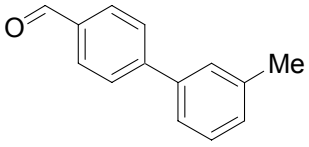

3'-Methyl-biphenyl-4-carbaldehyde (42a). Compound **42a** was prepared according to General Procedure E from 4-formylphenylboronic acid (0.50 g, 3.33 mmol) and 3-iodotoluene (0.73 g, 3.33 mmol) to afford a colorless solid (74 %) to afford a very viscous pale yellow oil (59 %): ^{1}H NMR (300 MHz, $CDCl_3$) δ 10.12 (s, 1H). 7.90-7.95 (d, *J*= 8.3 Hz, 2H), 7.83-7.88 (d, *J*= 8.1 Hz, 2H), 7.43-7.71 (m, 4H), 2.53 (s, 3H).

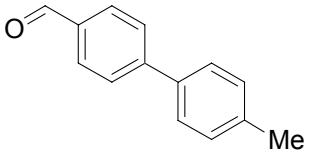

4'-Methyl-biphenyl-4-carbaldehyde (43a). Compound **43a** was prepared according to General Procedure E from 4-formylphenylboronic acid (0.50 g, 3.33 mmol) and 4-iodotoluene (0.73 g, 3.33 mmol) to afford a colorless solid (54 %); mp: 105 – 107 ^{o}C; ^{1}H NMR (300 MHz, $CDCl_3$) δ 2.41 (s, 3H), 7.32-7.38 (m, 1H), 7.41-7.76 (m, 3H), 7.81-7.89 (m, 2H), 8.03-8.31 (m, 2H), 10.11 (s, 1H).

2',4'-Dimethyl-biphenyl-4-carbaldehyde (44a).

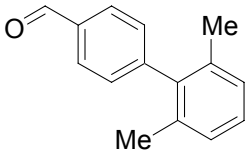

Compound **44a** was prepared according to General Procedure E from 4-formylphenylboronic acid (0.68 g, 4.5 mmol) and 2,6-dimethylbromobenzene (0.83 g, 4.5 mmol) to afford a colorless solid (96.2 %); mp: 48 – 50 ^{o}C; ^{1}H NMR (300 MHz, $CDCl_3$): δ 10.08 (s, 1H), 7.97 – 7.99 (d, *J*= 6 Hz, 2H), 7.34 –

7.35 (d, *J*= 3 Hz, 2H), 7.21 – 7.22 (m, 1H), 7.15 – 7.16 (d, *J*= 3 Hz, 2H), 2.06 (s, 6H); ^{13}C NMR (75 MHz, $CDCl_3$): δ 192.18, 148.21, 140.81, 135.67, 135.35, 130.26, 130.19, 127.98, 127.83, 21.01.

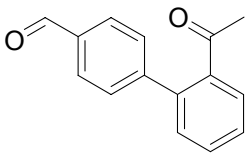

2'-Acetyl-biphenyl-4-carbaldehyde (45a).

Compound **45a** was prepared according to General Procedure E from 4-formylphenylboronic acid (0.75 g, 5.02 mmol) and 1-(2-bromo-phenyl)-ethanone (1.00 g, 5.02 mmol) to afford a colorless oil (63.1 %); ^{1}H NMR (300 MHz, $CDCl_3$): δ 10.05 (s, 1H), 7.91 – 7.93 (d, *J*= 6 Hz, 2H), 7.60 – 7.63 (d, *J*= 8.5 Hz, 1H), 7.60 – 7.63 (s, 1H), 7.51 – 7.54 (d, *J*= 8.5 Hz, 1H), 7.46 – 7.49 (m, 2H), 7.36 – 7.39 (d, *J*= 9 Hz, 1H), 2.14 (s, 3H); ^{13}C NMR (75 MHz, $CDCl_3$): δ 192.03, 147.43, 140.46, 139.60, 135.69, 131.30, 130.59, 130.16, 129.71, 128.55, 128.25, 30.52.

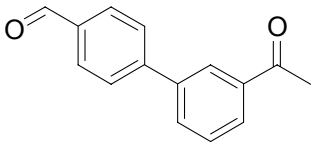

3'-Acetyl-biphenyl-4-carbaldehyde (46a).

Compound **46a** was prepared according to General Procedure E from 4-formylphenylbromide (1.10 g, 6.10 mmol) and 2-acetylphenylboronic acid (1.00 g, 6.10 mmol) to afford a colorless oil (66.6 %); ^{1}H NMR (300 MHz, $CDCl_3$): δ 10.10 (s, 1H), 8.26 (s, 1H), 8.00 – 8.03 (m, 3H), 7.80 – 7.88 (m, 3H), 7.59 – 7.65 (m, 1H), 2.71 (s, 3H); ^{13}C NMR (75 MHz, $CDCl_3$): δ 198.08, 192.09, 146.29, 140.50, 138.05, 135.83, 132.12, 130.63, 129.63, 128.64, 128.06, 127.31, 27.05.

4'-Acetyl-biphenyl-4-carbaldehyde (47a).

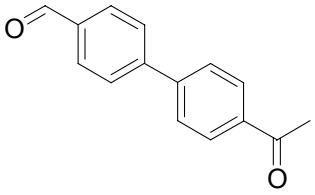

Compound **47a** was prepared according to General Procedure E from 4-formylphenylbromide (1.13 g, 6.1 mmol) and 4-acetylphenylboronic acid (1.00 g, 6.10 mmol) to afford a colorless oil (80.5 %); ^{1}H NMR (300 MHz, $CDCl_3$): δ 10.01 (s, 1H), 7.99 – 8.02 (d, *J*= 9 Hz, 2H), 7.90 – 7.93 (d, *J*= 9Hz, 2H), 7.71 – 7.73 (d, *J*= 6 Hz, 2H), 7.65 – 7.68 (d, *J*= 9 Hz, 2H), 2.59 (s, 3H); ^{13}C NMR (75 MHz, $CDCl_3$): δ 197.33, 191.55, 145.39, 143.82, 136.45, 135.57, 130.11, 128.83, 127.66, 127.32, 26.53.

[1,1';2',1'']Terphenyl-4-carbaldehyde (48a).

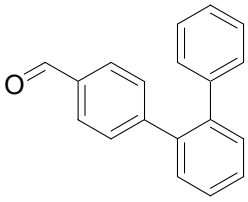

Compound **48a** was prepared according to General Procedure E from 4-formylphenylboronic acid (0.64 g, 4.29 mmol) and 2-bromobiphenyl (1.00 g, 4.29 mmol) to afford a colorless solid (40.3 %); mp: 73 – 75 ^{o}C; ^{1}H NMR (300 MHz, $CDCl_3$): δ 9.95 (s, 1H), 7.74 (s, 1H), 7.71 – 7.72 (d, *J*= 3 Hz, 1H), 7.44 – 7.46 (m, *J*= 6 Hz, 4H), 7.32 (s, 1H), 7.29 – 7.30 (d, *J*= 3 Hz, 1H), 7.21 – 7.23 (m, 3H), 7.11 – 7.14 (m, 2H); ^{13}C NMR (75 MHz, $CDCl_3$): 191.95, 147.97, 140.74, 140.56, 139.06, 134.32, 130.69, 130.42, 130.25, 129.71, 129.25, 128.28, 127.99, 127.56, 126.73.

[1,1';3',1'']Terphenyl-4-carbaldehyde (49a).

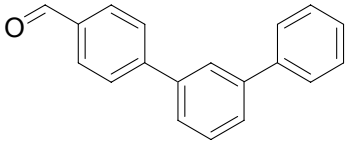

Compound **49a** was prepared according to General Procedure E from 4-formylphenylboronic acid (0.50 g, 3.33 mmol) and 3-bromobiphenyl (0.78 g, 3.33 mmol) to afford a colorless solid (72.1 %);

mp: 103 – 105 ^{o}C; ^{1}H NMR (300 MHz, $CDCl_3$): δ 10.08 (s, 1H), 7.97 – 8.00 (d, *J*= 9 Hz, 2H), 7.83 – 7.85 (d, *J*= 6 Hz, 2H), 7.80 (s, 1H), 7.61 – 7.67 (m, 4H), 7.56 – 7.58 (d, *J*= 5.5 Hz, 1H), 7.46 – 7.51 (t, *J*= 7.5 Hz, 2H), 7.40 – 7.42 (d, *J*= 6 Hz, 1H); ^{13}C NMR (75 MHz, $CDCl_3$): δ 192.19, 147.38, 142.36, 141.01, 140.51, 135.52, 130.56, 129.71, 129.15, 128.29, 128.05, 127.89, 127.50, 127.49, 126.52.

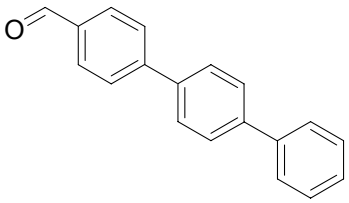

[1,1';4',1'']Terphenyl-4-carbaldehyde (50a).

Compound **50a** was prepared according to General Procedure E from 4-formylphenylboronic acid (0.64 g, 4.29 mmol) and 4-bromobiphenyl (1.00 g, 4.29 mmol) to afford a colorless solid (35 %); mp: 202 – 204 ^{o}C; ^{1}H NMR (300 MHz, $CDCl_3$): δ 10.08 (s, 1H), 7.96 – 8.00 (m, 2H), 7.81 – 7.84 (d, *J*= 9 Hz, 2H), 7.74 (s, 4H), 7.65 – 7.68 (m, 2H), 7.47 – 7.52 (m, 2H), 7.40 – 7.43 (t, *J*= 4.5 Hz, 1H); ^{13}C NMR (75 MHz, $CDCl_3$): δ 191.87, 146.61, 141.33, 140.26, 138.46, 135.21, 130.30, 128.87, 127.71, 127.49, 128.51, 127. 38, 127.05.

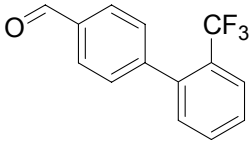

2'-Trifluoromethyl-biphenyl-4-carbaldehyde (51a).

Compound **51a** was prepared according to General Procedure E from 4-formylphenylboronic acid (0.50 g, 3.33 mmol) and 2-trifluoromethylphenyl bromide (0.75 g, 3.33 mmol) to afford a colorless solid (85.3 %); mp: 74 – 76 ^{o}C; ^{1}H NMR (300 MHz, $CDCl_3$): δ 10.04 (s, 1H), 7.88 – 7.91 (d, *J*= 9 Hz, 2H), 7.73 – 7.76 (d, *J*= 9 Hz, 1H), 7.55 – 7.58 (t, *J*= 4.5 Hz, 1H), 7.47 – 7.51 (m, 3H), 7.29 – 7.32 (d, *J*= 9 Hz, 1H); ^{13}C NMR (75 MHz, $CDCl_3$): δ 192.03, 146.24, 140.13, 135.81, 131.80, 131.70, 129.95, 129.37, 128.34, 126.48, 126.42, 126.05.

3'-Trifluoromethyl-biphenyl-4-carbaldehyde (52a).

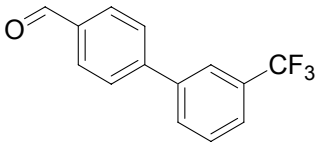

Compound **52a** was prepared according to General Procedure E from 4-formylphenylboronic acid (0.50 g, 3.33 mmol) and 3-trifluoromethylphenyl bromide (0.75 g, 3.33 mmol) to afford a colorless oil (72.1 %); ^{1}H NMR (300 MHz, $CDCl_3$): δ 10.05 (s, 1H), 7.97 – 7.98 (d, *J*= 3 Hz, 2H), 7.85 (s, 1H), 7.71 – 7.79 (m, 3H), 7.64 – 7.67 (m, 1H), 7.55 – 7.61 (m, 1H); ^{13}C NMR (75 MHz, $CDCl_3$): δ 191.93, 145.65, 140.72, 135.96, 130.85, 130.58, 128.78, 127.99, 127.63, 125.56, 124.31.

4'-Trifluoromethyl-biphenyl-4-carbaldehyde (53a).

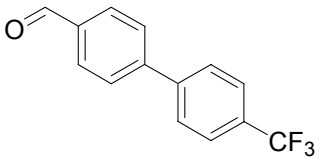

Compound **53a** was prepared according to General Procedure E from 4-formylphenylboronic acid (0.50 g, 3.33 mmol) and 4-trifluoromethylphenyl bromide (0.75 g, 3.33 mmol) to afford a colorless solid (91.3 %); mp: 64 – 66 ^{o}C; ^{1}H NMR (300 MHz, $CDCl_3$): δ 10.01 (s, 1H), 7.92 – 7.93 (t, *J*= 3.3 Hz, 1H), 7.89 – 7.90 (t, *J*= 3.6 Hz, 1H), 7.69 – 7.701, *J*= 3.3 Hz, 1H), 7.66 – 7.67 (m, 5H); ^{13}C NMR (75 MHz, $CDCl_3$): δ 191.82, 145.52, 143.35, 136.07, 130.47, 128.01, 127.85, 127.25, 126.11, 126.06, 122.52.

2',3',4',5',6'-Pentafluorobiphenyl-4-carbaldehyde (54a).

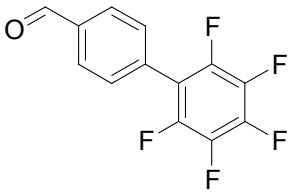

Compound **54a** was prepared according to General Procedure E from 4-formylphenylboronic acid (1.00 g, 6.67 mmol) and pentafluorophenylbromide (1.65 g, 6.67 mmol) to afford a colorless, amorphous solid (28.2 %) which was carried on slightly impure.

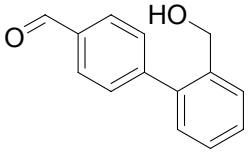

2'-Hydroxymethyl-biphenyl-4-carbaldehyde (55a).

Compound **55a** was prepared according to General Procedure E from 4-formylphenylboronic acid (0.50 g, 3.33 mmol) and 4-trifluoromethylphenyl bromide (0.77 g, 3.33 mmol) to afford a colorless solid (29.8 %); ^{1}H NMR (300 MHz, $CDCl_3$): δ 10.06 (s, 1H), 7.92 – 7.95 (d, *J*= 9 Hz, 2H), 7.55 – 7.60 (m 3H), 7.36 – 7.48 (m, 2H), 7.26 – 7.28 (m, 1H), 4.62 (s, 2H); ^{13}C NMR (75 MHz, $CDCl_3$): δ 192.26, 147.32, 140.30, 138.08, 135.43, 130.18, 130.02, 129.89, 129.08, 128.76, 128.15, 63.13.

4-Pyridin-3-yl-benzaldehyde (57a).

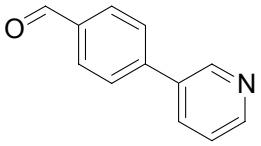

Compound **57a** was prepared according to General Procedure E from 4-formylphenylboronic acid (0.50 g, 3.33 mmol) and 3-bromopyridine (0.51 g, 3.33 mmol) to afford a colorless solid (50.8 %); mp: 51 – 52 ^{o}C; ^{1}H NMR (300 MHz, $CDCl_3$): δ 10.06 (s, 1H), 8.88 (s, 1H), 8.64 (s, 1H), 7.97 – 7.99 (d, *J*= 6 Hz, 2H), 7.91 – 7.93 (m, 1H), 7.73 – 7.75 (d, *J*= 6 Hz, 2H), 7.38 – 7.42 (m, 1H); ^{13}C NMR (75 MHz, $CDCl_3$): δ 191.60, 149.45, 148.28, 143.62, 135.68, 135.18, 134.49, 130.35, 127.65, 123.63.

4-Pyridin-4-yl-benzaldehyde (58a).

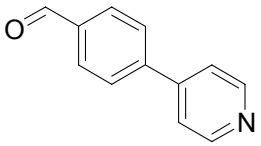

Compound **58a** was prepared according to General Procedure E from 4-formylphenylboronic acid (0.75 g, 5.00 mmol) and 4-bromopyridine (0.97 g, 5.00 mmol) to afford a colorless solid (50.8 %); mp: 83 – 85 ^{o}C; ^{1}H NMR (300 MHz, $CDCl_3$): δ 10.05 (s, 1H), 8.67 – 8.87 (m, 2H), 7.95 – 7.98 (d, *J*= 9

Hz, 2H), 7.74 – 7.77 (d, *J*= 9 Hz, 2H), 7.49 – 7.51 (d, *J*= 6 Hz, 2H); ^{13}C NMR (75 MHz, $CDCl_3$): δ 191.52, 150.38, 146.74, 143.80, 136.31, 130.29, 127.60, 121.62.

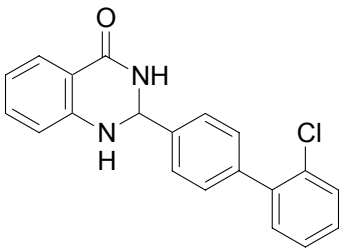

2-(2'-Chlorobiphenyl-4-yl)-2,3-dihydro-1H-quinazolin-4-one (32). Compound **32** was prepared according to General Procedure C from 4-(2-chlorophenyl)-benzaldehyde **32a** (0.52 g, 2.4 mmol) and anthranilamide (0.33 g, 2.4 mmol) to afford a colorless solid.(66.4 %); mp: 187-190 °C; ^{1}H NMR (300 MHz, DMSO-d_6) δ 8.31 (s, 1H), 7.22-7.65 (m, 11H), 6.63-6.81 (m, 2H), 5.83 (s, 1H); ^{13}C NMR (75 MHz, DMSO-d_6) δ 164.5, 148.7, 142.2, 140.3, 139.8, 134.3, 132.4, 132.2, 130.8, 130.2, 128.5, 128.3, 127.7, 118.1, 115.8, 115.4, 67.2; ESI *m/z* (rel intensity) 334.6 (M^+, 100), 336.5 (35); Anal. ($C_{20}H_{15}ClN_2O$) C, H, N; C: calcd, 71.75; found, 71.65; H: calcd, 4.52; found, 4.49; N: calcd, 8.37; found, 8.32.

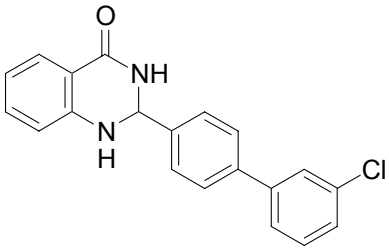

2-(3'-Chlorobiphenyl-4-yl)-2,3-dihydro-1H-quinazolin-4-one (33). Compound **33** was prepared according to General Procedure C from 4-(3-chlorophenyl)-benzaldehyde **33a** (0.40 g, 1.85 mmol) and anthranilamide (0.25 g, 1.85 mmol) to afford a colorless solid; mp: 225-228 °C (dec); ^{1}H NMR (300 MHz, DMSO-d_6) δ 8.31 (s, 1H); 7.10-7.75 (m, 11H), 6.61-6.72 (m, 2H), 5.80 (s, 1H); ^{13}C NMR (75 MHz, DMSO-d_6) δ 164.5, 148.7, 142.8, 142.6, 139.6, 134.7, 134.3, 131.7, 128.4, 128.3, 127.8, 127.3, 126.3, 118.1, 115.9, 115.4, 67.0; ESI *m/z* (rel intensity) 332.8 (100), 334.8 (M^+, 60). Anal.

($C_{20}H_{15}ClN_2O$) C, H, N; C: calcd, 71.75; found, 71.88; H: calcd, 4.52; found, 4.45; N: calcd, 8.37; found, 8.36.

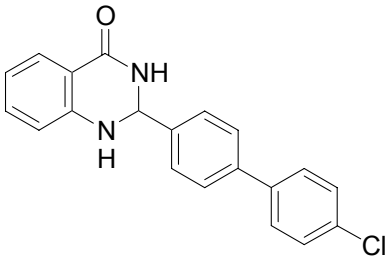

2-(4'-Chlorobiphenyl-4-yl)-2,3-dihydro-1H-quinazolin-4-one (34). Compound **34** was prepared according to General Procedure C from 4-(4-chlorophenyl)benzaldehyde **34a** (0.33 g, 1.52 mmol) and anthranilamide (0.21 g, 1.52 mmol) to afford a colorless solid (71.1%); mp >300 °C; ^{1}H NMR (300 MHz, DMSO-d_6) δ 8.31 (s, 1H), 7.52-7.76 (m, 9H), 7.17-7.22 (m, 2H), 6.64-6.74 (m, 2H), 5.81 (s, 1H); ^{13}C NMR (75 MHz, DMSO-d_6) δ 163.6, 147.8, 141.4, 138.9, 138.5, 133.4, 132.5, 128.9, 128.5, 127.5, 126.7, 117.2, 115.0, 114.5, 66.1; ESI *m/z* (rel intensity) 334.8 (M^+, 100), 336.8 (35); Anal. ($C_{20}H_{15}ClN_2O$) C, H, N; C: calcd, 71.75; found, 71.70; H: calcd, 4.52; found, 4.43; N: calcd, 8.37; found, 8.33.

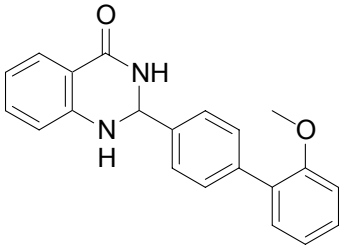

2-(2'-Methoxy-biphenyl-4-yl)-2,3-dihydro-1H-quinazolin-4-one (35).

Compound **35** was prepared according to General Procedure C from 4-(2-methoxyphenyl)benzaldehyde **35a** (0.20 g, 1.09 mmol) and anthranilamide (0.15 g, 1.09 mmol) to afford a colorless solid (68.3%); mp: 163 – 165 °C; ^{1}H NMR (300 MHz, DMSO): δ 8.33 (s, 1H), 7.61 – 7.63 (d, *J*= 6 Hz, 1H), 7.46 – 7.53 (m, 4H), 7.34 – 7.37 (t, *J*= 4.5 Hz, 1H), 7.23 – 7.27 (t, *J*= 6 Hz, 2H), 7.16 (s, 1H), 7.09 – 7.12 (d, *J*= 9 Hz, 1H), 6.99 – 7.04 (t, *J*= 7.5 Hz, 1H), 6.74 – 6.77 (d, *J*= 9 Hz,

1H), 6.65 – 6.70 (t, *J*= 7.5 Hz, 1H), 5.78 (s, 1H), 3.75 (s, 3H); ^{13}C NMR (75 MHz, DMSO): δ 163.64, 156.12, 147.90, 140.17, 138.41, 133.36, 130.33, 129.25, 129.23, 129.02, 127.40, 126.56, 120.78, 117.13, 114.94, 114.41, 111.70, 66.44, 55.44; ESI *m/z* (rel intensity) 330.8 (M^+, 100); Anal. ($C_{21}H_{18}N_2O\cdot.3H_2O$) C, H, N; C: calcd, 75.11; found, 75.34; H: calcd, 5.58; found, 5.50; N: calcd, 8.34; found, 8.30.

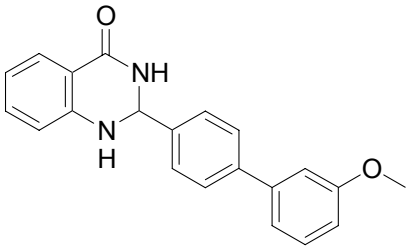

2-(3'-Methoxy-biphenyl-4-yl)-2,3-dihydro-1H-quinazolin-4-one (36).

Compound **36** was prepared according to General Procedure C from 4-(3-methoxyphenyl)benzaldehyde **36a** (0.47 g, 2.21 mmol) and anthranilamide (0.30 g, 2.21 mmol) to afford a colorless solid (42.5 %); mp: 163 – 165 °C; ^{1}H NMR (300 MHz, DMSO): δ 8.34 (s, 1H), 7.66 – 7.69 (d, *J*= 9 Hz, 2H), 7.58 – 7.62 (d, *J*= 11.5 Hz, 1H), 7.53 – 7.55 (d, *J*= 6 Hz, 2H), 7.33 – 7.38 (t, *J*= 7.5 Hz, 1H), 7.19 – 7.26 (m, 2H), 7.16 (s, 2H), 6.91 – 6.94 (d, *J*= 9 Hz, 1H), 6.73 – 6.75 (d, *J*= 6 Hz, 1H), 6.63 – 6.69 (m, 1H), 5.78 (s, 1H), 3.80 (s, 3H); ^{13}C NMR (75 MHz, DMSO): δ 163.59, 159.74, 147.81, 141.21, 141.03, 140.19, 133.35, 130.01, 127.37, 126.74, 119.01, 117.14, 114.99, 114.43, 113.09, 112.25, 66.12, 55.12; ESI *m/z* (rel intensity) 330.9 (M^+, 100); Anal. ($C_{21}H_{18}N_2O_2$) C, H, N; C: calcd, 76.34; found, 76.11; H: calcd, 5.49; found, 5.50; N: calcd, 8.48; found, 8.33.

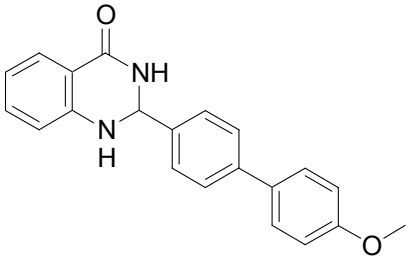

2-(4'-Methoxy-biphenyl-4-yl)-2,3-dihydro-1H-quinazolin-4-one (37).

Compound **37** was prepared according to General Procedure C from 4-(4-methoxyphenyl)benzaldehyde **37a** (0.19 g, .90 mmol) and anthranilamide (0.12 g, .90 mmol) to afford a colorless solid (33.8 %); mp: 203 – 204 °C; ^{1}H NMR (300 MHz, DMSO): δ 8.33 (s, 1H), 7.59 – 7.65 (m, 5H), 7.52 – 7.55 (d, *J*= 9 Hz, 2H), 7.23 – 7.28 (t, *J*= 7.5 Hz, 1H), 7.15 (s, 1H), 7.00 – 7.03 (d, *J*= 9 Hz, 2H), 6.74 – 6.77 (d, *J*= 9 Hz, 1H), 6.65 – 6.70 (t, *J*= 7.5 Hz, 1H), 5.78 (s, 1H), 3.79 (s, 3H); ^{13}C NMR (75 MHz, DMSO): δ 163.63, 159.03, 147.88, 140.07, 140.06, 133.35, 132.05, 127.79, 127.41, 126.10, 117.14, 115.01, 114.41, 66.23, 55.20; ESI *m/z* (rel intensity) 330.9 (M^{+}, 100); Anal. ($C_{21}H_{18}N_2O_2 \cdot 0.4H_2O$) C, H, N; C: calcd, 74.71; found, 74.77; H: calcd, 5.61; found, 5.39; N: calcd, 8.30; found, 8.31.

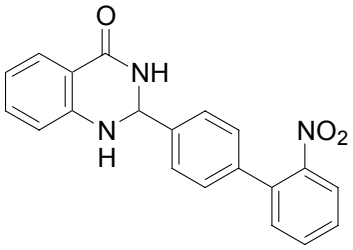

2-(2'-Nitro-biphenyl-4-yl)-2,3-dihydro-1H-quinazolin-4-one (38).

Compound **38** was prepared according to General Procedure C from 4-(2-nitrophenyl)benzaldehyde **38a** (0.70 g, 3.10 mmol) and anthranilamide (0.42 g, 3.10 mmol) to afford a colorless solid (71.9 %); mp: 198 – 200 °C; ^{1}H NMR (300 MHz, DMSO): δ 8.39 (s, 1H), 7.95 – 7.98 (d, *J*= 9 Hz, 1H), 7.71 – 7.77 (t, *J*= 9 Hz, 1H), 7.50 – 7.63 (m, 4H), 7.35 – 7.38 (d, *J*= 9 Hz, 2H), 7.22 – 7.27 (m, 2H), 6.76 – 6.78 (d, *J*= 6 Hz, 1H), 6.64 – 6.69 (t, *J*= 7.5 Hz, 1H), 5.82 (s, 1H); ^{13}C NMR (75 MHz, DMSO): δ 163.46, 148.79, 147.70, 141.81, 136.94, 134.54, 133.37,

132.89, 131.80, 128.90, 127.82, 127.34, 127.18, 124.06, 117.11, 114.80, 114.38, 66.07; ESI *m/z* (rel intensity) 345.3 (M^+, 100); Anal. ($C_{20}H_{15}N_3O_3$) C, H, N; C: calcd, 69.56; found, 69.14; H: calcd, 4.38; found, 4.53; N: calcd, 12.17; found, 12.05.

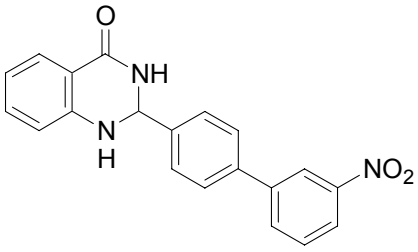

2-(3'-Nitro-biphenyl-4-yl)-2,3-dihydro-1H-quinazolin-4-one (39).

Compound **39** was prepared according to General Procedure C from 4-(3-nitrophenyl)benzaldehyde **39a** (0.50 g, 2.20 mmol) and anthranilamide (0.30 g, 2.20 mmol) to afford a colorless solid (36.8 %); mp: 236 – 237 °C (dec.); ^{1}H NMR (300 MHz, DMSO): δ 8.43 (s, 1H), 8.20 – 8.23 (d, *J*= 9 Hz, 1H), 8.13 – 8.15 (d, *J*= 6 Hz, 1H), 7.80 – 7.83 (d, *J*= 9 Hz, 2H), 7.72 – 7.78 (t, *J*= 9 Hz, 1H), 7.62 – 7.64 (d, *J*= 6 Hz, 3H), 7.23 – 7.28 (m, 2H), 6.76 – 6.80 (d, *J*= 12 Hz, 1H), 6.66 – 6.68 (t, *J*= 3 Hz, 1H), 5.84 (s, 1H); ^{13}C NMR (75 MHz, DMSO): δ 163.40, 148.38, 147.63, 142.16, 141.20, 137.76, 133.32, 133.21, 130.41, 127.55, 127.32, 126.96, 122.21, 120.98, 117.13, 114.92, 114.42, 65.86; ESI *m/z* (rel intensity) 345.3 (M^+, 100); Anal. ($C_{20}H_{15}N_3O_3$) C, H, N; C: calcd, 69.56; found, 69.87; H: calcd, 4.38; found, 4.39; N: calcd, 12.17; found, 12.22.

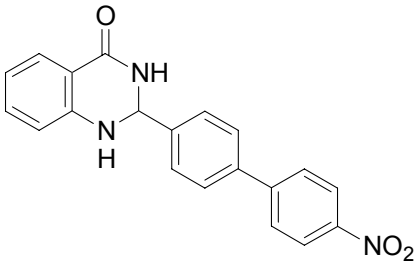

2-(4'-Nitro-biphenyl-4-yl)-2,3-dihydro-1H-quinazolin-4-one (40).

Compound **40** was prepared according to General Procedure C from 4-(4-nitrophenyl)benzaldehyde **40a**

(0.95 g, 3.91 mmol) and anthranilamide (0.53 g, 3.91 mmol) to afford a colorless solid (64.7 %); mp: 241 – 243 °C (dec.); ^{1}H NMR (300 MHz, DMSO): δ 8.42 (s, 1H), 8.29 – 8.32 (d, *J*= 9 Hz, 2H), 7.95 – 7.98 (d, *J*= 9 Hz, 2H), 7.81 – 7.84 (d, *J*= 9 Hz, 2H), 7.61 – 7.65 (m, 3H), 7.23 – 7.28 (m, 2H), 6.75 – 6.78 (d, *J*= 9 Hz, 1H), 6.66 – 6.71 (t, *J*= 7.5 Hz, 1H), 5.83 (s, 1H); ^{13}C NMR (75 MHz, DMSO): δ 163.50, 147.62, 146.63, 146.02, 142.61, 137.76, 133.33, 127.72, 127.56, 127.33, 127.20, 124.01, 117.15, 114.92, 114.41, 65.88; ESI *m/z* (rel intensity) 345.3 (M^{+},100); Anal. ($C_{20}H_{16}N_3O_3$) C, H, N; C: calcd, 69.56; found, 69.30; H: calcd, 4.38; found, 4.35; N: calcd, 12.17; found, 12.11.

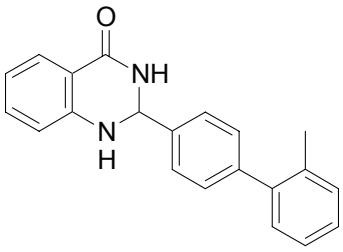

2-(2'-Methylbiphenyl-4-yl)-2,3-dihydro-1H-quinazolin-4-one (41). Compound **41** was prepared according to General Procedure C from 4-(2-methylphenyl)-benzaldehyde **41a** (0.47 g, 2.39 mmol) and anthranilamide (0.33 g, 2.39 mmol) to afford a colorless solid; mp: 169-171 °C; ^{1}H NMR (300 MHz, DMSO-d_6) δ 8.31 (s, 1H); 7.51-7.62 (m, 2H), 7.11-7.47 (m, 9H), 6.61-6.82 (m, 2H), 5.82 (s, 1H), 2.21 (s, 3H); ^{13}C NMR (75 MHz, DMSO-d_6) δ 164.5, 148.8, 142.4, 141.7, 141.3, 135.6, 134.3, 131.3, 130.4, 129.9, 128.3, 127.7, 126.9, 118.0, 115.8, 115.3, 109.8, 67.3, 21.1; ESI *m/z* (rel intensity) 314.7 (M^{+}, 100); Anal. ($C_{21}H_{18}N_2O$) C, H, N; C: calcd, 80.23; found, 80.19; H: calcd, 5.77; found, 5.79; N: calcd, 8.91; found, 8.83.

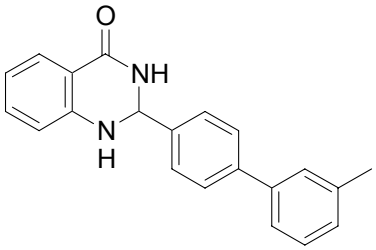

2-(3'-Methylbiphenyl-4-yl)-2,3-dihydro-1H-quinazolin-4-one (42). Compound **42** was prepared according to General Procedure C from 4-(3-methylphenyl)-benzaldehyde **42a** (0.38 g, 1.94 mmol) and anthranilamide (0.26 g, 1.94 mmol); mp: 213-216 °C; ^{1}H NMR (300 MHz, DMSO-d_6) δ 8.30 (s, 1H); 7.13-7.77 (m, 11H), 6.62-6.72 (m, 2H), 5.81 (s, 1H), 2.32 (s, 3H); ^{13}C NMR (75 MHz, DMSO-d_6) δ 164.5, 148.8, 141.7, 141.4, 140.6, 139.0, 134.3, 129.9, 129.8, 129.1, 128.7, 128.6, 128.3, 127.5, 124.8, 118.1, 115.9, 115.4, 67.2, 22.0; ESI *m/z* (rel intensity) 314.8 (M^+, 100); Anal. ($C_{21}H_{18}N_2O$) C, H, N; C: calcd, 80.23; found, 79.96; H: calcd, 5.77; found, 5.66; N: calcd, 8.91; found, 8.91.

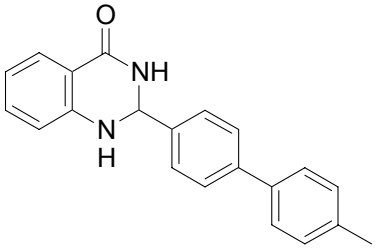

2-(4'-Methylbiphenyl-4-yl)-2,3-dihydro-1H-quinazolin-4-one (43). Compound **43** was prepared according to General Procedure C from 4-(4-methylphenyl)benzaldehyde **43a** (0.30 g, 1.53 mmol) and anthranilamide (0.21 g, 1.53 mmol); mp: 196-198 °C; ^{1}H NMR (300 MHz, DMSO-d_6) δ 8.33 (s, 1H); 7.43-7.74 (m, 9H), 7.18-7.39 (m, 2H), 6.63-6.72 (m, 2H), 5.81 (s, 1H), 2.31 (s, 3H); ^{13}C NMR (75 MHz, DMSO-d_6) δ 163.7, 147.9, 140.9, 140.6, 140.4, 140.3, 137.0, 136.9, 133.4, 129.6, 129.0, 127.5, 126.7, 126.4, 117.2, 115.0, 114.5, 66.2, 21.2; ESI *m/z* (rel intensity) 314.8 (M^+, 100); Anal. ($C_{21}H_{18}N_2O$) C, H, N; C: calcd, 80.23; found, 80.02; H: calcd, 5.77; found, 5.54; N: calcd, 8.91; found, 9.09.

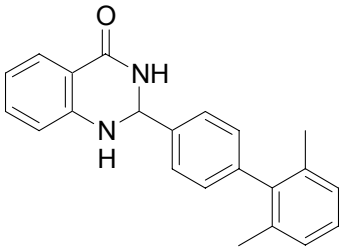

2-(2',6'-Dimethylbiphenyl-4-yl)-2,3-dihydro-1H-quinazolin-4-one (44). Compound **44** was prepared according to General Procedure C from 4-(2,6-dimethylphenyl)-benzaldehyde **44a** (0.25 g, 1.19 mmol) and anthranilamide (0.16 g, 1.19 mmol) to afford a colorless solid (68.9 %); mp: 198-201 °C; ^{1}H NMR (300 MHz, DMSO): δ 8.35 (s, 1H), 7.64 – 7.65 (d, *J*= 3 Hz, 1H), 7.57 – 7.58 (d, *J*= 3 Hz, 2H), 7.25 – 7.29 (t, *J*= 6 Hz, 1H), 7.15 – 7.20 (m, 4H), 7.11 – 7.12 (d, *J*= 3 Hz, 2H), 6.80 – 6.81 (d, *J*= 3 Hz, 1H), 6.68 – 6.71 (t, *J*= 4.5 Hz, 1H), 5.84 (s, 1H), 1.96 (s, 6H); ^{13}C NMR (75 MHz, DMSO): δ 163.45, 147.92, 140.93, 140.57, 140.17, 135.20, 133.37, 128.91, 127.33, 127.32, 127.07, 126.95, 117.05, 114.78, 114.36, 66.48, 20.64; ESI *m/z* (rel intensity) 326.8 (M^{+}, 100); Anal. ($C_{22}H_{20}N_2O \cdot 0.6H_2O$) C, H, N; C: calcd, 77.95; found, 78.29; H: calcd, 6.30; found, 6.08; N: calcd, 8.26; found, 8.13.

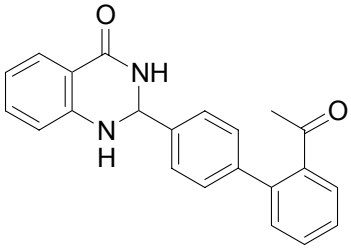

2-(2'-Acetyl-biphenyl-4-yl)-2,3-dihydro-1H-quinazolin-4-one (45). Compound **45** was prepared according to General Procedure C from 4-(2-acetylphenyl)-benzaldehyde **45a** (0.62 g, 2.77 mmol) and anthranilamide (0.38 g, 2.77 mmol) to afford a colorless solid (40.5 %); mp: 171-173 ° C; ^{1}H NMR (300 MHz, DMSO): δ 8.36 (s, 1H), 7.53 – 7.60 (m, 5H), 7.46 – 7.49 (m, 1H), 7.35 – 7.38 (d, *J*= 9 Hz, 1H), 7.30 – 7.32 (m, 2H), 7.21 – 7.26 (m, 1H), 7.18 (s, 1H), 6.75 – 6.77 (d, *J*= 6 Hz, 1H), 6.64 – 6.69 (t, *J*= 7.5 Hz, 1H), 5.80 (s, 1H), 2.18 (s, 3H); ^{13}C NMR (75 MHz, DMSO): δ 164.19, 148.50, 141.65, 141.22, 140.96, 140.10, 134.06, 131.53, 131.09, 129.30, 128.43, 128.22, 128.05, 127.72, 117.82, 115.57, 115.10, 66.91,

31.08; ESI *m/z* (rel intensity) 342.9 (M^+, 100); Anal. ($C_{22}H_{18}N_2O_2$) C, H, N; C: calcd, 77.17; found, 76.91; H: calcd, 5.30; found, 5.40; N: calcd, 8.18; found, 8.17.

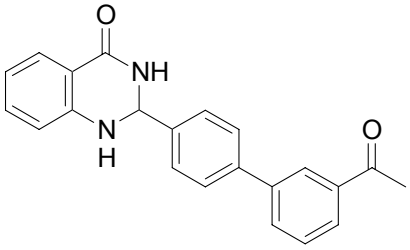

2-(3'-Acetyl-biphenyl-4-yl)-2,3-dihydro-1H-quinazolin-4-one (46).

Compound **46** was prepared according to General Procedure C from 4-(3-acetylphenyl)-benzaldehyde **46a** (0.90 g, 4.06 mmol) and anthranilamide (0.55 g, 4.06 mmol) to afford a colorless solid (39.7 %); mp: 179-181 °C; ^{1}H NMR (300 MHz, DMSO): δ 8.34 (s, 1H), 8.17 (s, 1H), 7.90 – 7.95 (t, *J*= 7.5 Hz, 2H), 7.74 – 7.77 (d, *J*= 9 Hz, 2H), 7.57 – 7.62 (m, 4H), 7.20 – 7.27 (m, 2H), 6.75 – 6.78 (d, *J*= 9 Hz, 1H), 6.65 – 6.69 (t, *J*= 6 Hz, 1H), 5.82 (s, 1H), 2.64 (s, 3H); ^{13}C NMR (75 MHz, DMSO): δ 197.92, 163.53, 147.71, 141.36, 140.05, 139.32, 137.42, 133.30, 131.28, 129.35, 127.45, 127.32, 127.17, 126.80, 126.26, 117.10, 114.94, 114.39, 65.99, 26.87; ESI *m/z* (rel intensity) 342.4 (M^+, 100); Anal. ($C_{22}H_{18}N_2O_2$) C, H, N; C: calcd, 77.17; found, 76.99; H: calcd, 5.30; found, 5.34; N: calcd, 8.18; found, 8.28.

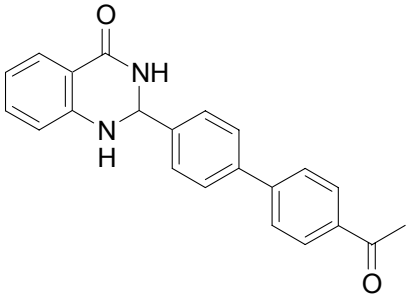

2-(4'-Acetyl-biphenyl-4-yl)-2,3-dihydro-1H-quinazolin-4-one (47).

Compound **47** was prepared according to General Procedure C from 4-(4-acetylphenyl)-benzaldehyde **47a** (1.10 g, 4.91 mmol) and anthranilamide (0.67 g, 4.91 mmol) to afford a colorless solid (71.9 %); mp: 271-273 °C; ^{1}H NMR (300 MHz,

DMSO): δ 8.44 (s, 1H), 8.02 – 8.05 (d, *J*= 9 Hz, 2H), 7.76 – 7.83 (m, 4H), 7.62 – 7.67 (t, *J*= 7.5 Hz, 3H), 7.24 – 7.27 (m, 2H), 6.78 – 6.81 (d, *J*= 9 Hz, 1H), 6.67 – 6.72 (t, *J*= 7.5 Hz, 1H), 5.85 (s, 1H), 2.61 (s, 3H); ^{13}C NMR (75 MHz, DMSO): δ 197.44, 163.58, 147.72, 143.95, 141.83, 138.93, 135.65, 133.35, 128.87, 127.52, 127.37, 126.93, 126.81, 117.16, 114.96, 114.43, 66.04, 26.74; ESI *m/z* (rel intensity) 342.4 (M^+, 100); Anal. ($C_{21}H_{18}N_2O \cdot 0.75H_2O$) C, H, N; C: calcd, 74.25; found, 73.85; H: calcd, 5.52; found, 5.13; N: calcd, 7.87; found, 7.86.

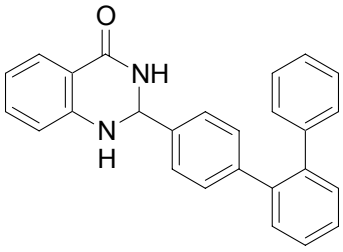

2-[1,1';2',1'']Terphenyl-4-yl-2,3-dihydro-1H-quinazolin-4-one (48).

Compound **48** was prepared according to General Procedure C from [1,1';2',1'']Terphenyl-4-carbaldehyde **48a** (0.40 g, 1.46 mmol) and anthranilamide (0.20 g, 1.46 mmol) to afford a colorless solid (85.5 %); mp: 257-259 °C; ^{1}H NMR (300 MHz, DMSO): δ 8.28 (s, 1H), 7.59 – 7.61 (d, *J*= 6 Hz, 1H), 7.45 – 7.47 (m, 2H), 7.39 – 7.40 (t, *J*= 1.5 Hz, 2H), 7.34 – 7.35 (d, *J*= 3 Hz, 2H), 7.23 – 7.25 (t, *J*= 3 Hz, 4H), 7.11 – 7.14 (m, 5H), 6.75 – 6.76 (d, *J*= 3 Hz, 1H), 6.65 – 6.69 (t, *J*= 6 Hz, 1H), 5.72 (s, 1H); ^{13}C NMR (75 MHz, DMSO): δ 163.42, 147.76, 141.09, 141.02, 140.08, 139.94, 139.37, 133.31, 130.59, 130.58, 129.48, 129.47, 128.08, 127.71, 127.31, 126.64, 126.39, 117.04, 114.85, 114.39, 66.04; ESI *m/z* (rel intensity) 374.8 (M^+, 100). Anal. ($C_{26}H_{20}N_2O \cdot 0.4H_2O$) C, H, N; C: calcd, 81.78; found, 81.91; H: calcd, 5.44; found, 5.50; N: calcd, 7.34; found, 7.22.

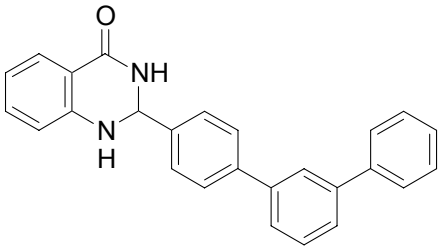

2-[1,1';3',1'']Terphenyl-4-yl-2,3-dihydro-1H-quinazolin-4-one (49).

Compound **49** was prepared according to General Procedure C from [1,1';3',1'']terphenyl-4-carbaldehyde **49a** (0.50 g, 1.94 mmol) and anthranilamide (0.26 g, 1.94 mmol) to afford a colorless solid (80.9 %); mp: 223-225 °C; ^{1}H NMR (300 MHz, DMSO): δ 8.41 (s, 1H), 7.90 – 7.92 (d, *J*= 6 Hz, 1H), 7.75 – 7.83 (m, 5H), 7.60 – 7.66 (m, 6H), 7.49 – 7.57 (m, 3H), 7.39 – 7.44 (t, *J*= 7.5 Hz, 1H), 6.78 – 6.84 (t, *J*= 9 Hz, 1H), 6.70 – 6.72 (d, *J*= 6 Hz, 1H), 5.84 (s, 1H); ^{13}C NMR (75 MHz, DMSO): δ 163.56, 147.77, 140.97, 140.96, 140.36, 140.19, 140.04, 133.28, 129.51, 128.86, 127.53, 127.37, 126.86, 125.93, 125.77, 125.07, 117.09, 114.95, 114.39, 66.12; ESI *m/z* (rel intensity) 374.8 (M^+, 100); Anal. ($C_{26}H_{20}N_2O \cdot 0.1H_2O$) C, H, N; C: calcd, 82.57; found, 82.31; H: calcd, 5.38; found, 5.44; N: calcd, 7.41; found, 7.52.

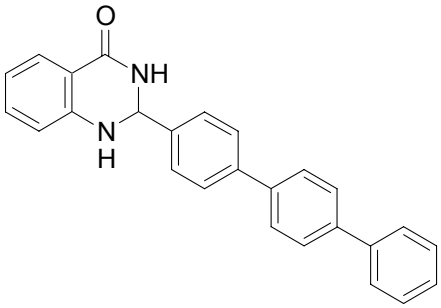

2-[1,1';4',1'']Terphenyl-4-yl-2,3-dihydro-1H-quinazolin-4-one (50).

Compound **50** was prepared according to General Procedure C from [1,1';4',1'']terphenyl-4-carbaldehyde **50a** (0.40 g, 1.55 mmol) and anthranilamide (0.21 g, 1.55 mmol) to afford a colorless solid (25.8 %); mp > 350 ° C; ^{1}H NMR (300 MHz, DMSO): δ 8.38 (s, 1H), 7.76 – 7.82 (m, 8H), 7.64 – 7.71 (m, 3H), 7.51 – 7.54 (t, *J*= 4.5 Hz, 2H), 7.43 – 7.45 (m, 1H),

7.30 - 7.33 (t, *J*= 4.5 Hz, 1H), 7.24 (s, 1H), 6.82 – 6.85 (d, *J*= 4.5 Hz, 1H), 6.72 – 6.77 (t, *J*= 7.5 Hz, 1H), 5.87 (s, 1H); ^{13}C NMR (75 MHz, DMSO): δ 163.52, 147.74, 140.88, 139.62, 139.47, 139.22, 138.56, 133.27, 128.91, 127.42, 127.31, 127.12, 126.49, 126.43, 117.06, 114.91, 114.36, 66.12; ESI *m/z* (rel intensity) 374.8 (M^+, 100); Anal. ($C_{26}H_{20}N_2O\cdot0.9H_2O$) C, H, N; C: calcd, 79.53; found, 79.27; H: calcd, 5.60; found, 5.20; N: calcd, 7.13; found, 7.35.

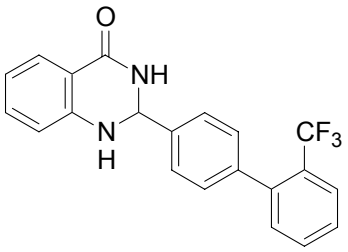

2-(2'-Trifluoromethyl-biphenyl-4-yl)-2,3-dihydro-1H-quinazolin-4-one (51).

Compound **51** was prepared according to General Procedure C from 2'-trifluoromethyl-biphenyl-4-carbaldehyde **51a** (0.63 g, 2.52 mmol) and anthranilamide (0.34 g, 2.52 mmol) to afford a colorless solid (99.2 %); mp: 180 - 182 °C; ^{1}H NMR (300 MHz, DMSO): δ 8.51 (s, 1H), 7.89 – 7.90 (d, *J*= 3 Hz, 1H), 7.68 – 7.76 (m, 5H), 7.34 – 7.43 (m, 5H), 6.92 (s, 1H), 6.77 (s, 1H), 5.96 (s, 5.96); ^{13}C NMR (75 MHz, DMSO): δ 163.56, 147.81, 141.39, 140.28, 139.42, 133.39, 132.16, 132.15, 128.74, 128.05, 127.40, 126.62, 126.37, 125.98, 117.13, 114.84, 114.44, 66.28; ESI *m/z* (rel intensity) 366.6 (M^+-1, 100); Anal. ($C_{21}H_{15}F_3N_2O$) C, H, N; C: calcd, 68.47; found, 68.54; H: calcd, 4.10; found, 4.30; N: calcd, 7.61; found, 7.44.

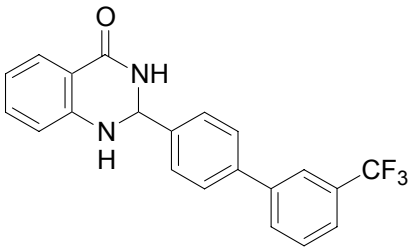

2-(3'-Trifluoromethyl-biphenyl-4-yl)-2,3-dihydro-1H-quinazolin-4-one (52).

Compound **52** was prepared according to General Procedure C from 3'-trifluoromethyl-biphenyl-4-carbaldehyde **52a** (0.55 g, 2.20 mmol) and anthranilamide (0.30 g, 2.20 mmol) to afford a colorless solid (52.3 %); mp: 242 - 244 °C; ^{1}H NMR (300 MHz, DMSO): δ 8.42 (s, 1H), 7.97 – 7.99 (d, *J*= 6 Hz, 2H), 7.77 – 7.80 (d, *J*= 9 Hz, 2H), 7.72 – 7.74 (m, *J*= 6 Hz, 2H), 7.61 – 7.65 (m, 3H), 7.24 – 7.29 (m, 2H), 6.77 – 6.80 (d, *J*= 9 Hz, 1H), 6.66 – 6.71 (t, *J*= 7.5 Hz, 1H), 5.84 (s, 1H); ^{13}C NMR (75 MHz, DMSO): δ 163.54, 147.70, 141.79, 140.68, 138.53, 133.34, 130.77, 130.02, 127.50, 127.34, 126.92, 124.12, 123.04, 117.12, 114.96, 114.42, 65.94; ESI *m/z* (rel intensity) 366.6 (M^{+}, 100); Anal. ($C_{21}H_{15}F_3N_2O$) C, H, N; C: calcd, 68.47; found, 68.64; H: calcd, 4.10; found, 4.12; N: calcd, 7.61; found, 7.71.

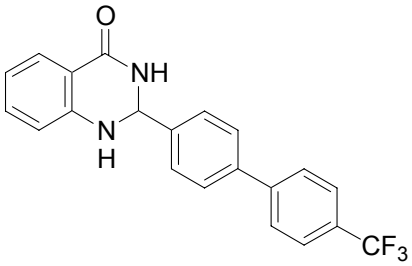

2-(4'-Trifluoromethyl-biphenyl-4-yl)-2,3-dihydro-1H-quinazolin-4-one (53).

Compound **53** was prepared according to General Procedure C from 4'-trifluoromethyl-biphenyl-4-carbaldehyde **53a** (0.60 g, 2.40 mmol) and anthranilamide (0.33 g, 2.4 mmol) to afford a colorless solid (45.1 %); mp: 274 - 276 °C; ^{1}H NMR (300 MHz, DMSO): δ 8.44 (s, 1H), 7.87 – 7.90 (d, *J*= 9 Hz, 2H), 7.75 – 7.82 (m, 4H), 7.63 – 7.68 (t, *J*= 7.5 Hz, 3H), 7.24 – 7.27 (m, 2H), 6.79 – 6.82 (d, *J*= 9 Hz, 1H), 6.80 – 7.10 (m, 1H), 5.86 (s, 1H); ^{13}C NMR (75 MHz, DMSO): δ 163.58, 147.72, 143.62,

141.95, 138.62, 133.33, 128.12, 127.55, 127.40, 126.98, 125.73, 117.15, 114.97, 114.43, 66.05; ESI *m/z* (rel intensity) 366.6 (M^+, 100). Anal. ($C_{21}H_{15}F_3N_2O$) C, H, N; C: calcd, 68.47; found, 68.48; H: calcd, 4.10; found, 4.11; N: calcd, 7.61; found, 7.62.

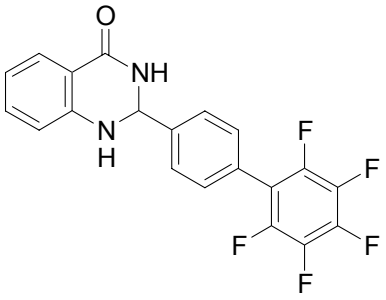

2-(2',3',4'5',6'-pentafluoro-biphenyl-4-yl)-2,3-dihydro-1H-quinazolin-4-one (54).

Compound **54** was prepared according to General Procedure C from 2',3',4',5',6'-tetrafluorobiphenyl-4-carbaldehyde **54a** (0.25 g, 1.84 mmol) and anthranilamide (0.25 g, 1.84 mmol) to afford a colorless solid (33.5 %); mp: 317 - 319 °C; ^{1}H NMR (300 MHz, DMSO): δ 8.39 (s, 1H), 7.61 – 7.69 (m, 3H), 7.53 – 7.56 (d, *J*= 9 Hz, 2H), 7.21 – 7.29 (m, 2H), 6.75 – 6.77 (d, *J*= 6 Hz, 1H), 6.67 – 6.72 (t, *J*= 7.5 Hz, 1H), 5.84 (s, 1H); ^{13}C NMR (75 MHz, DMSO): δ 163.43, 147.64, 145.20, 142.98, 141.94, 138.83, 135.55, 133.35, 130.07, 127.37, 126.78, 126.63, 125.80, 117.18, 114.80, 114.34, 68.15; ESI *m/z* (rel intensity) 390.9 (M^+, 100); Anal. ($C_{20}H_{11}N_2OF_5$) C, H, N; C: calcd, 61.55; found, 61.71; H: calcd, 2.84; found, 2.94; N: calcd, 7.18; found, 6.98.

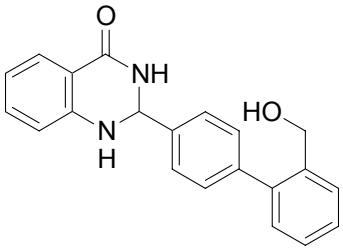

2-(2'-Hydroxymethyl-biphenyl-4-yl)-2,3-dihydro-1H-quinazolin-4-one (55).

Compound **55** was prepared according to General Procedure C from 2'-hydroxymethyl-biphenyl-4-carbaldehyde **55a** (1.29 g, 6.08 mmol) and anthranilamide (0.83 g, 6.08 mmol) to afford a colorless solid (38.3 %); mp: 165 - 167 °C; ^{1}H NMR (300 MHz, DMSO): δ 8.39 (s, 1H), 7.66 – 7.69 (d,

J= 9 Hz, 1H), 7.59 – 7.63 (m, 3H), 7.44 – 7.46 (d, *J*= 6 Hz, 2H), 7.23 – 7.44 (m, 4H), 6.80 – 6.83 (d, *J*= 9 Hz, 1H), 6.66 – 6.75 (m, 2H), 5.86 (s, 1H), 5.17 – 5.21 (t, *J*= 6 Hz, 1H), 4.43 – 4.44 (d, *J*= 3 Hz, 2H); ^{13}C NMR (75 MHz, DMSO): δ 164.36, 148.66, 141.39, 141.24, 140.40, 140.00, 134.14, 130.00, 129.78, 128.88, 128.17, 127.66, 277.49, 117.91, 115.67, 115.19, 67.18, 61.56; ESI *m/z* (rel intensity) 330.8 (M^+, 100); Anal. ($C_{20}H_{18}N_2O_2$) C, H, N; C: calcd, 76.34; found, 76.21; H: calcd, 5.49; found, 5.73; N: calcd, 8.48; found, 8.52.

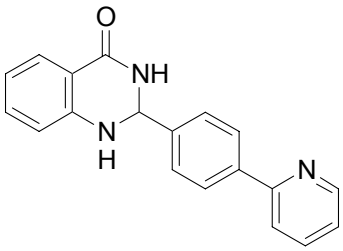

2-(4-Pyridin-2-yl-phenyl)-2,3-dihydro-1H-quinazolin-4-one (56).

Compound **56** was prepared according to General Procedure C from 4-pyridin-2-yl-benzaldehyde **56a** (1.00 g, 5.46 mmol) and anthranilamide (0.74 g, 5.46 mmol) to afford a colorless solid (76.0 %); mp: 196 - 198 °C; ^{1}H NMR (300 MHz, DMSO): δ 8.65 – 8.66 (d, *J*= 4.8 Hz, 1H), 8.36 (s, 1H), 8.07 – 8.10 (d, *J*= 9 Hz, 2H), 7.94 – 7.97 (d, *J*= 9 Hz, 1H), 7.84 – 7.87 (d, *J*= 9 Hz, 1H), 7.58 – 7.62 (m, 3H), 7.18 – 7.37 (m, 3H), 6.74 – 6.77 (d, *J*= 8.1 Hz, 1H), 6.65 – 6.70 (t, *J*= 7.5 Hz, 1H), 5.81 (s, 1H); ^{13}C NMR (75 MHz, DMSO): δ 164.26, 156.20, 150.40, 150.18, 148.49, 143.14, 138.17, 134.04, 128.93, 127.96, 127.39, 127.19, 123.45, 121.07, 117.86, 115.13, 66.86; ESI *m/z* (rel intensity) 301.3 (M^+, 100); Anal. ($C_{19}H_{15}N_3O$) C, H, N; C: calcd, 75.73; found, 75.77; H: calcd, 5.02; found, 4.94; N: calcd, 13.94; found, 13.92.

2-(4-Pyridin-3-yl-phenyl)-2,3-dihydro-1H-quinazolin-4-one (57).

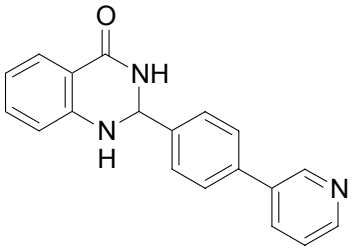

Compound **57** was prepared according to General Procedure C from 4-pyridin-3-yl-benzaldehyde **57a** (0.28 g, 1.53 mmol) and anthranilamide (0.21 g, 1.53 mmol) to afford a colorless solid (26.1 %); mp: 185 - 186 °C; ^{1}H NMR (300 MHz, DMSO): δ 8.90 (s, 1H), 8.57 – 8.58 (d, *J*= 3 Hz, 1H), 8.49 (s, 1H), 8.05 – 8.09 (d, *J*= 12 Hz, 1H), 7.74 – 7.77 (d, *J*= 9 Hz, 2H), 7.59 – 7.62 (m, 3H), 7.47 – 7.51 (d, *J*= 12 Hz, 1H), 7.21 – 7.28 (m, 2H), 6.75 – 6.78 (d, *J*= 9 Hz, 1H), 6.65 – 6.70 (t, *J*= 7.5 Hz, 1H), 5.82 (s, 1H); ^{13}C NMR (75 MHz, DMSO): δ 163.57, 148.61, 147.74, 147.67, 141.74, 137.15, 135.13, 134.12, 133.39, 127.57, 127.39, 126.87, 123.90, 117.17, 115.01, 114.46, 66.00; ESI *m/z* (rel intensity) 301.7 (M^{+}, 100); Anal. ($C_{19}H_{15}N_3O\cdot0.1H_2O$) C, H, N; C: calcd, 75.28; found, 75.27; H: calcd, 5.05; found, 5.11; N: calcd, 13.86; found, 13.91.

2-(4-Pyridin-4-yl-phenyl)-2,3-dihydro-1H-quinazolin-4-one (58).

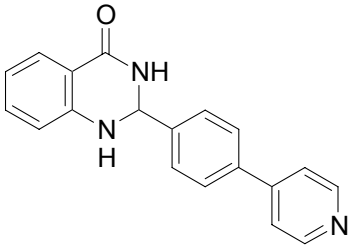

Compound **58** was prepared according to General Procedure C from 4-pyridin-4-yl-benzaldehyde **58a** (0.20 g, 1.09 mmol) and anthranilamide (0.15 g, 1.09 mmol) to afford a colorless solid (37.5 %); mp: 295 - 297 °C; ^{1}H NMR (300 MHz, DMSO): δ 8.60 – 8.63 (d, *J*= 9 Hz, 2H), 8.39 – 8.41 (d, *J*= 6 Hz, 1H), 7.80 – 7.83 (d, *J*= 9 Hz, 2H), 7.68 – 7.70 (d, J= 6 Hz, 2H), 7.59 – 7.62 (d, J= 9 Hz, 3H), 7.21 – 7.24 (m, 2 H), 6.74 – 6.76 (d, *J*= 6 Hz, 1H), 6.63 – 6.69 (t, *J*= 9 Hz, 1H), 5.81 (s, 1H); ^{13}C NMR (75 MHz, DMSO): δ

164.22, 150.93, 148.37, 147.18, 143.56, 137.86, 134.08, 128.28, 128.05, 127.51, 121.88, 117.88, 115.92, 115.13, 66.59; ESI *m/z* (rel intensity) 301.7 (M^+, 100); Anal. ($C_{19}H_{15}N_3O \cdot 0.6H_2O$) C, H, N; C: calcd, 73.11; found, 73.35; H: calcd, 5.23; found, 4.84; N: calcd, 13.46; found, 13.54.

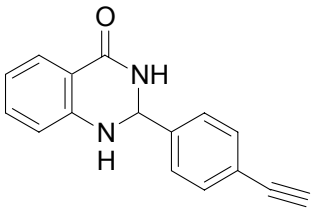

2-(4-ethynylphenyl)-2,3-dihydro-1H-quinazolin-4- one (59). Compound **59** was prepared according to General Procedure C from 4-ethynylbenzaldehyde (0.36 g, 2.78 mmol) and anthranilamide (0.38 g, 2.78 mmol) to afford a colorless solid; mp: 171-174 °C; ^{1}H NMR (300 MHz, DMSO-d_6) δ 8.34 (s, 1H), 6.64-7.63 (m, 9H), 5.77 (s, 1H), 4.21 (s, 1H), ^{13}C NMR (75 MHz, DMSO-d_6) δ 164.4, 148.6, 143.5, 134.3, 132.6, 128.3, 128.0, 122.7, 118.2, 115.8, 115.4, 84.1, 82.1, 66.9; APCI *m/z* (rel intensity) 233.0 (100), 249.7 (M^+, 50); Anal. ($C_{16}H_{12}N_2O$) C, H, N; C: calcd, 77.40; found, 77.17; H: calcd, 4.87; found, 4.88; N: calcd, 11.28; found, 11.25.

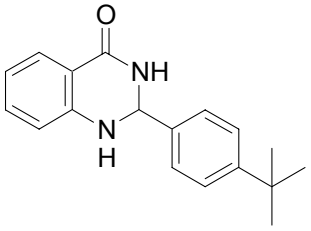

2-(4-tert-Butyl-phenyl)-2,3-dihydro-1H-quinazolin-4-one (60). Compound **60** was prepared according to General Procedure C from 4-tert-butyl-benzaldehyde (0.89 g, 5.51 mmol) and anthranilamide (0.75 g, 5.51 mmol) to afford a colorless solid; mp: 225 - 227 °C; ^{1}H NMR (300 MHz, DMSO): δ 8.25 (s, 1H), 7.62 – 7.65 (d, *J*= 9 Hz, 1H), 7.40 – 7.47 (m, 4H), 7.22 – 7.26 (t, *J*= 6 Hz, 1H), 7.08 (s, 1H), 6.74 – 6.76 (d, *J*= 6 Hz, 1H), 6.65 – 6.68 (t, *J*= 4.5 Hz, 1H), 5.73 (s, 1H), 1.28 (s, 9H); ^{13}C NMR (75 MHz, DMSO): δ 163.62, 150.95, 147.92, 138.52, 133.19, 127.31, 126.66,

125.04, 116.99, 114.90, 114.31, 66.44, 34.26, 31.06; APCI *m/z* (rel intensity) 287.50 (M^+, 100); Anal. ($C_{16}H_{12}N_2O$) C, H, N; C: calcd, 77.11; found, 76.99 H: calcd, 7.19; found, 7.39; N: calcd, 9.99; found, 10.08.

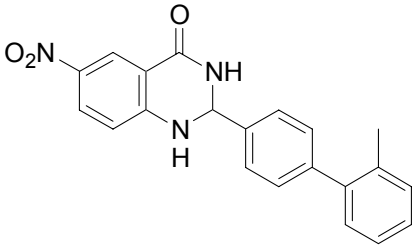

2-(2'-Methyl-biphenyl-4-yl)-5-nitro-2,3-dihydro-1H-quinazolin-4-one (61). Compound **61** was prepared according to General Procedure C from 2'-Methylbiphenylcarboxaldehyde (0.98 g, 5.00 mmol) and 5-nitroanthranilamide (0.91 g, 5.00 mmol) to afford a colorless solid; mp: 250 - 252 °C; ^{1}H NMR (300 MHz, DMSO-d_6) δ 8.82 (s, 1H), 8.66 (s, 1H), 8.49 (s, 1H), 8.13 – 8.17 (dd, J= 9.3, 2.7 Hz, 1H), 7.55 – 7.58 (d, J= 7.8 Hz, 2H), 7.42 – 7.45 (d, J= 8.1 Hz, 2H), 7.27 – 7.31 (m, 3H), 7.17 – 7.20 (m, 1H), 6.87 – 6.90 (d, J= 9.0 Hz, 1H), 6.11 (s, 1H), 2.25 (s, 3H); ^{13}C (75 MHz, DMSO-d_6) δ 162.0, 152.8, 142.6, 141.3, 140.4, 137.8, 135.3, 131.1, 130.2, 130.1, 130.0, 128.2, 127.4, 126.7, 124.9, 115.0, 113.3, 66.9, 20.9; ESI *m/z* (rel intensity) 359.1 (100); Anal. ($C_{21}H_{17}N_3O_3 \cdot 0.1\ H_2O$) C, H, N; C: calcd, 69.83; found, 69.75; H: calcd, 4.80; found, 4.65; N: calcd, 11.63; found, 11.67.

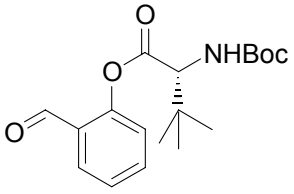

N-Boc-D-*tert*-leucine(salicylaldehyde) ester (74) D-*tert*-leucine (1.0 g, 7.6 mmol) was added to solution of dioxane (20 mL) and 1 M NaOH (7.6 mL, 7.6 mmol). Di-*tert*-butyldicarbonate (1.75 g, 8.0 mmol) was added and the reaction was allowed to continue at room temperature for 14 hours. The contents of the flask were then

concentrated and partitioned between EtOAc and water (ca. 100 mL each). The aqueous was separated from the organic layer and acidified to a pH of ~2 with concentrated HCl. The cloudy aqueous solution was then extracted 3 times with EtOAc (50 mL each) and the combined organics dried with $MgSO_4$. Filtration and concentration yielded the Boc-protected amino acid as a thick clear syrup, 0.75 g (3.45 mmol) of which was immediately taken up in DMF (25 mL). To this solution was added DCC (0.75 g, 3.63 mmol) followed by HOBt (0.49 g, 3.63 mmol) thirty minutes later. After an additional 30 minutes, salicylaldehyde (0.48 mL, 4.49 mmol) was added and the reaction proceeded for 12 hours, at which time 100 mL water was added. The mixture was extracted with EtOAc (3 x 50 mL), the combined organics dried with $MgSO_4$ then concentrated. The residue was purified by flash chromatograpy (Hexanes/EtOAc 7:1), the product aldehyde then recrystallized from hexanes to yield colorless crystals (0.58 g, 52.5 % over 2 steps); $[\alpha]_D$ = +2.1 (c = 1.0, $CHCl_3$); mp:104 – 106°C; ^{1}H NMR (300 MHz, $CDCl_3$) δ 10.22 (s, 1H), 7.91 – 7.95 (dd, *J*= 10.8 Hz, 1.5 Hz, 1H), 7.60 – 7.65 (dt, J= 8.1, 1.8 Hz, 1H), 7.36 – 7.41 (t, J= 7.8 Hz, 1H), 7.19 – 7.22 (d, J= 8.1 Hz, 1H), 5.13 – 5.16 (d, J= 0.9 Hz, 1H), 4.34 – 4.37 (d, J= 9.0 Hz, 1H), 1.47 (s, 9H), 1.14 (s, 9H); ^{13}C (75 MHz, $CDCl_3$) δ 188.8, 171.0, 156.0, 152.4, 135.5, 129.7, 128.5, 126.8, 123.2, 80.6, 62.6, 34.7, 28.6, 27.0; ESI *m/z* (rel intensity) 335.2 (100).

.

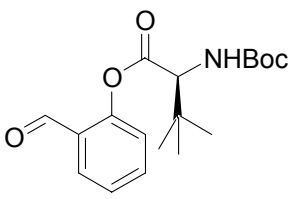

N-Boc-L-*tert*-leucine(salicylaldehyde) ester (75) L-*tert*-leucine (5.0 g, 38.12 mmol) was added to solution of dioxane (50 mL) and 1 M NaOH (38.12 mL, 8.12 mmol). Di-t-butyldicarbonate

(8.32 g, 38.12 mmol) was added and the reaction was allowed to continue at room temperature for 14 hours. The contents of the flask were then concentrated and partitioned between EtOAc and water (ca. 100 mL each). The aqueous was separated from the organic layer and acidified to a pH of ~2 with concentrated HCl. The cloudy aqueous solution was then extracted 3 times with EtOAc (100 mL each) and the combined organics dried with $MgSO_4$. Filtration and concentration yielded the Boc-protected amino acid as a thick clear syrup, 6.7 g (28.97 mmol) of which was immediately taken up in DMF (50 mL). To this solution was added DCC (6.6 g, 31.87 mmol) followed by HOBt (4.31 g, 31.87 mmol) thirty minutes later. After an additional 30 minutes, salicylaldehyde (4.01 mL, 37.66 mmol) was added and the reaction proceeded for 12 hours, at which time 100 mL water was added. The mixture was extracted with EtOAc (3 x 100 mL), the combined organics dried with $MgSO_4$ then concentrated. The residue was purified by flash chromatography (Hexanes/EtOAc 7:1), the product aldehyde then recrystallized from hexanes to yield colorless crystal 4.7 g (48.4 % over 2 steps); $[\alpha]_D$ = -2.1 (c = 1.0, $CHCl_3$); mp:104 – 106°C; ^{1}H NMR (300 MHz, $CDCl_3$) δ 10.22 (s, 1H), 7.92 – 7.95 (dd, *J*= 7.5 Hz, 1.5 Hz, 1H), 7.60 – 7.65 (dt, J= 7.5, 1.8 Hz, 1H), 7.36 – 7.41 (t, J= 7.8 Hz, 1H), 7.19 – 7.26 (d, J= 8.1 Hz, 1H), 5.12 – 5.15 (d, J= 0.9 Hz, 1H), 4.34 – 4.38 (d, J= 9.3 Hz, 1H), 1.47 (s, 9H), 1.14 (s, 9H); ^{13}C (75 MHz, $CDCl_3$) δ 188.7, 171.0, 156.0, 152.4, 135.4, 129.6, 128.5, 126.8, 123.1, 80.6, 62.6, 34.6, 28.5, 26.9; ESI *m/z* (rel intensity) 335.2 (100).

General Procedure F – Synthesis of Dihydroquinazolinone Diastereomers

To a 0°C solution of the anthranilamide (1 equiv.) and chiral aldehyde (1 equiv.) in MeCN (ca. 8 mL) was added 1 – 2 drops of trifluoroacetic acid. After 1.5 hours, the precipitate was collected by filtration and recrystallized from THF/Hexanes.

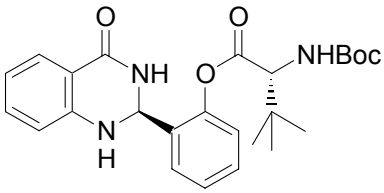

2S-(2'-N-Boc-D-*tert*-leucine phenyl ester)-4-quinazolinone (77a) Title compound was prepared according to General Procedure F from anthranilamide (0.13 g, 0.93 mmol) and aldehyde **74** (0.30 g, 0.93 mmol) to yield 0.29 g of colorless crystals (71 %); $[\alpha]_D$ = +120 (c = 0.1, THF); mp: 236-237°C; ^{1}H NMR (300 MHz, DMSO-d_6) δ 8.00 (s, 1H), 7.49-7.61 (m, 3H), 7.36 – 7.42 (t, J= 7.7 Hz, 1H), 7.25 – 7.30 (t, J= 7.2 Hz, 1H), 7.18 – 7.23 (t, J= 7.8 Hz, 1H), 7.10-7.13 (d, J=7.8 Hz, 1H), 6.64 – 6.73 (m, 3H), 5.95 (s, 1H), 4.08 – 4.11 (d, J=9.9 Hz, 1H), 1.33 (s, 9H), 1.06, (s, 9H); ^{13}C (75 MHz, DMSO-d_6) δ 171.3, 164.3, 157.09, 148.4, 148.3, 134.1, 133.8, 130.3, 128.5, 128.1, 126.8, 123.1, 118.0, 115.5, 115.1, 79.7, 64.0, 61.7, 34.0, 28.8, 27.4; ESI *m/z* (rel intensity) 453.2 (100); Anal. ($C_{25}H_{31}N_3O_5 \cdot 0.1\ H_2O$) C, H, N; C: calcd, 65.95; found, 65.80; H: calcd, 6.91; found, 6.86; N: calcd, 9.23; found, 9.19.

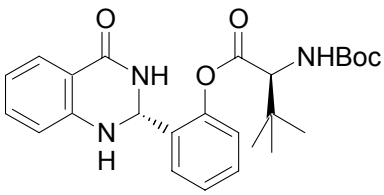

2R-(2'-N-Boc-D-*tert*-leucine phenyl ester)-4-quinazolinone (76b) Title compound was prepared according to General Procedure F from anthranilamide (0.20 g, 1.49 mmol) and aldehyde **75** (0.50 g, 1.49 mmol) to yield 0.57 g of colorless crystals (84.6 %); $[\alpha]_D$ = -126 (c = 0.1, THF); mp: 236-237°C;

^{1}H NMR (300 MHz, DMSO-d_6) δ 7.98 (s, 1H), 7.59-7.62 (dd, J= 7.8, 1.5 Hz, 1H), 7.54 – 7.57 (dd, J= 4.5, 1.2 Hz, 1H), 7.48 – 7.50 (d, J= 6.6 Hz, 1H), 7.36 – 7.42 (t, J= 7.8 Hz, 1H), 7.18-7.30 (m, 2H), 7.11-7.13 (d, J= 7.8 Hz, 1H), 6.64 – 6.73 (m, 3H), 5.95 (s, 1H), 4.09 – 4.11 (d, J= 6.9 Hz, 1H), 1.33 (s, 9H), 1.07, (s, 9H); ^{13}C (75 MHz, DMSO-d_6) δ 171.2, 164.2, 157.0, 148.4, 148.2, 134.0, 133.7, 130.3, 128.5, 128.1, 126.7, 123.0, 118.0, 115.5, 115.1, 79.6, 64.0, 61.6, 34.0, 28.8, 27.3; ESI *m/z* (rel intensity) 453.2 (100); Anal. ($C_{25}H_{31}N_3O_5$) C, H, N; C: calcd, 66.21; found, 66.12; H: calcd, 6.89; found, 6.92; N: calcd, 9.27; found, 9.14.

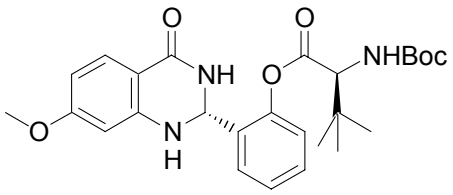

2R-(2'-N-Boc-D-*tert*-leucine phenyl ester)-7-methoxy-4-quinazolinone (76c) Title compound was prepared according to General Procedure A from 4-methoxyanthranilamide (0.20 g, 1.19 mmol) and aldehyde **75** (0.40 g, 1.19 mmol) to yield 0.45 g of colorless crystals (78.2 %); $[\alpha]_D$ = -105 (c = 0.1, THF); mp: 228-230°C; ^{1}H NMR (300 MHz, DMSO-d_6) δ 7.79 (s, 1H), 7.50-7.54 (m, 3H), 7.36 – 7.41 (t, J= 7.5 Hz, 1H), 7.24 – 7.29 (t, J= 7.5 Hz, 1H), 7.11 – 7.13 (d, J= 8.1 Hz, 1H), 6.67 (s, 1H), 6.22-6.27 (m, 2H), 5.92 (s, 1H), 4.09-4.11 (d, 1H), 3.67 (s, 3H), 1.35 (s, 9H), 1.07 (s, 9H); ^{13}C (75 MHz, DMSO-d_6) δ 171.2, 164.3, 164.2, 157.1, 149.8, 148.3, 134.1, 130.2, 130.0, 128.3, 126.7, 123.0, 108.9, 105.7, 98.5, 79.7, 64.0, 61.7, 55.8, 34.0, 28.8, 27.4; ESI *m/z* (rel intensity) 483.2 (100); Anal. ($C_{26}H_{33}N_3O_6$) C, H, N; C: calcd, 64.58; found, 64.58; H: calcd, 6.88; found, 6.99; N: calcd, 8.69; found, 8.93.

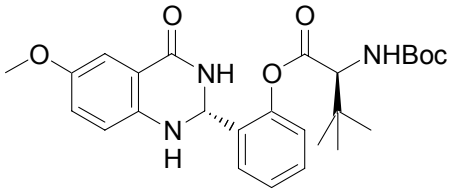

2R-(2'-N-Boc-D-*tert*-leucine phenyl ester)-6-methoxy-4-quinazolinone (76d) To a 0°C solution of the 5-methoxyanthranilamide (0.25 g, 1.51 mmol) and chiral aldehyde **75** (0.51 g, 1.51 mmol) in MeCN (ca. 8 mL) was added 1 – 2 drops of trifluoroacetic acid. After 1.5 hours, the solvent was removed *in vacuo* and the resulting residue purified by flash chromatography (Hexanes/EtOAc 2:1) to yield 0.26 g of a light green solid (35.8 %); $[\alpha]_D$ = -104 (c = 0.1, THF); mp: 192-194°C; ^{1}H NMR (300 MHz, DMSO-d_6) δ 7.73-7.75 (d, J=7.5 Hz, 1H), 7.40-7.41 (d, J= 3.3 Hz, 1H), 7.34 – 7.37 (dd, J= 7.8, 1.5 Hz, 1H), 7.24 – 7.29 (t, J= 7.5 Hz, 1H), 7.11 – 7.14 (d, J= 7.8 Hz, 1H), 6.87 – 6.911 (dd, J= 8.7, 4.8 Hz, 1H), 6.70 (s, 1H), 6.62 – 6.65 (d, 1H), 6.15 (s, 1H), 5.26 – 5.29 (d, J= 7.5 Hz, 1H), 5.04 (s, 1H), 4.21 – 4.23 (d, J= 7.8 Hz, 1H), 3.78 (s, 3H), 1.39 (s, 9H), 1.15 (s, 9H); ^{13}C (75 MHz, DMSO-d_6) δ 171.6, 165.5, 156.3, 153.2, 148.0, 141.4, 132.6, 130.2, 128.3, 126.9, 123.0, 122.4, 117.0, 116.1, 110.4, 80.8, 63.0, 62.6, 56.0, 34.1, 28.5, 27.1; ESI *m/z* (rel intensity) 483.2 (100); Anal. ($C_{26}H_{33}N_3O_6$) C, H, N; C: calcd, 64.58; found, 64.53; H: calcd, 6.88; found, 6.71; N: calcd, 8.69; found, 8.75.

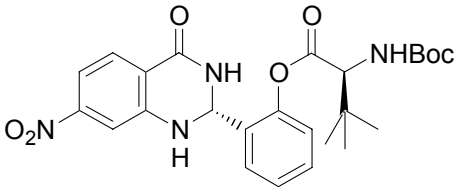

2R-(2'-N-Boc-D-*tert*-leucine phenyl ester)-7-nitro-4-quinazolinone (76e) To a room temperature solution of 4-nitroanthranilamide (0.22 g, 1.19 mmol) and chiral aldehyde **75** (0.40 g, 1.19 mmol) in MeCN (ca. 8 mL) was added 1 – 2 drops of trifluoroacetic acid. After 24 hours, the precipitate was collected and recrystallized from THF/Hexanes to yield 0.39 g

of a yellow solid (65.5 %); $[\alpha]_D$ = -167 (c = 0.1, THF); mp: 240-241°C; ^{1}H NMR (300 MHz, DMSO-d_6) δ 8.47 (s, 1H), 7.84 – 7.86 (d, J= 8.4 Hz, 1H), 7.58 – 7.61 (m, 2H), 7.42 – 7.50 (m, 3H), 7.30 – 7.35 (t, J= 6.6 Hz, 2H), 7.15 – 7.17 (d, J= 7.8 Hz, 1H), 6.13 (s, 1H), 4.08 – 4.10 (d, J= 6.6 Hz, 1H), 1.28 (s, 9H), 1.07 (s, 9H); ^{13}C (75 MHz, DMSO-d_6) δ 171.2, 162.7, 157.0, 151.4, 148.9, 148.4, 132.8, 130.7, 129.9, 128.6, 127.0, 123.1, 120.0, 111.9, 109.7, 79.6, 63.9, 61.6, 33.9, 28.7, 27.3; ESI *m/z* (rel intensity) 498.2 (100); Anal. ($C_{25}H_{30}N_4O_7 \cdot 0.1H_2O$) C, H, N; C: calcd, 60.02; found, 59.70; H: calcd, 6.08; found, 6.04; N: calcd, 11.24; found, 10.97.

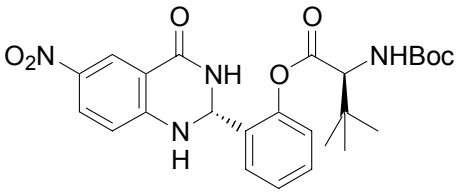

2R-(2'-N-Boc-D-*tert*-leucine phenyl ester)-6-nitro-4-quinazolinone (76f) To a 50°C solution of 5-nitroanthranilamide (0.27 g, 1.49 mmol) and chiral aldehyde **75** (0.50 g, 1.49 mmol) in MeCN (ca. 8 mL) was added 1 – 2 drops of trifluoroacetic acid. After 24 hours, the precipitate was collected and recrystallized from THF/Hexanes to yield 0.43 g of a yellow solid (57.7%); $[\alpha]_D$ = -182 (c = 0.1, THF); mp: 211-213°C; ^{1}H NMR (300 MHz, DMSO-d_6) δ 8.49 (s, 1H), 8.42 (d, J= 2.7 Hz, 1H), 8.15 (s, 1H), 8.07 – 8.11 (dd, J= 9.0, 2.7 Hz, 1H), 7.58 – 7.61 (d, J= 7.5 Hz, 1H), 7.43 – 7.47 (t, J= 6.3 Hz, 2H), 7.31 – 7.37 (t, J= 7.2 Hz, 1H), 7.14 – 7.16 (d, J= 8.1 Hz, 1H), 6.83 – 6.86 (d, J= 9.3 Hz, 1H), 6.21 (s, 1H), 4.06 – 4.08 (d, J= 6.9 Hz, 1H), 1.28 (s, 9H), 1.06 (s, 9H); ^{13}C (75 MHz, DMSO-d_6) δ 171.1, 162.0, 156.8, 153.0, 148.2, 137.8, 132.4, 130.7, 129.3, 128.5, 127.0, 124.6, 122.9, 114.9, 113.3, 79.4, 63.6, 61.3, 33.7, 28.5, 27.1; ESI *m/z* (rel intensity) 498.2 (100); Anal. ($C_{25}H_{30}N_4O_7$) C, H, N; C: calcd, 60.23; found, 60.35; H: calcd, 6.07; found, 6.25; N: calcd, 11.24; found, 11.19.

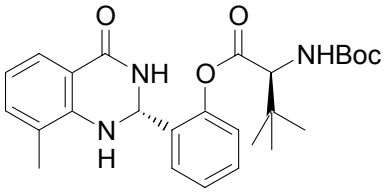

2R-(2'-N-Boc-D-*tert*-leucine phenyl ester)-8-methyl-4-quinazolinone (76g) To a 0°C solution of 3-methylanthranilamide (0.05 g, 0.30 mmol) and chiral aldehyde **75** (0.10 g, 0.30 mmol) in MeCN (ca. 8 mL) was added 1 – 2 drops of trifluoroacetic acid. After 2 hours the solvent was removed *in vacuo* and the resulting residue purified by flash chromatography (Hexanes/EtOAc 2:1), then recrystallized from THF/Hexanes to yield 0.09 g of a colorless solid (62.1%); $[\alpha]_D$ = -109 (c = 0.1, THF); mp: 177-179°C; ^{1}H NMR (300 MHz, DMSO-d_6) δ 7.76 – 7.82 (m, 2H), 7.37 – 7.43 (dt, J= 7.8, 1.5 Hz, 1H), 7.29 – 7.34 (t, J= 7.5 Hz, 1H), 7.13 – 7.16 (d, J= 7.2 Hz, 1H), 7.05 – 7.07 (d, J= 7.2 Hz, 1H), 6.71 – 6.76 (t, J= 7.5 Hz, 1H), 6.14 – 6.17 (d, J= 8.4 Hz, 2H), 5.10 – 5.12 (d, J= 8.7 Hz, 1H), 4.63 (s, 1H), 4.22 – 4.25 (d, J= 8.1 Hz, 1H), 2.08 (s, 3H), 1.30 (s, 9H), 1.12 (s, 9H); ^{13}C (75 MHz, DMSO-d_6) δ 172.3, 165.5, 156.0, 148.2, 145.5, 135.1, 132.9, 130.8, 128.6, 127.5, 126.6, 122.5, 122.3, 118.8, 115.1, 81.1, 62.7, 62.4, 34.3, 28.4, 27.0, 16.8; ESI *m/z* (rel intensity) 467.2 (100); Anal. ($C_{26}H_{33}N_3O_5$) C, H, N; C: calcd, 66.79; found, 66.42; H: calcd, 7.11; found, 7.23; N: calcd, 8.99; found, 8.62.

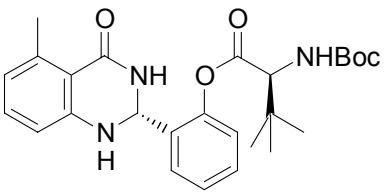

2R-(2'-N-Boc-D-*tert*-leucine phenyl ester)-5-methyl-4-quinazolinone (76h) To a 0°C solution of 6-methylanthranilamide (0.18 g, 1.19 mmol) and chiral aldehyde **75** (0.40 g, 1.19 mmol) in MeCN (ca. 8 mL) was added 1 – 2 drops of trifluoroacetic acid. After 2 hours the solvent was removed *in*

vacuo and the resulting residue purified by flash chromatography (Hexanes/EtOAc 2:1), then recrystallized from THF/Hexanes to yield 0.19 g of a colorless solid (33.6 %); $[\alpha]_D$ = -143 (c = 0.1, THF); mp: 148-150°C; ^{1}H NMR (300 MHz, DMSO-d_6) δ 7.73 – 7.74 (d, J= 4.5 Hz, 1H), 7.34 – 7.37 (t, J= 4.5 Hz, 1H), 7.25 – 7.27 (t, J= 3.3 Hz, 1H), 7.08 – 7.09 (d, J= 4.8 Hz, 1H), 7.03 – 7.07 (t, J= 4.5 Hz, 1H), 6.56 – 6.57 (d, J= 4.5 Hz, 1H), 6.49 – 6.50 (d, J= 4.8 Hz, 1H), 6.34 (s, 1H), 6.05 (s, 1H), 5.16 – 5.18 (d, J= 4.5 Hz, 1H), 5.07 (s, 1H), 4.18 – 4.20 (d, J= 4.8 Hz, 1H), 2.63 (s, 3H), 1.35 (s, 9H), 1.11 (s, 9H); ^{13}C (75 MHz, DMSO-d_6) δ 171.4, 165.6, 156.0, 148.3, 147.8, 142.1, 132.7, 132.2, 130.0, 128.2, 126.7, 122.7, 122.0, 113.6, 113.2, 80.5, 62.6, 61.6, 33.8, 28.2, 26.8, 22.3; ESI *m/z* (rel intensity) 467.2 (100); Anal. ($C_{26}H_{33}N_3O_5$) C, H, N; C: calcd, 66.79; found, 66.85; H: calcd, 7.11; found, 7.22; N: calcd, 8.99; found, 8.86.

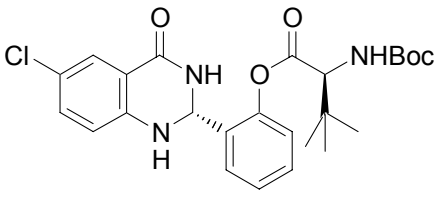

2R-(2'-N-Boc-D-*tert*-leucine phenyl ester)-6-chloro-4-quinazolinone (76i) Title compound was prepared according to General Procedure E from 5-chloroanthranilamide (0.05 g, 0.30 mmol) and aldehyde **75** (0.10 g, 0.30 mmol) to yield 0.11 g of colorless crystals (76.7 %); $[\alpha]_D$ = -123 (c = 0.1, THF); mp: 207-209°C; ^{1}H NMR (300 MHz, DMSO-d_6) δ 8.21 (s, 1H), 7.59 – 7.60 (d, J= 4.8 Hz, 1H), 7.54 (d, J= 1.2 Hz, 1H), 7.48 – 7.49 (d, J= 3.9 Hz, 1H), 7.41 – 7.44 (t, J= 4.5 Hz, 1H), 7.30 – 7.33 (t, J= 4.5 Hz, 1H), 7.26 – 7.28 (d, J= 5.1 Hz, 1H), 7.12 – 7.14 (d, J= 4.8 Hz, 1H), 6.93 (s, 1H), 6.76 – 6.78 (d, J= 4.8 Hz, 1H), 5.99 (s, 1H), 4.08 – 4.10 (d, J= 4.2 Hz, 1H), 1.31 (s, 9H), 1.07 (s, 9H); ^{13}C (75 MHz, DMSO-d_6) δ 171.3, 163.2, 157.0, 148.5, 147.3, 133.7, 133.1, 130.6, 128.7, 127.1, 126.9, 123.0, 121.7,

117.2, 116.8, 79.6, 63.9, 61.7, 34.0, 28.8, 27.4; ESI *m/z* (rel intensity) 487.2 (100); Anal. ($C_{25}H_{30}ClN_3O_5$) C, H, N; C: calcd, 61.53; found, 61.43; H: calcd, 6.20; found, 6.13; N: calcd, 8.61; found, 8.52.

General Procedure G – Ester Cleavage and Phenol Triflation

To a solution of the ester (1 equivalent) in THF (10 mLs) was added hydrazine monohydrate (3 equiv.). The reaction proceeded at room temperature until ester cleavage was complete by TLC (ca. 3 – 12 hours), at which time to solvent was removed *in vacuo* and the residue was taken up in 15 mLs chloroform, held at 0°C for 2 hours, then the precipitate collected by filtration. The mother liquor was concentrated and taken up in 5 – 10 mL chloroform and held at 0°C for another 2 hours, then filtered again. The combined precipitates were confirmed by ^{1}H NMR to be the corresponding phenol. The phenol (1 equivalent) was then taken up in 10 mLs THF and reacted with N-phenyl-bis(trifluorosulfonimide) (2 equiv.) and diisopropylethylamine (10 equiv.). After triflation was complete by TLC (ca. 3 – 12 hours at ambient temperature), the contents of the flask were concentrated and partitioned between ethyl acetate (ca. 50 mL) and water (ca. 50 mL). The aqueous was extracted twice more, the organics combined and dried with $MgSO_4$, then filtered and concentrated. The residue was purified by flash chromatography (Hexanes/ethyl acetate 1:1) and isolated as thick syrups.

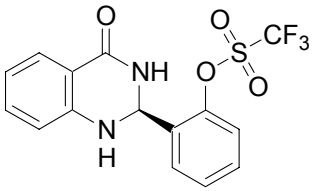

2S-(2'-trifluoromethane sulfonyl phenyl ester)-4-quinazolinone (78a)

The title compound was made according to General Procedure G from **77a** (0.15 g, 0.34 mmol) to first yield 0.076 g of the phenol (94.1 %); $[\alpha]_D$ = +122 (c = 0.1, THF); ^{1}H NMR (300 MHz, DMSO-d_6) δ 9.92 (s, 1H), 8.01 (s, 1H), 7.67 – 7.69 (d, J= 7.8 Hz, 1H), 7.39 – 7.41 (d, J= 7.5 Hz, 1H), 7.18 – 7.30 (m, 2H), 6.91 – 6.93 (d, J= 8.1 Hz, 1H), 6.81 – 6.88 (m, 3H), 6.70 – 6.75 (t, J= 7.5 Hz, 1H), 6.06 (s, 1H); The triflate was subsequently isolated as 0.10 g of a clear syrup (84.4 %); $[\alpha]_D$ = +120 (c = 0.1, THF); ^{1}H NMR (300 MHz, $CDCl_3$) δ 7.96 - 7.98 (d, J= 7.5 Hz, 1H), 7.89 – 7.92 (d, J= 7.2 Hz, 1H), 7.50 – 7.54 (m, 2H), 7.35 – 7.40 (m, 2H), 6.90 – 6.95 (t, J= 7.5 Hz, 1H), 6.70 – 6.73 (d, J= 8.1 Hz, 1H), 6.56 (s, 1H), 6.29 (s, 1H), 4.75 (bs, 1H); ^{13}C (75 MHz, $CDCl_3$) δ 165.11, 146.7, 146.5, 134.6, 132.9, 131.7, 130.1, 129.6, 128.7, 122.1, 120.1, 115.3, 115.1, 62.5 (CF_3 signal not detected due to the strong C-F coupling); ESI *m/z* (rel intensity) 372.0 (100).

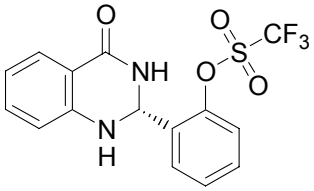

2R-(2'-trifluoromethane sulfonyl phenyl ester)-4-quinazolinone (78b)

The title compound was made according to General Procedure G from **76b** (0.40 g, 0.88 mmol) to first yield 0.20 g of the phenol (95.5 %); $[\alpha]_D$ = -128 (c = 0.1, THF); ^{1}H NMR (300 MHz, DMSO-d_6) δ 9.84 (s, 1H), 7.92 (s, 1H), 7.58 – 7.61 (d, J= 7.8 Hz, 1H), 7.30 – 7.33 (d, J= 7.5 Hz, 1H), 7.17 – 7.22 (dt, J= 7.2, 1.2 Hz, 1H), 7.10 – 7.15 (t, J= 6.6 Hz, 1H), 6.82 – 6.85 (d, J= 8.1 Hz, 1H), 6.73 – 6.80 (m, 3H), 6.61 – 6.66 (t, J= 7.5 Hz, 1H), 5.98 (s, 1H); The triflate was

subsequently isolated as 0.22 g of a clear syrup (93.7 %); $[\alpha]_D$ = -123 (c = 0.1, THF); ^{1}H NMR (300 MHz, $CDCl_3$) δ 7.93 (dd, J= 7.5, 2.1 Hz, 1H), 7.83 – 7.86 (dd, J= 7.8, 1.5 Hz, 1H), 7.42 – 7.50 (m, 2H), 7.26 – 7.34 (m, 2H), 6.84 – 6.89 (t, J= 7.8 Hz, 1H), 6.66 – 6.68 (d, J= 8.1 Hz, 1H), 6.63 (s, 1H), 6.24 (s, 1H), 4.78 (s, 1H); ^{13}C (75 MHz, $CDCl_3$) δ 165.1, 146.8, 146.5, 134.6, 132.9, 131.7, 130.1, 129.6, 128.7, 122.0, 120.0, 115.3, 115.0, 62.4 (CF_3 signal not detected due to the strong C-F coupling); ESI *m/z* (rel intensity) 372.0 (100).

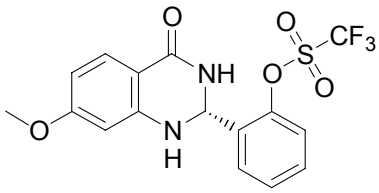

2R-(2'-trifluoromethane sulfonyl phenyl ester)-7-methoxy-4-quinazolinone (78c)

The title compound was made according to General Procedure G from **76c** (0.30 g, 0.62 mmol) to first yield 0.15 g of the phenol (88.7 %); $[\alpha]_D$ = -93 (c = 0.1, THF); ^{1}H NMR (300 MHz, DMSO-d_6) δ 9.85 (bs, 1H), 8.30 (s, 1H), 7.71 (s, 1H), 7.50 – 7.53 (d, J= 8.7 Hz, 1H), 7.27 – 7.30 (d, J= 7.8 Hz, 1H), 7.10 – 7.25 (t, J= 6.6 Hz, 1H), 6.72 – 6.85 (m, 2H), 6.20 – 6.30 (m, 2H), 5.94 (s, 1H), 3.68 (s, 3H); The triflate was subsequently isolated as 0.14 g of a clear syrup (77.3 %); $[\alpha]_D$ = -92 (c = 0.1, THF); ^{1}H NMR (300 MHz, $CDCl_3$) δ 7.93 – 7.94 (dd, J= 7.2, 2.4 Hz, 1H), 7.77 – 7.80 (d, J= 8.7 Hz, 1H), 7.43 – 7.53 (m, 2H), 7.30 – 7.33 (dd, J= 7.5, 1.8 Hz, 1H), 6.52 (s, 1H), 6.41 – 6.45 (dd, J= 8.7, 2.1 Hz, 1H), 6.22 (s, 1H), 6.16 – 6.17 (d, J= 2.1 Hz, 1H), 4.87 (bs, 1H), 3.79 (s, 3H); ^{13}C (75 MHz, $CDCl_3$) δ 165.0, 164.9, 148.5, 146.4, 133.2, 131.6, 130.6, 130.0, 129.6, 122.0, 108.7, 107.2, 98.9, 62.5, 55.6 (CF_3 signal not detected due to the strong C-F coupling); ESI *m/z* (rel intensity) 402.1 (100).

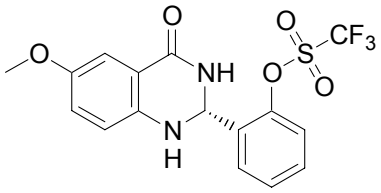

2R-(2'-trifluoromethane sulfonyl phenyl ester)-6-methoxy-4-quinazolinone (78d)

The title compound was made according to General Procedure G from **76d** (0.16 g, 0.32 mmol) to first yield 0.08 g of the phenol (87.5 %); $[\alpha]_D$ = -165 (c = 0.1, THF); ^{1}H NMR (300 MHz, DMSO-*d*$_6$) δ 9.86 (s, 1H), 7.99 (s, 1H), 7.37 – 7.39 (d, 7.8 Hz, 1H), 7.15 – 7.20 (m, 2H), 6.77 – 6.96 (m, 4H), 6.41 (s, 1H), 5.97 (s, 1H), 3.72 (s, 3H); The triflate was subsequently isolated as 0.10 g of a clear syrup (100 %); $[\alpha]_D$ = -78 (c = 0.1, THF); ^{1}H NMR (300 MHz, $CDCl_3$) δ 7.94 – 7.97 (dd, J= 6.9, 2.4 Hz, 1H), 7.50 – 7.55 (dt, J= 6.6, 1.5 Hz, 2H), 7.45 – 7.46 (d, 2.7 Hz, 1H), 7.38 – 7.40 (m, 2H), 7.01 – 7.04 (dd, J= 8.7, 2.7 Hz, 1H), 6.70 – 6.73 (d, J= 9 Hz, 1H), 6.59 (bs, 1H), 6.24 (s, 1H), 3.82 (s, 3H); ^{13}C (75 MHz, $CDCl_3$) δ 165.6, 154.0, 146.6, 140.9, 132.5, 131.8, 129.9, 129.6, 127.1, 123.5, 122.2, 117.2, 110.8, 62.8, 56.0 (CF_3 signal not detected due to the strong C-F coupling); ESI *m/z* (rel intensity) 402.1 (100).

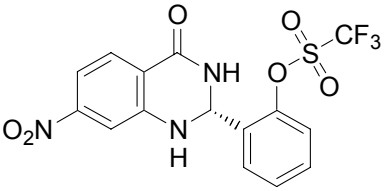

2R-(2'-trifluoromethane sulfonyl phenyl ester)-7-nitro-4-quinazolinone (78e)

The title compound was made according to General Procedure G from **78e** (0.17 g, 0.34 mmol) to first yield 0.09 g of the phenol (91.2 %); $[\alpha]_D$ = -233 (c = 0.1, THF); ^{1}H NMR (300 MHz, DMSO-*d*$_6$) δ 9.96 (s, 1H), 8.41 (s, 1H), 7.81 – 7.84 (d, 8.4 Hz, 1H), 7.60 (d, J= 1.8 Hz, 1H), 7.46 (s, 1H), 7.37 – 7.40 (dd, J= 8.7, 2.4 Hz, 1H), 7.25 – 7.28 (d, J= 8.4 Hz, 1H), 7.13 – 7.18 (t, J= 8.1 Hz, 1H), 6.76 – 6.87 (m, 2H), 6.08 (s, 1H); The triflate was subsequently

isolated as 0.12 g of a clear syrup (100 %); $[\alpha]_D$ = -132 (c = 0.1, THF); ^{1}H NMR (300 MHz, $CDCl_3$) δ 8.84 (s, 1H), 8.00 – 8.03 (d, J= 8.4 Hz, 1H), 7.86 – 7.89 (d, J= 7.5 Hz, 1H), 7.62 – 7.64 (d, J= 8.4 Hz, 1H), 7.48 – 7.58 (m, 3H), 6.76 (s, 1H), 6.33 (s, 1H), 5.17 (s, 1H); ^{13}C (75 MHz, $CDCl_3$) δ 158.7, 147.2, 142.3, 141.6, 127.5, 127.2, 125.7, 125.0, 122.5, 118.6, 117.7, 109.4, 105.3, 57.8 (CF_3 signal not detected due to the strong C-F coupling); ESI *m/z* (rel intensity) 417.0 (100).

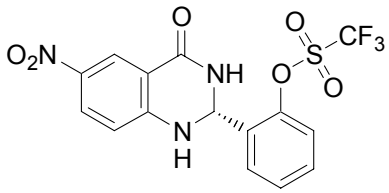

2R-(2'-trifluoromethane sulfonyl phenyl ester)-6-nitro-4-quinazolinone (78f)

The title compound was made according to General Procedure G from **76f** (0.46 g, 0.95 mmol) to first yield 0.23 g of the phenol (85.3 %); $[\alpha]_D$ = -292 (c = 0.1, THF); ^{1}H NMR (300 MHz, DMSO-d_6) δ 9.98 (s, 1H), 8.43 – 8.45 (m, 2H), 8.36 (s, 1H), 8.04 – 8.08 (dd, J= 9.0, 2.7 Hz, 1H), 7.24 – 7.27 (d, J= 7.5 Hz, 1H), 7.15 – 7.21 (t, J= 7.5, 1.5 Hz, 1H), 6.80 – 6.88 (m, 3H), 6.18 (s, 1H); The triflate was subsequently isolated as 0.34 g of a yellow syrup (100 %); $[\alpha]_D$ = -194 (c = 0.1, THF); ^{1}H NMR (300 MHz, $CDCl_3$) δ 9.77 (s, 1H), 8.77 (s, 1H), 8.20 – 8.23 (d, J= 9.0 Hz, 1H), 7.88 – 7.90 (d, J= 6.6 Hz, 1H), 7.47 – 7.60 (m, 2H), 7.03 (s, 1H), 6.76 – 6.80 (dd, J= 9.0, 2.7 Hz, 1H), 6.43 (s, 1H), 6.08 (s, 1H); ^{13}C (75 MHz, $CDCl_3$) δ 162.7, 151.0, 146.0, 139.8, 134.9, 131.9, 129.7, 129.4, 126.6, 125.5, 122.8, 122.1, 114.6, 62.2 (CF_3 signal not detected due to the strong C-F coupling); ESI *m/z* (rel intensity) 417.0 (100).

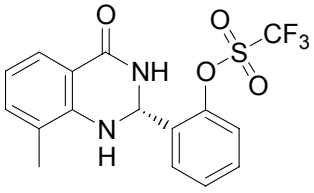

2R-(2'-trifluoromethane sulfonyl phenyl ester)-8-methyl-4-quinazolinone (78g)

The title compound was made according to General Procedure G from **76g** (0.50 g, 1.09 mmol) to first yield 0.20 g of the phenol (72.5 %); $[\alpha]_D$ = -97 (c = 0.1, THF); ^{1}H NMR (300 MHz, DMSO-d_6) δ 9.97 (s, 1H), 7.98 (s, 1H), 7.48 – 7.50 (d, J= 7.5 Hz, 1H), 7.16 – 7.19 (dd, J= 7.2, 1.2 Hz, 1H), 7.08 – 7.13 (t, J= 7.5 Hz, 2H), 6.82 – 6.84 (d, J= 8.1 Hz, 1H), 6.71 – 6.76 (t, J= 7.5 Hz, 1H), 6.57 – 6.62 (t, 7.5 Hz, 1H), 6.07 (s, 1H), 5.93 (s, 1H), 2.07 (s, 3H); The triflate was subsequently isolated as 0.18 g of a clear syrup (100 %); $[\alpha]_D$ = -88 (c = 0.1, THF); ^{1}H NMR (300 MHz, $CDCl_3$) δ 7.95 – 7.98 (dd, J= 7.5, 2.1 Hz, 1H), 7.74 – 7.76 (d, J= 7.8 Hz, 1H), 7.50 – 7.55 (m, 2H), 7.22 – 7.39 (m, 3H), 7.17 (s, 1H), 6.79 – 6.84 (t, J= 8.1 Hz, 1H), 6.29 (s, 1H), 2.15 (s, 3H); ^{13}C (75 MHz, $CDCl_3$) δ 165.8, 146.5, 145.1, 135.4, 133.2, 131.6, 130.1, 129.6, 126.5, 122.8, 122.0, 119.4, 115.2, 62.3, 16.7 (CF_3 signal not detected due to the strong C-F coupling); ESI *m/z* (rel intensity) 386.1 (100).

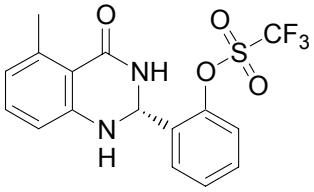

2R-(2'-trifluoromethane sulfonyl phenyl ester)-5-methyl-4-quinazolinone (78h)

The title compound was made according to General Procedure G from **76h** (0.22 g, 0.47 mmol) to first yield 0.10 g of the phenol (80.9 %); $[\alpha]_D$ = -114 (c = 0.1, THF); ^{1}H NMR (300 MHz, DMSO-d_6) δ 9.83 (s, 1H), 7.81 (s, 1H), 7.38 – 7.41 (dd, J= 7.5, 1.2 Hz, 1H), 7.15 – 7.21 (dt, J= 8.1, 1.5 Hz, 1H), 7.06 – 7.11 (t, J= 7.8 Hz, 1H), 6.81 – 6.90 (m, 2H), 6.64 – 6.69 (m, 2H), 6.48 – 6.51 (d, J= 7.5 Hz, 1H), 5.91 (s, 1H), 2.57 (s, 3H); The triflate was subsequently isolated as

0.10 g of a clear syrup (100 %); $[\alpha]_D$ = -116 (c = 0.1, THF); ^{1}H NMR (300 MHz, $CDCl_3$) δ 7.96 – 7.99 (dd, J= 6.9, 2.7 Hz, 1H), 7.47 – 7.52 (m, 2H), 7.31 – 7.35 (m, 2H), 7.16 – 7.21 (t, J= 7.5 Hz, 1H), 6.67 – 6.71 (m, 2H), 6.56 – 6.58 (d, J= 8.1 Hz, 1H), 6.16 (s, 1H), 2.64 (s, 3H); ^{13}C (75 MHz, $CDCl_3$) δ 165.7, 148.4, 146.7, 142.7, 133.4, 132.7, 131.6, 130.3, 129.5, 126.5, 123.8, 121.9, 113.4, 61.9, 22.5 (CF_3 signal not detected due to the strong C-F coupling); ESI *m/z* (rel intensity) 386.1 (100).

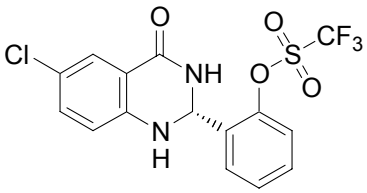

2R-(2'-trifluoromethane sulfonyl phenyl ester)-6-chloro-4-quinazolinone (78i)

The title compound was made according to General Procedure G from **76i** (0.24 g, 0.51 mmol) to first yield 0.11 g of the phenol (78.4 %); $[\alpha]_D$ = -172 (c = 0.1, THF); ^{1}H NMR (300 MHz, DMSO-d_6) δ 9.82 (s, 1H), 8.07 (s, 1H), 7.45 (s, 1H), 7.20 – 7.22 (d, J= 6.6 Hz, 1H), 7.14 – 7.17 (d, J= 7.2 Hz, 1H), 7.04 – 7.08 (t, J= 7.2 Hz, 1H), 6.92 (s, 1H), 6.68 – 6.78 (m, 3H), 5.92 (s, 1H); The triflate was subsequently isolated as 0.11 g of a clear syrup (100 %); $[\alpha]_D$ = -97 (c = 0.1, THF); ^{1}H NMR (300 MHz, $CDCl_3$) δ 9.37 (s, 1H), 7.86 – 7.89 (dd, J= 7.2, 3.2 Hz, 1H), 7.83 (d, J= 2.4 Hz, 1H), 7.46 – 7.55 (m, 2H), 7.24 – 7.24 (m, 1H), 6.63 – 6.69 (m, 2H), 6.24 (s, 1H), 4.79 (s, 1H); ^{13}C (75 MHz, $CDCl_3$) δ 164.5, 146.4, 145.2, 134.8, 132.0, 129.8, 129.7, 128.3, 127.1, 125.3, 123.2, 122.3, 116.7, 62.5 (CF_3 signal not detected due to the strong C-F coupling); ESI *m/z* (rel intensity) 406.0 (100).

General Procedure H – Reduction of Aryl Triflate

Triethylamine (15 equiv) and $Pd(dppf)Cl_2$ (0.02 equiv) were added to a solution of formic acid (10 equiv) in DMF (15 mL). After thoroughly degassing the resulting red solution, the corresponding aryl triflate (1 equiv) was added (the formic acid must be completely neutralized before adding the triflate, otherwise racemization may occur) and the reaction was heated at 90 – 100 ^oC until the starting material was completely consumed as indicated by TLC (ca. 1.5 hours). The dark solution was added to ~100 mLs H_2O, then extracted 3 times with ethyl acetate. The combined organics were dried with $MgSO_4$, filtered, and concentrated. The resulting residue was purified by flash chromatography (hexanes/ethyl acetate 1:1), then recrystallized from THF/hexanes.

General Procedure I – Reduction of Aryl Triflate for Nitro-Containing Compounds

Triethylamine (15 equiv) and $Pd(dppf)Cl_2$ (0.02 equiv) were added to a solution of formic acid (1.0 equiv) in 15 mL DMF (excess formic acid results in the reduction of nitro functional group). After thoroughly degassing the resulting red solution, the corresponding aryl triflate (1 equiv) was added (the formic acid must be completely neutralized before adding the triflate, otherwise racemization may occur) and the reaction was heated at 90 – 100 ^oC until the starting material was completely consumed as indicated by TLC (ca. 1.5 hours). The dark solution was added to ~100 mLs H_2O, then extracted 3 times with ethyl acetate. The combined organics were dried with $MgSO_4$, filtered, and concentrated. The resulting residue was purified by flash chromatography (hexanes/ethyl acetate 1:1), then recrystallized from THF/hexanes.

2S-(Phenyl)-4-quinazolinone (79a)

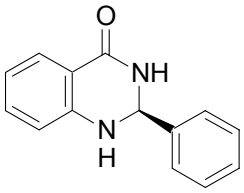

The title compound was synthesized according to General Procedure F from triflate **78a** (0.070 g, 0.19 mmol) to yield 0.038 g of a colorless solid (89.5 %); $[\alpha]_D$ = +160 (c = 0.1, THF); mp: 211-213^{o}C; ^{1}H NMR (300 MHz, DMSO-d_6) δ 8.32 (s, 1H), 7.60, 7.63 (d, J= 7.8 Hz, 1H), 7.47 – 7.50 (d, J= 6.6 Hz, 2H), 7.31 – 7.40 (m, 3H), 7.20 – 7.25 (t, J= 7.2 Hz, 1H), 7.12 (s, 1H), 6.73 – 6.76 (d, J= 8.1 Hz, 1H), 6.64 – 6.68 (t, J= 7.2 Hz, 1H), 5.75 (s, 1H); ^{13}C (125 MHz, DMSO-d_6) δ 164.4, 148.5, 142.3, 134.1, 129.2, 129.0, 128.1, 127.5, 117.8, 115.6, 115.1, 67.2; ESI *m/z* (rel intensity) 224.1 (100); Anal. ($C_{14}H_1N_2O$) C, H, N; C: calcd, 74.98; found, 74.84; H: calcd, 5.39; found, 5.35; N: calcd, 12.49; found, 12.46.

2R-(Phenyl)-4-quinazolinone (79b)

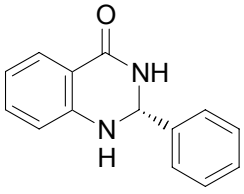

The title compound was synthesized according to General Procedure H from triflate **78b** (0.075 g, 0.20 mmol) to yield 0.044 g of a colorless solid (97.5 %); $[\alpha]_D$ = -158 (c = 0.1, THF); mp: 211-213^{o}C; ^{1}H NMR (500 MHz, DMSO-d_6) δ 8.33 (s, 1H), 7.63 – 7.64 (d, J= 3.0 Hz, 1H), 7.50 – 7.52 (d, J= 7.5 Hz, 2H), 7.33 – 7.40 (m, 3H), 7.23 – 7.26 (t, J= 7.0 Hz, 1H), 7.14 (s, 1H), 6.76 – 6.78 (d, J= 8.0 Hz, 1H), 6.66 – 6.69 (t, J= 8.0 Hz, 1H), 5.77 (s, 1H); ^{13}C (125 MHz, DMSO-d_6) δ 164.1, 148.4, 142.1, 133.8, 128.9, 128.8, 127.8, 127.3, 117.6, 115.4, 114.9, 67.1; ESI *m/z* (rel intensity) 224.1 (100); Anal. ($C_{14}H_1N_2O$) C, H, N; C: calcd, 74.98; found, 74.86; H: calcd, 5.39; found, 5.25; N: calcd, 12.49; found, 12.50.

2R-(Phenyl)-7-methoxy-4-quinazolinone (79c)

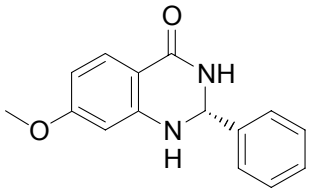

The title compound was synthesized according to General Procedure H from triflate **78c** (0.12 g, 0.30 mmol) to yield 0.049 g of a colorless solid (78.5 %); $[\alpha]_D$ = -135 (c = 0.1, THF); mp: 180-181^oC; ^1H NMR (300 MHz, DMSO-d_6) δ 8.10 (s, 1H), 7.52 – 7.53 (d, J= 5.7 Hz, 1H), 7.46 – 7.48 (d, J= 4.5 Hz, 2H), 7.32 – 7.39 (m, 3H), 7.11 (s, 1H), 6.25 – 6.26 (m, 2H), 5.7 (s, 1H), 3.69 (s, 3H); ^{13}C (75 MHz, DMSO-d_6) δ 164.0, 149.9, 142.3, 129.6, 128.8, 128.7, 127.4, 109.0, 105.5, 98.4, 67.2, 55.7; ESI *m/z* (rel intensity) 254.1 (100); Anal. ($C_{15}H_{14}N_2O_2$) C, H, N; C: calcd, 70.85; found, 70.49; H: calcd, 5.55; found, 5.49; N: calcd, 11.02; found, 10.87.

2R-(Phenyl)-6-methoxy-4-quinazolinone (79d)

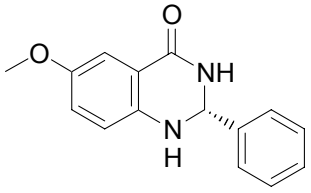

The title compound was synthesized according to General Procedure H from triflate **78d** (0.090 g, 0.22 mmol) to yield 0.042 g of a colorless solid (90.9 %); $[\alpha]_D$ = -200 (c = 0.1, THF); mp: 206-208 ^oC; ^1H NMR (300 MHz, DMSO-d_6) δ 8.35 (s, 1H), 7.51 – 7.53 (d, J= 7.5 Hz, 2H), 7.36 – 7.43 (m, 3H), 7.17 (s, 1H), 6.93 – 6.97 (dd, J= 8.7, 3.0 Hz, 1H), 6.74 – 6.78 (m, 2H), 5.71 (s, 1H), 3.70 (s, 3H); ^{13}C (75 MHz, DMSO-d_6) δ 164.4, 152.1, 143.0, 142.2, 129.1, 129.0, 127.7, 122.2, 116.9, 116.4, 110.5, 67.6, 56.0; ESI *m/z* (rel intensity) 254.1 (100); Anal. ($C_{15}H_{14}N_2O_2$) C, H, N; C: calcd, 70.85; found, 70.85; H: calcd, 5.55; found, 5.49; N: calcd, 11.02; found, 10.91.

2R-(Phenyl)-7-nitro-4-quinazolinone (79e)

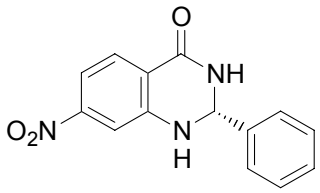

The title compound was synthesized according to General Procedure I from triflate **78e** (0.03 g, 0.07 mmol) to yield 0.015 g of a yellow solid (77.7 %); $[\alpha]_D$ = -279 (c = 0.1, THF); mp: 219-221^{o}C; ^{1}H NMR (300 MHz, DMSO-d_6) δ 8.73 (s, 1H), 7.82 – 7.84 (d, J= 5.1 Hz, 1H), 7.76 (s, 1H), 7.57 (d, J= 1.5 Hz, 1H), 7.48 – 7.49 (d, J= 4.2 Hz, 2H), 7.36 – 7.43 (m, 4H), 5.91 (s, 1H); ^{13}C (75 MHz, DMSO-d_6) δ 162.3, 151.2, 148.6, 141.5, 129.6, 129.2, 129.0, 127.2, 119.7, 111.4, 109.3, 66.8; ESI *m/z* (rel intensity) 269.1 (100); Anal. ($C_{14}H_{11}N_3O_3 \cdot 0.2\ H_2O$) C, H, N; C: calcd, 61.63; found, 61.59; H: calcd, 4.21; found, 4.00; N: calcd, 15.40; found, 15.29.

2R-(Phenyl)-6-nitro-4-quinazolinone (79f)

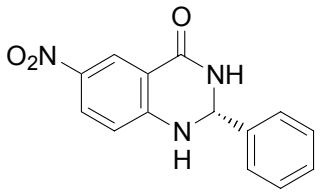

The title compound was synthesized according to General Procedure I from triflate **78f** (0.20 g, 0.48 mmol) to yield 0.044 g of a yellow solid (58.3 %); $[\alpha]_D$ = -240 (c = 0.1, THF); mp: 238-240 ^{o}C; ^{1}H NMR (300 MHz, DMSO-d_6) δ 8.75 (s, 1H), 8.57 (s, 1H), 8.42 (d, J= 1.5 Hz, 1H), 8.08 – 8.10 (d, J= 5.4 Hz, 1H), 7.36 – 7.47 (m, 5H), 6.81 – 6.83 (d, J= 5.7 Hz, 1H), 6.01 (s, 1H); ^{13}C (75 MHz, DMSO-d_6) δ 161.8, 152.6, 141.5, 137.5, 129.5, 129.4, 129.1, 127.0, 124.6, 114.7, 113.1, 66.7; ESI *m/z* (rel intensity) 269.1 (100); Anal. ($C_{14}H_{11}N_3O_3 \cdot 0.2\ H_2O$) C, H, N; C: calcd, 61.63; found, 61.57; H: calcd, 4.21; found, 4.02; N: calcd, 15.61; found, 15.24.

2R-(Phenyl)-8-methyl-4-quinazolinone (79g)

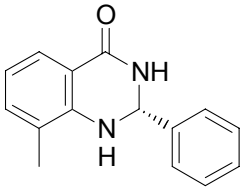

The title compound was synthesized according to General Procedure H from triflate **78g** (0.18 g, 0.47 mmol) to yield 0.069 g of a colorless solid (76.6 %); $[\alpha]_D$ = -150 (c = 0.1, THF); mp: 176-178 ^oC; ^1H NMR (300 MHz, DMSO-d_6) δ 8.40 (s, 1H), 7.48 – 7.50 (d, J= 4.5 Hz, 1H), 7.44 – 7.46 (d, J= 4.5 Hz, 2H), 7.32 – 7.35 (t, J= 4.5 Hz, 2H), 7.27 – 7.29 (m, 1H), 7.12 – 7.13 (d, J= 4.2 Hz, 1H), 6.56 – 6.61 (t, J= 4.5 Hz, 2H), 5.72 (s, 1H), 2.12 (s, 3H); ^{13}C (75 MHz, DMSO-d_6) δ 164.1, 145.9, 143.0, 134.5, 128.7, 128.5, 126.9, 125.7, 122.8, 117.2, 115.6, 65.9, 17.4; ESI *m/z* (rel intensity) 238.1 (100); Anal. ($C_{15}H_{14}N_2O$) C, H, N; C: calcd, 75.61; found, 75.55; H: calcd, 5.92; found, 5.87; N: calcd, 11.76; found, 11.68.

2R-(Phenyl)-5-methyl-4-quinazolinone (79h)

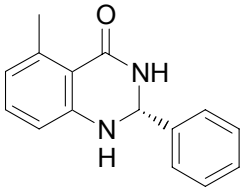

The title compound was synthesized according to General Procedure H from triflate **78h** (0.09 g, 0.23 mmol) to yield 0.035 g of a colorless solid (78.3 %); $[\alpha]_D$ = -172 (c = 0.1, THF); mp: 134-135 ^oC; ^1H NMR (300 MHz, DMSO-d_6) δ 8.22 (s, 1H), 7.53 – 7.56 (d, J= 6.6 Hz, 2H), 7.40 – 7.42 (d, J= 7.2 Hz, 3H), 7.09 – 7.13 (t, J= 7.5 Hz, 1H), 7.05 (s, 1H), 6.68 – 6.71 (d, J= 7.5 Hz, 1H), 6.50 – 6.52 (d, J= 6.9 Hz, 1H), 5.67 (s, 1H), 3.70 (s, 3H); ^{13}C (75 MHz, DMSO-d_6) δ 165.2, 150.1, 142.1, 141.2, 132.9, 129.1, 129.0, 127.7, 121.7, 114.3, 113.7, 67.1, 22.8; ESI *m/z* (rel intensity) 238.1 (100); Anal. ($C_{15}H_{14}N_2O$) C, H, N; C: calcd, 75.61; found, 75.63; H: calcd, 5.92; found, 5.94; N: calcd, 11.76; found, 11.74.

2R-(Phenyl)-6-chloro-4-quinazolinone (79i)

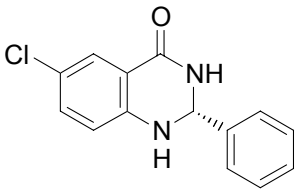

The title compound was synthesized according to General Procedure H from triflate **78i** (0.11 g, 0.27 mmol) to yield 0.045 g of a colorless solid (59.3 %); $[\alpha]_D$ = -111 (c = 0.1, THF); mp: 243-245 ^oC; ^1H NMR (300 MHz, DMSO-d_6) δ 8.53 (s, 1H), 7.59 (d, J= 2.1 Hz, 1H), 7.51 – 7.54 (d, J= 6.6 Hz, 2H), 7.38 – 7.45 (m, 4H), 7.30 – 7.33 (dd, J= 8.7, 2.4 Hz, 1H), 6.81 – 6.84 (d, J= 8.7 Hz, 1H), 5.83 (s, 1H); ^{13}C (75 MHz, DMSO-d_6) δ 163.2, 147.3, 142.0, 133.8, 129.3, 129.1, 127.6, 127.2, 121.5, 117.1, 116.8, 67.2; ESI *m/z* (rel intensity) 258.1 (100); Anal. ($C_{14}H_{11}ClN_2O$) C, H, N; C: calcd, 65.00; found, 64.91; H: calcd, 4.29; found, 4.19; N: calcd, 10.83; found, 10.81.

5-(2'-tolyl)-2-formylphenol (81)

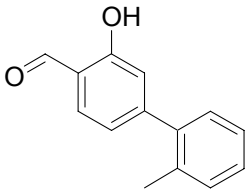

A solution of 3-bromophenylacetate (3.95 g, 18.39 mmol), 2-tolylboronic acid (2.50 g, 18.39 mmol), Cs_2CO_3 (8.97 g, 27.59 mmol), and $Pd(PP_3)_4$ (0.42 g, 0.37 mmol) in 50 mL dioxane was thoroughly degassed, then brought to reflux until the starting materials were consumed (ca. 12 hours). Ethanol (10 mL) was added and reaction continued for 1 hour more. The contents of the reaction flask were concentrated and partitioned between saturated ammonium chloride (100 mL) and ethyl acetate (100 mL). The organic layer was collected and the aqueous extracted twice more. The combined organics were dried with $MgSO_4$, filtered, concentrated and purified by flash chromatography (Hexanes/EtOAc 7:1) to yield 3.17 g of **80** as a brown oil (93.6 %). Methylmagnesium bromide (5.74 mL 3M in ether, 17.21 mmol) was added to a 0 ^oC solution of **80** (3.17 g, 17.21 mmol) in 25

mL THF. After 30 minutes, a precipitate had formed and all the THF was removed *in vacuo*. Benzene (25 mL) was added, removed *in vacuo*, then another 25 mL portion of benzene added again. Paraformaldehyde (6.61 g, 73.4 mmol) and triethylamine (6.1 mL, 44.1 mmol) were then added and the mixture was brought to reflux for 24 hours. The reaction was quenched by addition of 150 mLs saturated ammonium chloride which was then extracted with ethyl acetate (3 x 75 mLs). The combined organics were dried with $MgSO_4$, filtered, concentrated and purified by distillation (220 ^oC, 1 mmHg) to yield 2.4 g of a thick, pale yellow oil (65.7 %); ^1H NMR (300 MHz, $CDCl_3$) δ 11.22 (s, 1H), 9.97 (s, 1H), 7.62 – 7.65 (d, J= 7.8 Hz, 1H), 7.27 – 7.37 (m, 4H), 7.03 – 7.07 (m, 2H), 2.36 (s, 3H); ^{13}C (75 MHz, $CDCl_3$) δ 196.5, 161.7, 151.5, 140.6, 135.3, 133.7, 130.9, 129.5, 128.5, 126.3, 121.6, 119.6, 118.5, 20.7; ESI *m/z* (rel intensity) 212.1 (100).

N-Boc-D-*tert*-leucine [5-(2'-tolyl)-2-formyl]phenyl ester (82)

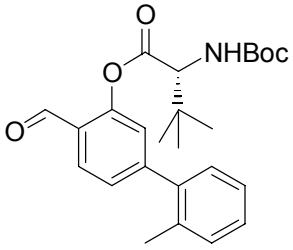

DCC (1.02 g, 4.95 mmol) was added to a room temperature solution of Boc-(L)-tert- leucine (1.07 g, 4.95 mmol), followed by addition of HOBt (0.67 g, 4.95 mmol) 45 minutes later. After an additional 45 minutes, aldehyde **81** (1.00 g, 4.70 mmol) was added and the reaction allowed to proceed overnight. Water (150 mL) was added and the mixture was extracted with ethyl acetate (3 x 75 mLs). The combined organic layers were dried with $MgSO_4$, filtered, concentrated and purified by flash chromatography (Hexanes/EtOAc 6:1) to yield 1.20 g of a thick oil (59.0 %); ^1H NMR (300 MHz,$CDCl_3$) δ 10.29 (s, 1H), 8.00 – 8.03 (d, J= 8.1 Hz, 1H), 7.28 – 7.40 (m, 5H), 7.21 (s, 1H), 5.19 –

5.22 (d, J= 8.7 Hz, 1H), 4.40 – 4.43 (d, J= 8.4 Hz, 1H), 2.32 (s, 3H), 1.51 (s, 9H), 1.18 (s, 9H); ESI *m/z* (rel intensity) 425.2 (100).

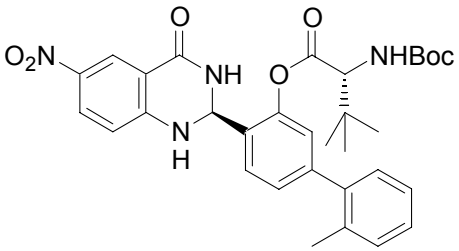

2S-[4'-(2''-tolyl)-2'-N-Boc-D-*tert*-leucine phenyl ester)-6-nitro-4-quinazolinone (83)

The title compound was prepared according to General Procedure F from 5-nitroanthranilamide (0.28 g, 1.55 mmol) and aldehyde **82** (0.70 g, 1.55 mmol) to yield 0.44 g of a yellow foam (49.7 %); $[\alpha]_D$ = +213 (c = 0.1, THF); ^{1}H NMR (300 MHz, DMSO-d_6) δ 8.78 – 8.79 (d, J= 2.4 Hz, 1H), 8.05 – 8.09 (dd, J= 9.0, 2.4 Hz, 1H), 7.61 – 7.63 (m, 2H), 7.16 – 7.27 (m, 6H), 6.84 (s, 1H), 6.74 -6.77 (d, J= 9.3 Hz, 1H), 6.48 (s, 1H), 5.18 – 5.20 (d, J= 5.7 Hz, 1H), 4.10 – 4.13 (dd, J= 7.2, 2.4 Hz, 1H), 2.25 (s, 3H), 1.44 (s, 9H), 1.11 (s, 9H); ^{13}C (75 MHz, DMSO-d_6) δ 171.0, 163.9, 156.8, 151.1, 145.9, 144.3, 140.0, 139.2, 135.6, 130.9, 130.8, 129.9, 129.5, 128.2, 127.6, 127.0, 126.2, 125.8, 123.4, 115.0, 113.0, 81.3, 63.3, 61.8, 34.1, 28.6, 27.1, 20.6; ESI *m/z* (rel intensity) 588.3 (100).

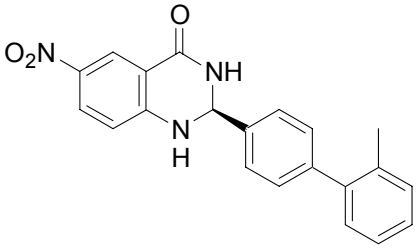

2S-[4'-(2''-tolyl)-phenyl]-6-nitro-4-quinazolinone (84)

The title compound was prepared by making the triflate according to General Procedure G, followed by reduction of the triflate according to General Procedure I. Reacting the ester **83** (0.22 g, 0.38 mmol) with hydrazine (0.056 mL, 1.15 mmol)

formed 0.14 g of the corresponding phenol as a yellow solid (94.7 %); $[\alpha]_D$ = +293 (c = 0.1, THF); ^{1}H NMR (300 MHz, DMSO-d_6) δ 10.13 (s, 1H), 8.45 – 8.52 (m, 3H), 8.08 – 8.12 (dd, J= 9.0, 2.7 Hz, 1H), 7.22 – 7.36 (m, 5H), 7.13 – 7.16 (m, 1H), 6.81 – 6.87 (m, 3H), 6.26 (s, 1H), 2.23 (s, 3H); To the phenol (0.11 g, 0.28 mmol) was added N-phenyl-bis(trifluoromethanesulfonimide) (0.20 g, 0.56 mmol) and diisopropylethyl amine (0.49 mL, 2.80 mmol) to form 0.14 g of the triflate as a thick yellow oil (100 %); $[\alpha]_D$ = +155 (c = 0.1, THF); ^{1}H NMR (300 MHz, $CDCl_3$) δ 8.77 – 9.78 (d, J= 2.7 Hz, 1H), 8.17 – 8.21 (dd, J= 9.0, 2.7 Hz, 1H), 7.87 – 7.89 (d, J= 8.1 Hz, 1H), 7.45 – 7.48 (dd, J= 8.1, 1.5 Hz, 1H), 7.25 – 7.38 (m, 4H), 7.16 – 7.19 (d, J= 7.2 Hz, 1H), 7.07 (s, 1H), 6.73 – 6.6.76 (d, J= 9.0 Hz, 1H), 6.44 (s, 1H), 5.65 (s, 1H), 2.26 (s, 3H); ^{13}C (75 MHz,$CDCl_3$) δ 163.0, 150.9, 146.7, 145.7, 140.4, 138.8, 135.4, 131.1, 130.7, 130.3, 130.0, 129.8, 129.3, 128.9, 127.3, 126.5, 125.8, 123.3, 123.1, 114.9, 62.3, 20.5 (CF_3 signal not detected due to the strong C-F coupling); The triflate was reduced according to General Procedure D from formic acid (0.010 mL, 0.27 mmol), triethylamine (0.36 mL, 2.56 mmol) and Pd(dppf)Cl_2 (0.004 g, 0.005 mmol) to yield 0.050 g of **84** as yellow crystals (53.8 %); $[\alpha]_D$ = +209 (c = 0.1, THF); mp: 258-260 ^{o}C; ^{1}H NMR (300 MHz, DMSO-d_6) δ 8.82 (s, 1H), 8.66 (s, 1H), 8.49 (s, 1H), 8.13 – 8.17 (dd, J= 9.3, 2.7 Hz, 1H), 7.55 – 7.58 (d, J= 7.8 Hz, 2H), 7.42 – 7.45 (d, J= 8.1 Hz, 2H), 7.27 – 7.31 (m, 3H), 7.17 – 7.20 (m, 1H), 6.87 – 6.90 (d, J= 9.0 Hz, 1H), 6.11 (s, 1H), 2.25 (s, 3H); ^{13}C (75 MHz, DMSO-d_6) δ 162.0, 152.8, 142.6, 141.3, 140.4, 137.8, 135.3, 131.1, 130.2, 130.1, 130.0, 128.2, 127.4, 126.7, 124.9, 115.0, 113.3, 66.9, 20.9; ESI *m/z* (rel intensity) 359.1 (100); Anal. ($C_{21}H_{17}N_3O_3$ · 0.1 H_2O) C, H, N; C: calcd, 69.83; found, 69.75; H: calcd, 4.80; found, 4.65; N: calcd, 11.63; found, 11.67.

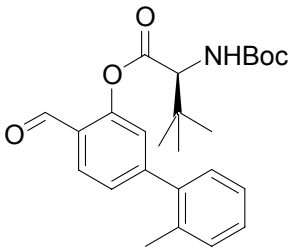

N-Boc-L-*tert*-leucine [5-(2'-tolyl)-2-formyl]phenyl ester (85)

DCC (1.57 g, 7.60 mmol) was added to a room temperature solution of Boc-(D)-tert-leucine (1.50 g, 6.91 mmol), followed by addition of HOBt (1.03 g, 7.60 mmol) 45 minutes later. After an additional 45 minutes, aldehyde **81** (1.10 g, 5.18 mmol) was added and the reaction allowed to proceed overnight. Water (150 mL) was added and the mixture was extracted three times with ethyl acetate. The combined organic layers were dried with $MgSO_4$, filtered, concentrated and purified by flash chromatography (Hexanes/EtOAc 6:1) to yield 0.8 g of a thick oil (37.5 %); ^{1}H NMR (300 MHz,$CDCl_3$) δ 10.25 (s, 1H), 7.96 – 7.99 (d, J= 8.1 Hz, 1H), 7.17 – 7.36 (m, 5H), 7.16 (s, 1H), 5.14 – 5.17 (d, J= 8.1 Hz, 1H), 4.35 – 4.38 (d, J= 8.4 Hz, 1H), 2.29 (s, 3H), 1.47 (s, 9H), 1.13 (s, 9H); ESI *m/z* (rel intensity) 425.2 (100).

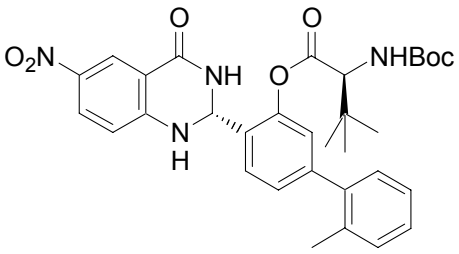

2R-[4'-(2''-tolyl)-2'-N-Boc-L-*tert*-leucine phenyl ester)-6-nitro-4-quinazolinone (86)

The title compound was prepared according to General Procedure F from 5-nitroanthranilamide (0.27 g, 1.50 mmol) and aldehyde **85** (0.64 g, 1.50 mmol) to yield 0.33 g of a yellow foam (37.3 %); $[\alpha]_D$ = -210 (c = 0.1, THF); ^{1}H NMR (300 MHz, DMSO-d_6) δ 8.79 - 8.80 (d, J= 2.7 Hz, 1H), 8.06 – 8.10 (dd, J= 9.0, 2.7 Hz, 1H), 7.62 – 7.64 (m, 2H), 7.16 – 7.28 (m, 6H), 6.83 (s, 1H), 6.74 – 6.77 (d, J= 9.0 Hz, 1H), 6.48 (s, 1H), 5.18 – 5.20 (d, J= 6.0 Hz, 1H), 4.11 – 4.14 (m, 1H), 2.90 (s, 3H), 1.44 (s, 9H), 1.17 (s, 9H); ^{13}C (75 MHz,

DMSO-d_6) δ 171.0, 164.2, 156.8, 151.3, 147.0, 144.2, 140.0, 139.1, 135.5, 131.0, 130.8, 129.9, 129.5, 128.2, 127.5, 127.0, 126.2, 125.7, 123.4, 115.0, 113.0, 81.2, 63.4, 61.8, 33.7, 28.6, 27.1, 20.6; ESI *m/z* (rel intensity) 588.3 (100).

2S-[4'-(2''-tolyl)-phenyl]-6-nitro-4-quinazolinone

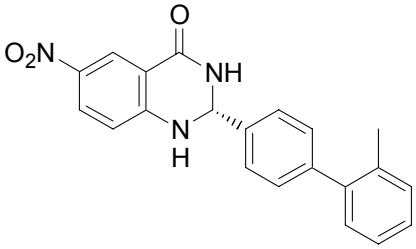

(87)

The title compound was prepared by making the triflate according to General Procedure G, followed by reduction of the triflate according to General Procedure I. Reacting the ester **86** (0.33 g, 0.56 mmol) with hydrazine (0.82 mL, 1.68 mmol) formed 0.17 g of the corresponding phenol as a yellow solid (80.4 %); $[\alpha]_D$ = -288 (c = 0.1, THF); ^{1}H NMR (300 MHz, DMSO-d_6) δ 10.17 (s, 1H), 8.49 – 8.57 (m, 2H), 8.12 – 8.17 (dd, J= 9.0, 2.7 Hz, 1H), 7.28 – 7.40 (m, 5H), 7.18 – 7.20 (m, 1H), 6.85 – 6.92 (m, 3H), 6.30 (s, 1H), 2.27 (s, 3H); To the phenol (0.08 g, 0.22 mmol) was added N-phenyl-bis(trifluoromethanesulfonimide) (0.16 g, 0.44 mmol) and diisopropylethyl amine (0.38 mL, 2.20 mmol) to form 0.11 g of the triflate as a thick yellow oil (100 %); $[\alpha]_D$ = -156 (c = 0.1, THF); ^{1}H NMR (300 MHz, $CDCl_3$) δ 8.87 (s, 1H), 8.29 – 8.31 (d, J= 6.6 Hz, 1H), 7.98 – 8.01 (d, J= 7.8 Hz, 1H), 7.56 – 7.59 (d, J= 8.1 Hz, 1H), 7.36 – 7.51 (m, 4H), 7.23 – 7.28 (m, 2H), 6.85 – 6.88 (d, J= 9.0 Hz, 1H), 6.56 (s, 1H), 5.79 (s, 1H), 2.38 (s, 3H); ^{13}C (75 MHz, $CDCl_3$) δ 163.1, 151.0, 146.8, 145.8, 140.5, 138.9, 135.5, 131.2, 130.8, 130.5, 130.2, 129.9, 129.4, 129.0, 127.3, 126.6, 125.9, 123.4, 123.2, 115.0, 62.5, 20.6 (CF_3 signal not detected due to the strong C-F coupling); The triflate was reduced according to General Procedure D from formic acid (0.013 mL, 0.35 mmol), triethylamine (0.17 mL, 1.20 mmol) and Pd(dppf)Cl_2

(0.004 g, 0.005 mmol) to yield 0.058 g of **87** as yellow crystals (66.7 %); $[\alpha]_D$ = -213 (c = 0.1, THF); mp: 258-260 ^oC; ^1H NMR (300 MHz, DMSO-d_6) δ 8.86 (s, 1H), 8.69 (s, 1H), 8.51 (s, 1H), 8.15 – 8.19 (dd, J= 9.0, 2.4 Hz, 1H), 7.58 – 7.61 (d, J= 8.4 Hz, 2H), 7.44 – 7.47 (d, J= 8.1 Hz, 2H), 7.29 – 7.32 (m, 3H), 7.21 – 7.22 (m, 1H), 6.90 – 6.93 (d, J= 9.0 Hz, 1H), 6.14 (s, 1H), 2.27 (s, 3H); ^{13}C (75 MHz, DMSO-d_6) δ 162.0, 152.9, 142.7, 141.4, 140.5, 137.9, 135.4, 131.1, 130.2, 130.1, 129.8, 128.2, 127.3, 126.7, 125.0, 115.0, 113.3, 67.0, 20.9; ESI *m/z* (rel intensity) 359.1 (100); Anal. ($C_{21}H_{17}N_3O_3$) C, H, N; C: calcd, 70.18; found, 70.05; H: calcd, 4.77; found, 4.65; N: calcd, 11.69; found, 11.71.

8.4 Biological Methods

Cell culture

HCT-116 colon cancer cells (ATCC) were maintained in McCoy's 5a Medium with 1.5mM L-glutamine (Invitrogen) supplemented with 5% FBS (Atlanta Biologicals) and MDA-MB-435 breast cancer cells (ATCC) were maintained in D-MEM with 1.5mM L-glutamine(Invitrogen) supplemented with 5% FBS (Optima) at 37ºC in a humidified, 5% CO_2 incubator.

Cell proliferation Assay

Cells grown to confluency were trypinized, counted and diluted to 6400 cells per 100 mcl. 3200 cells/well were added to a clear 96 well tissue culture treated plate (Falcon). Cells were allowed to attach and 50 mcl of media with concentrations of drug at 10nM, 30nM, 100nM, 300nM, 1mcM, 3mcM or vehicle added to each well (n=8). The cells were incubated 72 hours at 37ºC in a humidified, 5% CO_2 incubator. The CellTiter 96®

AQ_{ueous} Non-Radioactive Cell Proliferation Assay (Promga) was used to measure the number of living cells in culture. The absorbance was read at 490nm on a ELISA plate reader and the numbers are evaluated for a dose response curve and EC_{50} for each cell line and drug (GraphPad Prism 4 software).

[^{3}H] Colchicine Binding Assay

The binding of [^{3}H] colchicine to tubulin was measured by the DEAE-cellulose filter method, as described in detail previously.[1] The tubulin concentration was 1.0 μM (0.1 mg/ml), and the [^{3}H] colchicine concentration was 5.0 μM and 50.0 μM.

In Vitro Tubulin Depolymerization Assay

Tubulin polymerization was followed turbidimetrically at 350 nm in a Beckman model DU-7400 and Du7500 spectrophotometers equipped with electronic temperature controllers, as described in detail previously.[2] The tubulin concentration was 10 μM (1.0 mg/ml).

Cellular Tubulin Depolymerization Assay

The ability of the compounds to depolymerize cellular microtubules was evaluated in A-10 cells as previously described.[3] Briefly, cells were treated for 18 h with a range of concentrations of each compound and then fixed and microtubules visualized by indirect immunofluorescent techniques. The percent microtubule loss was estimated for each compound concentration and then the EC_{50} values for microtubule depolymerization were calculated from the linear portion of the log dose response curves.

Cellular Antiproliferation Studies

The human colon cancer cell line, HCC-2998, was obtained from the National Cancer Institute (NCI-Frederick Cancer DCTD Tumor/Cell Line Repository) and grown in RPMI-1640 Medium (1x), liquid, with L-glutamine (Gibco, Cat# 11875-119) supplemented with 10% Fetal Bovine Serum (Gibco, Cat# 16000-044, Lot# 1222352). The pooled neonatal human microvascular endothelial cell line, HMVEC-d (Cambrex, CC-2516, Lot# 1F0379) was grown in Clonetics Endothelial Growth Media (EBM2: Cambrex, CC-3156) supplemented with the EGM-2-MV Bulletkit (Cambrex, CC-3202). The pooled neonatal human umbilical vein endothelial cell line, HUVEC (Cambrex, C2519A, Lot# 1F1625) was grown in Clonetics Endothelial Growth Media (EBM2: Cambrex, CC-3156) supplemented with the EGM-2 Bulletkit (Cambrex, CC-3162).

Routine Tissue Culture

Cells were routinely grown in Nunc EasY filter-capped T-25 and/or T-75 flasks (Fisher Scientific, Cat# 12-565-351, Cat# 12-565-349) at 37 ± 0.5 °C in an Isotemp Fisher Scientific humidified (90 ± 1%) incubator under an air/CO_2 (95%/5% ± 0.5%) atmosphere. Cells were regularly re-fed 2 - 3 times per week including a once per week passage. Upon passaging, cells received a 30 ± 3 second rinse with Phosphate Buffered Saline (PBS) 7.4, 1x, liquid, (Gibco, Cat# 10010-064), and were then treated with Trypsin-EDTA (.05% Trypsin, with EDTA 4Na) (1x) (Gibco, Cat# 25300-120) for 2-7 minutes. Trypsin was inactivated by resuspending cells in their appropriate media containing FBS. Cell cultures were re-fed 24 ± 3 hours prior to seeding.

Assay Proliferation

All three cell lines were seeded into Nunclon* Δ MicroWell flat bottom 96-well culture plates (Fisher Scientific, 12-565-66) in 100 µl of their respective media as described above: HCC-2998's at 10 x 10^3 cells per well, and HMVEC's and HUVEC's at 20 x 10^3 cells per well. Compound dosing occurred at 24 ± 3 hours post-plating to give a final volume of 200 µl per well. Compounds were dissolved in DMSO (SIGMA, Cat# D 8779) at 100 mM and diluted 1:10 in ETOH (SIGMA, Cat# E 7023). Final concentrations were in log steps inclusively between 100 and 0.100 µM with a constant DMSO:EtOH concentration of 0.1%:1.0%.

Crystal Violet Staining

At 72 ± 3 hours cells were fixed with 1% gluteraldehyde (SIGMA, Cat# G 6257) in PBS (as described above) for 15 minutes ± 30 seconds and then stained with 5 mg/L crystal violet (Fisher Scientific, Cat# C581-100) in sterilized deionized water for 15 minutes ± 30 seconds. No less than 3 rinses (3 – 5) were performed to remove excess concentrated stain using deionized water. The resulting dilute stain was then removed through passive diffusion in tap water immersion and the stained plates were dried. At ≥3 hours under minimal light conditions cells received 100 µl/well Sorenson's solution: 8.967 g trisodium citrate (Fisher Scientific, Cat# S279-500), 19.5 mL 1 N HCl (SIGMA, Cat# H 9892), 480 mL distilled water, in 500 mL 90% Ethanol (as described above). Cells were shaken for 1 hour ± 15 minutes at low speed under minimal light conditions and read using a Thermo Labsystems Multiskan Ascent plate reader at 492 nm.

GI_{50} Determination

Raw data (n=3) was converted to corrected percent of control by subtracting blank averages (on a per plate basis) from all data points and then dividing the corrected average triplicate absorbance of a particular end point by the corrected average negative carrier control end point (n=6). Concentrations were plotted vs. the resulting corrected percent of control values. A linear trendline was fit to the linear portion of the data ($R^2 > 0.95$) and a resulting GI_{50} was calculated. To obtain errors the standard deviation was added and subtracted to each of the corrected raw data points to generate two separate corrected percent of controls. Separate plots and trendlines were generated as described above and the absolute value of the difference between the resultant high GI_{50} and the actual GI_{50} was averaged with the respective absolute value of the difference between the low GI_{50} and the actual GI_{50}.

8.5 Molecular Modeling Methods

Docking

The X-ray structure of tubulin originating from the complex of two α/β-heterodimers with podophylotoxin, and the stathmin-like domain (SLD) (PDB entry 1SA1) was applied for all docking experiments. The binding site chosen was a 6.5 Å radius surrounding the co-crystallized podophylotoxin and tyrosine 224. Hydrogen atoms were added to the protein using the Build/Edit Add feature on Sybyl 7.0. The flexible docking experiments were done with the FlexX module using energy minimized ligands (1000 iterations to 0.05 kcal/mol using the Powell Gradient method) prior to

docking. The top 30 results (default setting) were analyzed using visual inspection, FlexX scoring, G-Score, PMF Score, D-Score, Chem-Score, and C-Score.

8.5 Chapter 8 References

1. Verdier-Pinard, P.; Lai, J. Y.; Yoo, H. D.; Yu, J.; Marquez, B.; Nagle, D. G.; Nambu, M.; White, J. D.; Falck, J. R.; Gerwick, W. H.; Day, B. W.; Hamel, E. Structure-activity analysis of the interaction of curacin A, the potent colchicine site antitmitotic agent, with tubulin and effects of analogues on the growth of MCF-7 breast cancer cells. *Mol. Pharmacol.* **1998**, *53*, 62-76.
2. Li, L.; Wang, H. K.; Kuo, S. C.; Wu, T. S.; Mauger, A.; Lin, C. M.; Hamel, E.; Lee, K. H. Synthesis and biological evaluation of 3′,6′,7-substituted 2-phenyl-4-quinolones as antimitotic antitumor agents. *J. Med. Chem.* **1994**, *37*, 3400-3407.
3. Rao, P. N., Cessac, J.W. Tinley, T.L. and Mooberry, S.L**.** Synthesis and antimitotic activity of novel 2-methoxyestradiol analogs. *Steroids.* **2002,** *67*, 1079-1089.